PREDICTABILITY AND TRENDS OF ANNUAL POLLUTANT LOADS IN MIDWESTERN WATERSHEDS

BY

SIDDHARTHA VERMA

DISSERTATION

Submitted in partial fulfillment of the requirements
for the degree of Doctor of Philosophy in Agricultural and Biological Engineering
in the Graduate College of the
University of Illinois at Urbana-Champaign, 2013

Urbana, Illinois

Doctoral Committee:

Associate Professor Richard A. Cooke, Chair
Professor Prasanta K. Kalita
Assistant Professor Momcilo Markus
Alena Bartosova
Professor Praveen Kumar

ABSTRACT

The effect of multiple stressors on global water resources have been increasing rapidly over the past few decades. Anthropogenic activities such as rapid industrialization, urbanization, deforestation and increased application of agricultural nutrients have led to a decline in overall quality of our aquatic environment. Additionally, these activities have increased greenhouse gas concentrations globally, warming the earth's atmosphere and eventually having a detrimental effect on global water and energy balances. The global water cycle has been altered, leading to its overall intensification and an increase in frequency of extreme events and such as floods and droughts. Also, the demands of higher quality water have been rising globally attributed to a burgeoning world population, further stressing the water resources. To address the increased water demands worldwide coupled with declining water quality and depletion of water resources requires new approaches in water management along with improvement in water use efficiencies.

To facilitate development of newer approaches of water management and solutions to alleviate global water problems requires an overall comprehensive assessment of our water resources. A key step in these assessments is water quality monitoring which will help improve our ability to predict water quantity, quality and distribution on a global scale. In this research, I aim to improve our knowledge of anthropogenic and natural impacts on global water resources, largely focusing on water quality monitoring by evaluating and refining the science of predicting pollutant (nutrient and sediment) export from large scale watersheds. To enable these goals, this research is centered on large watersheds in Midwestern United States, which have been some of the primary sources of nutrient and sediment export to downstream water bodies such as the Gulf of Mexico and Lake Erie leading to massive eutrophication. In total, fourteen watersheds with extensive water quality datasets are analyzed in different stages of this research. Typically,

these large watersheds are predominantly agricultural with intensive row-cropped farmlands having a network of sub-surface tile drain systems.

The science of pollutant export and various hydrological processes associated with it have been simulated using three major modeling approaches namely statistical and empirical modeling, physically-based modeling and data mining methods. In this research I improve, apply or evaluate all three approaches to meet specific objectives related to annual pollutant load predictions and trend assessments. In the first part of this research, I use regression techniques to assess the role of large load events in predicting annual pollutant (Suspended Solids (SS), Total Phosphorus (TP) and Nitrate-Nitrogen (NO3-N)) loads. In doing so, a novel baseflow separation technique based on mechanistic differences in nutrient and sediment export is proposed and applied. Then, I assess the spatio-temporal patterns of pollutant export from large Midwestern watersheds using circular statistics. This enables identification of critical periods of high load export and also gaging impacts of landuse, management practices, and sources of pollution on overall annual loads. These analyses constitute the first such application of these approaches on a large spatio-temporal scale especially for nutrient export dynamics. I next calibrate a physically-based SWAT model for hydrology and water quality predictions in the largest watershed in the Lake Erie basin. I use this calibrated model to gage the impacts of future projected climate changes from the mid-century and late-century time periods on the hydrology and water quality in the watershed. Further, I evaluate two data mining techniques namely the nearest-neighbor method and decision trees which have scarcely been used in hydrology to predict missing NO_3-N concentrations for two extensively monitored watersheds in the Lake Erie basin. Lastly, I evaluate the impacts of available water quality data for concentration and load predictions and trend calculations based on traditional statistical methods and some new improved and modified approaches which have not yet been applied extensively.

ACKNOWLEDGEMENTS

I would like to thank everyone who has offered help, words of encouragement and support over the past two years thereby helping me complete my PhD dissertation.

Firstly, I would like to express my gratitude to my advisor Dr. Richard Cooke, who has been a constant source of motivation. His passion towards research, his optimism and the ever smiling persona has been highly inspiring for me over the past few years. He has always challenged me to become a better researcher and made sure I have access to all the tools I need to be one. He has been instrumental in my growth over the last few years both on the professional and personal front.

I'll also like to thank Dr.Momcilo Markus and Dr. Alena Bartosova for giving me this great opportunity to work on this project. They have been wonderful mentors who always encouraged me think independently as a researcher and were instrumental in keeping the project on track and ensuring high overall quality was maintained.

I'll also like to thank my committee members Dr. Prasanta Kalita and Dr. Praveen Kumar, for taking time out to review my thesis and also for their invaluable suggestions and comments.

I am grateful to Dr. Amit Desai, Dr.Rabin Bhattarai and Dr. Huzefa Raja who have been role models for me and also for addressing my innumerable technical and professional queries. I would also like to thank Joe Monical, Carlos Bulnes Garcia, Natasha Bell, Ana Martin, Tim Rendall, Doug Barker, Chris Cirone, and Mitch Minarick for sharing their graduate experiences with me and making the workplace fun to be at.

I am really thankful to Neha Bisht, who has always lent a patient ear and has helped me keep my priorities in line. Her enthusiasm and optimism have kept my spirits high throughout the past several years.

Finally I'll thank my parents and brother, without whom my journey thus far wouldn't have been possible. I'm really fortunate to have received their unwavering love and support throughout. They have always taught me to dream big and to work diligently to turn those dreams into reality.

TABLE OF CONTENTS

CHAPTER 1

Introduction

"Spirit of the water
Give us all the courage and the grace
To make genius of this tragedy unfolding
The genius to save this place"

-Joni Mitchell

We live in an era in which the impacts of human activities on earth have never been greater. There is a growing scientific evidence of enormous anthropogenic disruption of water, energy and climate cycles over the past several decades. A growing group of scientists around the world are even pushing to define this period as the "Anthropocene", a new geological epoch in which humans are the primary drivers for change in environmental systems and processes (Balter, 2013). Among all environmental changes that are attributed to humans, the alteration of the water cycle is perhaps the most detrimental for sustainable existence of life. Globally, rapid industrialization, intensification of agriculture, and the needs to fulfill the growing demands of an increasing population have led to severe water stresses and degradation of water resources. Our activities have altered the intensities of the water cycle, changed patterns of precipitation and river flow, increased sediment and nutrient pollution, drained wetlands, depleted groundwater resources and increased non-natural sedimentation by dams (Postel, 2013). Moreover, the impacts of these changes have led to a loss in water biodiversity, rise of eutrophic water bodies and an overall decline of aquatic environment aesthetics.

Water is critical for the future growth of humanity, but at the same time it can be its biggest limiting factor. The human population is projected to reach nine billion by the year 2050, with the majority of growth occurring in regions which are already water stressed. The fulfilling of

water needs of the additional two billion people while maintaining the life-support functions of freshwater systems is possibly one of the biggest challenges of the 21st century. To address these water challenges in the coming future, it will be vital to meet the additional water quantity requirements with an increased emphasis on higher water quality. However, given the current nature of water management and the existing pressures on water resources, it might not be sustainably possible to meet the demand for high quality water in the future. It will require new ways and approaches in water management and improvement in efficiency of water use. It is likely that large-scale advances in water management and gains in efficiencies of water utilization may be able to meet the demands of a growing global population and economy. However, there are large degree of uncertainties associated with the amount of improvements needed, the efficiency levels that can be achieved and if there is enough time to make significant and relevant gains.

The answers to these questions lie in assessing the current status of our water resources as well as in determining the direction in which they are headed. A key step in these assessments is comprehensive water quality monitoring of our aquatic environments. As stated by Jackson et al. (2001), better monitoring and forecasting of the water resources will help in improved allocation of water for competing demands. Water quality monitoring is essential to verify suitability of water resources for their intended purposes, both locally and on bigger spatial scales. It is vital for characterizing any changes and trends in water quality over time. It helps in quantifying existing or new emerging water quality problems. Additionally, monitoring is also critical to gage compliance of water bodies with existing pollution regulations.

Over the past few decades, water quality monitoring studies have increasingly been carried out to estimate sediment and nutrient loads delivered by rivers to receiving lakes and oceans. Nutrients such as nitrogen and phosphorus have been the engines of agriculture for some time now. Globally, more than a hundred million tons of nutrients are applied each year to

agricultural farms to enhance crop yields. This has enabled human civilization to survive by increasing global food production to meet the ever increasing demands. Yet, this modern miracle has come with a price of its own. More than 50% of the nutrients applied each year, are not used up by crops and are lost to the environment by leaching, erosion and emissions. These excess nutrients have been primarily responsible for degradation of river and lake water quality, loss of wildlife habitat, groundwater pollution and overall decline in usability of water resources. Thereby, it has become critical to quantify these losses to help design pollution abatement programs and agricultural best management practices and also to evaluate their effectiveness.

In quantifying sediment and nutrient loads delivered by rivers to lakes and oceans, the main concern for water resource managers is to accurately estimate loading rates while minimizing associated uncertainties. However, resource constraints such as manpower and financial limitations prohibit intensive water quality monitoring to achieve accurate load estimates (Yaksich and Verhoff, 1983). Additionally, increasing water quality pollution in historically pristine resources warrants the need to monitor more water resources than ever before (Meybeck and Helmer, 1989). So, limited resources coupled with more monitoring demand call for efficient approaches for obtaining accurate and reliable load estimates.

Some research studies have evaluated inventive approaches to estimate annual pollutant loads such as developing regression relationships between a few critical storm (high flow event) loads and annual loads. Richards and Holloway (1987), Preston et al. (1989), Lewis (1996), Robertson and Roerish (1999), Cooper and Watts (2002), Markus and Demissie (2006) and Salles et al. (2007) have reported that a few high flow events carry significant amounts of nutrients exported over a year. Yaksich and Verhoff(1983) analyzed high flow event based sampling strategies for watersheds in the Lake Erie basin and recommended intensively sampling two to three largest events in a year to get annual loading estimates with small errors. Thus, development of robust statistical relationships between observed loads during a few

critical high flow events and observed total annual loads could provide an alternative approach to estimate annual pollutant loads for a certain watershed. If successful, such an approach will provide watershed managers and sampling programs with an option of estimating annual pollutant loadings by just sampling a few high flow events in a year thereby leading to significant reduction in monitoring costs over a year. In spite of some studies that have emphasized the importance of a few high load export periods on annual pollutant loads, a comprehensive analysis hasn't been done to validate this hypothesis for a wide range of combinations of watershed sizes, locations, land uses and pollutants. Specifically, there is a dearth of such studies examining predictability of nutrient loads from a few large load events annually in the large agricultural Midwestern watersheds, particularly when they are the principal sources of nutrients and sediment export to the Gulf of Mexico and Lake Erie eventually causing extreme eutrophication. Thereby, in the first part of this study, multiyear water quality data comprising of Suspended Solids (SS), Total Phosphorus (TP) and Nitrate-Nitrogen (NO_3-N) concentrations from ten large Midwestern watersheds was used to statistically evaluate the relationships between nutrient and sediment loads exported through a few large events (the biggest load events) and total annual loads. Most of the watersheds analyzed in the study are typical agricultural Midwestern watersheds which drain into the Lake Erie and the Mississippi River basins.

If a watershed-specific correlation exists between the few biggest load events and total annual load, this information can possibly be used to precisely and efficiently predict annual loads. However, a major challenge associated with this approach is the *a priori* prediction of a large load event which might be critical to predict total annual loads. Although it is virtually impossible to precisely forecast the occurrence of an event which will be important to predict annual loads, analyzing temporal patterns in load export might enable water managers to majorly focus on periods of high load export. Royer et al. (2006) stated that from the perspective of quantifying annual pollutant loads from agricultural watersheds the temporal distributions of

load export patterns and consequently critical load events are largely unclear. Despite the widely acknowledged seasonality in load export patterns from large agricultural Midwestern watersheds and the importance of a few biggest load events in total annual loads, few comprehensive efforts have been made to quantify these patterns on large spatio-temporal scales. Rather, the few studies that exist simply analyzed pollutant export patterns from very small experimental watersheds limited to a smaller geographical extent. Therefore, the second part of this study aims at analyzing the spatio-temporal patterns in nutrient and sediment load export from eight large Midwestern watersheds over long monitoring durations (8-32 years). The spatio-temporal analysis was done in two phases, with one focusing on the temporal occurrence of the top load events annually for SS, TP and NO_3-N loads which were identified in the first part of this study. The second phase of the analysis focused on examining the timing of mean annual flow, pollutant concentrations and corresponding loads over the complete monitoring durations for each watershed. These analysis would potentially reveal the temporal patterns of pollutant load export which can then then be further used to design more efficient monitoring programs which focus on periods of high load export. Identification of temporal patterns in load export would also help in designing targeted regulatory programs and policies for reducing riverine pollutant loads.

Water resources and water managers in the future face a host of challenges such as population growth, land use changes, economic development, changing social values and climate change. Amongst these challenges, climate change is one of the biggest and most dynamic. Globally, there is growing scientific and observational evidence about climate change due to the rise of greenhouse gas concentrations in the earth's atmosphere and its overall warming. It is likely to impact the fundamental drivers of the hydrological cycle and influence outcomes linked to it such as water quantity, water quality, floods, droughts, navigation and hydropower. Moreover as stated by the IPCC report, current water management practices might not be robust enough to cope up with climate change and its impacts on water resources.

Additionally, there are knowledge gaps in observational data and understanding the complex dynamics of climate change and its impacts a wide range of watersheds in different global regions. Thus, it has become ever more crucial for water managers and environmental scientists to propose newer water management approaches by tracking, anticipating and responding to climate change (Brekke et al., 2009). Specifically, it is vital to estimate the impacts of projected climate change on water resources and hydrological processes on both global and local scales (Jackson et al., 2001). This would enable water managers to determine the necessary adaptation options and mitigating measures which might reduce the impacts of climate change on water resources. As rivers, lakes and oceans are key components of the global hydrological cycle and they face increasing pressures with growing nutrient and sediment pollution, it is critical to understand the impacts of impending climate change on the functionality of these water bodies. Typically this is done using physically-based hydrologic models coupled with future climate data from General Circulation Models (GCMs). As these hydrologic models are physically based, they utilize commonly measured hydro-climatic parameters along with spatial watershed data to recreate the hydrological processes in a watershed. Once calibrated, future projections of climate from General Circulation Models (GCMs) can be used as model inputs to understand the sensitivity of the watershed processes to climate change. Thus, the third part of this research uses the Soil and Water Assessment Tool (SWAT) to evaluate the impacts of projected change in temperature and precipitation for the mid-century (2045-2055) and late-century (2089-2099) time-periods on the flow, sediment and nutrient loading in the largest watershed in the Lake Erie basin. Also, this watershed is the largest contributor of nutrient and sediment loads to Lake Erie annually, and typifies a Midwestern agriculture watershed with intensive row-crop agriculture and a high density of sub-surface tile drain systems.

With the advent of low-cost sensing in general, we are fast moving towards an era in which observational time-series data are being collected at greater amounts than ever before. This can been beneficial in hydrologic sciences as it aids in creation of better statistical and physically-

based models which are able to simulate real world hydrological processes more accurately. However, there is still a long way to reach a stage where low-cost sensing becomes ubiquitous, especially to measure water quality parameters. Additionally, with an increasing need to monitor newer sites with diminishing budgets makes multiyear daily water quality time-series datasets uncommon. Conversely, the necessity for intensive water quality monitoring is increasing on a global scale given the pressures of an increasing population, economic development, land use change and climate change on water resources. A majority of the water quality monitoring programs globally measure streamflow inexpensively at high temporal resolutions typically ranging from 15-minute intervals or lower using automated stage recorders and stage-discharge rating curves. However, financial and manpower shortages lead to water quality parameters being measured at much lower temporal resolutions typically ranging from daily to a few samples per year. Thereby, a lot of hydrologists have explored and developed various approaches to predict missing water quality data from sparse time-series datasets. These approaches have ranged from simple empirical averaging and interpolation to statistical modeling, and even neural networks. Yet, a lot of data mining techniques which are frequently used in other scientific and economic fields for missing time-series estimation have not been widely applied in hydrological sciences. Hence, the fourth part of this study aims at evaluating data mining techniques such as nearest-neighbor methods and decision trees to predict missing NO_3-N concentrations for two extensively monitored watersheds in the Lake Erie basin. The streamflow and time of the year (Julian day) were the only parameters used to predict missing concentrations after calibrating the data mining models using cross validation and percentage split techniques. If effective, these data mining methods may help monitoring networks to estimate missing sediment and nutrient concentrations in sparse datasets for watersheds with limited or even no water quality monitoring altogether.

Even with the introduction of newer approaches in pollutant concentration and load estimation like data mining methods, typically the majority of pollutant concentration and load

estimation is still done using traditional empirical and statistical approaches. These approaches include the widely applied seven-parameter regression model (Cohn et al., 1992) and simple ratio and averaging estimators which have been tested and evaluated in numerous studies globally. Recently, these approaches have been modified and improved by various residual correction techniques (Aulenbach and Hooper, 2006; and Verma et al., 2012) and using weighted regressions (Hirsch et al., 2010). As these improved techniques have been fairly recent, they have not yet been applied and evaluated independently on newer datasets. Therefore, the fifth and final part of this study targets quantifying the variability in selection of these new improved techniques by calculating average annual nitrate concentrations, loads and their respective trends for the Lower Illinois River and its tributaries for an extensive monitoring period from 1975-2010.

References

Aulenbach, B. T. and R. P. Hooper. 2006. "The Composite Method: An Improved Method for Stream-Water Solute Load Estimation." *Hydrological Processes* 20 (14): 3029-3047.

Balter, M. 2013. "Archaeologists Say the 'Anthropocene' is here - but it Began Long Ago." *Science* 340 (6130): 261-262.

Brekke, L.D., J.E. Kiang, J.R.Olsen, R.S. Pulwarty, D.A. Raff, D.P. Turnipseed, R.S.Webb, and K.D.White. 2002. "Climate change and water resources management—A federal perspective." *U.S. Geological Survey Circular* 1331, 65 p.

Cohn, T. A., D. L. Caulder, E. J. Gilroy, L. D. Zynjuk, and R. M. Summers. 1992. "The Validity of a Simple Statistical Model for Estimating Fluvial Constituent Loads: An Empirical Study Involving Nutrient Loads Entering Chesapeake Bay." *Water Resources Research* 28 (9): 2353-2363.

Cooper, D. M. and C. D. Watts. 2002. "A Comparison of River Load Estimation Techniques: Application to Dissolved Organic Carbon." *Environmetrics* 13 (7): 733-750.

Jackson, R. B., S. R. Carpenter, C. N. Dahm, D. M. McKnight, R. J. Naiman, S. L. Postel, and S. W. Running. 2001. "Water in a Changing World." *Ecological Applications* 11 (4): 1027-1045.

Lewis, J. 1996. "Turbidity-Controlled Suspended Sediment Sampling for Runoff-Event Load Estimation." *Water Resources Research* 32 (7): 2299-2310.

Markus, M. and M. Demissie. 2006. "Predictability of Annual Sediment Loads Based on Flood Events." *Journal of Hydrologic Engineering* 11 (4): 354-361.

Meybeck, M. and R. Helmer. 1989. "The Quality of Rivers: From Pristine Stage to Global Pollution." *Palaeogeography, Palaeoclimatology, Palaeoecology* 75 (4): 283-309.

Postel, S. 2013. "Water – and Us – in the "Anthropocene"." *National Geographic Freshwater Initiative in Water Currents*

Preston, S. D., V. J. Bierman Jr, and S. E. Silliman. 1989. "An Evaluation of Methods for the Estimation of Tributary Mass Loads." *Water Resources Research* 25 (6): 1379-1389.

Richards, R. P. and Holloway J. 1987. "Monte Carlo Studies of Sampling Strategies for Estimating Tributary Loads." *Water Resources Research,* 23 (10): 1939-1948.

Robertson, D. M. and E. D. Roerish. 1999. "Influence of various Water Quality Sampling Strategies on Load Estimates for Small Streams." *Water Resources Research* 35 (12): 3747-3759.

Royer, T. V., M. B. David, and L. E. Gentry. 2006. "Timing of Riverine Export of Nitrate and Phosphorus from Agricultural Watersheds in Illinois: Implications for Reducing Nutrient Loading to the Mississippi River." *Environmental Science and Technology* 40 (13): 4126-4131

Salles, C., M. G. Tournoud, and Y. Chu. 2008. "Estimating Nutrient and Sediment Flood Loads in a Small Mediterranean River." *Hydrological Processes* 22 (2): 242-253.

Verma, S., M. Markus, and R. A. Cooke. 2012. "Development of Error Correction Techniques for Nitrate-N Load Estimation Methods." *Journal of Hydrology* 432-433: 12-25.

Yaksich, S. M. and F. H. Verhoff. 1983. "Sampling Strategy for River Pollutant Transport." *Journal of Environmental Engineering* 109 (1): 219-231.

CHAPTER 2

Objectives

The overall aim of this study is to improve the understanding of anthropogenic and natural impacts on the climate-watershed-stream-lake processes in the hydrologic cycle, primarily focusing on export of pollutants (agricultural nutrients and sediment) from large Midwestern watersheds. Specific objectives of this study are summarized as follows:

(i) Characterize statistical relationships between large load events and total annual pollutant loads (Chapter 3)

(ii) Analyze spatio-temporal patterns of pollutant export (Chapter 4)

(iii) Quantify the impacts of projected future climate change on hydrology and pollutant export using physically-based hydrologic modeling (Chapter 5)

(iv) Apply new data mining methods in hydrology to predict nutrient loads (Chapter 6)

(v) Evaluate modified and improved statistical approaches to estimate nutrient concentrations, loads and corresponding trends (Chapter 7)

CHAPTER 3

Annual riverine pollutant load export in Midwestern watersheds: The role of large load events [1]

Abstract

Accurately estimating riverine pollutant loads is a key challenge for hydrologists and water resource managers around the world. Limited financial and manpower resources, along with the ever increasing demand for monitoring new watersheds, require the development of efficient approaches to accurately estimate riverine pollutant loads. In this research, the authors assess the role of a few large load events in a year which export a majority of annual riverine pollutant loads. Regression relationships were developed between total annual loads and loads exported by a few of the largest load events in a year for Nitrate plus Nitrite Nitrogen (NO_2-N+NO_3-N, [1]indicated as N), Total Phosphorus (TP), and Suspended Solids (SS) for eight watersheds in the Lake Erie and Ohio River basins. These regression relationships for various spatial scales were evaluated by comparing estimated annual loads (based on a few large load events) with observed (monitored) annual loads. The median prediction errors for annual N, TP, and SS loads from the top 5 load events for a spatial aggregation of all agricultural watersheds were 10.5%, 10%, and 12.5%, respectively. To test if these regression lines could be transferred to different watersheds in the region, they were applied to predict annual N loads for two agricultural watersheds in Illinois, producing an average median error of approximately 8%. The regional application of these regression relationships did not result in any loss of predictive accuracy, suggesting that the relationships between annual loads and large load events are regionally transferable. Therefore, these regression relationships can potentially be used for estimating riverine pollutant loads for similar watersheds within the same geographical region where large load events have been monitored. Additionally, as most of these large load events are concurrent with large flow peaks annually, they can be forecasted with reasonable accuracy and would lead to more efficient monitoring with a focus on a few largest load events.

Keywords: Nitrate, phosphorus, sediment, monitoring, loads, storm

[1]This chapter is part of a manuscript, Verma et al., 2013, currently in review in the *Journal of Hydrology*

3.1 Introduction

Increased pollutant loading from non-point sources around the world has been one of the foremost factors in degrading water quality in receiving streams, rivers, lakes, and estuaries (Howarth, 1998; Kronvang et al., 2005). In the US, increased pollutant loading, specifically nitrogen and phosphorus from the intensively cropped and tile-drained Midwestern watersheds, has been a major cause of severe ecological damage in the Gulf of Mexico (Goolsby et al., 2001; Rabalais et al., 2002) and Great Lakes (Smith et al., 2008). The adverse effects of increased pollutant loading range from eutrophication, hypoxia, and consequently reduced biodiversity, to human health issues such as methemoglobinemia (Camargo and Alonso, 2006).

Among the Great Lakes, the central basin of Lake Erie has been the most adversely affected by seasonal eutrophication and hypoxic conditions over the past few decades. Nutrient abatement programs (mainly phosphorus) were successfully implemented by the Great Lakes Water Quality Agreement signed between the US and Canada in 1972. This led to a continuous decline in phosphorus export from the Lake Erie basin, thereby reducing the extent of hypoxic zones in the 1970s-1980s (DePinto et al., 1986; Rao et al., 2008). Changes in nutrient application, higher temperatures, and reduced water levels during the 1990s potentially led to a reemergence of hypoxic zones in the lake. In 2005, a 10,000-square kilometer hypoxic region was reported in Lake Erie, which was one of the largest over the previous few decades (Hawley et al., 2006).

Hypoxic conditions in lakes and estuaries attributed to pollutant (nitrates and phosphorus) delivery from agricultural watersheds make the export of pollutants from such watersheds a topic of great interest. It is essential to regularly monitor streams and rivers draining into these water bodies to estimate annual pollutant delivery rates. Furthermore, frequent long-term monitoring is essential to assess trends in pollutant loading over a period of a few decades, to evaluate the efficacy of best management practices and pollutant abatement programs, climate

change, urbanization, land-use change, and measure relative loading contributions of two streams to a receiving water body (Yaksich and Verhoff, 1983).

In quantifying annual loading estimates, water managers are usually concerned with improving estimation accuracies and minimizing uncertainties involved. However, resource constraints such as inadequate funding and limited manpower can impede the collection of a large number of samples (Yaksich and Verhoff, 1983). Over a period of past several decades, water quality sampling strategies have also changed, moving from traditional fixed-frequency water sampling (bi-weekly, monthly, quarterly) to mixed strategies such as fixed-frequency water sampling supplemented with some storm-based sampling to capture high flows (Robertson, 2003; Hirsch et al., 2010). These approaches are time and resource intensive, as it is essential to characterize all flow regimes and capture most of the high load periods throughout the year in order to avoid underestimation of annual pollutant loading values. There are a few less data- and resource-intensive empirical or statistically-based approaches such as the Universal Soil Loss Equation, USLE (NRCS, 1983), SPAtially Referenced Regression On Watershed attributes, SPARROW (Smith et al., 1997), GIS Pollutant Load, PLOAD (USEPA, 2001), or Spreadsheet Tool for Estimating Pollutant Loads, STEPL (USEPA, 2006), but these approaches lack a high temporal resolution in load estimation and only estimate long-term average loadings.

Alternatively, to minimize monitoring costs some research studies have evaluated different ways to estimate annual pollutant loadings, such as developing regression relationships between a few critical storm (high flow event) loads and annual loads. Richards and Holloway (1987), Preston et al. (1989), Lewis (1996), Robertson and Roerish (1999), Cooper and Watts (2002), Markus and Demissie (2006) and Salles et al. (2007) have reported that a few high flow periods carry significant amounts of sediment and nutrients exported over a year. Yaksich and Verhoff (1983) analyzed high flow events based on sampling strategies for watersheds in the Lake Erie

basin and recommended intensively sampling two to three largest storm events in a year to get annual suspended solids, soluble orthophosphorus, and total phosphorus loading estimates with small errors. Since water quality monitoring strategies have been shifting over the past few decades and water quality managers are still searching for the most cost effective monitoring plans, a statistical approach based on large load events has the potential to estimate annual pollutant loadings with a reduction in fixed-frequency sampling, thereby reducing annual monitoring costs.

This study utilized a multiyear daily time series of water quality data from ten watersheds in northern and central Ohio, southeastern Michigan, northeastern Indiana, and central Illinois. Six watersheds are in the Lake Erie basin and two drain southwards into the Ohio River. In this study, these eight watersheds are referred to as the Ohio watersheds. The remaining two watersheds drain westwards into the Mississippi River (referred to as the Illinois watersheds). Agriculture was the predominant land-use in these watersheds with a few having significant areas of wooded forests and urbanization. A novel approach to identify and separate high flow events based on pollutant loading was developed by comparing the local-minimum and recursive digital base-flow filters from the WHAT base-flow separation tool (Kyoung et al., 2005). Regression relationships were developed between total pollutant loads exported by the few largest load events and total annual pollutant loads. Analysis of covariance (ANCOVA) was used to evaluate the statistical similarity of developed regression lines by comparing regressions for different watersheds for a particular pollutant. In summary, the main objectives of this study were to (i) assess the role of a few large load events on annual pollutant loads using regression relationships, (ii) test the statistical similarity between these regression relationships developed for different watersheds in close proximity (the Ohio watersheds), and (iii) test the applicability of developed regression relationships for watersheds in the same geographical region with a similar land-use (the Illinois watersheds).

3.2 Material and Methods

3.2.1 Watershed descriptions

Six of the watersheds analyzed in this study, namely, Cuyahoga, Grand, Maumee, Raisin, Sandusky and Vermilion, drain into Lake Erie. Two watersheds, Great Miami and Muskingum, drain southwards into the Ohio River basin and two watersheds in Illinois, Vermilion and Upper Sangamon, drain into the Upper Mississippi River basin (Figure 3.1). A majority of these watersheds primarily have an agricultural land use, except for Cuyahoga, which is about 47% urbanized and Grand, which is about 52% forested (Table 3.1). Most of the land classified as agriculture in these watersheds is row-crop agriculture with rotational schedules composed mostly of corn, soybean, and wheat crops. The most common soils in the Sandusky, the northern reaches of Maumee, and Raisin watersheds were formed in lake and beach sediments and glacial till associated with the glacial lakes. These soils are characterized by clayey topsoils with 3% or greater organic matter content in the upper 25 cm of the soil profile (ODNR Division of Soil and Water Resources-Soil Regions). The central part of Maumee, most of Great Miami, and the southern part of Sandusky watersheds are characterized by coarse-textured soils formed by glacial deposits. These soils are better drained than soils formed by lake and beach sediments but are relatively older and thereby more weathered and less fertile for agricultural production. The Muskingum watershed is characterized by clayey soils with high slopes and little organic matter content. These soils are well drained and have heavily wooded areas. The soils in the Grand and Cuyahoga watersheds were also formed by glacial deposits and range from coarse to fine-textured with better drained soils seen in the southern parts of these watersheds. Most of the land in the northwest part of Ohio, eastern Indiana, and Southern Michigan is characterized by low slopes and fertile but poorly drained soils; therefore large parts are artificially drained using sub-surface tile drain systems. The Vermilion and the Upper Sangamon watersheds in Illinois are characterized by highly fertile but poorly drained prairie soils formed by the loamy

glacial drifts. These Illinois watersheds are also extensively drained using subsurface drainage systems. Muskingum is the largest watershed analyzed in this study with a drainage area of about 19,200 square kilometers upstream of the sampling station sampling gage. Among the watersheds draining into the Lake Erie basin, Maumee is the largest with about 16,400 square kilometers of watershed area upstream of the sampling station. Vermilion is the smallest watershed analyzed in this study with a drainage area of about 700 square kilometers. Cuyahoga and Grand watersheds experience slightly higher annual precipitations compared to the western watersheds which is attributed to more lake-effect precipitation (Bosch et al., 2011).

Table 3.1: Characteristics of studied watersheds for modeled areas upstream of the USGS gaging station (*Land-use data for Cuyahoga, Grand, Maumee, Raisin, and Sandusky as reported by Bosch et al., 2011)

	USGS Station Number	Monitoring Period	Watershed size (km^2)	Land-use (%)*		
				Agriculture	Urban	Wooded
OHIO WATERSHEDS						
Lake Erie basin						
Cuyahoga	04208000	1982-2009	1,843	17	47	35
Grand	04212100	1989-2006	1,758	37	10	52
Maumee	04193500	1975-2009	16,427	81	11	8
Raisin	04176500	1982-2007	2,755	72	11	16
Sandusky	04198000	1975-2005	3,285	83	9	8
Vermilion	04199500	2001-2008	697	71	1	26
Ohio River basin						
Great Miami	03271601	1996-2009	6,953	82	5	10
Muskingum	03150000	1995-2009	19,208	52	2	43
ILLINOIS WATERSHEDS						
Upper Mississippi River basin						
Upper Sangamon	05572000	1993-1999	1,406	90	5	1
Vermilion, IL	05554500	1988-1999	1,492	95	3	2

3.2.2 Data descriptions and selection

The Water Quality Lab (WQL) at the National Center for Water Quality Research at Heidelberg College intensively sampled the Ohio watersheds for monitoring periods ranging from 8 to 32 years for different watersheds. This sampling program was designed to characterize annual pollutant loads, thus daily samples were collected during low flows with additional samples collected during storm events. The sampling stations were coupled with existing United

States Geological Survey (USGS) gaging stations. Simple grab samples using an auto-sampler were collected at the sampling stations as opposed to depth and width-integrated samples, but were comparable as stations were located in regions where water was well mixed (Richards et al., 2001). In-depth details about the sampling program and chemical analysis are described in Baker (1985), Richards and Baker (1993), and Richards et al. (2001). Three pollutants, Suspended Solids (SS), Total Phosphorus as P (TP), and Nitrate plus Nitrite Nitrogen (NO_2-N+NO_3-N, indicated as N from here on), were analyzed in this study.

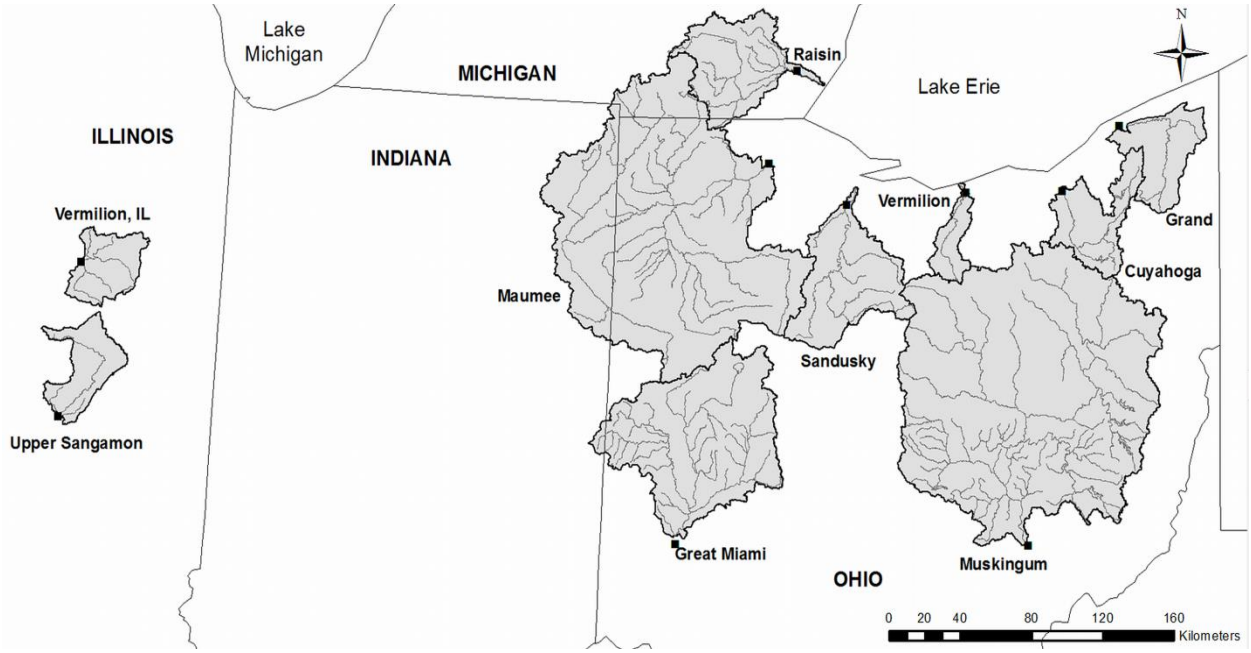

Figure 3.1: Locations of watersheds and gaging stations. The Cuyahoga, Grand, Maumee, Raisin, Sandusky, and Vermilion watersheds drain into western and central Lake Erie while Great Miami and Muskingum watersheds drain into the Ohio River basin. The Vermilion, IL and Upper Sangamon watersheds drain west into the Upper Mississippi River basin.

The WQL datasets reported laboratory-analyzed pollutant concentrations along with the corresponding 15-minute flow measurements at the sampling stations from the USGS gage. Yaksich and Verhoff (1983) reported that if water quality measurements are not made during high flow events, the annual pollutant loads can be underestimated significantly. As one of the primary objectives of this study was to assess the role of large load events on annual loads, data

preprocessing was conducted to eliminate water years with considerable missing concentration and flow data. Missing flow volumes attributed to a lack of sampling coverage in a water year were computed by comparing the water year flow volumes from WQL datasets and water year flow volumes from daily flows reported by the USGS. For example, Figure 3.2 shows hydrographs from the Sandusky watershed for water years 1988 and 1989. In this figure, the continuous curve indicates the mean daily flows which are derived from the 15-minute measurements as reported by the USGS. The points on the figure indicate the 15-minute flows from the USGS gages as reported by the WQL datasets which correspond to the time of water sample collection for pollutant concentration analysis. In the water year 1988, the WQL did not report any pollutant concentrations till late January and therefore it was excluded from this study to avoid underestimation of total annual pollutant loads and probable overestimation of the contributions of high flow loads to annual loads. On the other hand, the water year 1989 was included in the study as the WQL covered the whole year with consistent daily sampling coupled with multiple samples during high flow events.

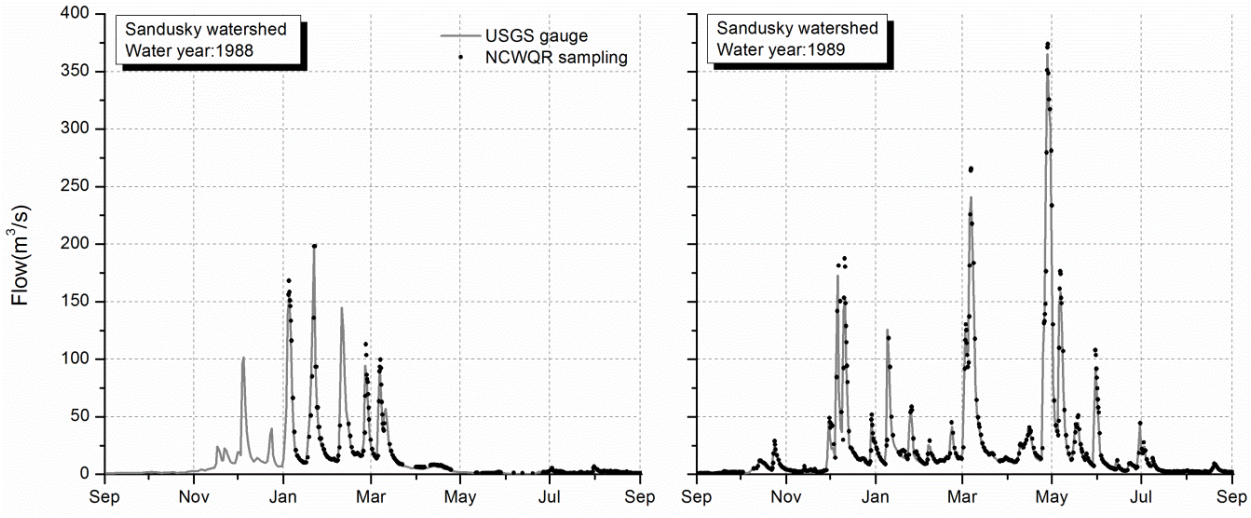

Figure 3.2: Hydrographs from the Sandusky watershed for water years 1988 and 1989 showing the example years excluded (1988) and included (1989) from this study based on completeness of flow measurement sampling conducted by the National Center for Water Quality Research, Heidelberg College and USGS gaging stations.

3.2.3 High flow event separation

To assess the role of large load events on annual pollutant loads, it is essential to identify and separate high flow events in a water year as most of the loads are exported during high flows. The watersheds analyzed in this study were fairly large, and thus identifying the beginning of high flow events isn't very complicated as a precipitation event is usually followed by a steep rise in the hydrograph. Identifying the exact end of a high flow event is more complicated in these watersheds as the receding limb of the hydrograph was generally more gradual. Additionally, after a high flow event, the flow stabilized at a higher value as compared to the beginning of the event. There was some overlapping of closely occurring events with two or more hydrograph peaks separated by a flow value that was lower than peak flows but could not be considered low flow. Similar to Richards et al. (2001), snowmelt-driven events were treated similarly to precipitation events as flow volumes for both kinds of events were similar.

In this study, a novel approach to identify high flow events was developed and tested. This approach used two base-flow separation filters from the Web-based Hydrograph Analysis Tool (WHAT) (Kyoung et al., 2005) and compared them to identify the beginning and end of high flow events. The results of using a local minimum filter, which linearly connects local minima to separate out the base-flow from a hydrograph, were compared with results from a recursive digital filter, which separates base-flow and direct runoff similarly to separating high frequency and low frequency signals in signal processing. To minimize the subjective influence of different Baseflow Index (BFI_{max}, ratio of base-flow to total flow) values on the performance of the recursive digital filter, a BFI_{max}=0.80 for perennial streams with porous aquifers was selected as recommend by Kyoung et al., (2005). The points of intersection of base-flow curves from both these filters defined the beginning and end of a high flow event (Figure 3.3).

The high flow event begins where flow starts to increase above the base-flow, i.e., when the first non-zero value is encountered for direct runoff. Since, the last non-zero value appeared on

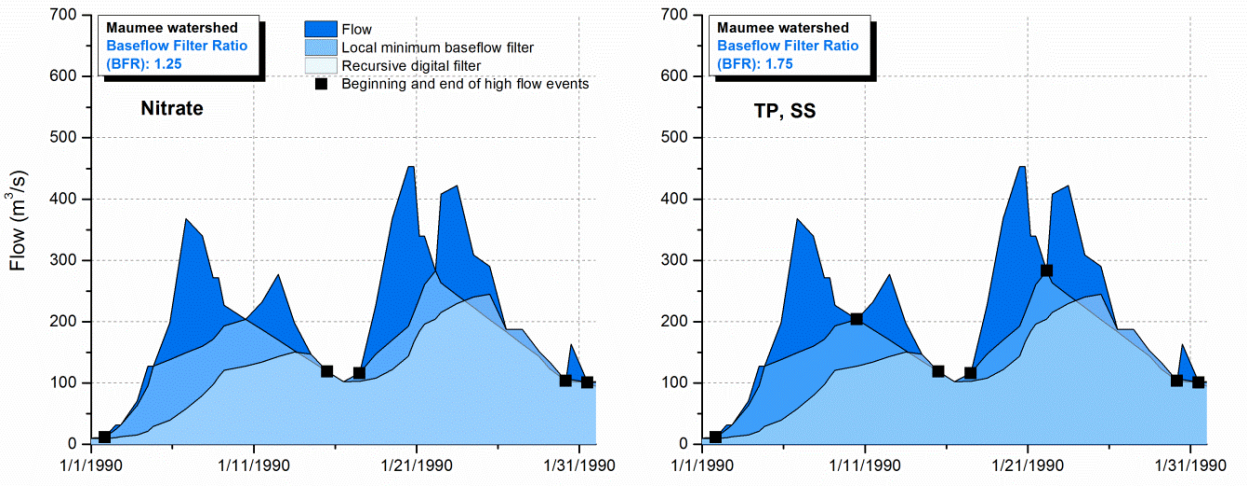

Figure 3.3: Example of different high flow event separations based on the Base-flow Filter Ratio (BFR) for a typical high flow period for the Maumee watershed, resulting in different numbers of high flow events

the receding limb of the hydrograph, the end point was selected as the first local minimum encountered after the last non-zero value for direct runoff. Markus and Demissie (2006) reported that in loading analysis, the uncertainty in identification of the beginning and end of high flow events results in insignificant errors due to negligible loads exported during low flows. Similarly, in this study small errors in identifying the correct endings of high flow events were neglected.

In the watersheds analyzed in this study, the SS concentration peaks coincided or just preceded the hydrograph peaks as SS is generally transported through overland surface flow. The pollutograph for SS indicated a much steeper rise in concentration compared to the hydrograph (Figure 3.4). Similarly, TP is also exported through overland flow (Royer et al., 2006; Richards et al., 2001), and its concentration peaks also closely align with hydrograph peaks as TP is generally bound to sediment particles. It was observed that N concentrations decreased as hydrographs reached their peak values; mainly due to dilution as most of the large stream flow increases were caused by surface flow. Later, when the surface flow contribution to stream flow decreased, N concentrations increased and reached their peaks later than the hydrograph peaks as N is exported mainly through subsurface flow (Richards et al., 2001;

Schilling and Zhang, 2004; Royer et al., 2006; Zhang et al., 2010; and Zhu et al., 2011), which is slower than surface flow export. Also, during a few large precipitation events the subsurface tile drain outlets might get submerged, backing up the tile, which eventually starts flowing once the water levels in drainage ditches subside, further delaying the N concentration peaks.

Given the mechanistic differences in export of SS, TP, and N from watersheds and the criticality of high flow event loads, hydrographs were separated differently for different pollutants. Additionally, as this research is based on loads exported during high flow events, it was essential to accurately separate pollutographs to identify periods of high load export. This was done using a new index called the Base-flow Filter Ratio (BFR), which for any local minima was defined as the ratio of local minimum filter base-flow value and digital recursive filter base-flow value. As the intersection of both base-flow filter curves identified the beginning and ending of high flow events, the BFR was used to further split these events into smaller individual events based on pollutants being evaluated. If the BFR exceeded a set threshold at any local minima point in an identified high flow event, the event was further split at that point into two smaller events. Setting a high threshold for the BFR split an identified high flow event with multiple peaks into smaller events, and conversely, setting a low BFR did not split the hydrograph with multiple peaks into smaller events.

For fast-response pollutants such as SS and TP, for which pollutographs closely follow or just precede hydrographs, a high BFR of 1.75 was used, which very closely identified individual high flow events as each peak in the hydrograph was separated and accounted as a different event. For slow-response pollutants such as N for which pollutographs recede more gradually than hydrographs and concentration peaks tends to lag hydrograph peaks, a lower BFR of 1.25 closely identified individual high flow events as events occurring very closely (two or more close peaks) were accounted as one to better characterize high flow event N loads. Figure 3.4 shows

the impact of BFRs in separating hydrographs into high flow events based on the pollutant being evaluated.

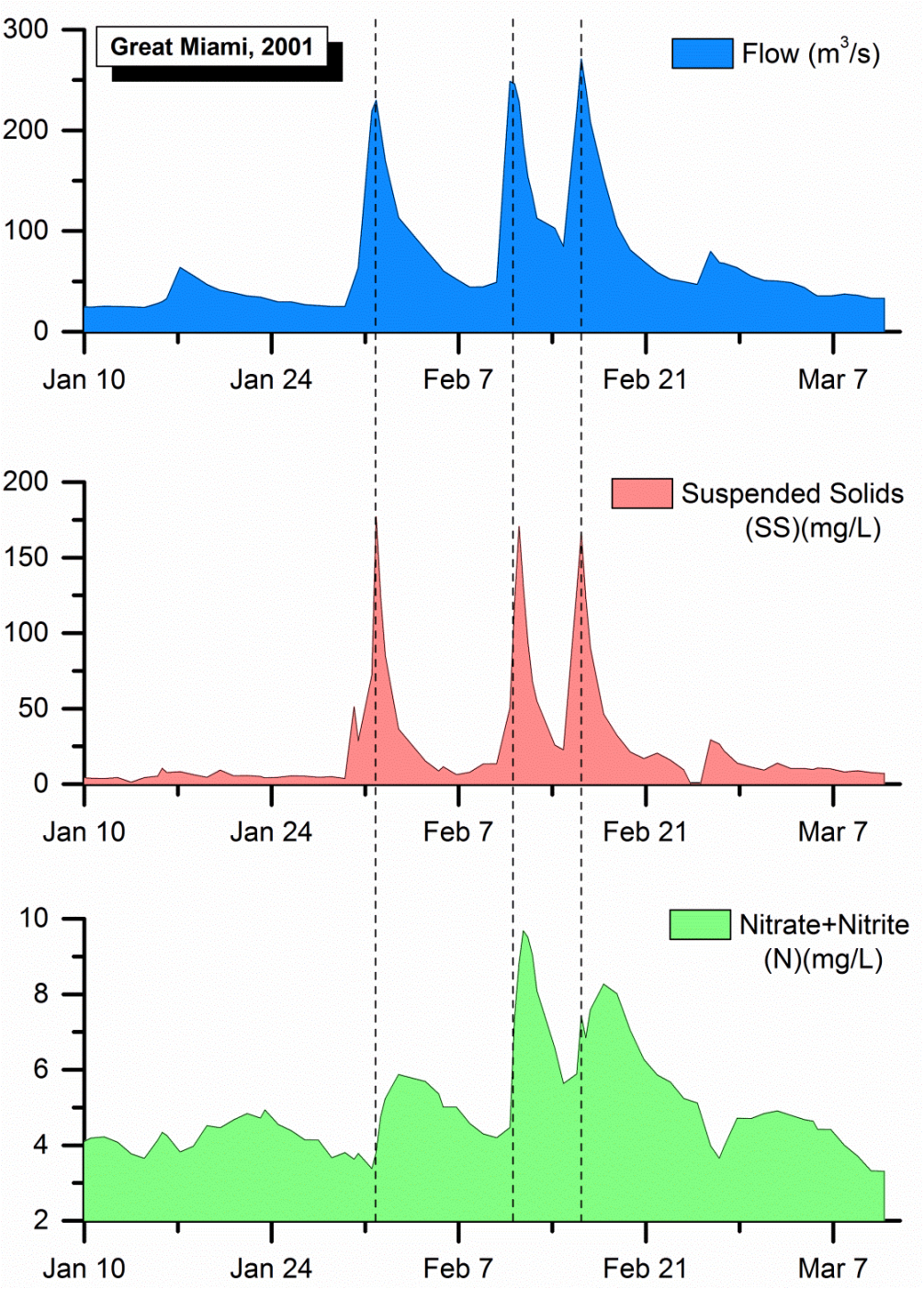

Figure 3.4: Typical hydrographs with Suspended Solids (SS) and Nitrate plus Nitrite Nitrogen (N) pollutographs for a high flow event in the Great Miami watershed. Total Phosphorus (TP) pollutographs were very similar to SS and therefore not included in this figure

3.2.4 High flow loads and annual loads

For all the water years included in this study for each of the eight watersheds, the WQL databases reported daily and high flow event pollutant concentrations and flow data. Given the high number of observations for each water year, annual water year loads were computed for SS, TP, and N using a simple numeric integration approach (El-Shaarawi et al., 1986; Preston et al., 1989; Richards et al., 2001; Guo et al., 2002, Aulenbach and Hooper, 2006; Toor et al., 2008; Verma et al., 2012). In cases where nearly continuous data are available, a numeric integration approach is the most desirable as it is free from statistical assumptions of normality and is simple to implement (Richards et al., 2001). Annual loads were computed as:

$$\text{Load} = \int C(t)Q(t)dt \tag{3.1}$$

where C is the pollutant concentration, Q is the flow, and *dt* is the duration represented by the sample. The duration associated with each sample collected comprised half the time between the preceding and current samples plus half the time between the current and following samples.

Similarly, pollutant loads were also computed for all high flow events separately for each water year and watershed. These high flow events for each pollutant, water year, and watershed were then ranked based on decreasing loads exported. From now on, these high flow events will be referred to as load events. Further analysis was performed to check whether top load events were also the events with the highest peak flows. This was done to establish if load events are a function of flows in these watersheds. Figure 3.5 shows the average percentage of common top events based on total loads exported and on peak flows for all the Ohio watersheds over their complete monitoring durations. The analysis was performed for both BFR values used in this study, viz., 1.25 for N and 1.75 for SS and TP. The size of the circles in Figure 3.5 is relatively proportional to the watershed sizes (not to scale), and the figure indicated that for most of the

agricultural watersheds roughly more than 75% of the top 5 load events were common with the top 5 events based on peak flows.

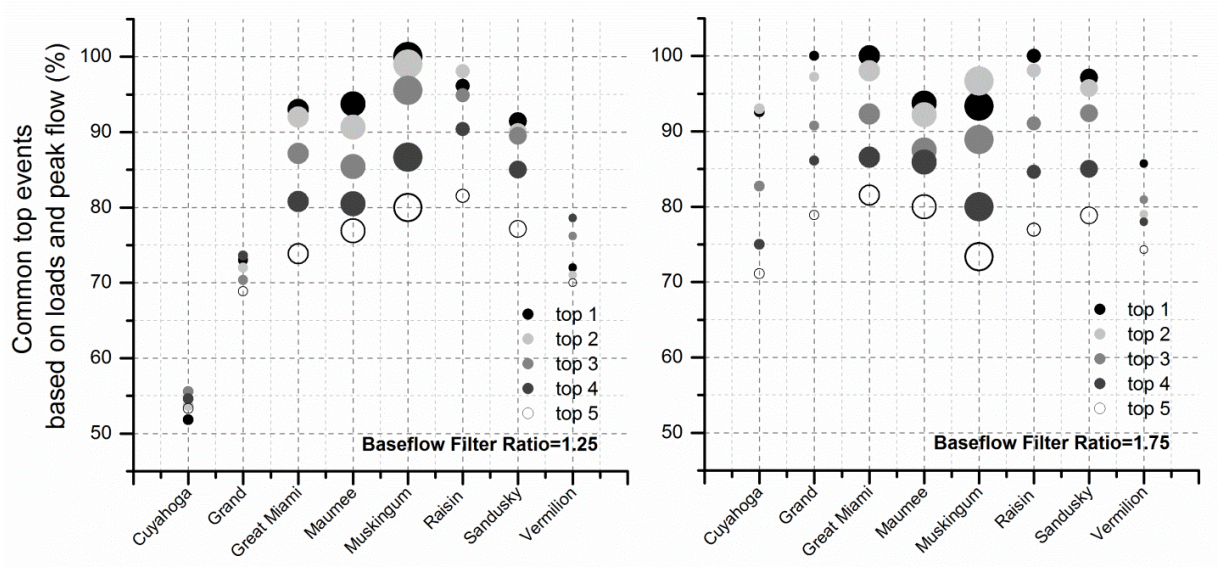

Figure 3.5: Percentage of common top events based on loads exported and peak flows for BFR=1.25 (N) and BFR=1.75 (SS, TP). For example, the hollow circle for the Muskingum watershed for the BFR=1.25 case shows that 80% of the top 5 events based on N loading and peak flows were common over the 15 years of monitoring. The size of points are based on relative watershed sizes (not to scale)

An analysis of top load event contributions to annual loads for all combinations of pollutants, water years, and watersheds indicated that the biggest 5 load events cumulatively carried a large percentage of the annual loads which declined rapidly after the top 6 to 7 events on average. Figure 3.6 shows the contribution of the top 25 load events to annual loads for a typical agricultural watershed, i.e., Maumee and an urbanized watershed, i.e., Cuyahoga. The average contribution of the top 5 load events to annual loads for all pollutants was substantial for Maumee and other agricultural watersheds. On the other hand, for the urbanized watershed Cuyahoga, the annual loads were more evenly distributed amongst the top 10 load events. Overall, the top 5 load events were chosen for predicting annual loads as for a majority of scenarios they carried a large percentage of annual loads. There were some scenarios where the contributions from the 6^{th}-10^{th} biggest events were substantial, but such cases were rare.

Therefore, the total cumulative loads exported by the top 1, 2, 3, 4, and 5 load-producing events each year were computed for all watersheds and pollutants.

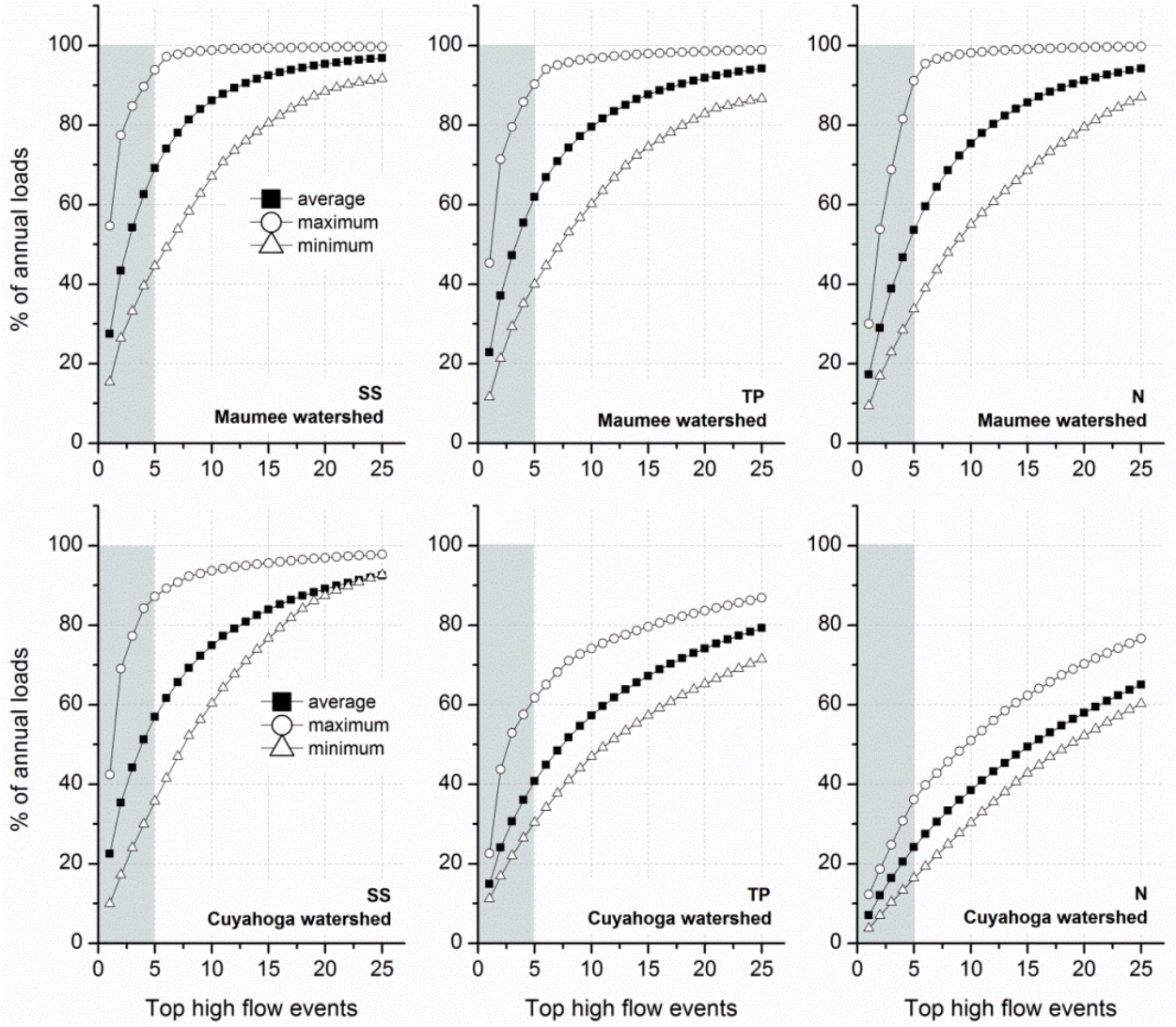

Figure 3.6: Contribution of top high flow events to annual SS, TP, and N loads for Maumee and Cuyahoga watersheds. The average of all years is indicated by the solid square symbols while the maximum and minimum contribution by top 5 events to annual loads are indicated by hollow circle and triangle symbols.

3.2.5 Regression relationships

Markus and Demissie (2006) reported that annual sediment loads and loads during the top high flow events based on peak flows have a high correlation, and thus annual loads can be

predicted based on flood event loads using regression relationships. In this study, such regression relationships were developed for annual SS, TP, and N loads and loads exported during the top 1, 2, 3, 4, and 5 load events. The following equation describe the relationship between annual loads and top load events:

$$\log(L_a) = a + b \log(L_{le}) \tag{3.2}$$

where L_a and L_{le} are pollutant loads exported annually during a water year and cumulatively during top load events in a year, respectively (le=1, 2, 3, 4, 5), and a and b are regression parameters. The annual and top load event loads were log-transformed to normalize residual variances and reduce the skewness towards extreme values (Troutman, 1985; Driver and Troutman, 1989; and Kocic et al., 2008).

Distinct regression relationships were developed for each combination of watershed and pollutant. Additionally, regression relationships were developed by spatially aggregating data for a given pollutant from all eight Ohio watersheds and similar watersheds for annual loads and the top 1,2,3,4, and 5 load events in a water year. This analysis could also have been performed using loads per unit area for different watersheds, but actual loads were selected to predict loads more directly, similar to Yaksich and Verhoff (1983), Demissie (1996), Öztürk et al., (2001) and Markus and Demissie (2006).

3.2.6 Analysis of covariance (ANCOVA)

To test the similarity between regression lines developed for a pollutant for different watersheds and also the spatially aggregated data, analysis of covariance (ANCOVA) was used (Snedecor and Cochran, 1980 pp 390-393; Markus and Demissie, 2006). The purpose was to examine whether linear regressions of annual pollutant loads and top load events for a watershed are the same as other watersheds or the same as the spatially aggregated data from all

watersheds. These regressions can differ in slope, intercept, and residual variances. ANCOVA was used to compare the following model:

$$Y_{i,j} = \alpha_i + \beta_i X_{i,j} + \varepsilon_{i,j} \quad (3.3)$$

where X=independent variable, high flow loads in this case; Y=dependent variable, annual load; *i*= watershed 1, watershed 2, all watersheds together; j=observations, pollutants being evaluated; α= intercept; β=slope; and ε=residuals.

This approach compares the slope, intercept, and residual variances for two regression equations based on a two-tail F test. If heterogeneous slopes, intercepts, or residual variances are found, then the regression lines are regarded as statistically different. The slope represents a rate of increase in annual loads based on top load events. For similar slopes, the intercept generally represents the overall magnitude of annual loads compared to top high flow event loads.

Regression relationships from watersheds having statistically similar regression slopes and intercepts can possibly be used interchangeably to predict annual loads based on top load events or combined to produce statistically stronger relationships. If the regression lines are similar, then regional water quality monitoring would likely be beneficial for new monitoring sites with limited data. Secondly, it also helps identify watersheds which have similar contributions of top load events to annual loads for a certain pollutant. This would aid in designing uniform sampling strategies for such watersheds and also identify representative watersheds for long-term continuous monitoring (Rozemeijer et al., 2010).

3.2.7 Evaluation of regression relationships (Illinois watersheds)

To evaluate the applicability of developed regression relationships to watersheds with limited water quality data, regression relationships from all Ohio watersheds (both Lake Erie and Ohio River basins) were used to estimate loads for the Upper Sangamon and Vermilion

watersheds in central Illinois. The Upper Sangamon and Vermilion watersheds drain an area of 3,161 km^2 and 3,424 km^2, respectively. These watersheds are predominantly agricultural with an extensive adoption of sub-surface drainage. Daily monitored flow and N concentration data were available for 6 years for the Upper Sangamon watershed and 11 years for the Vermilion watershed. High flow events were separated for each water year using the same method (described earlier) which was used for the watersheds from Ohio. The separated high flow events were ranked based on loads exported, and the cumulative loads exported in the top 5 load events were used as an input for regression relationships developed from Ohio watersheds to predict annual N loads.

3.2.8 Data Preprocessing

Data preprocessing was conducted to identify and remove water years with a significant portion of missing flow data and to keep only those years with more complete data. This was done to avoid underestimation of annual pollutant loads and possible incorrect estimation of the top load event. From exploratory runs it was found that years with more than 20% missing flow volume underestimated annual loads and generally missed sampling of one to two major load events. Thus, any water year in the database with more than 20% of flow data without water quality data was excluded from the analysis. Table 3.2 shows the percentage of missing flow volumes along with missing water quality data for each year, which were then used to identify years excluded from the analysis for Cuyahoga and Maumee watersheds. For a few years, the numerical integration of WQL flows reported higher annual flow volumes than that computed using average daily flows as reported by the USGS. This happened as WQL reported 15-minute flows corresponding to sample collection time-stamps, and as they intensively sampled high flow events, there were a few reported flows which were much higher than the average flow for that day. As the WQL sampling wasn't at uniform time intervals, numerical integration to compute daily flow volumes resulted in higher volumes than from USGS daily flows. As the

authors compared total annual flow volumes, higher volumes over a few days resulted in higher annual volumes overall. Such years are indicated by a negative missing flow volume in Table 3.2. The maximum number of years excluded was 6 from the 32-year monitoring record from the Sandusky watershed. Just 1 out of the 8 years of monitoring record was excluded for the Vermilion watershed (Table 3.3).

Table 3.2: Missing flow volumes and days in each water year for Cuyahoga and Maumee watersheds, based on flow measurements reported by National Center for Water Quality Research, Heidelberg College and USGS gaging stations. Years with more than 20% flow volume missing are highlighted and were excluded from this study.

Watershed	Cuyahoga		Maumee	
Year	Missing flow	Missing days	Missing flow	Missing days
1982	*21.2%*	19.3%	10.4%	13.3%
1983	5.0%	2.8%	-0.4%	0.0%
1984	4.3%	4.4%	-1.7%	0.5%
1985	5.5%	1.8%	0.8%	3.5%
1986	1.6%	1.9%	0.1%	2.2%
1987	1.8%	6.5%	1.7%	2.1%
1988	*24.3%*	23.6%	7.4%	4.5%
1989	13.4%	17.6%	0.8%	2.0%
1990	*36.1%*	40.1%	-0.2%	0.2%
1991	9.3%	10.9%	4.9%	4.6%
1992	*55.1%*	34.6%	*27.1%*	10.3%
1993	9.8%	8.0%	17.7%	12.1%
1994	8.5%	6.0%	8.2%	6.3%
1995	14.6%	10.6%	0.3%	5.6%
1996	15.6%	8.5%	7.8%	8.0%
1997	10.9%	12.8%	-4.6%	3.1%
1998	-0.7%	2.0%	-1.1%	0.3%
1999	1.2%	0.7%	-2.8%	0.6%
2000	7.1%	7.2%	0.5%	3.6%
2001	3.3%	3.1%	19.7%	8.6%
2002	9.2%	7.1%	17.3%	7.1%
2003	0.9%	8.1%	-10.0%	1.3%
2004	4.9%	10.4%	10.6%	13.9%
2005	*46.3%*	24.1%	*43.6%*	14.2%
2006	10.0%	7.1%	*23.2%*	14.9%
2007	-2.1%	2.7%	4.6%	2.6%
2008	4.5%	3.8%	-2.6%	1.3%
2009	8.3%	4.1%	-9.7%	4.5%

Table 3.3: Monitoring periods, years of record, and number of years included in this study for all watersheds

	Monitoring period	Years of record	Years selected in this study
Lake Erie basin			
Cuyahoga	1982-2009	28	24
Grand	1989-2006	18	13
Maumee	1975-2009	32	29
Raisin	1982-2007	26	23
Sandusky	1975-2005	31	25
Vermilion	2001-2008	8	7
Ohio River basin			
Great Miami	1996-2009	14	10
Muskingum	1995-2009	15	14

3.3 Results

3.3.1 Top five load events

Contributions of top load events towards annual loads and their durations were computed for three pollutants (Tables 3.4, 3.5). For N the average duration of the top load event ranged from about 14 days (4% of the number of days annually) to 26 days (7%) for Cuyahoga and Muskingum, respectively. On average, the minimum contribution of the top 1 load event was 7% of the annual N load for Cuyahoga, and the maximum contribution was about 23% for Raisin. The top 5 load events combined lasted for a minimum of 60 days (16%) for Maumee and a maximum of about 90 days (25%) for Sandusky carrying a minimum of 24% of annual N load for Cuyahoga and a maximum of 67% for Raisin. On average, the biggest jump between loads carried by top load events was found between the top 1 and top 2 events.

For TP, the average duration of the top 1 load event ranged from just 8 days (2%) for Grand to about 18 days (5%) for Muskingum, carrying a minimum of 15% of annual TP load for Cuyahoga and a maximum of 28% for Sandusky. The top 5 load events carried a minimum of about 41% and a maximum of about 71% of the annual TP load for Cuyahoga and Sandusky,

respectively, jointly lasting for a minimum of 36 days (10%) for Cuyahoga and a maximum of 76 days (21%) for Sandusky.

As expected, results were very similar for SS loads, with the top 1 load event lasting from 8 days (2%) to 19 days (5%) for Cuyahoga and Muskingum, respectively, carrying a minimum of 22% of annual SS load for Cuyahoga and a maximum of 31% for Sandusky. The top 5 load events carried a minimum of about 57% and a maximum of about 75% of annual SS load for Cuyahoga and Sandusky respectively, jointly lasting for a minimum of 34 days (9%) for Cuyahoga and a maximum of 72 days (20%) for Sandusky.

Among the three pollutants analyzed, the least variance for the loads contributed by the top 1 to 5 load events was observed for N, followed by TP and SS. Among the watersheds, for N, Cuyahoga had the smallest variance while Sandusky and Vermilion had the largest variance in top load events. For TP and SS, Great Miami had the least variance while Maumee and Vermilion had the greatest variance in contributions of top 1 to 5 load events towards annual loads.

Table 3.4: Average contribution percentages (%) and standard deviations (SD) for annual Nitrate plus Nitrite Nitrogen (N), Total Phosphorus (TP) and Suspended Solids (SS) loads from top load events per water year.

Contribution to annual loads (%)	Top load events	Cuyahoga		Grand		Great Miami		Maumee		Muskingum		Raisin		Sandusky		Vermilion	
		%	SD	%	SD	%	SD	%	SD	%	SD	%	SD	%	SD	%	SD
Nitrate+ Nitrite Nitrogen (N)	1	7	2	21	10	16	6	16	6	19	5	23	8	20	7	18	9
	2	12	3	33	11	25	6	27	7	32	7	38	9	36	11	30	11
	3	16	4	42	11	33	7	37	8	42	8	50	10	48	13	39	13
	4	20	4	49	11	40	7	44	9	50	7	60	10	57	13	46	13
	5	24	5	55	11	46	7	51	9	57	7	67	9	64	13	52	13
Total Phosphorus (TP)	1	15	6	23	7	16	4	21	9	18	6	26	10	28	11	22	10
	2	24	8	36	8	26	4	35	12	30	7	41	12	44	14	36	14
	3	31	8	46	9	34	4	45	13	39	7	52	12	56	14	45	14
	4	36	8	54	9	41	5	53	13	46	7	60	11	64	13	53	13
	5	41	8	61	10	47	5	60	12	52	7	66	10	71	12	60	13
Suspended Solids (SS)	1	22	10	31	10	23	6	26	13	23	7	27	11	31	10	25	09
	2	35	12	47	11	36	7	41	14	38	7	42	12	48	12	42	17
	3	44	12	59	11	46	7	51	14	50	7	54	13	60	13	54	17
	4	51	12	67	10	54	7	60	14	57	7	63	13	68	12	63	14
	5	57	11	72	9	61	7	67	13	64	7	69	11	75	11	71	12

Table 3.5: Average yearly durations (%) and standard deviations (SD) for annual Nitrate plus Nitrite Nitrogen (N), Total Phosphorus (TP) and Suspended Solids (SS) top load events.

Duration of high flow periods per water year (%)	Top load events	Cuyahoga		Grand		Great Miami		Maumee		Muskingum		Raisin		Sandusky		Vermilion	
		%	SD	%	SD	%	SD	%	SD	%	SD	%	SD	%	SD	%	SD
Nitrate+ Nitrite Nitrogen (N)	1	4	1	6	5	4	2	4	1	7	3	5	2	6	4	4	1
	2	7	2	10	7	7	4	8	3	12	4	10	3	11	8	6	2
	3	10	5	14	9	10	5	11	4	16	5	15	5	17	12	8	4
	4	14	7	16	10	14	6	14	5	21	7	19	7	21	15	10	5
	5	17	9	19	12	16	7	16	7	25	8	23	8	25	18	13	6
Total Phosphorus (TP)	1	2	2	2	1	3	2	3	1	5	2	4	1	4	4	2	1
	2	4	3	6	3	7	5	7	3	9	4	9	3	9	6	4	1
	3	6	4	9	5	11	7	10	4	12	5	12	4	13	10	7	3
	4	8	5	11	5	13	9	12	5	15	6	15	5	17	13	9	4
	5	10	6	14	7	15	10	14	6	18	8	19	8	21	17	11	6
Suspended Solids (SS)	1	2	1	2	1	3	1	3	1	5	2	4	2	5	4	2	1
	2	4	3	5	3	5	3	7	3	9	4	8	3	9	7	5	3
	3	6	4	8	4	7	4	9	4	11	5	12	5	13	10	6	4
	4	8	5	10	6	9	5	12	5	14	6	15	6	16	13	8	4
	5	9	6	13	7	12	8	14	6	17	7	19	8	20	16	10	5

3.3.2 Regression lines

For all the watersheds studied, Figure 3.7 shows the total annual N loads plotted against the loads contributed by the top 5 load events. Part (a) shows the individual regression lines for each watershed while Part (b) shows spatially aggregated regression lines for the top 1 and top 5 load events. It is clearly evident from Part (a) that for N, Cuyahoga follows a distinctly different relationship as compared to the other watersheds. Regression lines from the other watersheds align closely to one another having visibly similar slopes and having large differences in the amounts of total annual N loads and top 5 load event contributions. Regression lines for contributions of top 2, 3, and 4 load events towards annual loads were also developed similar to top 1 and top 5 lines, as shown in Part (b), but were omitted from the figure for better representation. Two regression lines were created for the contributions of top 5 load events, with and without including data from Cuyahoga. A high correlation with an adjusted R^2 of 0.937 was observed for loads during the top 5 load events and total annual load for spatially aggregated data from all watersheds including Cuyahoga (Table 3.6).

Similarly, Figures 3.8 and 3.9 show the regression lines developed for TP and SS export from these watersheds. In case of TP export, individual regression lines from all watersheds lie in the same region, with potential differences in slopes and intercepts. Unlike N, TP export from Cuyahoga is more closely aligned with export from other watersheds. Watershed scale phosphorus management changes coupled with phosphorus abatement programs implemented in these watersheds over the 1970s and 1980s potentially caused an additional variation in TP export over the years. For spatially aggregated regression lines, the adjusted R^2 for loads exported during top load events and total annual TP loads was high, increasing from 0.88 to 0.95 for the top 1 and top 5 load events, respectively. For SS export, individual regression lines are shown in Figure 3.9 (a). These regression lines were visibly the most similar among all the three monitored pollutants, with most lines being indistinguishable from one another. As SS export from these watersheds was largely unaffected by land management and nutrient abatement programs, consistent patterns were observed for SS export during top load events. For spatially aggregated regression lines, high adjusted R^2 increasing from 0.89 to 0.97 was observed to annual SS load contributions from the top 1 and top 5 load events (Table 3.6). These adjusted R^2 for spatially aggregated regression lines were the highest among the three monitored pollutants.

3.3.3 ANCOVA

ANCOVA was used to compare linear regression lines developed for total annual load estimates using loads exported during the top 1 to 5 load events for all eight watersheds in the Lake Erie and Ohio River basins (Ohio watersheds) and three monitored pollutants. Further, for each pollutant, these individual watershed-specific regression lines were compared with a spatially aggregated regional regression line for similarity. ANCOVA analysis was performed to gauge a statistical similarity between linear regression slopes, intercepts, and residual variances at $\alpha=0.05$ and $\alpha=0.01$ levels of significance. The results from the ANCOVA analysis are shown in

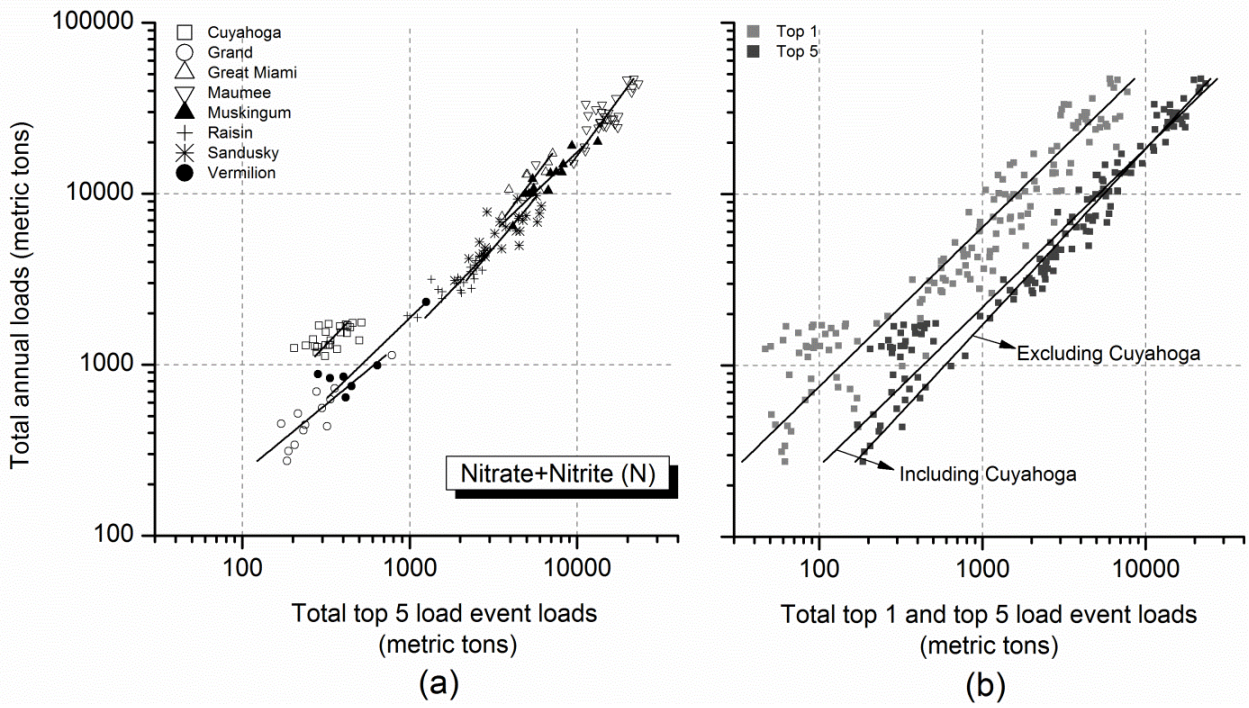

Figure 3.7: Regression relationships for total annual and top event Nitrate plus Nitrite Nitrogen (N) loads on an individual watershed (a) and spatially aggregated regional scale (b). Most watersheds in the study are predominantly agricultural, unlike the mostly urbanized Cuyahoga River watershed.

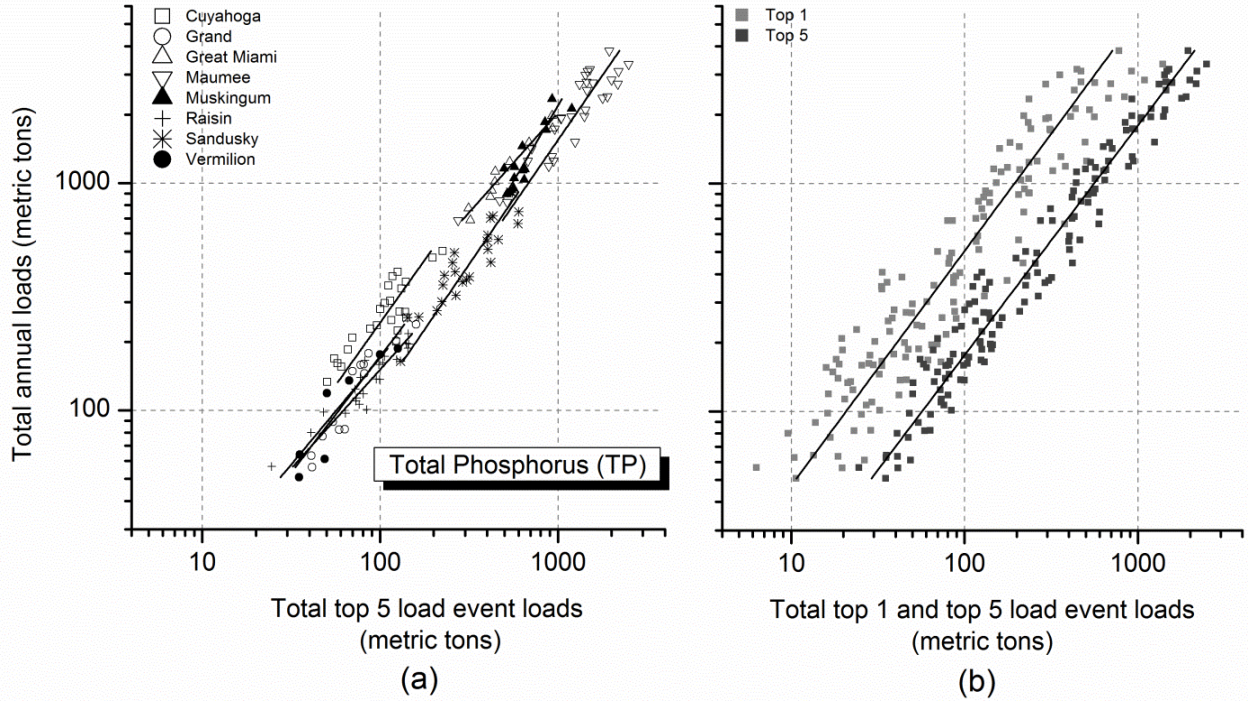

Figure 3.8: Regression relationships for total annual and top event Total Phosphorus (TP) loads on an individual watershed (a) and spatially aggregated regional scale (b).

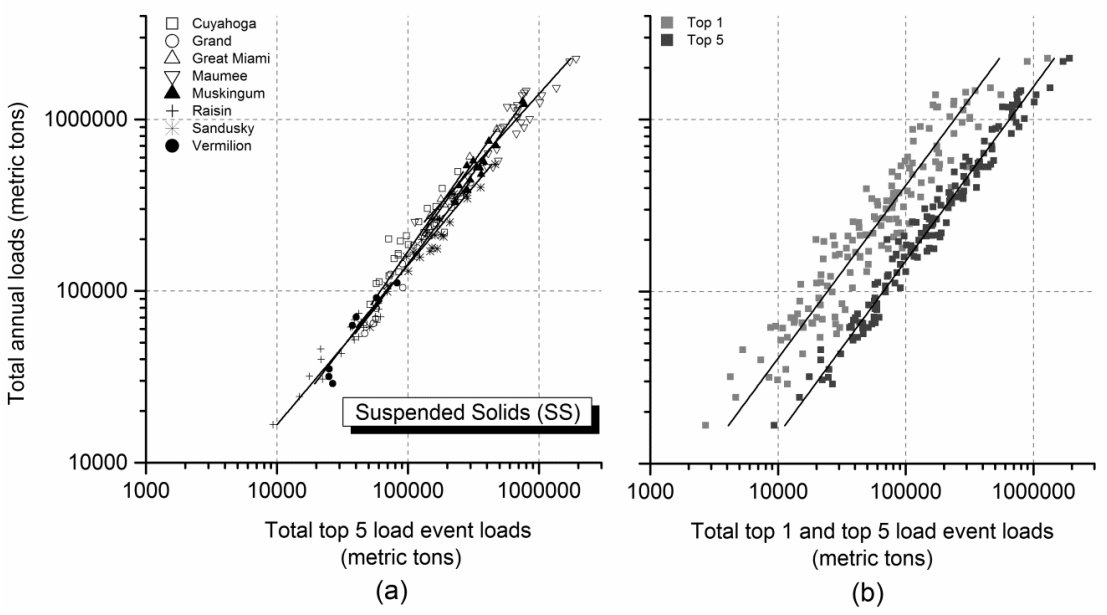

Figure 3.9: Regression relationships for total annual and top event Suspended Solids (SS) loads on an individual watershed (a) and spatially aggregated regional scale (b).

Table 3.6: Correlation coefficient for annual and top 1 to 5 Nitrate plus Nitrite Nitrogen (N), Total Phosphorus (TP) and Suspended Solids (SS) load events for spatially aggregated data from all watersheds

High flow event by loads	Top 1	Top 2	Top 3	Top 4	Top 5
Constituent	Adjusted R2 (all watersheds together)				
(Nitrate + Nitrite)-N (N)	0.89	0.91	0.92	0.93	0.94
Total Phosphorus (TP)	0.88	0.92	0.93	0.94	0.95
Suspended Solids (SS)	0.89	0.93	0.95	0.96	0.97

Tables 3.7, 3.8, and 3.9 for N, TP, and SS, respectively. R, S, and I indicate residual variances, slope, and intercept, respectively. Significant differences at both α=0.05 and α=0.01 are indicated by a "2" value in the tables, while differences significant at α=0.05 and insignificant at α=0.01 are indicated by a "1" value in the tables. A "0" value indicated that differences between two regression lines were insignificant for that particular case. Watershed names indicate watershed-specific regression lines while "all watersheds together" indicates spatially aggregated data from all the watersheds. A comparison of watershed A to watershed B would be similar to a comparison of watershed B to watershed A for slope and intercept differences, while it would be different for comparing residual variances. This difference arises as the slope and intercept comparisons between two regression lines are done on pooled data (which would be similar in

both cases), while residual variance comparisons are done using individual data and their associated degrees of freedom (Snedecor and Cochran, 1980 pp. 392).

Table 3.7 summarizes results for N. As was clearly evident from Figure 3.6, regression lines for Cuyahoga are different from other watershed regression lines. The ANCOVA analysis indicates that slopes and residual variances of the regression lines from Cuyahoga are statistically the same as the other lines, but the intercepts are different. For N, most of the statistical differences in regression lines were in the intercepts. The slopes and residual variances of most lines were consistently statistically similar. Four out of eight watersheds, Great Miami, Maumee, Muskingum, and Vermilion, were found to have statistically similar regression relationships when compared to the spatially aggregated regional regression line. Among the watersheds, Maumee, Muskingum, Sandusky, and Raisin were found to have statistically similar regression relationships to each other for N top load event contributions to annual loads.

In case of TP regression lines, statistical differences were more common than for N. Cuyahoga, Grand, and Great Miami had statistically different lines when compared to most of the other watersheds (Table 3.8). In most cases the statistical differences rose from different line intercepts, except in a few comparisons such as Raisin and Grand, where regression line slopes were different. For TP, Grand, Maumee, Muskingum, and Vermilion were found to have statistically similar regression lines as the spatially aggregated regional regression line. Among the individual watersheds, a few groups of watersheds were found to have statistically similar regression lines such as Great Miami and Grand, and Maumee and Sandusky.

For SS regression lines, the fewest statistical differences were observed among the three pollutants studied. Five out of the eight watersheds had similar regression lines to the spatially aggregated regional regression line (Table 3.9). Cuyahoga had statistically similar regression lines to Maumee and Vermilion, unlike N and TP, where it had statistically different lines as

compared to all the other watersheds. A few groups of watersheds were found to have statistically similar regression lines, for example, Maumee, Raisin, and Sandusky.

Table 3.7: ANCOVA-based statistical comparison for annual and top 1 to 5 Nitrate plus Nitrite Nitrogen (N) load event regression relationships, for individual watershed and spatially aggregated data. R, S, and I indicate residual variances, slope, and intercept, respectively. Significant differences at both α=0.05 and α=0.01 are indicated a "2" value, while differences significant at α=0.05 and insignificant at α=0.01 are indicated by "1" value. A "0" value indicates no statistical difference between two lines at both α=0.05 and α=0.01.

Nitrate + Nitrite Watershed	High flow event	Cuyahoga			Grand			Great Miami			Maumee			Muskingum			Raisin			Sandusky			Vermilion			All watersheds together		
		R	S	I	R	S	I	R	S	I	R	S	I	R	S	I	R	S	I	R	S	I	R	S	I	R	S	I
Cuyahoga	top1				0	0	2	0	0	0	0	0	2	0	0	1	0	0	2	0	0	2	0	0	2	1	0	2
	top2				0	0	2	0	0	1	0	0	2	0	0	1	0	0	2	0	0	2	1	0	2	2	0	2
	top3				0	0	2	0	0	1	0	0	2	0	0	2	0	0	2	0	0	2	1	0	2	2	0	2
	top4				0	0	2	0	0	2	0	0	2	0	0	2	0	0	2	0	0	2	0	0	2	2	0	2
	top5				0	0	2	0	0	2	0	0	2	0	0	2	0	0	2	0	0	2	0	0	2	2	0	2
Grand	top1	0	0	2				0	0	0	0	0	0	0	0	0	0	0	0	0	0	0	0	0	0	0	0	1
	top2	0	0	2				0	0	0	0	0	0	0	0	0	0	0	0	0	0	0	0	0	0	0	0	1
	top3	0	0	2				0	0	0	0	0	0	0	0	0	0	0	0	0	0	0	0	0	0	0	0	1
	top4	0	0	2				0	0	0	0	0	0	0	0	0	0	0	1	0	0	0	0	0	0	1	0	1
	top5	0	0	2				0	0	0	0	0	1	0	0	0	0	0	1	0	0	0	0	0	0	1	0	1
Great Miami	top1	0	0	0	0	0	0				0	0	1	0	0	1	0	0	0	0	0	0	0	0	0	0	0	0
	top2	0	0	1	0	0	0				0	0	2	0	0	2	0	0	0	0	0	0	1	0	0	1	0	0
	top3	0	0	1	0	0	0				0	0	2	0	0	2	0	0	0	0	0	1	1	0	0	2	0	0
	top4	0	0	2	0	0	0				0	0	2	0	0	2	0	0	0	0	0	1	1	0	0	2	0	0
	top5	0	0	2	0	0	0				0	0	2	0	0	2	0	0	0	0	0	1	1	0	0	2	0	0
Maumee	top1	0	0	2	0	0	0	0	0	1				0	0	0	0	0	0	0	0	0	1	0	0	2	0	2
	top2	0	0	2	0	0	0	0	0	2				0	0	0	0	0	0	0	0	0	1	0	0	2	0	2
	top3	0	0	2	0	0	0	0	0	2				0	0	0	0	0	0	0	0	0	1	0	0	2	0	2
	top4	0	0	2	0	0	0	0	0	2				0	0	0	0	0	0	0	0	0	1	0	0	2	0	2
	top5	0	0	2	0	0	1	0	0	2				0	0	0	0	0	0	0	0	0	0	0	1	2	0	2
Muskingum	top1	0	0	1	0	0	0	0	0	1	0	0	0				0	0	0	0	0	0	1	0	0	1	0	0
	top2	0	0	1	0	0	0	0	0	2	0	0	0				0	0	0	0	0	0	1	0	0	2	0	0
	top3	0	0	2	0	0	0	0	0	2	0	0	0				0	0	0	0	0	0	1	0	0	2	0	0
	top4	0	0	2	0	0	0	0	0	2	0	0	0				0	0	0	0	0	0	1	0	0	2	0	0
	top5	0	0	2	1	0	0	0	0	2	0	0	0				0	0	0	1	0	0	2	0	0	2	0	0
Raisin	top1	0	0	2	0	0	0	0	0	0	0	0	0	0	0	0				0	0	0	1	0	0	2	0	2
	top2	0	0	2	0	0	0	0	0	0	0	0	0	0	0	0				0	0	0	1	0	0	2	0	2
	top3	0	0	2	0	0	0	0	0	0	0	0	0	0	0	0				0	0	0	1	0	1	2	0	2
	top4	0	0	2	0	0	1	0	0	0	0	0	0	0	0	0				0	0	0	1	0	1	2	0	2
	top5	0	0	2	0	0	1	0	0	0	0	0	0	0	0	0				0	0	0	1	0	1	2	0	2
Sandusky	top1	0	0	2	0	0	0	0	0	0	0	0	0	0	0	0	0	0	0				1	0	0	2	0	1
	top2	0	0	2	0	0	0	0	0	0	0	0	0	0	0	0	0	0	0				0	0	0	2	0	2
	top3	0	0	2	0	0	0	0	0	1	0	0	0	0	0	0	0	0	0				0	0	0	2	0	2
	top4	0	0	2	0	0	0	0	0	1	0	0	0	0	0	0	0	0	0				0	0	0	2	0	2
	top5	0	0	2	0	0	0	0	0	1	0	0	0	0	0	0	0	0	0				0	0	0	2	0	2
Vermilion	top1	0	0	2	0	0	0	0	0	0	0	0	0	0	0	0	0	0	0	0	0	0				0	0	0
	top2	0	0	2	0	0	0	0	0	0	0	0	0	0	0	0	0	0	0	0	0	0				0	0	0
	top3	0	0	2	0	0	0	0	0	0	0	0	0	0	0	0	0	0	1	0	0	0				0	0	0
	top4	0	0	2	0	0	0	0	0	0	0	0	0	0	0	0	0	0	1	0	0	0				0	0	0
	top5	0	0	2	0	0	0	0	0	0	0	0	1	0	0	0	0	0	1	0	0	0				0	0	0
All watersheds together	top1	0	0	2	0	0	1	0	0	0	0	0	0	0	0	0	0	0	2	0	0	1	0	0	0			
	top2	0	0	2	0	0	1	0	0	0	0	0	0	0	0	0	0	0	2	0	0	2	0	0	0			
	top3	0	0	2	0	0	1	0	0	0	0	0	0	0	0	0	0	0	2	0	0	2	0	0	0			
	top4	0	0	2	0	0	1	0	0	0	0	0	0	0	0	0	0	0	2	0	0	2	0	0	0			
	top5	0	0	2	0	0	1	0	0	0	0	0	0	0	0	0	0	0	2	0	0	2	0	0	0			

Table 3.8: ANCOVA based statistical comparison for annual and top 1-5 Total Phosphorus (TP) load event regression relationships, for individual watershed and spatially aggregated data. R, S and I indicate residual variances, slope and intercept respectively. Significant differences at both α=0.05 and α=0.01 are indicated a "2" value, while differences significant at α=0.05 and insignificant at α=0.01 are indicated by "1" value. A "0" value indicates no statistical difference between two lines at both α=0.05 and α=0.01.

Total Phosphorus Watershed	High flow event	Cuyahoga			Grand			Great Miami			Maumee			Muskingum			Raisin			Sandusky			Vermilion			All watersheds together		
		R	S	I	R	S	I	R	S	I	R	S	I	R	S	I	R	S	I	R	S	I	R	S	I	R	S	I
Cuyahoga	top1				0	0	0	0	0	0	0	0	0	0	0	0	0	0	2	0	0	2	0	0	0	0	0	2
	top2				0	0	1	0	0	0	0	0	0	0	0	1	0	0	2	0	0	2	0	0	0	0	0	2
	top3				0	0	2	0	0	0	0	0	1	0	0	1	0	0	2	0	0	2	0	0	0	0	0	2
	top4				0	0	2	0	0	0	0	0	1	0	0	2	0	0	2	0	0	2	0	0	1	0	0	2
	top5				0	0	2	0	0	0	0	0	2	0	0	2	0	0	2	0	0	2	0	0	1	0	0	2
Grand	top1	0	0	0				0	0	0	0	0	0	0	0	1	0	2	0	0	0	2	0	0	0	0	0	0
	top2	0	0	1				0	0	0	1	0	0	0	0	1	1	1	0	0	0	2	1	0	0	1	0	0
	top3	0	0	2				0	0	0	1	0	0	0	0	1	0	2	0	0	0	2	1	0	0	2	0	0
	top4	0	0	2				0	0	0	1	0	0	0	0	1	0	2	0	0	0	2	1	0	0	2	0	0
	top5	0	0	2				0	0	0	0	0	0	0	0	1	0	2	0	0	0	2	0	0	0	1	0	0
Great Miami	top1	1	0	0	0	0	0				2	0	0	0	0	1	1	1	1	1	0	1	1	0	0	2	0	1
	top2	2	0	0	0	0	0				2	0	1	0	0	1	2	0	2	2	0	2	2	0	0	2	0	1
	top3	2	0	0	0	0	0				2	0	2	0	0	2	2	0	2	2	0	2	2	0	0	2	0	1
	top4	1	0	0	0	0	0				2	0	2	0	0	2	1	0	2	1	0	2	1	0	0	2	0	2
	top5	1	0	0	0	0	0				1	0	2	0	0	1	0	0	2	0	0	2	1	0	0	2	0	1
Maumee	top1	0	0	0	0	0	0	0	0	0				0	0	0	0	0	1	0	0	0	0	0	0	0	0	0
	top2	0	0	0	0	0	0	0	0	1				0	0	0	0	0	0	0	0	0	0	0	0	0	0	0
	top3	0	0	1	0	0	0	0	0	2				0	0	0	0	0	0	0	0	0	0	0	0	0	0	0
	top4	0	0	1	0	0	0	0	0	2				0	0	1	0	0	0	0	0	0	0	0	0	0	0	0
	top5	0	0	2	0	0	0	0	0	2				0	0	2	0	0	0	0	0	0	0	0	0	0	0	0
Muskingum	top1	0	0	0	0	0	1	0	0	1	0	0	0				0	1	0	0	0	0	0	0	0	0	0	0
	top2	0	0	1	0	0	1	0	0	1	1	0	0				0	1	0	0	0	0	0	0	0	1	0	0
	top3	0	0	1	0	0	1	0	0	2	1	0	0				0	1	0	0	0	0	0	0	0	1	0	0
	top4	0	0	2	0	0	1	0	0	2	1	0	1				0	1	0	0	0	1	1	0	0	2	0	0
	top5	1	0	2	0	0	1	0	0	1	1	0	2				0	1	0	0	0	1	1	0	0	2	0	0
Raisin	top1	0	0	2	0	2	0	0	1	1	0	0	1	0	1	0				0	1	0	0	0	0	0	1	0
	top2	0	0	2	0	1	0	0	0	2	0	0	0	0	1	0				0	0	0	0	0	0	0	0	0
	top3	0	0	2	0	2	0	0	0	2	0	0	0	0	1	0				0	1	0	0	0	0	0	0	1
	top4	0	0	2	0	2	0	0	0	2	0	0	0	0	1	0				0	0	0	0	0	0	1	0	1
	top5	0	0	2	0	2	0	0	0	2	0	0	0	0	1	0				0	0	0	0	0	0	2	0	1
Sandusky	top1	0	0	2	0	0	2	0	0	1	0	0	0	0	0	0	0	1	0				0	0	1	0	0	2
	top2	0	0	2	0	0	2	0	0	2	0	0	0	0	0	0	0	0	0				0	0	1	0	0	2
	top3	0	0	2	0	0	2	0	0	2	0	0	0	0	0	0	0	1	0				0	0	1	0	0	2
	top4	0	0	2	0	0	2	0	0	2	0	0	0	0	0	1	0	0	0				0	0	1	1	0	2
	top5	0	0	2	0	0	2	0	0	2	0	0	0	0	0	1	0	0	0				0	0	1	2	0	2
Vermilion	top1	0	0	0	0	0	0	0	0	0	0	0	0	0	0	0	0	0	0	0	0	1				0	0	0
	top2	0	0	0	0	0	0	0	0	0	0	0	0	0	0	0	0	0	0	0	0	1				0	0	0
	top3	0	0	0	0	0	0	0	0	0	0	0	0	0	0	0	0	0	0	0	0	1				0	0	0
	top4	0	0	1	0	0	0	0	0	0	0	0	0	0	0	0	0	0	0	0	0	1				0	0	0
	top5	0	0	1	0	0	0	0	0	0	0	0	0	0	0	0	0	0	0	0	0	1				0	0	0
All watersheds together	top1	0	0	2	0	0	0	0	0	1	0	0	0	0	0	0	0	1	0	0	0	2	0	0	0			
	top2	0	0	2	0	0	0	0	0	1	0	0	0	0	0	0	0	0	0	0	0	2	0	0	0			
	top3	0	0	2	0	0	0	0	0	1	0	0	0	0	0	0	0	0	1	0	0	2	0	0	0			
	top4	0	0	2	0	0	0	0	0	2	0	0	0	0	0	0	0	0	1	0	0	2	0	0	0			
	top5	0	0	2	0	0	0	0	0	1	0	0	0	0	0	0	0	0	1	0	0	2	0	0	0			

Table 3.9: ANCOVA based statistical comparison for annual and top 1-5 Suspended Solids (SS) load event regression relationships, for individual watershed and spatially aggregated data. R, S and I indicate residual variances, slope and intercept respectively. Significant differences at both α=0.05 and α=0.01 are indicated a "2" value, while differences significant at α=0.05 and insignificant at α=0.01 are indicated by "1" value. A "0" value indicates no statistical difference between two lines at both α=0.05 and α=0.01.

Suspended Solids Watershed	High flow event	Cuyahoga			Grand			Great Miami			Maumee			Muskingum			Raisin			Sandusky			Vermilion			All watersheds together		
		R	S	I	R	S	I	R	S	R	R	R	I	R	S	I	R	S	I	R	S	I	R	S	I	R	S	I
Cuyahoga	top1				0	0	1	0	0	0	0	0	0	0	0	0	0	0	0	0	0	2	0	0	0	0	0	1
	top2				0	0	1	0	0	0	0	0	0	0	0	0	0	0	0	0	0	2	0	0	0	0	0	2
	top3				0	0	2	0	0	0	0	0	0	0	0	0	0	0	1	0	0	2	0	0	0	0	0	2
	top4				0	0	2	0	0	0	0	0	0	0	0	0	0	0	1	0	0	2	0	0	0	0	0	2
	top5				0	0	2	0	0	0	0	0	0	0	0	0	0	0	1	0	0	2	0	0	0	0	0	2
Grand	top1	0	0	1				0	0	0	0	0	0	0	0	0	0	0	0	0	0	0	0	0	1	0	0	0
	top2	1	0	1				0	0	1	1	1	0	0	0	0	0	1	0	0	0	0	0	0	2	0	0	0
	top3	1	0	2				0	0	2	2	2	0	0	0	0	0	1	0	0	0	0	0	0	1	0	0	0
	top4	1	0	2				0	0	2	2	2	0	0	0	0	0	1	0	0	0	0	0	0	1	0	0	0
	top5	1	0	2				0	0	1	1	1	0	0	0	0	0	1	0	0	0	0	0	0	0	1	0	0
Great Miami	top1	2	0	0	0	0	0				2	2	0	0	0	0	2	1	0	1	0	0	0	0	2	2	0	0
	top2	2	0	0	0	0	0				2	2	0	0	0	1	2	1	0	1	0	1	1	0	2	2	0	0
	top3	2	0	0	0	0	0				2	2	0	0	0	1	2	1	0	1	0	2	0	0	1	2	0	0
	top4	2	0	0	0	0	0				2	2	0	0	0	1	1	1	0	1	0	2	0	0	0	2	0	0
	top5	1	0	0	0	0	0				2	2	0	0	0	1	0	1	0	0	0	2	0	0	0	1	0	0
Maumee	top1	0	0	0	0	0	0	0	1	0				0	0	0	0	0	0	0	0	0	0	0	0	0	0	0
	top2	0	0	0	0	0	0	0	0	0				0	0	0	0	0	0	0	0	0	0	0	0	0	0	0
	top3	0	0	0	0	0	0	0	0	0				0	0	0	0	0	0	0	0	0	0	0	0	0	0	0
	top4	0	0	0	0	0	0	0	0	0				0	0	0	0	0	0	0	0	0	0	0	0	0	0	0
	top5	0	0	0	0	0	0	0	0	0				0	0	0	0	0	0	0	0	0	0	0	0	0	0	0
Muskingum	top1	0	0	0	0	0	0	0	0	0	0	0	0				0	0	0	0	0	0	0	0	0	0	0	0
	top2	1	0	0	0	0	0	0	0	1	1	1	0				1	0	0	0	0	0	0	0	1	1	0	0
	top3	1	0	0	0	0	0	0	0	1	1	1	0				1	0	0	0	0	0	0	0	1	1	0	0
	top4	1	0	0	0	0	0	0	0	2	2	2	0				1	0	0	0	0	0	0	0	0	1	0	0
	top5	1	0	0	0	0	0	0	0	2	2	2	0				0	0	0	0	0	1	0	0	0	1	0	0
Raisin	top1	0	0	0	0	0	0	0	1	0	0	0	0	0	0	0				0	0	0	0	1	0	0	0	0
	top2	0	0	0	0	1	0	0	1	0	0	0	0	0	0	0				0	0	0	0	1	0	0	0	0
	top3	0	0	1	0	1	0	0	1	0	0	0	0	0	0	0				0	0	0	0	1	0	0	0	0
	top4	0	0	1	0	1	0	0	1	1	1	1	0	0	0	0				0	0	0	0	1	0	0	0	0
	top5	0	0	1	0	1	0	0	1	2	2	2	0	0	0	0				0	0	0	0	1	0	0	0	0
Sandusky	top1	0	0	2	0	0	0	0	0	0	0	0	0	0	0	0	0	0	0				0	0	1	0	0	1
	top2	0	0	2	0	0	0	0	0	0	0	0	0	0	0	0	0	0	0				0	0	0	0	0	1
	top3	0	0	2	0	0	0	0	0	0	0	0	0	0	0	0	0	0	0				0	0	0	0	0	1
	top4	0	0	2	0	0	0	0	0	1	1	1	0	0	0	0	0	0	0				0	0	0	0	0	2
	top5	0	0	2	0	0	0	0	0	2	2	2	0	0	0	1	0	0	0				0	0	0	0	0	2
Vermilion	top1	0	0	0	0	0	1	0	0	0	0	0	0	0	0	0	0	1	0	0	0	1				0	0	0
	top2	0	0	0	0	0	2	0	0	0	0	0	0	0	0	1	0	1	0	0	0	0				0	1	0
	top3	0	0	0	0	0	1	0	0	0	0	0	0	0	0	1	0	1	0	0	0	0				0	0	0
	top4	0	0	0	0	0	1	0	0	0	0	0	0	0	0	0	0	1	0	0	0	0				0	0	0
	top5	0	0	0	0	0	0	0	0	0	0	0	0	0	0	0	0	1	0	0	0	0				0	0	0
All watersheds together	top1	0	0	1	0	0	0	0	0	0	0	0	0	0	0	0	0	0	0	0	0	1	0	0	0			
	top2	0	0	2	0	0	0	0	0	0	0	0	0	0	0	0	0	0	0	0	0	1	0	1	0			
	top3	0	0	2	0	0	0	0	0	0	0	0	0	0	0	0	0	0	0	0	0	1	0	0	0			
	top4	0	0	2	0	0	0	0	0	0	0	0	0	0	0	0	0	0	0	0	0	2	0	0	0			
	top5	0	0	2	0	0	0	0	0	0	0	0	0	0	0	0	0	0	0	0	0	2	0	0	0			

3.3.4 Error Analysis

The various regression lines developed in the study were used to predict total annual loads, and the distributions of relative errors in predicting annual loads are presented using box and whisker plots. Regression analysis was carried out for different levels of watershed aggregations, ranging from individual watersheds to aggregation by similarity, i.e., watersheds with similar land use and aggregation by proximity, i.e., all watersheds in the Lake Erie and Ohio River basins (Ohio watersheds). Firstly, for all three pollutants analyzed in this study, the spatially aggregated regional regression line using all 8 Ohio watersheds was used to predict annual loads from the top 1 to 5 load events (Figure 3.10). Secondly, based on the results from the ANCOVA analysis, watersheds with statistically similar regressions (predominantly agricultural watersheds) were grouped together to create aggregated regressions for just the top 5 load events, and these grouped regressions were used to predict annual loads (Figure 3.11). Thirdly, individual watershed-specific regressions for the top 5 load events to predict annual loads were used to calculate prediction errors (Figure 3.12).

Figure 3.10 shows the relative errors in annual loads predicted using the spatially aggregated regression lines. Relative errors were defined as (Toor et al., 2008):

$$Absolute\ Relative\ Error\ (\%) = \left|\left(\frac{Observed\ annual\ load - Estimated\ annual\ load}{Observed\ annual\ load}\right)\right| \qquad (3.4)$$

The median relative errors for annual load predictions from the top 1, 2, 3, 4, and 5 load events for N were 29%, 27%, 28%, 27%, and 26% respectively for all Ohio watersheds. For predictions using the top 5 load events, two regression relationships were developed, one each by including and excluding results from Cuyahoga. The median relative errors for these regressions were 26% and 14%, respectively. Although, the median errors for annual load predictions from the top 1 to 5 load events, including data from Cuyahoga, were fairly similar, the maximum relative errors declined from 233% to 95%, with standard deviations also

declining from 36% to 19% for top 1 and top 5 load events. The new regression relationship for the top 5 load events excluding data from Cuyahoga considerably improved annual load predictions for the remaining watersheds as was evident by the reduction in median relative error. The maximum relative error and standard deviations were also the smallest at 61% and 12%, respectively.

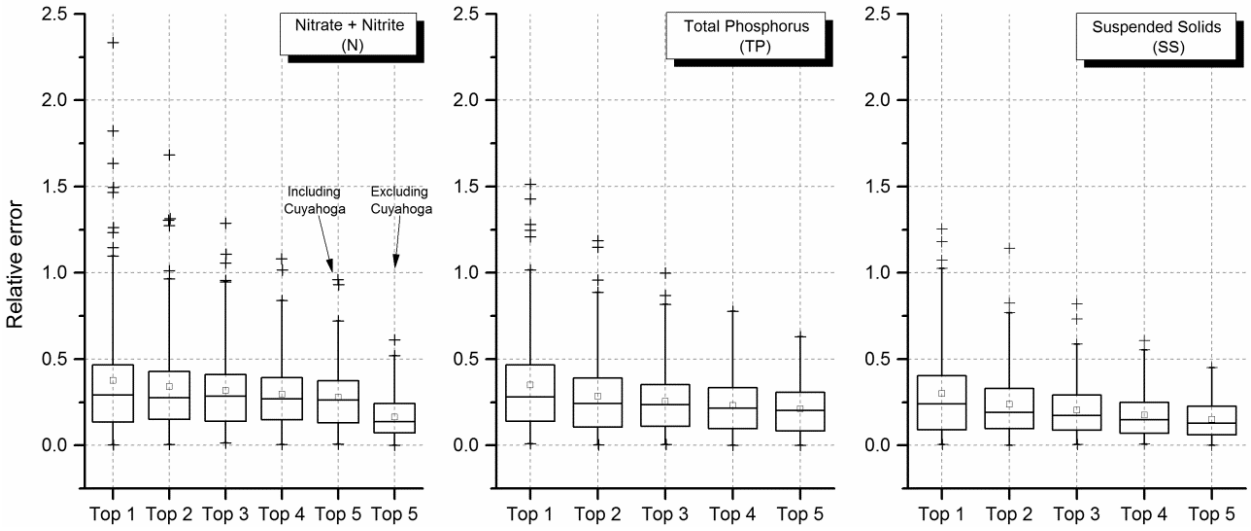

Figure 3.10: Relative error distributions for observed annual loads and annual loads estimated using top 1 to 5 Nitrate plus Nitrite Nitrogen (N), Total Phosphorus (TP) and Suspended Solids (SS) load events for spatially aggregated data from all watersheds. Cross (+) symbol beyond the length of whiskers indicates outliers and a small square symbol within the boxes indicates the mean of the distributions.

The median relative errors for annual load predictions were lower for TP and SS as compared to N. For TP, the median relative errors for annual load predictions for the top 1, 2, 3, 4 and 5, load events were 28%, 24%, 23%, 22%, and 20%, respectively. The maximum relative errors and standard deviations also declined from 151% to 63% and 30% to 14% for the top 1 and top 5 load events, respectively. SS annual load predictions had the least relative errors among all three pollutants with the median values being 24%, 19%, 17%, 15%, and 13% for the top 1, 2, 3, 4, and 5 load events. The maximum relative errors and standard deviations for SS annual load predictions declined from 125% to 45% and 26% to 11% for the top 1 and top 5 load events,

respectively. Overall, results showed that the top load events for N tend to last longer, carry a smaller percentage of annual loads and had higher prediction errors than TP and SS load events.

Based on results from the ANCOVA analysis, for every pollutant, a few watersheds were found to have statistically similar regression relationships for annual load predictions using loads exported in top 1 to 5 load events. Data from these similar watersheds were aggregated together and new regressions were developed for annual load predictions from the total loads exported in the top 5 load events. Distributions in relative errors in predicted loads using these new regressions are presented using box and whisker plots in Figure 3.11.

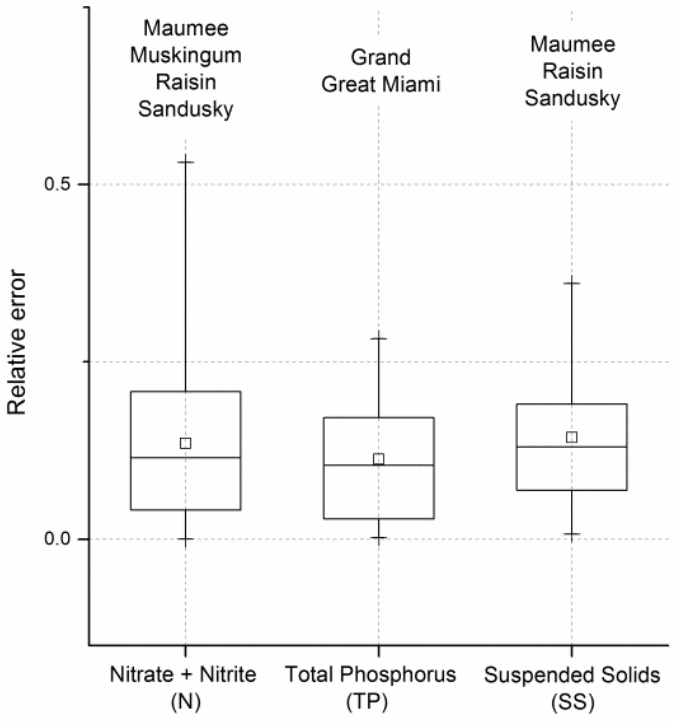

Figure 3.11: Relative error distributions for observed annual loads and annual loads estimated using top 5 Nitrate plus Nitrite Nitrogen (N), Total Phosphorus (TP), and Suspended Solids (SS) load events for spatially aggregated data from a few watersheds with statistically similar regression relationships between annual loads and top load events. Cross (+) symbol beyond the length of whiskers indicates outliers and a small square symbol within the boxes indicates the mean of the distributions.

For N, data from the four agricultural watersheds, Maumee, Muskingum, Raisin, and Sandusky, were aggregated as their individual watershed specific regressions were statistically

similar to each other. The median and maximum relative error for this new regression was 11% and 53% with a standard deviation of about 12%. The median and maximum relative errors reduced from 14% and 61% for spatially aggregated regression from all watersheds excluding Cuyahoga. For TP, a statistical similarity was found in a few watersheds such as Grand and Great Miami. A new regression relationship using aggregated data from these two watersheds was developed. The median and maximum relative errors for this regression reduced from 20% to 10% and 63% to 28% as compared to spatially aggregated regression from all watersheds. For SS, a new regression for data from Maumee, Raisin, and Sandusky was developed. The median relative error for this regression was similar to that from a spatially aggregated regression for data from all watersheds at 13%, but the maximum relative error and standard deviations declined from 45% to 36% and 10% to 9%.

Figure 3.12 shows distributions of relative errors for annual load predictions using watershed and pollutant-specific regression equations from the top 5 load events. These watershed-specific regressions performed better as compared to spatially aggregated regressions. For N, the median relative errors ranged from 7% for Muskingum to 19% for Vermilion, while the average median relative error for all watersheds was 12%. The maximum relative error ranged from 37% for Sandusky to 23% for Muskingum, while the average maximum relative error was 29%.

For TP, the median relative errors ranged from 5% for Great Miami to 16% for Maumee, while the average median relative error for all watersheds was 12%. The maximum relative error ranged from 49% for Cuyahoga to 11% for Great Miami, while the average maximum relative error was 30%. For SS, the median relative errors ranged from 6% for Great Miami to 16% for Maumee, while the average median relative error for all watersheds was 11%. The maximum relative error ranged from 44% for Cuyahoga to 18% for Great Miami, while the average

maximum relative error was 26%. The average standard deviation observed for these individual watershed specific regressions was 7%.

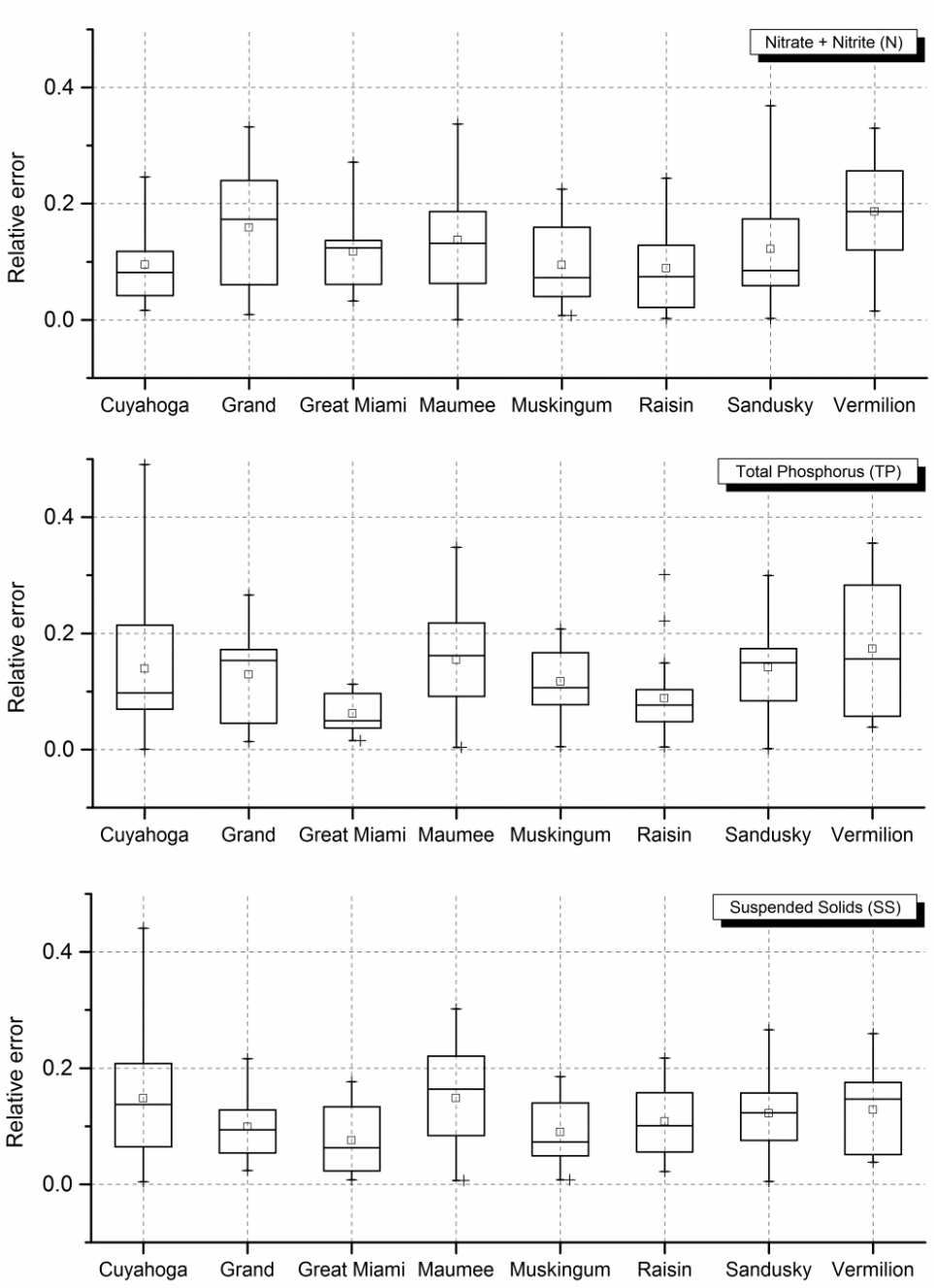

Figure 3.12: Relative error distributions for observed annual loads and annual loads estimated using top 5 Nitrate plus Nitrite Nitrogen (N), Total Phosphorus (TP), and Suspended Solids (SS) load events for data from individual watersheds. Cross (+) symbol beyond the length of whiskers indicates outliers and a small square symbol within the boxes indicates the mean of the distributions.

3.3.5 Spatial transferability of results on Illinois watersheds

The regression relationship for predicting annual N loads developed using spatially aggregated data from all Ohio watersheds (except Cuyahoga, the only watershed with high urbanization) was used to predict annual N loads for two non-urbanized agricultural watersheds in Illinois namely Upper Sangamon and Vermilion. This process was repeated using the spatially aggregated regression relationship from similar land-use watersheds from Ohio. As Maumee, Muskingum, Raisin, and Sandusky watersheds from Ohio had similar land-use patterns and statistically similar individual regressions, spatially aggregated regression relationship for these watersheds for N was used to estimate annual N loads for both Illinois watersheds (Figure 3.13).

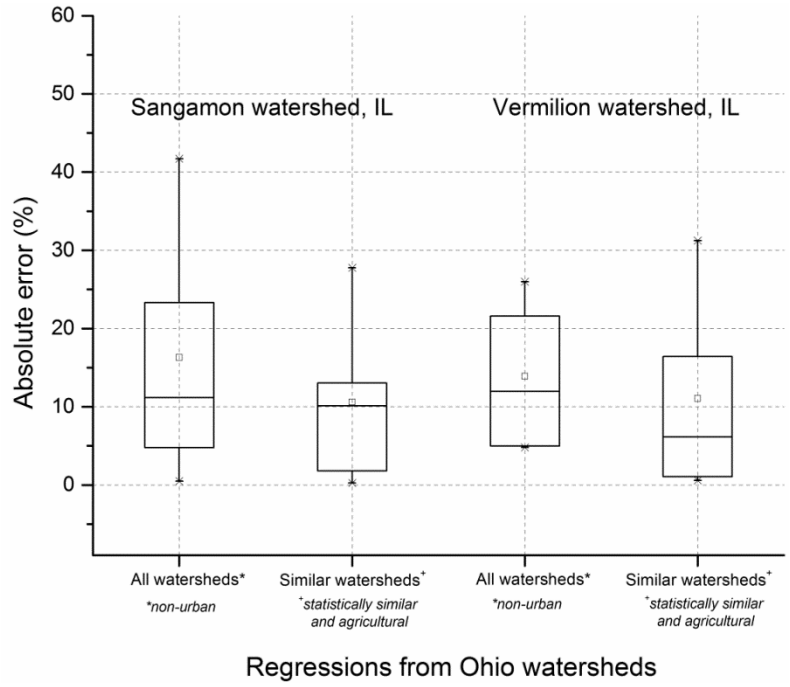

Figure 3.13: Relative error distributions for observed annual loads and annual loads estimated using top 5 Nitrate plus Nitrite Nitrogen (N) load events for watersheds in Illinois using regression equations from Ohio watersheds. Small square symbol within the boxes indicates the mean of the distributions.

The results indicated that the median absolute prediction error for annual N loads using the spatially aggregated regression relationship from all watersheds in Ohio (non-urban watersheds, which excludes the urbanized Cuyahoga watershed) was about 11% and 12% for the Upper

Sangamon and Vermilion watersheds, respectively. The maximum errors were slightly higher than 41% for the Upper Sangamon watershed and about 26% for the Vermilion watershed. The median absolute prediction error declined to 10% and 6% on using the spatially aggregated regression from statistically similar watersheds (which were all agricultural) for the Upper Sangamon and Vermilion watersheds, respectively. The maximum error declined to about 28% for the Upper Sangamon watershed but increased to about 31% for the Vermilion watershed.

3.4 Discussions

For most of the watersheds analyzed in this study, a majority of annual pollutant loads were exported in a few large load events. For example, data from all Ohio watersheds excluding Cuyahoga indicated that on average 56% of the total annual N loads were exported during the top 5 load events, which lasted for about 17% of days in a year. Similarly, data from all Ohio watersheds indicated that on average for TP and SS the top 5 load events carried 57% and 67% of annual loads in just 15% and 14% of the days in a year, respectively. So, these results clearly indicate the critical contribution of top load events to annual loads in these Midwestern watersheds. Additionally, these top load events lasted longer while carrying a lesser percentage of annual N loads than TP and SS loads.

Among the three pollutants analyzed in this study, the most accurate regression relationships to predict annual loads from top load events were observed for SS. SS loading patterns in these watersheds were largely unaffected by nutrient abatement programs implemented over the 1970s and 1980s as they mainly focused on point sources . This was validated by Richards and Baker (1993) who showed a statistically non-significant trend was observed in SS concentrations in some of the Ohio watersheds between the years 1975 to 1990. Thus, this relative stationarity in SS concentration trends possibly led to fewer variations in both annual loads and top load event loads leading to better predictability. For most of the predominantly agricultural watersheds, the regression relationships created to predict annual

SS loads were fairly strong. However, in a few of these agricultural watersheds, changes in land management practices possibly affected the performance of the regression relationships. For example, increased conservation tillage and changes in other agricultural practices were implemented in Maumee and Sandusky watersheds in the 1990s. These changes have been linked to a decline in SS loads exported from these watersheds (Richards et al., 2001), and possibly caused a relative higher variation in predicted annual loads as compared to other agricultural watersheds, over a span of few decades assessed in this study. Cuyahoga, which is the least agricultural and most urbanized of all watersheds, had the weakest watershed scale regression relationship to predict annual SS loads from top load events. Despite having the least percentage of agricultural land, Cuyahoga had one of highest total annual SS load contributions to Lake Erie. This hydrological behavior, coupled with its least agricultural and most urbanized land cover, potentially led to a weak regression relationship with the highest maximum relative error.

Given the mechanistic similarities in TP and SS export from watersheds, the performance of the regression relationships was similar for both these pollutants. Among the Ohio watersheds, the point-source inputs to total riverine loads are highest for Cuyahoga at about 33% (Bosch et al., 2011). In addition to a primarily urban land cover, significant point-source inputs led to an even weaker regression relationship for Cuyahoga for TP annual load predictions. Similar to SS, over the years Maumee and Sandusky had variations in total annual TP loads exported which can be attributed to land management changes implemented in these watersheds. It can be speculated that these annual variations led to a weaker regression relationship between top load events and annual loads, which is evident from the higher median and maximum relative errors for TP predictions in these watersheds. For TP, the strongest regression relationships were observed for Great Miami and Raisin watersheds. Over the monitoring period for Raisin, relatively consistent total annual and top event TP loads were observed, possibly due to the presence of impoundments in the upper Raisin watershed. These impoundments tend to slow

down the river flow acting as sediment sinks, altering the amount and timing of TP load export from Raisin (Bosch, 2008). Impoundments also possibly minimize impacts of any land management and nutrient abatement programs on relative contributions of top load events loads to annual loads, leading to robust regression relationships. A strong regression relationship for TP loads was also observed for Grand, indicating that such an approach can successfully be applied to watersheds that are not predominantly agricultural and in which loads exported are forest driven.

For N, fairly strong regression relationships were observed for all Ohio watersheds. Cuyahoga, which is mainly a point-source driven watershed, had the lowest contributions to annual N loads from top load events, but they were consistent over the complete monitoring duration. In addition to climate-driven variations in annual loads across the region, significant land management changes were particularly important for Maumee and Sandusky, resulting in an increased variation in annual N loads.

In this research, the predictability of annual pollutant loads from top load events were evaluated at three different levels of spatial aggregation. Firstly, a spatially aggregated and pollutant-specific regional regression relationship with data from all Ohio watersheds was developed. Secondly, spatially aggregated regression relationships were developed using data from a few similar watersheds, i.e., all agricultural watersheds. Thirdly, watershed-specific regression relationships to predict annual loads from top load events were developed. As expected, results indicated that the predictability of annual pollutant loads from top load events increases as the level of spatial aggregation decreases. Regression relationships were weakest for an aggregation of all watersheds by proximity at the regional level and the strongest at the individual watershed level. Watersheds differ in hydrological characteristics, geology, soils, climate, point-sources, land-use, and cropping patterns and thereby have different pollutant loading patterns. Thus, a bigger spatial aggregation of watersheds is expected to have a larger

variation in pollutant loading patterns leading to weaker regression relationships between annual loads and top load events. These variations are smaller in similar watersheds and the least at the individual watershed-scale as evident by relatively stronger regression relationships with smaller prediction errors. However, despite the expected weaker performance of the regional-level spatially aggregated regression relationships, they still had median relative errors below 25% for annual load predictions. These errors are comparable or lower to other studies which have utilized the commonly used 6 to 8-week monitoring frequency for estimating pollutant loads for short monitoring periods (Guo et al., 2002; Robertson, 2003; Johnes, 2006; Verma et al., 2012)

To test the applicability of the developed approach to predict annual loads for watersheds with limited water quality data, annual N loads for two watersheds in Illinois were estimated using regression relationships from Ohio. The results indicated a reasonable estimate with absolute median errors less than 12% for both watersheds were obtained using the regression relationship from all Ohio watersheds. This further improved to an average median error of 8.14% for both Illinois watersheds by using regression relationships just from the similar land-use watersheds (agricultural). This validated the merits of this approach by showing that a regional regression relationship can be utilized for predicting annual N loads for similar watersheds which have the top load events monitored.

Lastly, there are a few limitations of this proposed approach. This research clearly demonstrated that loads exported during top load events in a year can be used to predict annual loads, but it is a challenge to *a priori* predict which high flow events should be sampled for accurate annual load predictions. As suggested by Markus and Demissie (2006), a few monitoring "triggers" can be setup for each watershed based on past flow records. A majority of these top load events also have the highest peak flows in a water year (Figure 3.5), and as flows are forecasted, better triggers could be based on flow thresholds. Data mining can be used to

determine which auxiliary parameters such as the antecedent moisture index, time of the year, total predicted precipitation, number of dry days, fertilizer application time, etc. are most critical and should be included in determining the events to be sampled. Care should be taken in applying this methodology in cases with short monitoring records, as variations in annual load contributions from top load events in extremely wet or dry years might affect the regression relationships towards extreme values. Similarly, changes in nutrient application patterns and land management practices within a watershed might skew a regression relationship developed from short monitoring records.

However, in spite of the described potential pitfalls and limitations of this proposed approach, our analysis indicates that this approach can be used for efficiently predicting annual pollutant loads in watersheds by monitoring high flow events which carry the most loads on an annual scale. By reducing regular monitoring during low flow periods in a given water year and increasing focus on big load events which are generally linked to peak flows, annual pollutant loads can possibly be predicted at lower monitoring costs overall. Additionally, annual pollutant loads for watersheds without historical water quality records can be predicted by focusing on monitoring the events likely to produce high loads and applying the appropriate spatially aggregated regional regression equations. This can be done without expecting a significant loss of predictive accuracy as validated from results of applying regressions from watersheds in Ohio to similar land-use watersheds in Illinois. This approach focusing on a few large load events would potentially result in manpower and financial savings, which can then be utilized to monitor additional sites with the same resource pool.

3.5 Summary and Conclusions

The research results provided additional understanding of the pollutant dynamics as it relates to hydrologic variations. Water quality and flow data collected at 10 watersheds with different land-uses in the US Midwest were analyzed. In particular, this study evaluated the role

of large load events on annual pollutant load export by assessing the predictability of annual N, TP, and SS loads by the top 1 to 5 load events in a year for eight watersheds in the Lake Erie and Ohio River basins. To capture the mechanistic differences in pollutant export, a novel pollutant-specific technique was designed to identify high flow events, and consequently, loads exported during these high flow events. The results confirmed and illustrated the existence of strong correlations between the pollutant loads exported during a few top load events and the total annual loads. Therefore, regression relationships can be developed using top load events to predict total annual loads, and thus, monitoring programs can be designed to focus more on loads exported during these few top load events. These regression relationships were developed and evaluated at three levels of spatial aggregation: at the watershed level, spatial aggregation of similar watersheds, and spatial aggregation of all watersheds in a region. Analysis of Covariance (ANCOVA) was used to assess the similarity of regression relationships developed for different watersheds individually and spatially aggregated data from multiple watersheds. The regression relationships from similar land use watersheds were found to be statistically similar to each other, indicating that they can be transferred spatially without the loss of predictive accuracy. Consequently, the study results can be used in estimating annual and long-term pollutant loads at sites with most of the largest load events sampled.

Predictability of SS annual loads was the highest among the three pollutants analyzed, with the prediction errors declining on reducing the spatial aggregation of regression relationships for all three pollutants. Additionally, for all regression relationships evaluated, the variation and mean errors for annual load predictions declined as more top load events were used for setting up the regression relationships, indicating a trade-off in overall monitoring costs and annual load prediction accuracies. This approach based on high flow improves our understanding of the variability in pollutant loads under various hydrologic conditions.

Acknowledgements

Partial support for the research was provided by the United States Environmental Protection Agency (Grant EPA GL-00E00683-0) and the Great Lakes Water Quality Consortium. We would like to thank Brian Miller and Lisa Merrifield from Illinois Indiana Sea Grant at the University of Illinois for their role in research design and administration, and for serving as a liaison with EPA. We would also like to thank Greg McIsaac from the University of Illinois for valuable discussions in early stages of this research, and Peter Richards from Heidelberg University, who provided useful explanations and suggestions regarding the NCWQR data used in this study. Finally, we would like to acknowledge the contribution of the Illinois State Water Survey (ISWS) staff, Amy Russell and Daeryong Park, for helpful review comments, and Lisa Sheppard for editorial assistance.

References

Aulenbach, B. T. and R. P. Hooper. 2006. "The Composite Method: An Improved Method for Stream-Water Solute Load Estimation." *Hydrological Processes* 20 (14): 3029-3047.

Baker, D. B. 1985. "Regional Water Quality Impacts of Intensive Row-Crop Agriculture: A Lake Erie Basin Case Study." *Journal of Soil & Water Conservation* 40 (1): 125-132.

Bosch, N. S. 2008. "The Influence of Impoundments on Riverine Nutrient Transport: An Evaluation using the Soil and Water Assessment Tool." *Journal of Hydrology* 355 (1-4): 131-147.

Bosch, N. S., J. D. Allan, D. M. Dolan, H. Han, and R. P. Richards. 2011. "Application of the Soil and Water Assessment Tool for Six Watersheds of Lake Erie: Model Parameterization and Calibration."*Journal of Great Lakes Research* 37 (2): 263-271.

Camargo, J. A. and Á. Alonso. 2006. "Ecological and Toxicological Effects of Inorganic Nitrogen Pollution in Aquatic Ecosystems: A Global Assessment." *Environment International* 32 (6): 831-849.

Cooper, D. M. and C. D. Watts. 2002. "A Comparison of River Load Estimation Techniques: Application to Dissolved Organic Carbon." *Environmetrics* 13 (7): 733-750.

Demissie, M. 1996. "Sediment Load during Flood Events for Illinois Streams." *Water Int.* 21: 131-137.

Depinto, J. V., T. C. Young, and D. K. Salisbury. 1986. "Impact of Phosphorus Availability on Modelling Phytoplankton Dynamics." *Hydrobiological Bulletin* 20 (1-2): 225-243.

Driver, N. E. and B. M. Troutman. 1989. "Regression Models for Estimating Urban Storm-Runoff Quality and Quantity in the United States." *Journal of Hydrology* 109 (3-4): 221-236.

El-Shaarawi, A. H., K. W. Kuntz, and A. Sylvestre. 1986. "Estimation of Loading by Numerical Integration." *Developments in Water Science* 27.

Goolsby, D. A., W. A. Battaglin, B. T. Aulenbach, and R. P. Hooper. 2001. "Nitrogen Input to the Gulf of Mexico." *Journal of Environmental Quality* 30 (2): 329-336.

Guo, Y., M. Markus, and M. Demissie. 2002. "Uncertainty of Nitrate-N Load Computations for Agricultural Watersheds." *Water Resources Research* 38 (10): 31-312.

Hawley, N., T. H. Johengen, Y. R. Rao, S. A. Ruberg, D. Beletsky, S. A. Ludsin, B. J. Eadie, D. J. Schwab, T. E. Croley, and S. B. Brandt. 2006. "Lake Erie Hypoxia Prompts Canada-U.S. Study." *Eos* 87 (32): 313-315.

Hirsch, R.M., L. M. Douglas, and S. A. Archfield. 2010. "Weighted Regressions on Time, Discharge, and Season (WRTDS), with an Application to Chesapeake Bay River Inputs. Journal of the American Water Resources Association 46: 857-880.

Howarth, R. W. 1998. "An Assessment of Human Influences on Fluxes of Nitrogen from the Terrestrial Landscape to the Estuaries and Continental Shelves of the North Atlantic Ocean." *Nutrient Cycling in Agroecosystems* 52 (2-3): 213-223.

Johnes, P. J. 2007. "Uncertainties in Annual Riverine Phosphorus Load Estimation: Impact of Load Estimation Methodology, Sampling Frequency, Baseflow Index and Catchment Population Density." *Journal of Hydrology* 332 (1-2): 241-258.

Kočić, A., T. Hengl, and J. Horvatić. 2008. "Water Nutrient Concentrations in Channels in Relation to Occurrence of Aquatic Plants: A Case Study in Eastern Croatia." *Hydrobiologia* 603 (1): 253-266.

Kronvang, B., E. Jeppesen, D. J. Conley, M. Søndergaard, S. E. Larsen, N. B. Ovesen, and J. Carstensen. 2005. "Nutrient Pressures and Ecological Responses to Nutrient Loading Reductions in Danish Streams, Lakes and Coastal Waters." *Journal of Hydrology* 304 (1-4): 274-288.

Kyoung, J. L., B. A. Engel, Z. Tang, J. Choi, K. -S Kim, S. Muthukrishnan, and D. Tripathy. 2005. "Automated Web GIS Based Hydrograph Analysis Tool, WHAT." *Journal of the American Water Resources Association* 41 (6): 1407-1416.

Lewis, J. 1996. "Turbidity-Controlled Suspended Sediment Sampling for Runoff-Event Load Estimation." *Water Resources Research* 32 (7): 2299-2310.

Markus, M. and M. Demissie. 2006. "Predictability of Annual Sediment Loads Based on Flood Events." *Journal of Hydrologic Engineering* 11 (4): 354-361.

Natural Resources Conservation Service. 1983. National engineering handbook, Section 3 sedimentation. U.S. Department of Agriculture.

Öztürk, F., Apaydin, H., and Walling, D. E. 2001. "Suspended Sediment Loads through Flood Events for Streams of Sakarya River Basin." *Turk. J. Eng. Environ. Sci.* 25: 643-650.

Preston, S. D., V. J. Bierman Jr, and S. E. Silliman. 1989. "An Evaluation of Methods for the Estimation of Tributary Mass Loads." *Water Resources Research* 25 (6): 1379-1389.

Rabalais, N. N., R. E. Turner, and D. Scavia. 2002. "Beyond Science into Policy: Gulf of Mexico Hypoxia and the Mississippi River." *Bioscience* 52 (2): 129-142.

Rao, Y. R., N. Hawley, M. N. Charlton, and W. M. Schertzer. 2008. "Physical Processes and Hypoxia in the Central Basin of Lake Erie." *Limnology and Oceanography* 53 (5): 2007-2020.

Richards, R. P. and D. B. Baker. 1993. "Pesticide Concentration Patterns in Agricultural Drainage Networks in the Lake Erie Basin." *Environmental Toxicology and Chemistry* 12 (1): 13-26.

Richards, R. P., D. B. Baker, J. W. Kramer, D. E. Ewing, B. J. Merryfield, and N. L. Miller. 2001. "Storm Discharge, Loads, and Average Concentrations in Northwest Ohio Rivers, 1975-1995." *Journal of the American Water Resources Association* 37 (2): 423-438.

Richards, R. P. and Holloway J. 1987. "Monte Carlo Studies of Sampling Strategies for Estimating Tributary Loads." *Water Resources Research,* 23 (10): 1939-1948.

Robertson, D. M. and E. D. Roerish. 1999. "Influence of Various Water Quality Sampling Strategies on Load Estimates for Small Streams." *Water Resources Research* 35 (12): 3747-3759.

Robertson, D. M. 2003. "Influence of Different Temporal Sampling Strategies on Estimating Total Phosphorus and Suspended Sediment Concentration and Transport in Small Streams." *Journal of the American Water Resources Association* 39 (5): 1281-1308.

Royer, T. V., M. B. David, and L. E. Gentry. 2006. "Timing of Riverine Export of Nitrate and Phosphorus from Agricultural Watersheds in Illinois: Implications for Reducing Nutrient Loading to the Mississippi River." *Environmental Science and Technology* 40 (13): 4126-4131.

Rozemeijer, J. C., Y. Van Der Velde, F. C. Van Geer, G. H. De Rooij, P. J. J. F. Torfs, and H. P. Broers. 2010. "Improving Load Estimates for NO3 and P in Surface Waters by Characterizing the Concentration Response to Rainfall Events." *Environmental Science and Technology* 44 (16): 6305-6312.

Salles, C., M. G. Tournoud, and Y. Chu. 2007. "Estimating Nutrient and Sediment Flood Loads in a Small Mediterranean River." *Hydrological Processes* 22 (2): 242-253.

Schilling, K. and Y.–K. Zhang. 2004. "Base-flow Contribution to Nitrate-Nitrogen Export from a Large, Agricultural Watershed, USA." *Journal of Hydrology* 295 (1-4): 305-316.

Smith, R. A., G. E. Schwarz, and R. B. Alexander. 1997. "Regional Interpretation of Water-Quality Monitoring Data." *Water Resources Research* 33 (12): 2781-2798.

Smith, D. R., S. J. Livingston, B. W. Zuercher, M. Larose, G. C. Heathman, and C. Huang. 2008. "Nutrient Losses from Row Crop Agriculture in Indiana." *Journal of Soil and Water Conservation* 63 (6): 396-409.

Snedecor, G. W. and W. G. Cochran. 1980. *Statistical Methods* 7th ed., The Iowa State University Press, Ames, Iowa.

Toor, G. S., R. D. Harmel, B. E. Haggard, and G. Schmidt. 2008. "Evaluation of Regression Methodology with Low-Frequency Water Quality Sampling to Estimate Constituent Loads for Ephemeral Watersheds in Texas." *Journal of Environmental Quality* 37 (5): 1847-1854.

Troutman, B. M. 1985. "Errors and Parameter Estimation in Precipitation-Runoff Modeling 1. Theory." *Water Resources Research* 21 (8): 1195-1213.

United States Environmental Protection Agency (USEPA). 2001. PLOAD version 3.0: An ArcView GIS Tool to Calculate Nonpoint Sources of Pollution in Watershed and Stormwater Projects, User's Manual. Developed for USEPA by CH2M HILL.

United States Environmental Protection Agency (USEPA). 2006. User's Guide. Spreadsheet Tool for the Estimation of Pollutant Load (STEPL), Version 4.0. Developed for USEPA by Tetra Tech, Inc. Fairfax, VA

Verma, S., M. Markus, and R. A. Cooke. 2012. "Development of Error Correction Techniques for Nitrate-N Load Estimation Methods." *Journal of Hydrology* 432-433: 12-25.

Verma, S., A. Bartosova, M. Markus, and R. A. Cooke. 2013. " Annual riverine pollutant load export in Midwestern watersheds: The role of large load events". *Submitted, Journal of Hydrology*

Yaksich, S. M. and F. H. Verhoff. 1983. "Sampling Strategy for River Pollutant Transport." *Journal of Environmental Engineering* 109 (1): 219-231.

Zhang, S., Z. Wang, B. Zhang, K. Song, D. Liu, and C. Ren. 2010. "Characteristics of Nonpoint Source Pollution from an Agricultural Watershed during Rainfall Events. *International Conference on Mechanic Automation and Control Engineering, MACE2010, Wuhan, 26-28th June 2010.*

Zhu, Q., J. P. Schmidt, A. R. Buda, R. B. Bryant, and G. J. Folmar. 2011. "Nitrogen Loss from a Mixed Land use Watershed as Influenced by Hydrology and Seasons." *Journal of Hydrology* 405 (3-4): 307-315.

CHAPTER 4

Spatio-Temporal patterns of pollutant export in Midwestern watersheds using circular statistics

Abstract

This study analyzed the spatio-temporal patterns in nutrient and sediment export from eight large Midwestern watersheds in the Lake Erie and Ohio River basins over long term monitoring durations (8-32 years). These predominantly agricultural watersheds are the major source of pollutants delivered to Lake Erie and also contribute to the annual loading in the Gulf of Mexico through the Mississippi River system. The spatio-temporal analysis was done in two phases, with one focusing on the temporal occurrence of the top load events annually for Suspended Solids (SS), Total Phosphorus (TP) and Nitrate-Nitrogen (NO_3-N) loads while the other examining the timing of mean annual flow, pollutant concentrations and corresponding loads over the complete monitoring durations for each watershed. The results indicated that mechanistic, temporal and spatial differences exist in the export of different pollutants from the watersheds studied. The analysis revealed that most of the pollutant export in these watersheds happened during high flow conditions observed over the cooler months of the year. NO_3-N was predominantly exported from these watersheds between the months of November and April while SS and TP loads were exported mainly between February and May. The SS loads were more evenly distributed over the year as compared to the TP and NO_3-N loads. There were no statistically significant trends observed in the timing of mean annual flow, pollutant concentrations and corresponding loads over the complete monitoring durations in these watersheds. The results showed that pollutant concentrations are more dispersed on a temporal scale with their corresponding loads concentrated over the high flow periods in the winter-early spring months. Additionally, the analysis qualitatively highlighted the impacts of impoundment dams in limiting sediment and nutrient export from watersheds and also the differences in pollutant load patterns attributed to different sources and land uses. Lastly, the results underlined the temporal separation in peak pollutant export from these watersheds and the poorest water quality conditions in the receiving water bodies stressing on the need to focus the management and regulatory efforts on periods of high load export.

Keywords: Circular statistics, temporal load export, nutrient, sediment, Lake Erie

4.1 Introduction

Nutrient and sediment export from agricultural watersheds has been identified as a major cause of eutrophication and hypoxia throughout the world. Around the United States, the Gulf of Mexico and Lake Erie have been known as areas most highly affected by eutrophication caused by anthropogenic activities over the past few decades (Goolsby et al., 2001; Rabalais et al., 2002; and Dolan, 1993). Lake Erie's drainage basin is the most populated and has the most amount agricultural land among the five Laurentian Great Lakes. Moreover, it is also the shallowest and the southernmost of the five lakes. The extensive application of phosphorus as fertilizer in the 1960-70s within the agricultural farmlands in the Lake Erie basin led to large algal blooms in the lake (Michalak et al. 2013). Consequently, the US and Canadian governments implemented the Great Lakes Water Quality Agreement in the late 1970s and early 1980s which brought down excessive phosphorus loading from point and non-point sources into Lake Erie (GLWQA, 1978 and De Pinto et al. 1986). After a period of few years with low nutrient loading to the lake and smaller algal blooms, the mid-1990s saw their reemergence which has further increased drastically over the past few years. Hawley et al. (2006) reported one of the largest hypoxic zones over the past few decades which extended to approximately 10.000 km^2 within the lake was observed in the year 2005. Recently Michalak et al. (2013) reported that the western and central basins of Lake Erie experienced the largest algal bloom in its recorded history with peak intensities over three times greater than the previously largest bloom recorded in 2008. Studies have listed changes in land use, agricultural practices, water levels, temperatures and rise in severe meteorological conditions together contributed to the occurrence of these huge blooms (Hawley et al., 2006 and Michalak et al., 2013).

Such algal blooms in receiving water bodies primarily caused by anthropogenic application of N and P fertilizers in agricultural farmlands, makes it very critical to understand the nutrient export dynamics from such farmlands. It is essential to quantify the amount and timing of

nutrient export to assess trends in nutrient loadings, evaluate the impacts of land management and policy regulations and for accurate estimation of loadings in future scenarios. Moreover, quantifying the temporal trends in timing of nutrient export and delivery from agricultural watersheds is critical to develop efficient nutrient criteria, numeric standards and total maximum daily loads (TMDLs) for impaired receiving streams, rivers and lakes (Royer et al., 2006). Further, as explained by Limburg et al. (1986), large rivers are important for fish production, water supply systems and recreational usage and these values may be affected by nutrient concentrations (Soballe and Kimmel, 1987 and Heathwaite et al. 1996). Thus, analyzing temporal trends in nutrient export patterns may help in better management and utilization of the river systems. Typically nutrient concentrations in agricultural rivers have some seasonal variability which needs to be characterized to quantify annual export from the system (Lampman et al., 1999). Zhang et al. (1995) concluded that if this seasonal variability is not characterized it may contribute to the difficulty in determining long-term changes in nutrient concentrations and export. Additionally the seasonal variability in nutrient export may influence the impact of these nutrients in the receiving water bodies and also give an insight into the nature if the nutrient sources contributing to the river systems (Lampman et al., (1999).Thereby, quantification of the temporal variability in nutrient export could help address these issues and also enable smarter and more efficient water quality sampling focusing on periods which generally see higher nutrient losses and are vital for annual export estimations. Grimvall et al. (2000) reported inertia of the aquatic and terrestrial systems that control nutrient export, to reduced application rates and regulatory changes. Temporal analysis of nutrient export might also highlight any changes in nutrient export patterns due to inertia in the response of watersheds.

Eutrophic conditions in Lake Erie have generally been observed in late summer- early fall periods, when low flow conditions exist in the streams draining into these water bodies. Low flow conditions favor nutrient uptake and extensive algae growth eventually leading to hypoxic

conditions. Eutrophication in such water bodies is largely driven by nutrient export from agricultural lands which is primarily driven by hydrological processes such as precipitation and drainage from the farmlands (Royer et al., 2006). The export of nutrients is largely dependent on the landscape characteristics, geological and climatological factors along with agricultural management practices and their influences on hydrological processes (Mourad and van der Perk, 2009). Streams in the Midwestern United States generally see peak flows in late winter and early spring months which coincides with the fallow period in the agricultural watersheds contributing to these streams. This period of high flow is usually accompanied by large nutrient export from these watersheds. Agricultural management practices such as no cover crops, fall fertilizer application, and broadcasting of fertilizers rather than soil injection are possibly major reasons for higher nutrient export during such high flows. Additionally, the Midwestern watersheds are characterized by intensive installation of sub-surface tile drain systems. The installation of these tile drain systems modifies the natural landscape characteristics and affects the natural nutrient transport processes by expediting the export of dissolved nutrients by bypassing the preferential groundwater flow paths. This nutrient rich water is delivered to downstream lakes and estuaries eventually causing algal blooms and eutrophic conditions.

This study aims at identifying temporal patterns in pollutant loads (suspended solids, total phosphorus, and nitrate-N) from six watersheds in the Lake Erie basin and two watersheds lying in the Ohio River basin. The six watersheds in the Lake Erie basin are amongst the largest draining into the lake and receive some of the highest nutrient and sediment inputs of any watersheds in all of the Great Lake basins mainly attributed to the intensive agriculture practiced in the region (Bosch et al., 2011). Majority of these watersheds are primarily agricultural, along with a few watersheds which are predominantly urbanized and forested. Collectively, they have a wide range of combinations of watershed sizes and land uses. This allows comparisons of temporal patterns in export of different nutrients and sediment based on variations in watershed characteristics. The temporal analysis in the study was performed in two

phases, with one focusing on the few top load events annually (high flow events carrying the maximum loads) while other evaluating temporal patterns in mean annual values of hydrological variables, both over a substantial period of monitoring data (8-32 years). Specifically the objectives of this study were to apply circular statistics to (i) Identify temporal patterns in export of pollutants from the top load events in watersheds in the Lake Erie and Ohio River basins (ii) Evaluate the temporal distribution of daily average precipitation, flow, pollutant concentrations and loads within a year in watersheds in the Lake Erie and Ohio River basins.

4.2 Methods

4.2.1 Watershed and data descriptions

Long term flow and pollutant concentration namely suspended solids (SS), total phosphorus (TP) and nitrate plus nitrite-nitrogen ($NO_{2\text{-}3}$-N) data from eight watersheds were analyzed in this study. Typically in these watersheds the nitrite forms a very small percentage of nitrite +nitrate mixture, therefore the nitrate plus nitrite-nitrogen is simply referred as nitrate-N and NO_3-N in this study. Six of these watersheds namely Raisin, Maumee, Sandusky, Vermilion, Cuyahoga and Grand drain into Lake Erie and lie on the western and southern sides of the lake, primarily in northern Ohio, southern Michigan and eastern Indiana. Two watersheds namely Great Miami and Muskingum lie in central Ohio and are part of the Ohio River basin. Table 4.1 summarizes the watershed sizes, land use characteristics and their respective durations of monitoring. All watersheds except Cuyahoga and Grand are primarily agricultural with majority of their land area under row-crop agriculture with mostly corn-soybean annual rotations. The Cuyahoga watershed is a predominantly urbanized watershed with the Greater Cleveland urban area covering most of the northern half of the watershed. The Grand watershed is the only watershed which is mostly forested with about 52% of its land area occupied by wooded forests.

The Raisin watershed is the northernmost watershed with virtually all its land area in Michigan. It is a typical Midwestern watershed which is predominantly agricultural, however it is different from other watersheds due to the higher degree of river impoundment in the middle and lower sections of the watershed. The Raisin watershed has about 14 impoundments having surface area of at least 10 ha, including artificial reservoirs, natural lakes and small ponds (Bosch, 2008). The soils in these watersheds especially in the northern Ohio, eastern Indiana and southern Michigan are composed of fine glacial till and are generally very fertile but poorly drained, leading to extensive adoption of tile-drainage in these areas. Soils in central and northeastern Ohio are also of glacial origin but are coarser and less fertile.

Table 4.1: Characteristics of studied watersheds for modeled areas upstream of the USGS gaging station (*Land use data for Cuyahoga, Grand, Maumee, Raisin, and Sandusky as reported by Bosch et al., 2011)

	USGS Station Number	Monitoring Period	Watershed size (km^2)	Land-use (%)*		
				Agriculture	Urban	Wooded
Lake Erie basin						
Cuyahoga	04208000	1982-2009	1,843	17	47	35
Grand	04212100	1989-2006	1,758	37	10	52
Maumee	04193500	1975-2009	16,427	81	11	8
Raisin	04176500	1982-2007	2,755	72	11	16
Sandusky	04198000	1975-2005	3,285	83	9	8
Vermilion	04199500	2001-2008	697	71	1	26
Ohio River basin						
Great Miami	03271601	1996-2009	6,953	82	5	10
Muskingum	03150000	1995-2009	19,208	52	2	43

The data used in this study was collected by the Water Quality Lab (WQL) at the National Center for Water Quality Research at Heidelberg College, Ohio. The data comprises of daily concentrations during low flow conditions with up to three samples per day during storm events. The sample collection sites comprised of automatic samplers and were installed in conjunction with USGS gaging stations. In-depth details about the sampling program and

chemical analysis are described in Baker (1985), Richards and Baker (1993), and Richards et al. (2001).

4.2.2 Precipitation

As precipitation is the main driver of water movement from the agricultural fields to the drainage ditches, it is essential to calculate the daily mean areal precipitation across these watersheds over the monitoring period. Daily precipitation data was used from all the available weather stations lying within these watersheds from the Midwestern Regional Climate Center (MRCC) database. Daily mean areal precipitations across a watershed were computed by using Thiessen weighted precipitations from all the weather stations in and around a watershed. Table 4.2 shows the drainage areas of all watersheds upstream of the gaging stations and the total number of weather stations used to calculate the Thiessen weighted daily mean areal precipitation across the watersheds.

Table 4.2: The total number of weather stations used to calculate Thiessen weighted daily precipitation in all the watersheds analyzed in this study.

Watershed	Number of weather stations used as Thiessen weights
Cuyahoga	5
Grand	4
Great Miami	10
Maumee	19
Muskingum	17
Raisin	6
Sandusky	6
Vermilion	2

Figure 4.1 shows the location of all the watersheds analyzed in this study and the weather stations used to calculate the Thiessen weighted daily precipitation values across the watersheds. The watershed areas ranged from approximately 700 to 19,000 square kilometers with the total number of weather stations ranging from 2 to 19 for calculation of Thiessen weighted daily precipitations.

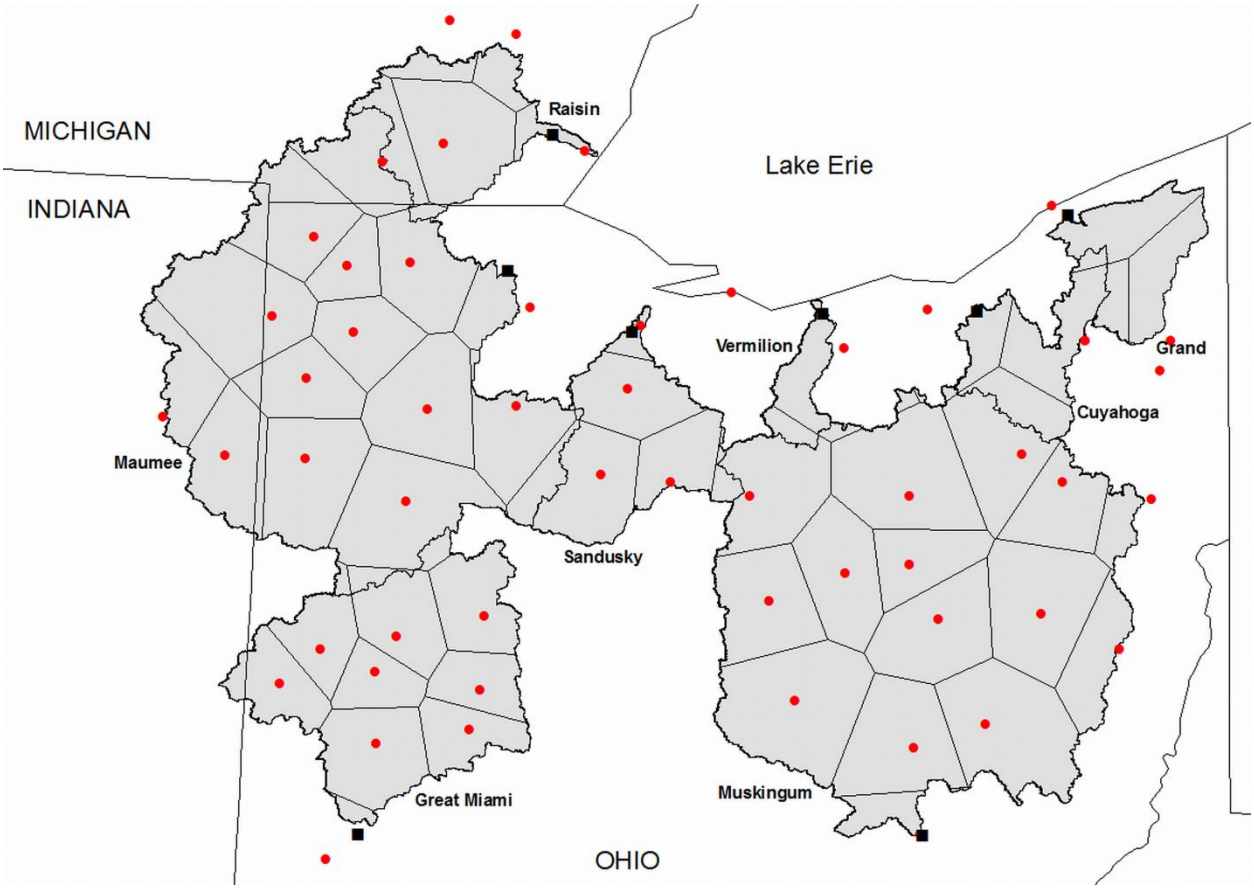

Figure 4.1: Location of all the watersheds with their respective gaging stations and weather stations along with Thiessen polygons for calculating daily mean areal precipitations over watersheds

4.2.3 Analysis of timing

Lag in concentration

The watersheds analyzed in this study are characterized by extensive fertilization and presence of tile-drain systems. Most of the fertilization comprises of N (nitrogen) and P (phosphorus) addition to the soils. In these watersheds the patterns in export of N and P were observed to be different from one another. P binds to the soil particles and is mainly exported by surface runoff and N which is highly soluble is removed from agricultural fields primarily through sub-surface tile drainage. The timing of peaks of TP and SS concentrations were almost identical to each other and also aligned very closely with the hydrograph peaks. On the other

hand, a lag in N concentration peaks compared to the hydrograph peaks was observed in agricultural watersheds (Figure 4.2).

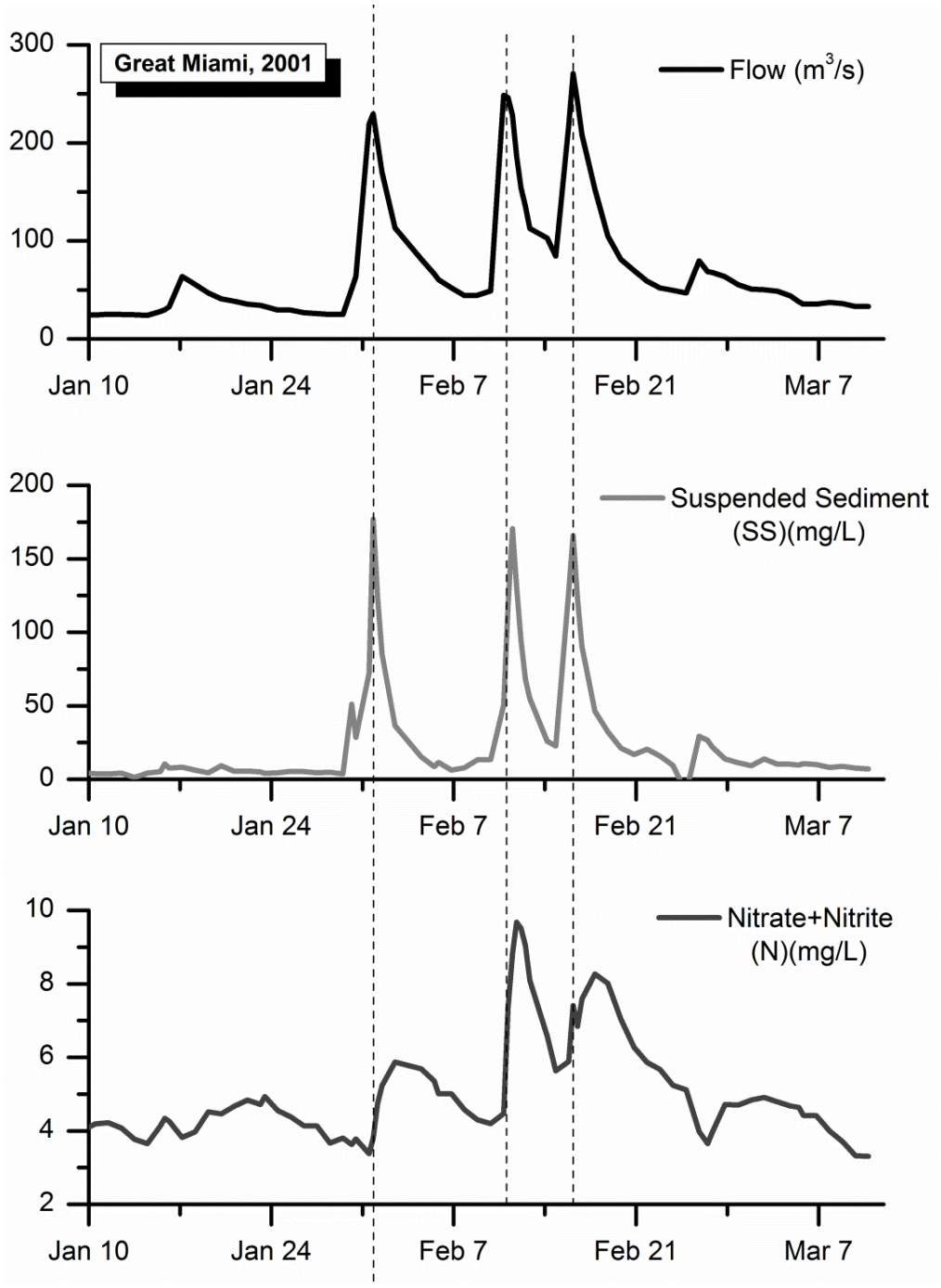

Figure 4.2: Typical hydrographs with Suspended Solids (SS) and Nitrate-N (NO_3-N) pollutographs for a high flow event in the Great Miami watershed. Total Phosphorus (TP) pollutographs were very similar to SS and therefore not included in this figure

This lag possibly occurs due to the "dilution effect" in which the rising limb and peaks of the hydrographs mostly consist of surface runoff which exports very little amounts of N. Additionally, the submergence of tile outlets during larger events backs up the tile drains which possibly contributes to the lag in N concentrations and also slower receding to base values. Such mechanistic differences between fast and slow moving pollutants make it essential to understand the export dynamics for an accurate characterization of load events. Fast moving pollutants loads such as SS and TP loads are exported mainly during high flow events and N loads are exported during high flow events and some duration beyond, as N concentration peaks tend to recede slower than hydrograph peaks.

Critical Storms-high load periods

Numerous studies have reported that pollutant export from watersheds mainly happens during a few high flow periods in a year (Richards and Holloway, 1987; Preston et al., 1989; Lewis, 1996; Robertson and Roerish, 1999; Cooper and Watts, 2002; Markus and Demissie, 2006; and Salles et al., 2007). To quantify the timing of nutrient export within a year it is essential to identify the timing of these critical high flow periods which export most of the loads from the watersheds. One such way is to compute the loads exported during these high flow periods and then to evaluate temporal patterns of the top (largest) load events in a watershed over a year. As there are mechanistic differences between export of fast moving pollutants such as SS and TP and slow moving pollutants such as N, the critical high flow periods were identified differently. A novel base-flow separation technique was used by combining the local minimum and digital recursive filter in the WHAT base-flow separation tool (Kyoung et al., 2005). In-depth details about the pollutant specific high flow period separation is described in Verma et al., (2013). High flow periods were separated for the complete monitoring period of each watershed analyzed in this study. Pollutant loads exported and precipitation totals were then

calculated for these separated high flow periods. Consequently, on a water year scale these high flow periods were arranged in descending order of pollutant loads (top load events) and precipitation totals.

Annual averages- Circular statistics

In hydrology, a lot of commonly measured parameters which show temporal periodicity may be represented on a circular scale instead of the traditionally used linear scale. There is no fixed zero on a circular scale which perhaps better characterizes the parameters which are periodically continuous. For example, the mean daily flow at a gaging station on December 31st would be very similar to that on January 1st. This continuity is better represented on a circular scale rather than on the discontinuous linear scale. Therefore apart from parameters measured in angles (example: wind-speed), circular scales and statistics can also be applied to data such as day of year which exhibit a certain periodicity (Berens, 2009). Continuous or average periodic data can be represented on a circular scale using circular histograms along with its mean resultant vector or it can be used to compute the mean daily value over each periodic cycle with its corresponding regularity. The mean daily value (MDV) represents the temporal occurrence of the mean of the angular data (through direction) with the regularity denoting the concentration of the data around this mean direction. The regularity is usually normalized, ranging between 0 and 1 with higher regularity, indicating that the data is more concentrated around the mean direction. It is important to note that the MDV only denotes the timing of the mean on a circular scale and not its magnitude.

The daily linear time series can be converted to the angular scale using the following set of equations. The day of the maximum parameter value (example: precipitation, flow) in a year i can be expressed on an angular scale in radians (θ_i) by applying the following transformation (Eq. 4.1):

$$\theta_i = JD_i \frac{2\pi}{ND_i} \tag{4.1}$$

where, JD_i is the Julian day of the maximum parameter value in a year and ND_i is the total number of days in year i. After linear data has been transformed to an angular scale, the mean of these transformed values cannot be calculated by simply averaging the data points. The angular values need to be transformed to unit vectors in the two-dimensional plane by using the sine and cosine functions. The regularity can then calculated by taking the square root of the sum of squares of the unit vectors. The mean angular direction $\bar{\theta}$ is then computed using the inverse tangent function. Thereby the MDV is calculated which indicates the occurrence of the maximum parameter value over N years of time-series data (Eq. 4.2).

$$\bar{x} = \frac{1}{N} \sum_{i=1}^{N} \cos(\theta_i)$$

$$\bar{y} = \frac{1}{N} \sum_{i=1}^{N} \sin(\theta_i)$$

$$\bar{r} = \sqrt{\bar{x}^2 + \bar{y}^2} \; ; \; (0 \leq \bar{r} \leq 1) \tag{4.2}$$

$$\bar{\theta} = \tan^{-1}\left(\frac{\bar{y}}{\bar{x}}\right) ; (0 \leq \bar{\theta} \leq 2\pi)$$

$$MDV = \bar{\theta} \frac{\overline{ND}}{2\pi}$$

Markus et al. (2012) modified the traditional MDV and regularity calculations by incorporating weights corresponding to daily parameter values in the calculations. These

modified MDV and regularity calculations added more significance to the extreme parameter values which are essential when temporal trends are being examined. The weighted MDV and regularity values can be calculated using the following set of equations (Eq. 4.3):

$$\bar{x}_w = \frac{1}{N}\sum_{i=1}^{N} w_i \cos(\theta_i)$$

$$\overline{y_w} = \frac{1}{N}\sum_{i=1}^{N} w_i \sin(\theta_i)$$

$$\overline{\theta_w} = \tan^{-1}\left(\frac{\overline{y_w}}{x_w}\right); (0 \leq \bar{\theta} \leq 2\pi) \tag{4.3}$$

$$\overline{r_w} = \sqrt{\bar{x}_w{}^2 + \bar{y}_w{}^2}; \ (0 \leq \overline{r_w} \leq 1)$$

$$MDV = \overline{\theta_w}\frac{\overline{ND}}{2\pi}$$

where, the subscript *w* indicates the weighted estimates and w_i denotes the weight calculated using the maximum parameter value P_i in the year *i* for the N years of record (Equation 4).

$$w_i = N \times \frac{P_i}{\sum_{j=1}^{N} P_j} \tag{4.4}$$

Mean daily values and their corresponding regularity were calculated for flow, precipitation, pollutant concentrations and loads to assess the changes in hydrology of the watersheds analyzed in this research for each water year during the monitoring period. Four watersheds with the longest duration of monitoring data namely Maumee, Sandusky, Cuyahoga and Raisin were selected for this analysis. The Maumee, Sandusky and Raisin watersheds are primarily

agricultural while the Cuyahoga watershed is predominantly urbanized. The Raisin watershed is unique as it has a lot of impoundments dotting the course of Raisin River.

4.3 Results and Discussion

4.3.1 Top load events

Nitrate-N

For each watershed and water year across its monitoring duration, nitrate-N loads (NO_3-N loads) exported and Thiessen weighted precipitation totals during high flow (storm) events were tabulated. In each water year, the top 5 event (storms) in terms of load exported and top 5 precipitation totals during separated events were separated out for further analysis. The top 5 load events carried a large percentage of the annual NO_3-N loads ranging from 24% for the urbanized and point source dominated Cuyahoga watershed to 67% for the agricultural Raisin watershed (Verma et al., 2013). The beginning months of each of these top 5 load events were identified and tabulated. A circular histogram was plotted with total number of monthly top 5 load events and precipitation totals (Figure 4.3). The scales were normalized, by dividing the monthly totals by the maximum total number of top 5 events that occurred over a specific month for both loads exported and precipitation totals. For example from Figure 4.3, for the Cuyahoga watershed over the 25 year monitoring duration most number of top 5 events based on precipitation totals began in September and May. Similarly, most number of top 5 NO_3-N load events began in February. A vector resultant indicated by an arrow (Figure 4.3) was also plotted within the circular charts indicating the net resultant direction and magnitude of the circular histogram.

The results indicated that NO_3-N export from these watersheds mainly occurred in the months between November and April. It was observed that in the agricultural watersheds which

are dominated by non-point sources, typically the most top 5 NO_3-N load events occurred in February-April, while in the forested Grand watershed most top 5 NO_3-N load events occurred in November-December. Conversely, most of the larger precipitation events in these watersheds occurred over the late summer months. It was observed that for top 5 load events, the precipitation totals in winter months were lower than that during summer months. From the results it can be speculated that NO_3-N export typically occurred during winter months as it coincides with the fallow period in these Midwestern agricultural watersheds. The lack of crops results in very little water being taken up by vegetation and thereby mean monthly flows are higher during such months. Snow melt also potentially contributes to higher flows in late winter and early spring months. Thus any precipitation falling over these watersheds in the winter-early spring months coupled with snow melt exports a significant amount of nitrate rich water from agricultural fields. As nitrates are highly soluble in water, any residual and excess amount within the fields get dissolved and exported quickly through the extensive sub-surface tile drain network which is a typical characteristic commonly present in the watersheds studied. Moreover, the practice of fall application of nutrients is still observed in parts of these watersheds which adds nutrients to the fields leaving them highly susceptible to leaching with any significant precipitation event and snow melt. Additionally, the lack of cover crops, conservation tillage and broadcasting of fertilizers rather than injecting them in soil potentially contribute to higher nitrate load export over the winter months in these watersheds. On the other hand very few top 5 NO_3-N load events were observed over the summer months in spite of higher precipitation totals during such events. In summer months, the crop growing cycle is at its peak with significant uptake of water and nutrients by the crops. This inhibits nitrate losses considerably as compared to the winter months evident from very few top 5 load events in the warmer months. However, a large precipitation event after a long dry spell can export substantial N loads. Such occurrences are termed as “first flush” events and were usually seen in

the beginning of summer months albeit only once or twice each year, thereby accounting for a few top 5 NO3-N load events.

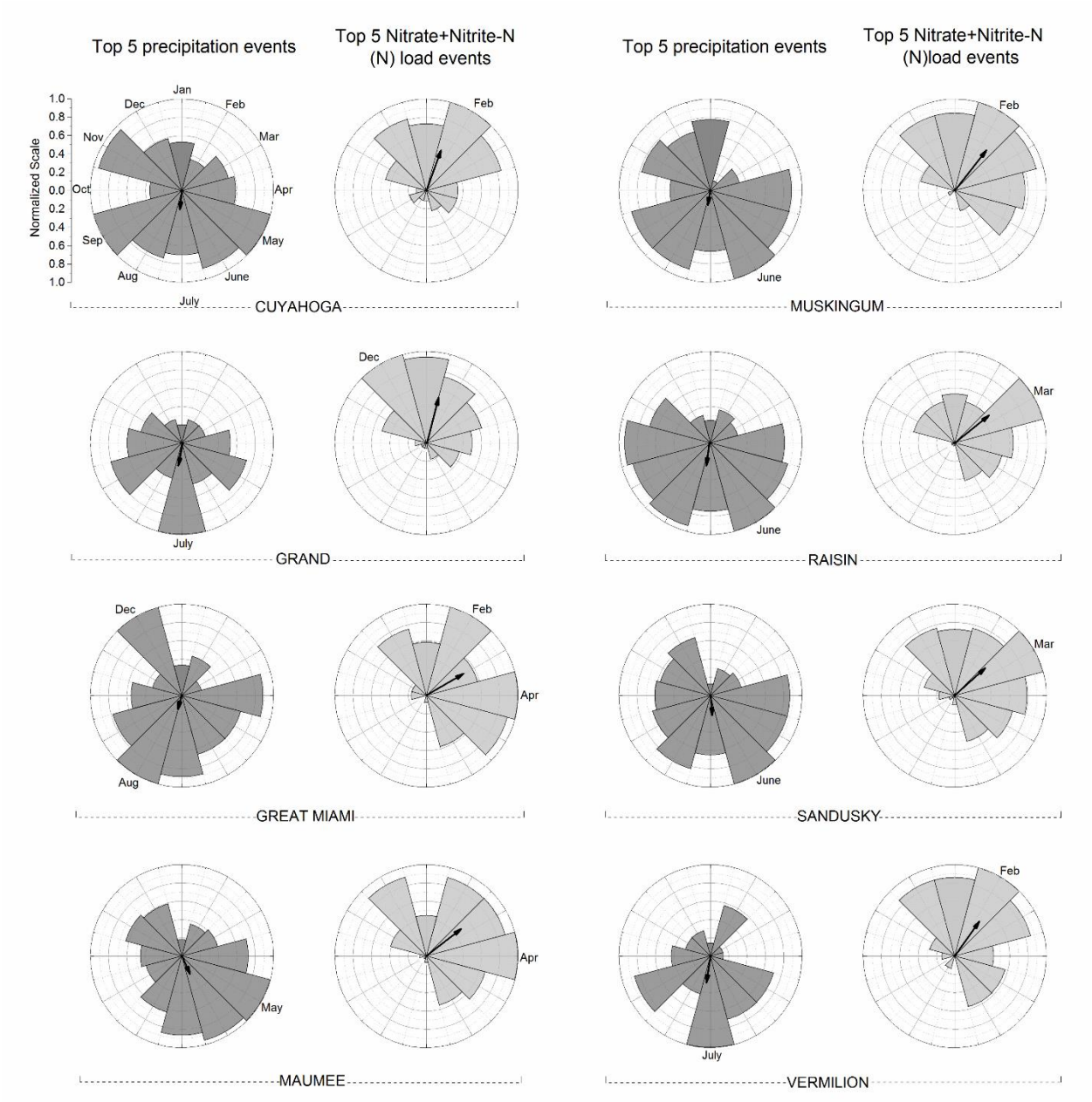

Figure 4.3: Circular histograms on a normalized scale showing number of top 5 NO3-N load events per water year and the top 5 events in terms of precipitation totals over the complete monitoring durations for all eight watersheds analyzed in this study. The months in which the most number of these top 5 events began are highlighted along with the mean resultant vector of the circular histograms indicating the timing (direction) and degree of concentration around the timing (magnitude).

TP and SS

Similar to the NO_3-N load export and precipitation circular histograms, circular histograms were also created for Total Phosphorus (TP) and Suspended Solids (SS). As the patterns in the concentration peaks for these constituents is similar i.e. very close alignment with hydrograph peaks, the top 5 load events separated for both pollutants were concurrent with very few exceptions. The top 5 load events for TP and SS loads exported a large percentage of annual loads ranging from a minimum of 41% and 57% of annual loads exported for the Cuyahoga watershed to a maximum of 71% and 75% of annual loads for the Sandusky watershed respectively (Verma et al., 2013).

Figures 4.4(a) and 4.4(b) show the timing of removal of TP, and SS and timing of most of the precipitation in all eight watersheds in the study. The results indicate that export of TP, and SS was more evenly distributed around the year. Most of the top 5 load events for TP, and SS loads in a water year began sometime from February to May. This result was different from N export which primary occurred earlier from November to April. It can be speculated that as TP, and SS are largely exported by surface runoff and are more influenced by precipitation events. Most of the major export of these constituents occurred in late spring-early summer months, which are characterized by no or small crop presence with very shallow rooting depths. This leaves any applied fertilization susceptible to surface runoff. As the growing season progresses, both the increased plant uptake and deeper rooting depths limits export of these constituents which is characterized by lesser number of critical high flow events in terms of loads exported from June to October. However, any significant precipitation event has the potential to erode loose particulate matter on the soil surface thereby exporting SS and TP primarily through surface runoff. Thus, relatively larger storm events are likely to export substantial amounts of SS and TP leading to a few top 5 load events more evenly distributed throughout the year compared to the top 5 NO_3-N load events. The Cuyahoga watershed, which is predominantly urbanized and has a

higher contribution to annual loads from point sources saw the most even distribution of the top 5 SS and TP load events on an annual scale as compared to the other watersheds which are non-point source dominated agricultural watersheds.

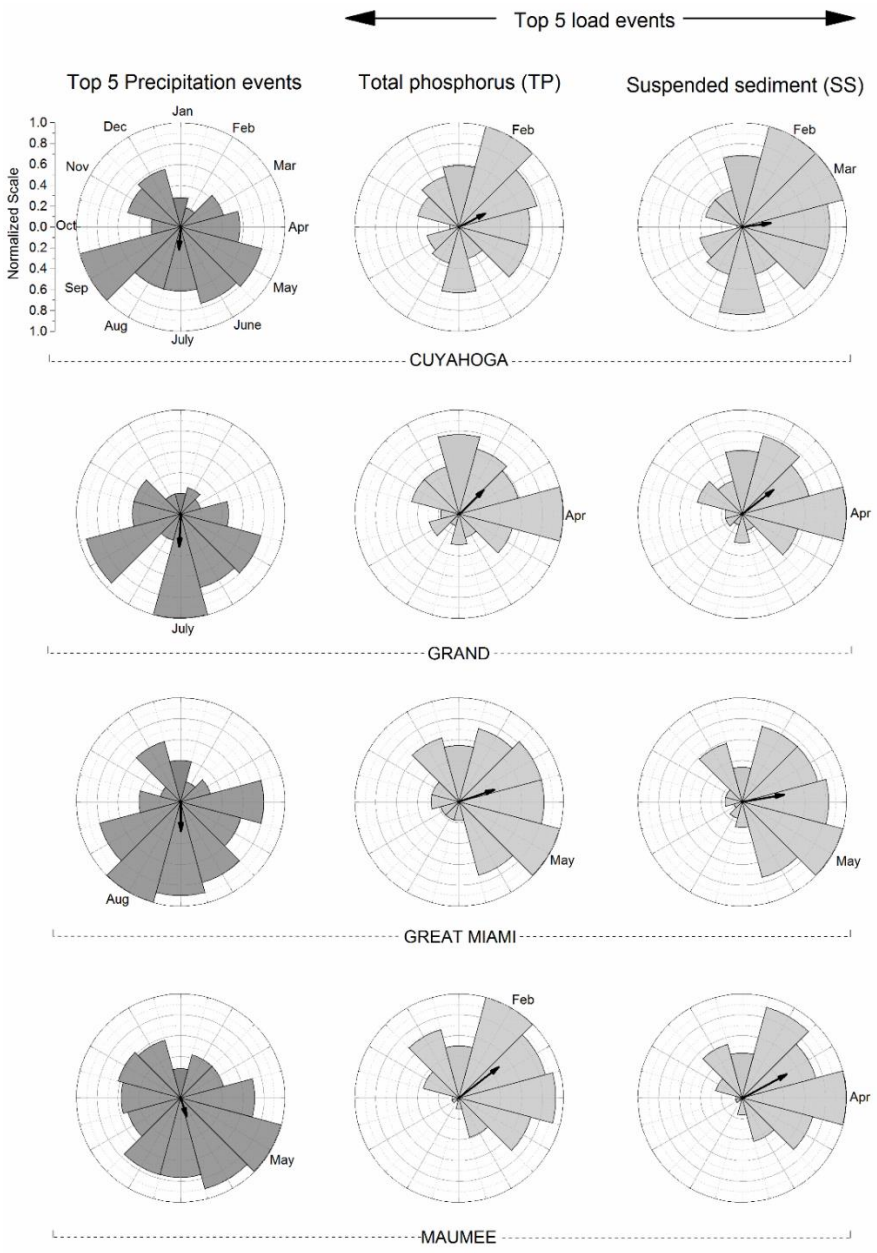

Figure 4.4(a): Circular histograms on a normalized scale showing number of top 5 load events for TP and SS loads per water year and the top 5 events in terms of precipitation totals over the complete monitoring durations for the Cuyahoga, Grand, great Miami and Maumee watersheds. The months in which the most number of these top 5 events began are highlighted along with the mean resultant vector of the circular histograms indicating the timing (direction) and degree of concentration around the timing (magnitude).

Figure 4.4 (cont.)

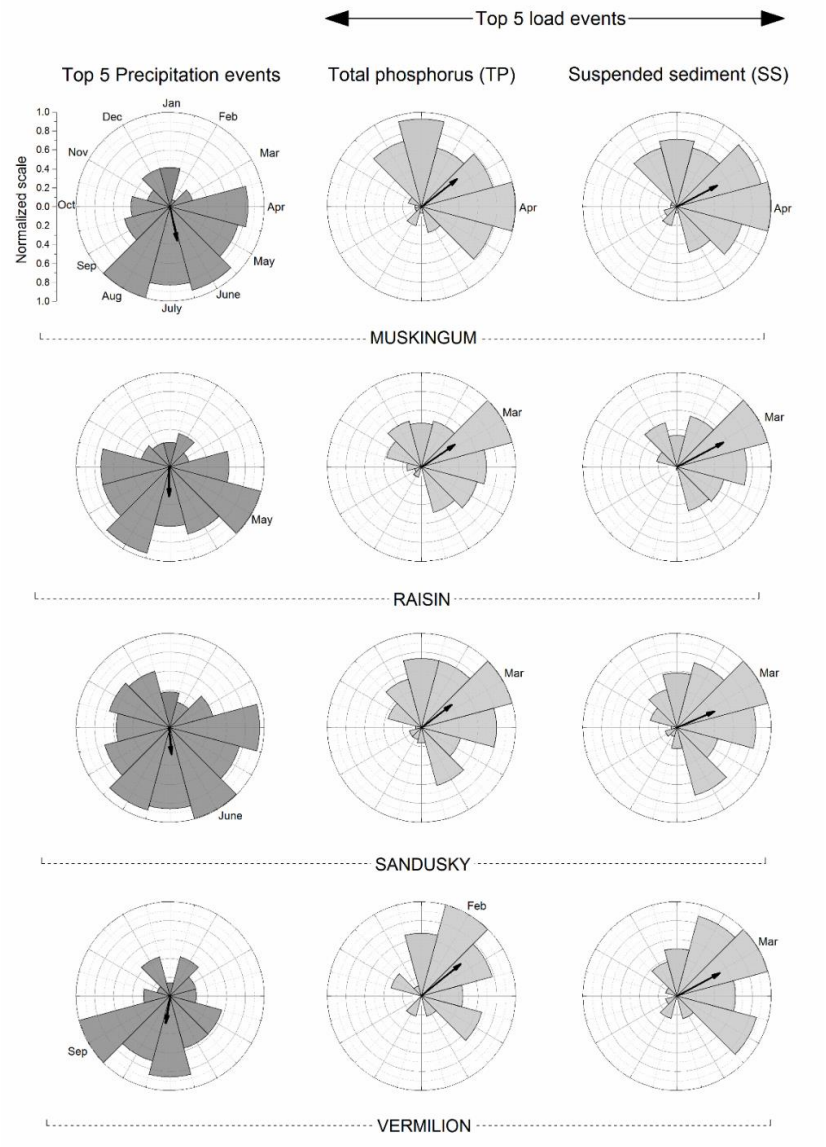

Figure 4.4(b): Circular histograms on a normalized scale showing number of top 5 load events for TP and SS loads per water year and the top 5 events in terms of precipitation totals over the complete monitoring durations for the Muskingum, Raisin, Sandusky and Vermilion watersheds. The months in which the most number of these top 5 events began are highlighted along with the mean resultant vector of the circular histograms indicating the timing (direction) and degree of concentration around the timing (magnitude).

Vector resultants

The results from the circular histograms were compiled together to quantify the timing of NO_3-N and TP (similar to SS) load export through the top load events during a water year in all

watersheds analyzed in the study. Similar results were also computed for precipitation totals over the identified top load events. The vector resultants were plotted on a scale with time on the X axis and their magnitude on the Y axis (Figure 4.5). The timing corresponds to the direction of the vector resultants in the circular histograms and the normalized vector length (vector magnitude) corresponds to the size of the resultant vector. All the vector resultants from the NO_3-N and TP load and precipitation circular histograms were plotted together. The results indicated that the highest precipitation during top load events were concentrated around June-July while the top load events were concentrated around January-April.

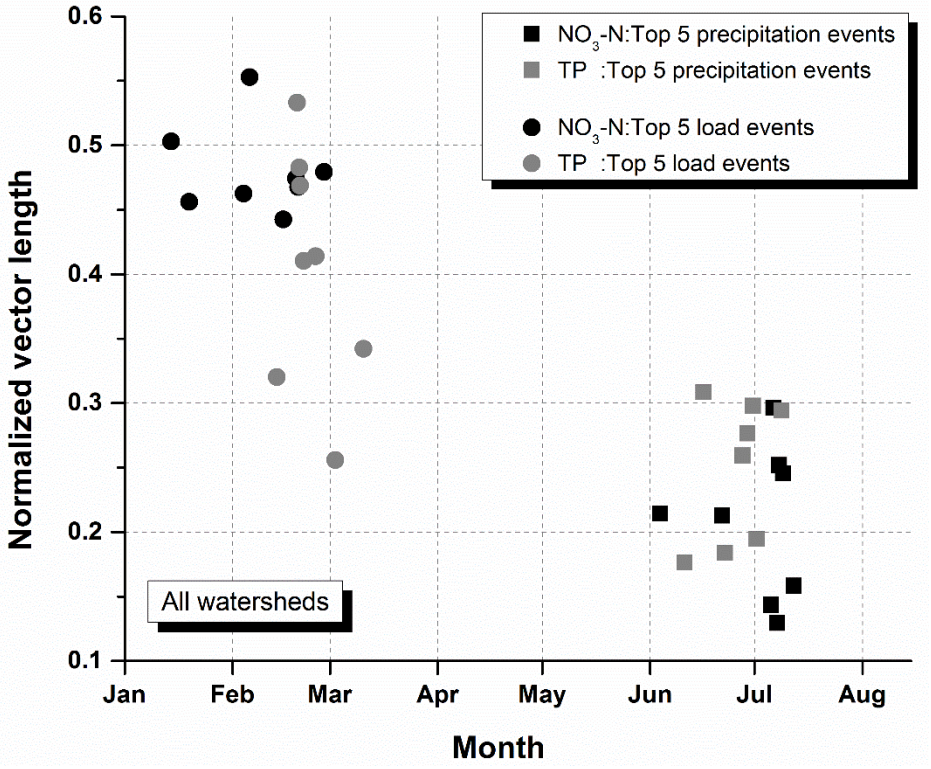

Figure 4.5: Resultant vector magnitudes and temporal occurrences of the top 5 NO_3-N and TP load events per water year and the top 5 events in terms of their precipitation totals for all the eight watersheds analyzed in this study.

The magnitude of these precipitation resultant vector points ranged from about 0.12 to 0.32 indicating a wider spread over a water year. The magnitudes of the top load event vectors were higher compared to precipitation resultant vectors and ranged from 0.45-0.55 and 0.26-0.55 for

NO_3-N and TP respectively. Higher vector magnitudes for NO_3-N indicated that critical high flow events were concentrated around a small period in a water year. Lower vector magnitudes for TP indicated a more even spread of top load events over a water year. These asynchrony in timing of the top load events and top precipitation totals and also in the temporal patterns of NO_3-N and TP export were largely explained by the agricultural practices, the agricultural landscape, pollutant transport mechanisms, primary pollutant sources and land use in the watersheds.

Moving averages of critical high flow events

To analyze the impact of precipitation on criticality of load export in a high flow event a sample watershed, Maumee was selected from the watersheds analyzed in this study. A 30-point moving average was computed for high flow event precipitations separately for critical and non-critical (in terms of NO_3-N loads exported) high flow events (Figure 4.6).

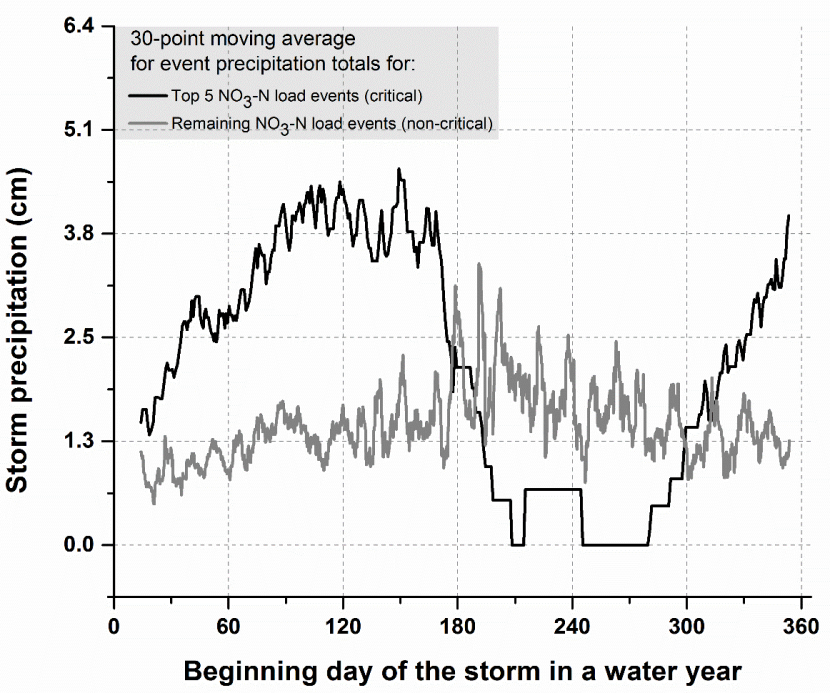

Figure 4.6: 30-point moving average of Thiessen weighted mean areal precipitation for the top 5 NO_3-N load events (critical) and the remaining events (non-critical) over each water year in the complete monitoring duration for the Maumee watershed.

The results indicated that for critical high flow events i.e. high flow events in a water year which were amongst the top 5 by NO_3-N loads exported , total precipitation moving average was higher compared to non-critical high flow events over the first few months (from January to May). This indicated that bigger precipitation events during this period caused a substantial export of NO_3-N. Over the summer months, the very few critical high flow events existed indicated by the presence of flat regions in the curve. The 30-point moving average of critical high flow events was lower as compared to non-critical high flow events indicating that over these summer months fairly large storms too did not export substantial NO_3-N. A bump in the critical high flow precipitation curve is cause by a few very high precipitation totals which occurred in the summer months and likely caused the first flush carrying substantial NO_3-N loads.

Land use impact

To assess the impacts of land-use on export of SS and NO_3-N two similar sized watersheds with different land-usage were selected amongst the eight watersheds used in this study. The Cuyahoga watershed is a fairly urbanized watershed with almost 45% of its land-usage being urban. Only about 20% of its land cover is used for agriculture, with the remaining being under wooded forests. The Raisin watershed is predominantly characterized by row-crop agriculture with about 70% of its land cover being agricultural. Only about 10% of the Raisin watershed has urban land-usage with the remaining being wooded forests.

The contribution of top 5 SS load events per water year to annual loads was calculated for both these watersheds. The results were plotted over their monitoring duration ranging from 1977-2009. The results indicated that although the SS load contributions from top 5 load events were generally slightly lower for Cuyahoga as compared to Raisin, there wasn't any appreciable difference (Figure 4.7). On the other hand, a similar plot for NO_3-N export indicated that Raisin had a much higher percentage of loads that were exported in the top 5 load events in a water

year. The Raisin watershed has a much higher percentage of land-cover under row-crop agriculture and also has a high density of tile-drainage compared to Cuyahoga. Moreover, the Cuyahoga watershed is dominated by point sources unlike the Raisin watershed which is largely non-point source driven. Thus, it can be inferred that NO_3-N export is largely affected by the agricultural presence and the agricultural landscape in a watershed. It can be concluded from this analysis that watersheds in the upper Midwest which are characterized by row-crop agriculture and high density of tile-drainage are more likely to export a significant amount of NO_3-N loads in a few critical high flow events occurring over late winter and early spring months.

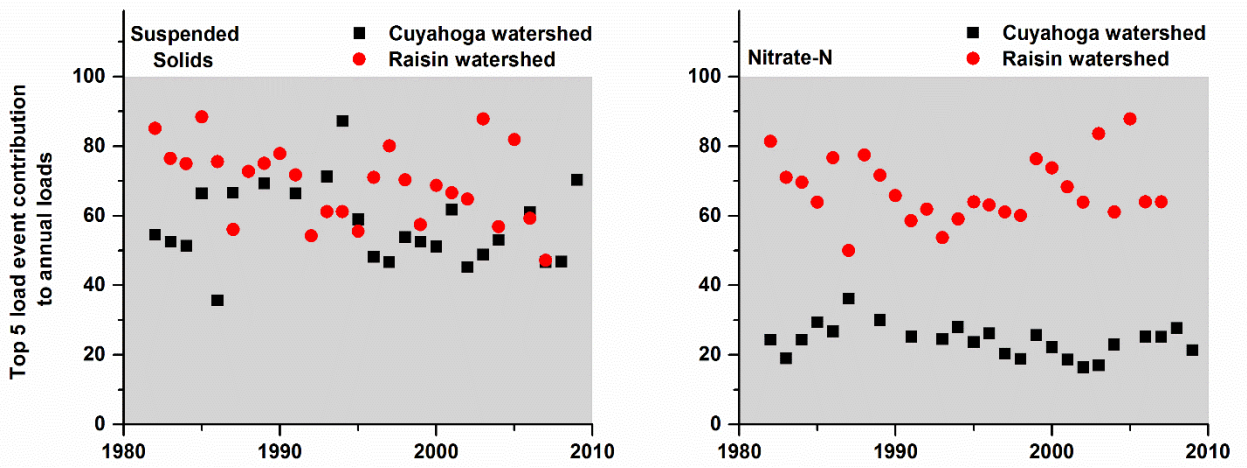

Figure 4.7: A comparison between percentage annual load contributions by Top 5 SS and NO_3-N load events from Cuyahoga and Raisin watersheds over their complete monitoring durations

Maumee average monthly precipitation, loads, and flow

To validate the findings using the critical high flow event analysis, monthly averages of Thiessen weighted precipitation, flow, total phosphorus (TP) and nitrate-N (NO_3-N) loads were computed over the complete monitoring duration of 28 years ranging from 1976-2009. Data were missing for 3 years from 1978-81 and data for 3 years 1977, 1992 and 2007 were removed due to significant gaps in sampling.

The results are presented in Figure 4.8, and they indicate that March had the highest total flow volumes at Maumee. The average monthly NO_3-N and TP loads were very closely aligned with the flow pattern. Relatively lower flow volumes were observed over the summer and fall months and thereby lower loads were exported in these months. Conversely, most of the Thiessen weighted precipitation occurred in late summer to early winter period.

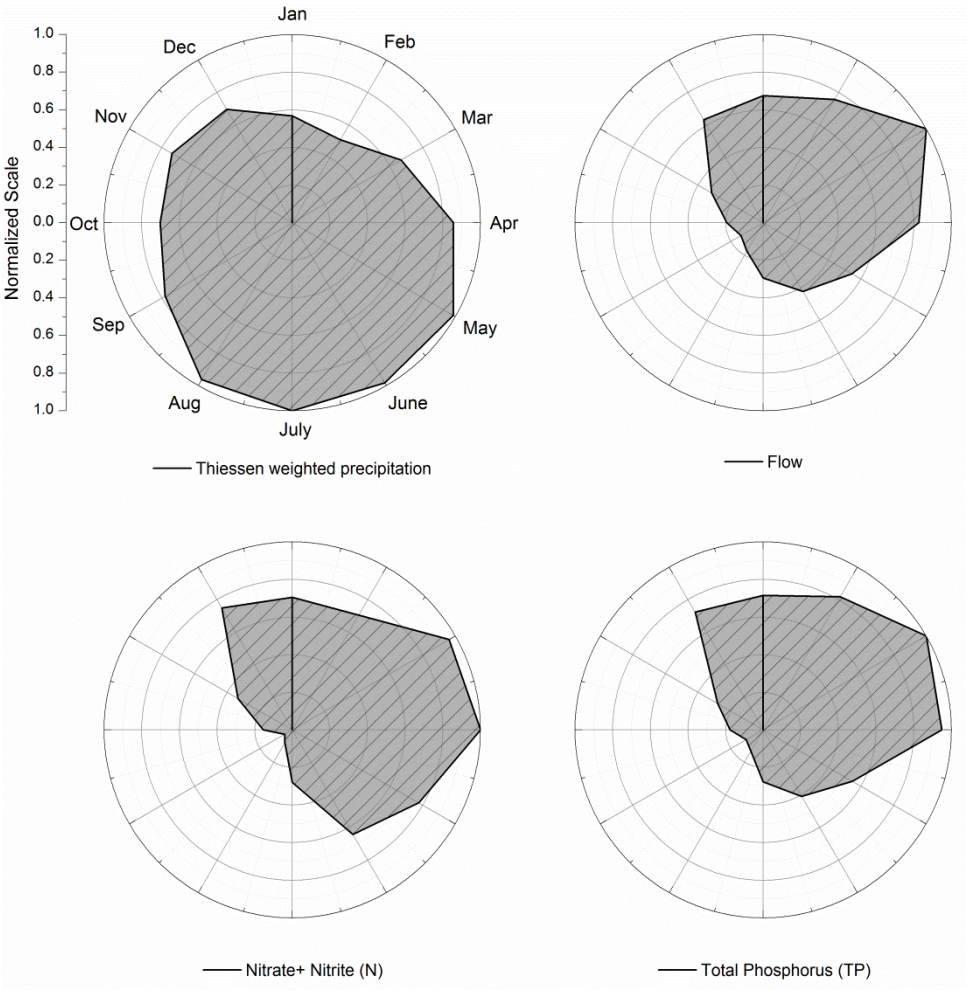

Figure 4.8: Monthly averages of Thiessen weighted mean areal precipitation, flow volumes, TP and NO_3-N loads from the Maumee watershed over 28 years of monitoring duration

This analysis confirms that loads are very closely correlated with flow volumes and snow melt along with frozen ground conditions that significantly affect the nutrient export. Frozen ground conditions coupled with some snow melt over late winter and early spring months carry

a lot of surface runoff and reduce infiltration of water. Thereby, higher flow volumes are observed in such upper Midwestern watersheds over early spring months. However, presence of extensive tile drainage does export a large quantity of NO_3-N with any water that is drained by these systems.

4.3.2 Mean daily values and Regularity

Precipitation

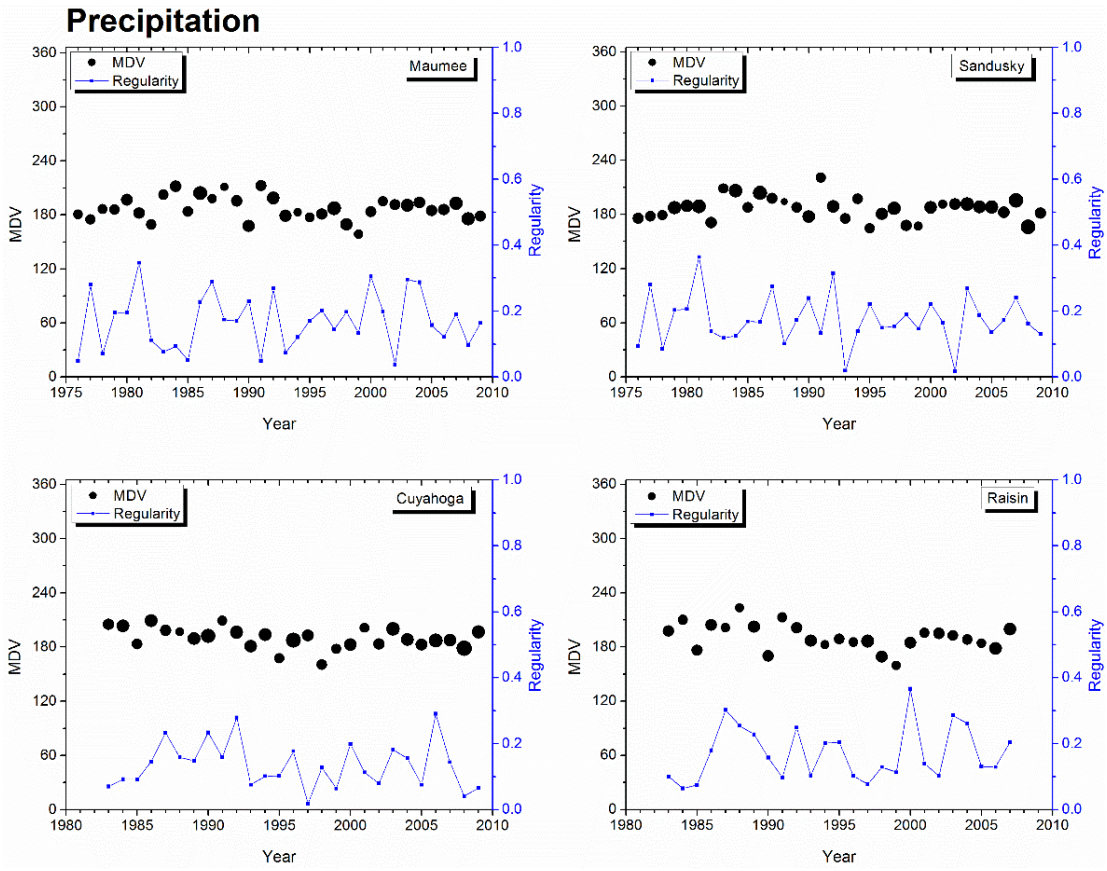

Figure 4.9: Temporal patterns of the mean daily values (MDVs) and their corresponding regularity values for precipitation for the Maumee, Sandusky, Cuyahoga and Raisin watersheds. The MDVs are represented by the black circular dots and their temporal is shown in days after the beginning of the water year. The sizes of the circular dots are proportional to the maximum precipitation observed in a single water year for the four watersheds over their complete monitoring durations.

Figure 4.9 and Table 4.3 summarizes the MDVs and the corresponding regularities for precipitation over the four watersheds for each water year in the monitoring duration. The black

circular dots in the figure denote the timing (1-366 days after the beginning of the water year i.e. October 1st) of the MDVs for precipitation for different water years. The sizes of the circular dots have been rescaled based on total maximum precipitation observed in a single water year in all the four watersheds. As expected, the results indicated that the precipitation patterns in these watersheds are fairly similar to each other with comparable annual amounts, timing of MDVs and also the temporal distribution of precipitation over a water year. The timing of the average MDVs for the four watersheds individually ranged between 187 and 191 days after the start of the water year with standard deviations ranging between 12.6 and 14.5 days. The regularity of the MDVs for the three agricultural watersheds was the same at 0.17 and slightly lower at 0.13 for Cuyahoga. The standard deviation of the average regularity values for all the four watersheds was very close averaging about 0.08. These results implied that precipitation is fairly evenly distributed throughout the year in all these watersheds and there are no significant differences or trends in precipitation occurrence and amounts over the years these watersheds were monitored.

Table 4.3: The average annual mean daily values (MDVs) and regularity values along with the standard deviations for precipitation, flow and SS, TP and NO_3-N concentrations and loads for the Maumee, Sandusky, Raisin and Cuyahoga watersheds over their complete monitoring durations. The MDVs are represented in days after the beginning of the water year (October 1st).

	Precip.		Flow		SS conc.		SS loads		TP conc.		TP loads		NO_3-N conc.		NO_3-N loads	
	μ	σ	μ	σ	μ	σ	μ	σ	μ	σ	μ	σ	μ	σ	μ	σ
MDV																
Maumee	187	12.8	145	26.4	169	20.3	141	38.9	177	13.4	143	35.7	161	18.9	147	29.4
Sandusky	187	12.6	138	27.8	162	18.9	134	34.6	170	16.5	137	36.1	154	25.9	137	33.1
Raisin	191	14.5	146	23.7	172	20.7	139	37.9	182	14.1	142	35.9	163	18.5	143	35.8
Cuyahoga	190	11.7	161	16.1	176	24.3	163	38.8	191	10.6	166	25.3	200	10.8	176	13.7
Regularity																
Maumee	0.17	0.08	0.45	0.17	0.26	0.12	0.56	0.20	0.13	0.07	0.51	0.18	0.31	0.13	0.48	0.17
Sandusky	0.17	0.07	0.49	0.13	0.36	0.13	0.57	0.16	0.19	0.1	0.55	0.16	0.33	0.15	0.50	0.14
Raisin	0.17	0.08	0.42	0.12	0.21	0.10	0.53	0.15	0.12	0.08	0.5	0.14	0.30	0.11	0.51	0.17
Cuyahoga	0.13	0.07	0.30	0.11	0.27	0.12	0.39	0.17	0.15	0.07	0.28	0.11	0.21	0.07	0.15	0.07

Flow

Figure 4.10 and Table 4.3 review the MDVs and their corresponding regularities for the four watersheds assessed. The position of the black circular dots in the figure indicates the MDVs for each water year monitored while their sizes are corresponding to the average annual flow per unit area for the different watersheds. The MDVs indicate the timing of the mean flow occurrence in a watershed, ranging between 1-365 or 366 depending on the number of days in the water year analyzed.

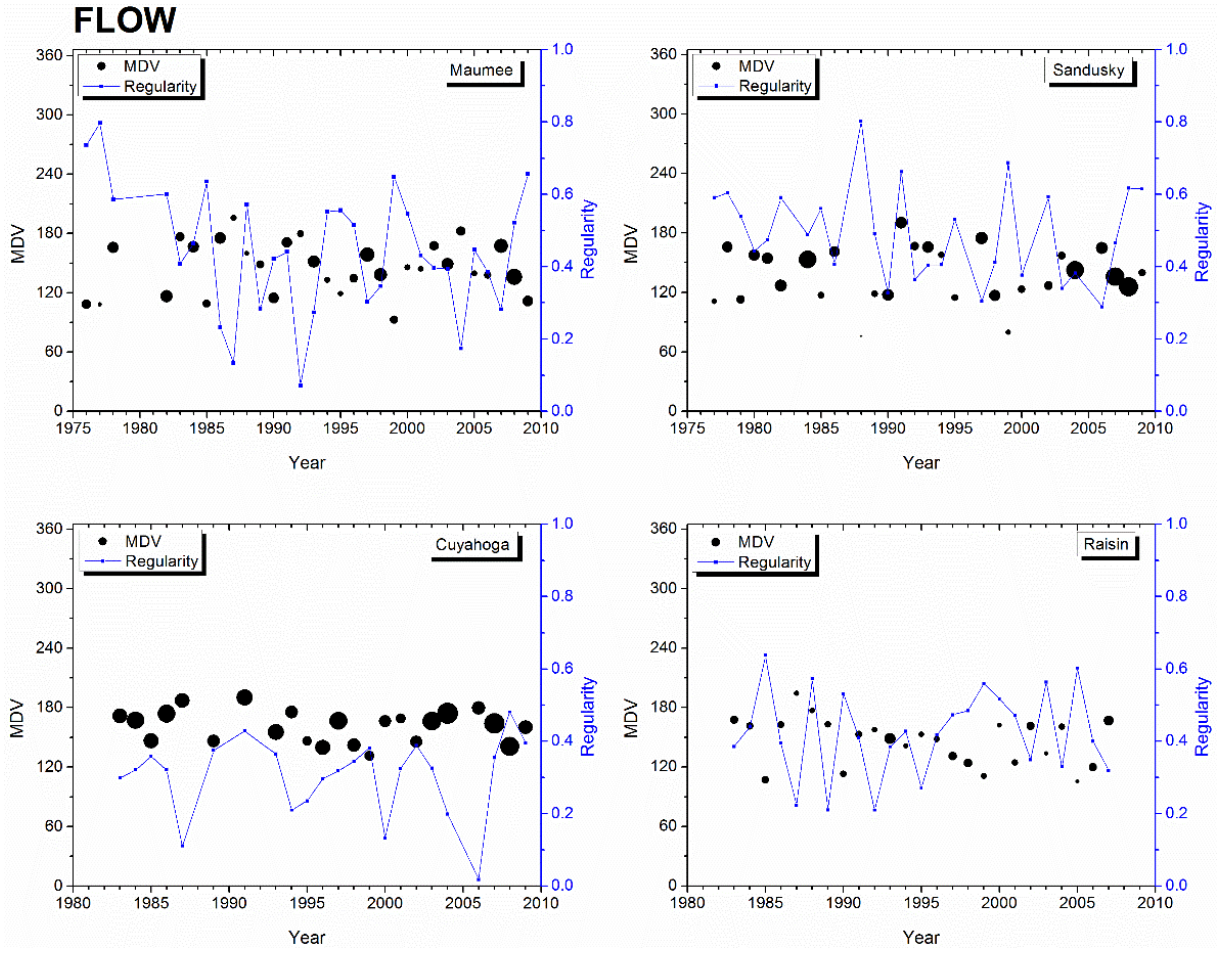

Figure 4.10: Temporal patterns of the mean daily values (MDVs) and their corresponding regularity values for flow for the Maumee, Sandusky, Cuyahoga and Raisin watersheds. The MDVs are represented by the black circular dots and their timing is shown in days after the beginning of the water year. The sizes of the circular dots are proportional to the annual flow per unit area for each water year in the four watersheds over their complete monitoring durations.

No significant trends were observed in the MDV values indicating there hasn't been a change in the temporal distribution of flow over the 2-3 decades of monitoring in these watersheds. However, the results indicated that the average MDVs for the three agricultural watersheds was around 140 days after the beginning of the water year. Some variability was seen in the flow MDVs and the average annual flow per unit area for the Maumee and Sandusky watersheds which can potentially be attributed to the natural variations in precipitation. For these watersheds, the average annual flow per unit area saw some increases especially for the Sandusky watershed towards the end of the monitoring period. The MDVs for flow for the Raisin watershed which is agricultural and very similar in size to the Sandusky watershed were slightly less variable, with a standard deviation of about 24 days compared to 28 days for the Sandusky watershed. Also the average annual flow per unit area from the Raisin watershed was the smallest amongst the four watersheds. These low flow conditions probably occurred due to the presence of impoundments in the watershed which increase the water residence time and surface storage. Many of these actively operated dams managing impoundments, are regulated to be managed as " instantaneous run-of-river mode" as recommended by the Michigan Department of Natural Resources ensuring impoundment inflows equal outflow limiting water level fluctuations (Bosch, 2008). However, as also reported by Bosch (2008) it is not clear if these requirements are followed closely as inferred by communications from downstream communities regarding seasonal fluctuations in lake levels and lowering in preparation for large precipitation events for flood control. The average annual flow per unit area was the highest for the Cuyahoga watershed due to its predominantly urbanized land use. Additionally, the average MDV for flow for the Cuyahoga watershed was 161 which was about 15-20 days later than the average MDVs of the agricultural watersheds. Even the variation in flow MDVs was lower at 16 days which is about 10 days smaller than the average for the agricultural watersheds. Urbanization limits water seepage and storage in the soil profile and the presence of significant impervious land cover aids in greater surface runoff leading to higher flows in the watershed.

The flow regularity results indicated that the highest regularity was observed for the Sandusky watershed being 0.49. This was comparable to the other two agricultural watersheds with flow regularity for Maumee and Raisin watersheds being 0.45 and 0.42 respectively. The variability in the regularity was the highest for the Maumee watershed, with the average standard deviation for the three agricultural watersheds being 0.14. The average regularity for flow for the Cuyahoga watershed was the lowest amongst the four watersheds at 0.30 along with the least variability with a standard deviation of 0.11. These results clearly indicated that the flows in the Cuyahoga watershed is more evenly distributed throughout the year and has the least amount of variation in it due to hydro-climatic and land use forcing. It was observed that for the agricultural watersheds the typically the years with the highest regularities generally had the lower average annual flow per unit area. It can be speculated that this happened in the drier years, when the annual flow was lower and more concentrated in the winter months leading to a higher regularity and a smaller average annual flow per unit area.

Suspended Solids (SS)

Figure 4.11 summarizes the MDV and regularity computations for SS concentrations for the four watersheds analyzed. The sizes of the circular dots is proportional to the maximum average annual SS concentration observed in any of the four watersheds over all the water years the watersheds were monitored respectively. Table 4.3 summarizes the mean and standard deviations for the average SS concentration MDVs and regularity values observed in the watersheds. The MDVs for SS concentrations for all the watersheds were very close to each other with individual averages ranging between 162 and 179 days after the start of the water year. The standard deviations in the MDVs were also similar for all the watersheds ranging between 19 and 25 days. The regularity results indicated that the Raisin watershed had the lowest average regularity value at 0.21 with it being the highest for the Sandusky watershed at 0.36. Thereby, it can inferred that the SS concentrations were more evenly distributed throughout the year in the

Raisin watershed compared to the other watersheds. Interestingly these extremes in average regularity values were found between the Raisin and Sandusky watersheds which are very similar in size and land use. However, the presence of numerous impoundment dams along the Raisin River possibly altered the river nutrient and sediment export dynamics.

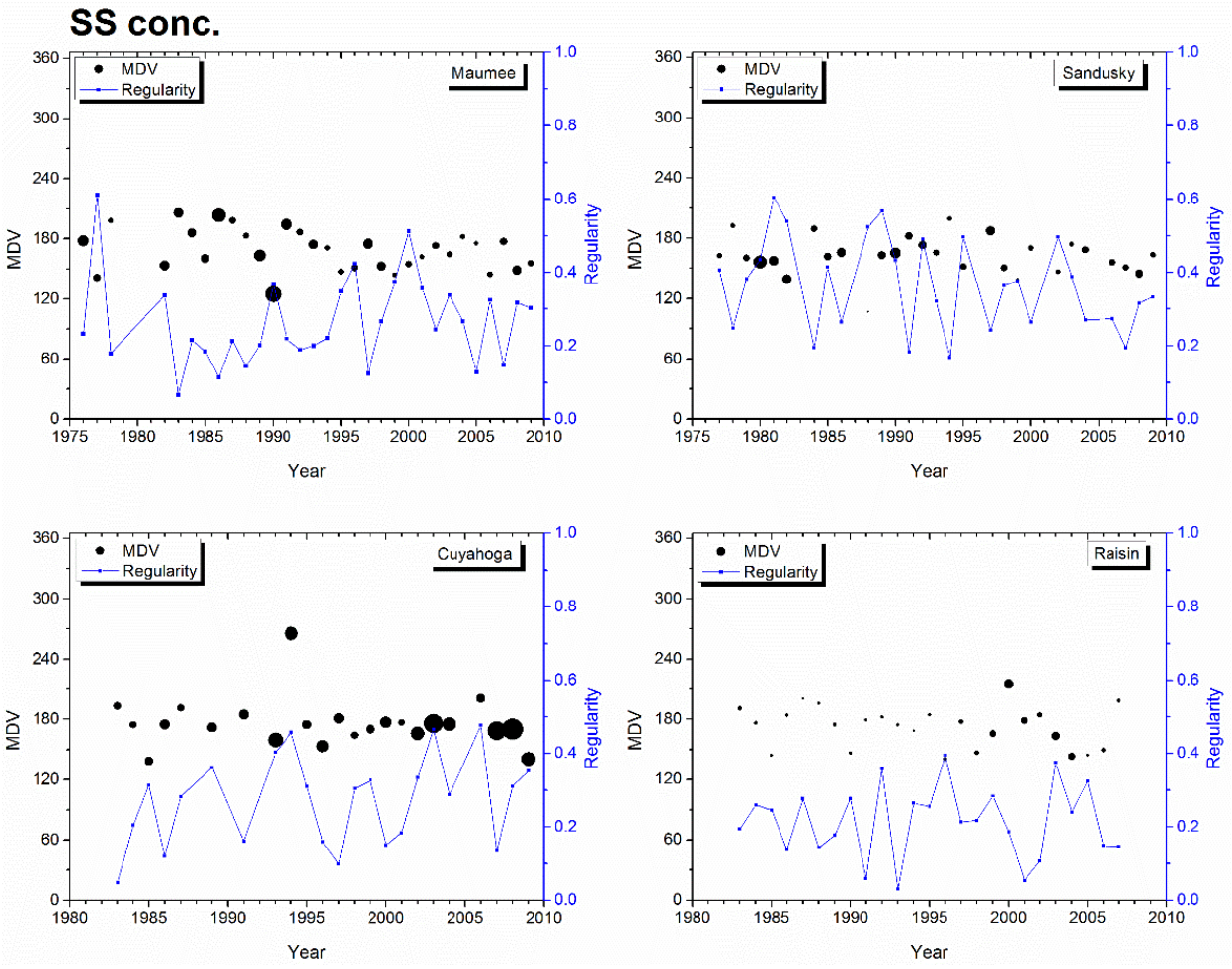

Figure 4.11: Temporal patterns of the mean daily values (MDVs) and their corresponding regularity values for SS concentrations for the Maumee, Sandusky, Cuyahoga and Raisin watersheds. The MDVs are represented by the black circular dots and their timing is shown in days after the beginning of the water year. The sizes of the circular dots are proportional to the maximum annual average SS concentrations observed in a single water year for the four watersheds over their complete monitoring durations.

Impoundments are expected to act as nutrient and sediment sinks in river systems as reported by numerous studies (Alexander et al., 2002; Dixit et al., 2000; Kling et al., 2000). The impoundments have merits in nutrient and sediment removal as they increase water residence

time allowing sediment and associated nutrients to settle down thereby removing them from the river flow (Stanley and Doyle, 2002). Vorosmarty et al. (2003) validated the sediment retention processes in impoundments, reporting that possibly 25-30% of world's annual sediment flux in rivers is trapped in them. This likely reduces the average sediment concentrations, and also possibly offset the impacts of extreme events which might export high SS concentrations from the watershed. The small size of the circular dots for the Raisin watershed confirms the low SS concentrations that were observed in the watershed. The results also indicated that SS concentrations in the Maumee and Sandusky watersheds were higher in the first half of their respective monitoring periods, with some of the highest average annual concentrations recorded after the drier water years (1988 was a dry year and higher concentrations were observed in 1989-1990). The highest annual average SS concentrations were observed in the Cuyahoga watershed, even though it was the smallest amongst all the watersheds. The highly urbanized landscape coupled with the largest share of the point source pollution probably caused export of SS with higher concentrations.

The MDV and regularity results for SS loads are summarized in Figure 4.12 and Table 4.3. The circular black dots denoting MDVs were sized according to average annual SS loads normalized by watershed areas. The average MDVs for SS loads for the three agricultural watersheds was found to be similar ranging between 134 and 141 days. Their corresponding average regularity values were also similar to each other ranging between 0.53 to 0.57 with similar standard deviations for both regularity and MDVs. The peaks in regularity for the Maumee and Sandusky watershed typically occurred during water years with smaller annual average SS loads per unit area as is visually evident from the Figure 4.12. Higher average annual SS loads per unit area for the Sandusky watershed were observed in the earlier part of its monitoring period before 1985. The regularity values were a lot higher for SS loads as compared to SS concentrations indicating that loads exported were more concentrated rather than evenly distributed over the year. The Cuyahoga watershed saw the highest amount of average annual SS

loads per unit area amongst all watersheds evident by the biggest dots showing the MDVs. The average of MDVs for SS loads for the Cuyahoga watershed was 22-29 days later than the agricultural watersheds and was more distributed over the water year evident by its lowest average regularity at 0.39. The effects of different annual average SS concentrations in these watersheds was magnified in the SS loads analysis as is seen by the relatively large dots for the Cuyahoga watershed and virtually indistinguishable ones for the Raisin watershed.

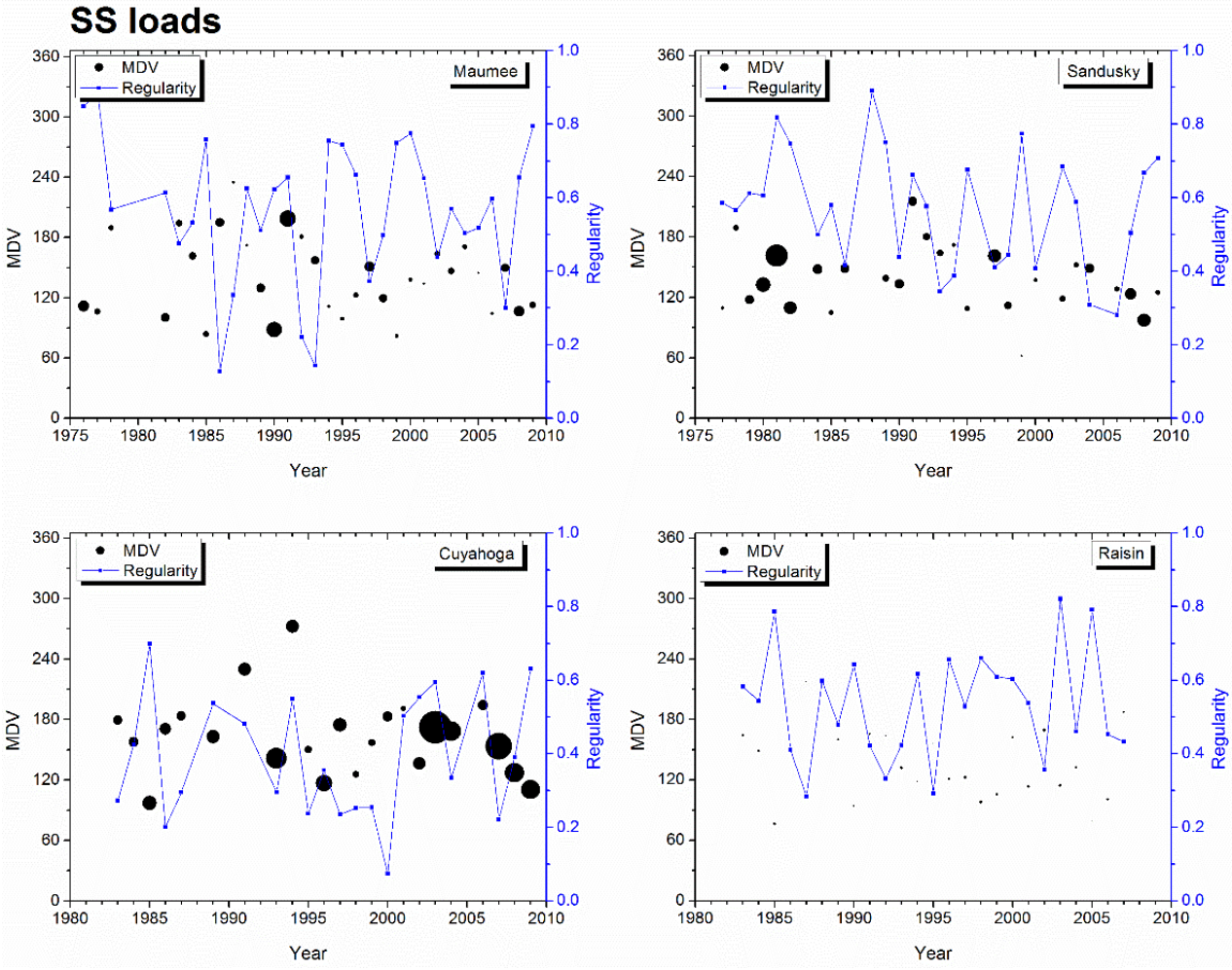

Figure 4.12: Temporal patterns of the mean daily values (MDVs) and their corresponding regularity values for SS loads for the Maumee, Sandusky, Cuyahoga and Raisin watersheds. The MDVs are represented by the black circular dots and their timing is shown in days after the beginning of the water year. The sizes of the circular dots are proportional to the annual SS loads per unit area for each water year in the four watersheds over their complete monitoring durations.

Total Phosphorus (TP)

The MDVs and regularity results for TP concentrations in the four watersheds are summarized in Table 4.3 and Figure 4.13. The results for TP concentrations in all the watersheds followed similar trends to SS concentrations. The average MDVs for the three agricultural watersheds was lower than the urbanized Cuyahoga watershed ranging between 170 and 182 days compared to the 191 days for the latter (Table 4.3). The variability in MDVs for TP concentrations within each watershed was the lowest amongst the three pollutants analyzed. The standard deviations for the MDVs averaged 14.6 days and 10.6 days for the three agricultural and Cuyahoga watersheds respectively. The regularity results were also the lowest for TP concentrations when compared to the other pollutant concentrations, ranging between 0.12 and 0.19 for the Raisin and Sandusky watersheds respectively. The size of the circular dots representing MDVs in the Figure 4.13 was normalized based on the maximum average annual concentration recorded at any of the watersheds studied. Higher annual average TP concentrations were seen for all the watersheds in the first half of their monitoring periods. There was a distinct decline in the annual average TP concentrations for the Cuyahoga watersheds after the mid-1980s, very likely due to the implementation of the NPDES programs regulating point source pollution. Even the Maumee watershed and the Sandusky watershed to some extent saw declines in annual average TP concentrations after policy regulations were placed to reduce P export to the receiving water bodies downstream. Another inference that can be drawn from the Figure 4.13 is that the Cuyahoga watershed had the highest annual average TP concentrations that were observed in these four watersheds, while the Raisin watershed consistently had the lowest annual concentrations potentially due to the presence of the impoundment dams in the watershed.

The MDVs and regularity results for the TP loads are visually represented in the Figure 4.14 and summarized in the Table 4.3. These results were very similar to SS loads with virtually the

same averages and standard deviations for the MDVs and regularity. The sizes of the black circular dots indicating MDVs were sized based on annual TP loads normalized by area.

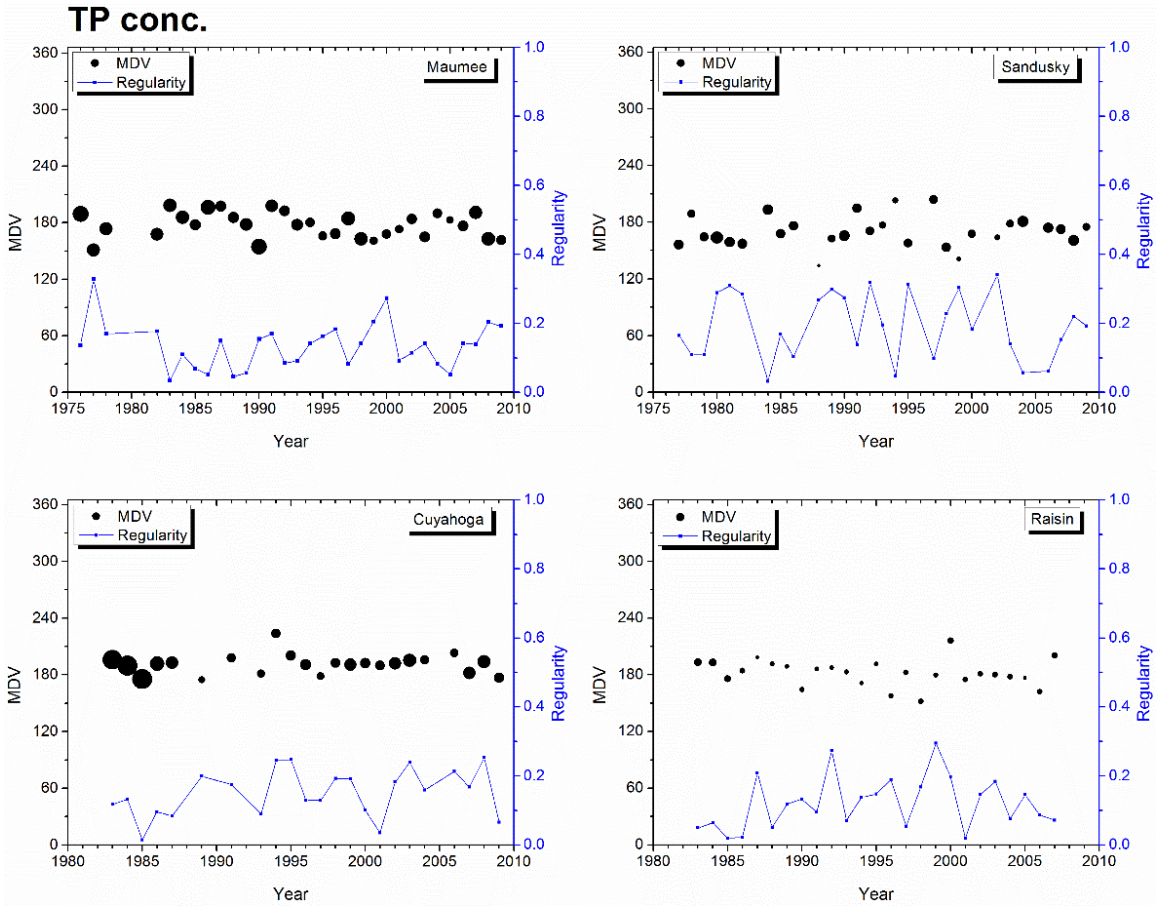

Figure 4.13: Temporal patterns of the mean daily values (MDVs) and their corresponding regularity values for TP concentrations for the Maumee, Sandusky, Cuyahoga and Raisin watersheds. The MDVs are represented by the black circular dots and their timing is shown in days after the beginning of the water year. The sizes of the circular dots are proportional to the maximum annual average TP concentrations observed in a single water year for the four watersheds over their complete monitoring durations.

Overall there was a lot more variation in the temporal averages of the TP loads compared to the TP concentrations over the years these watersheds were monitored. The average MDVs and standard deviations for the three agricultural watersheds was about 141 and 36 days respectively. The average for the MDVs for the Cuyahoga watershed was 166 days with a standard deviation of 25 days. Similar to the SS loads, this average was about 23-29 days later than that of the agricultural watersheds. The regularity results indicated that the TP loads in

these watersheds were a lot more concentrated temporally compared to the TP concentrations, averaging 0.52 and 0.28 for the agricultural and the Cuyahoga watersheds respectively. The relatively lower average regularity seen in the Cuyahoga watershed was likely due to the higher percentage of point sources in the total pollutant loads which are not affected by seasonal changes seen in loading patterns in agricultural watersheds attributed to crop growing cycles.

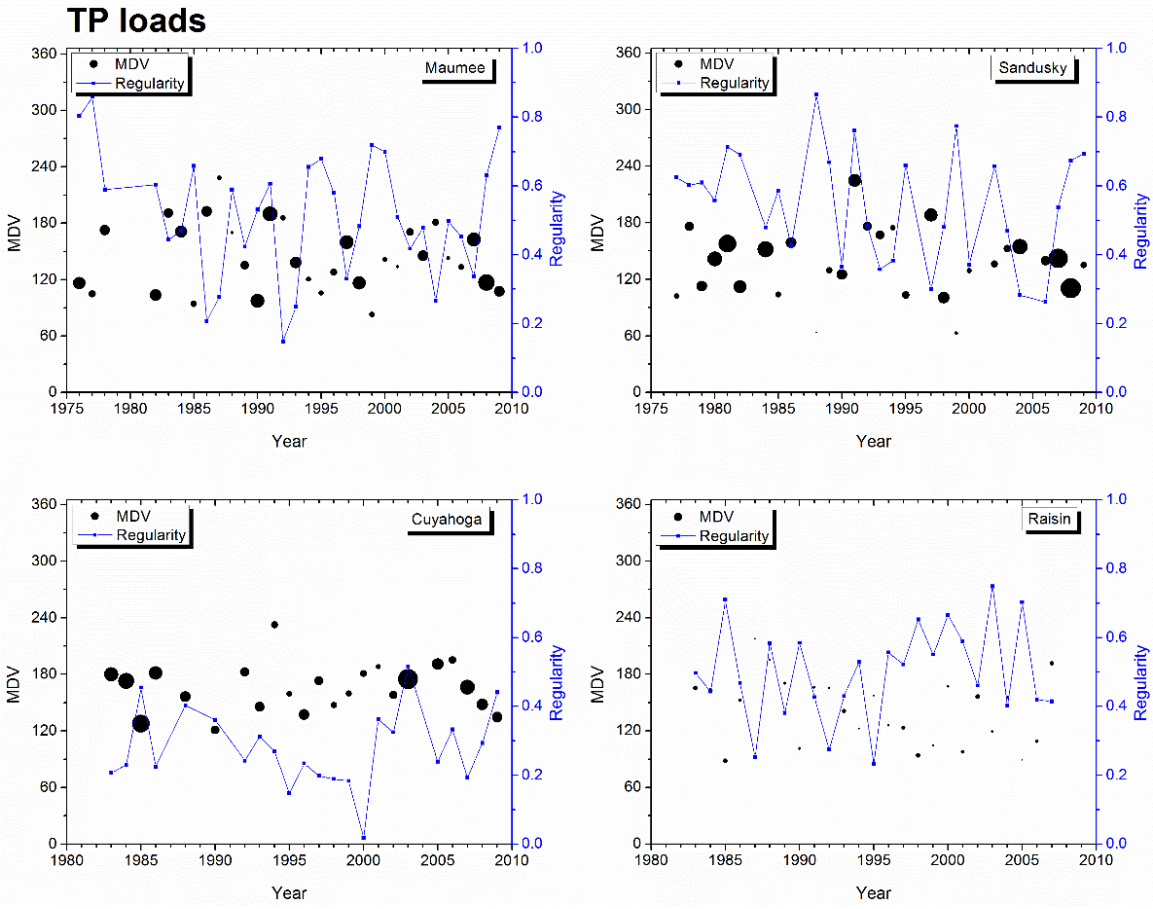

Figure 4.14: Temporal patterns of the mean daily values (MDVs) and their corresponding regularity values for TP loads for the Maumee, Sandusky, Cuyahoga and Raisin watersheds. The MDVs are represented by the black circular dots and their timing is shown in days after the beginning of the water year. The sizes of the circular dots are proportional to the annual TP loads per unit area for each water year in the four watersheds over their complete monitoring durations.

The peaks in regularity values for the Maumee and Sandusky watershed were typically accompanied by lower average annual TP loads, very likely occurring during drier years in which the load export was low and concentration over a small period temporally. For example some of

the lowest annual average TP loads per unit area along with high regularity were observed in the 1988 which was one of the driest years in the past few decades. Conversely in 1993 a relatively wet year the TP loads per unit area had lower regularities indicating they were more distributed temporally. The effects of TP concentrations coupled with watershed sizes were more pronounced on the loads as indicated by the variations in the sizes of the dots indicating MDVs. In the Sandusky and the Cuyahoga watersheds, TP load export was higher prior to 1985 and declined considerably over the next few years. However these loads started rising again in these watersheds over the mid-2000s probably attributed to land management and climatic changes. The average annual TP loads in the Maumee watershed were more consistent with roughly cyclic periods of high and low annual loads. The Raisin watershed saw the lowest amount of TP loads per unit area evident by the small and virtually indistinguishable dots representing the MDVs, very likely due to the impacts of impoundment dams along the Raisin River.

Nitrate-N (NO_3-N)

The MDVs and their corresponding regularity values for NO_3-N concentrations are shown in Figure 4.15 and their averages are summarized in Table 4.3. The patterns in temporal averages of NO_3-N concentrations were distinctly different than SS and TP concentrations. The MDVs represented by black circular dots in the figure were sized relative to the maximum annual average NO_3-N concentration recorded in all of the four watersheds. The MDVs for NO_3-N concentrations for the agricultural watersheds were very similar averaging 159 days along with an average standard deviation of 21 days. For the Cuyahoga watershed the average MDV was 200 days which was about a month and a half later than the agricultural watersheds. It was also less variable with a standard deviation of just about 11 days for close to three decades of monitoring. The regularity results showed that the NO_3-N concentrations in the agricultural watersheds were fairly concentrated around the MDVs averaging 0.31. This was very different than the urbanized and point source dominated Cuyahoga watershed with had a regularity of

0.21, indicating the NO_3-N concentrations were a lot more evenly distributed on a temporal scale as it is devoid of any variations attributed to general agricultural processes and crop growth cycles. The sizes of the dots representing the MDVs indicated that as expected, the highest NO_3-N concentrations were seen in the Maumee and Sandusky watershed which are the traditional agricultural watersheds.

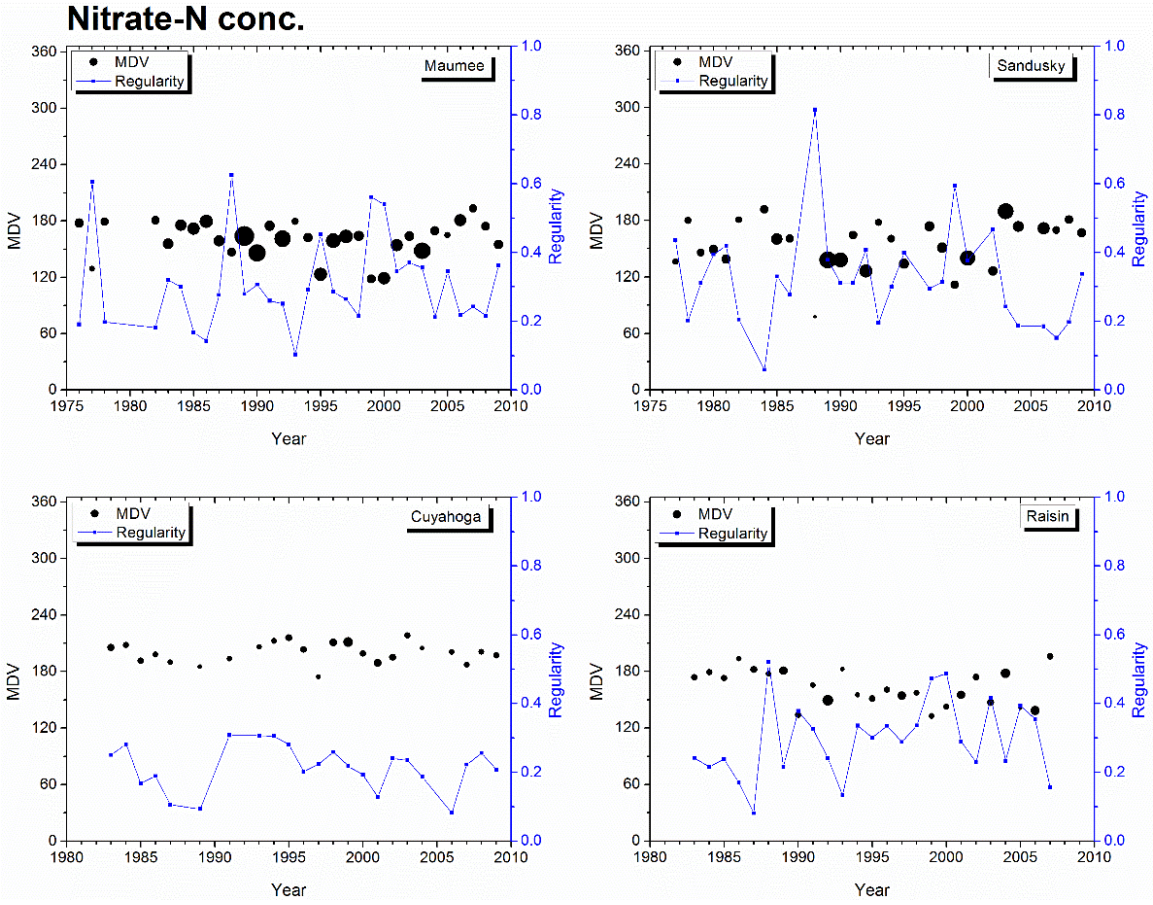

Figure 4.15: Temporal patterns of the mean daily values (MDVs) and their corresponding regularity values for NO_3-N concentrations for the Maumee, Sandusky, Cuyahoga and Raisin watersheds. The MDVs are represented by the black circular dots and their timing is shown in days after the beginning of the water year. The sizes of the circular dots are proportional to the maximum annual average NO_3-N concentrations observed in a single water year for the four watersheds over their complete monitoring durations.

The average annual NO_3-N concentrations in these watersheds peaked around 1990, rising from the earlier monitoring periods concentrations. It has been speculated that this rise occurred due to higher nitrate application rates and increased atmospheric depositions

(Richards and Baker, 1993). Similar to the SS and TP concentrations the peaks in regularity were typically accompanied by lower annual NO_3-N concentrations likely during the drier years (example: 1988) and vice-versa (example: 1993). Years with high regularity which were presumably drier years were followed by years with increased NO_3-N concentrations partly explained by the export of stored nitrates which were not exported in the drier years. Similar findings have also been reported in Midwestern agricultural watersheds by other studies such as (Raymond et al., 2012; Randall and Mulla, 2001; Gentry el al., 2009; and David et al., 1997) The average annual NO_3-N concentrations were low for the Cuyahoga watershed as a result of the urban landscape, and lower for the Raisin watershed as compared to the other agricultural watersheds. However, the differences in NO_3-N concentrations for the Raisin watershed and the other two agricultural watersheds wasn't as large as SS and TP concentrations. This difference is very likely due to the transport of nitrates in the soluble form rather than the particulate form for SS and P, which are more likely affected by the sedimentation in the impoundment dams, a common characteristic in the Raisin watershed.

The MDVs and regularity results for the NO_3-N loads are presented in the Figure 4.16 and Table 4.3. The MDVs are shown by black circular dots which are sized based on average annual NO_3-N loads normalized by watershed areas. The MDVs results indicated that the average values for the three agricultural watersheds was similar ranging between 137 and 147 days and was more than a month earlier for the urbanized and point source dominated Cuyahoga watershed. The variations in the MDVs for the agricultural watersheds was higher than the Cuyahoga watershed with an average standard deviation of 33 days which was a lot higher than about 14 days for the latter. The variations in the MDVs for the agricultural watersheds in over two decades of monitoring was very likely due to the natural variations in precipitation patterns coupled with the changes in land cover and agricultural practices. There were no statistical trends that were observed in the MDVs for NO_3-N loads indicating some stationarity in the timings of the NO_3-N load export in these watersheds for the 2-3 decades of monitoring data.

Similar to the other pollutants, the regularity for NO_3-N loads was a lot higher than its concentrations averaging 0.50 and 0.15 for the agricultural and the Cuyahoga watersheds respectively. As expected, similar to the NO_3-N concentrations the highest NO_3-N loads per unit area were observed in the Maumee and the Sandusky watersheds which are predominantly agricultural.

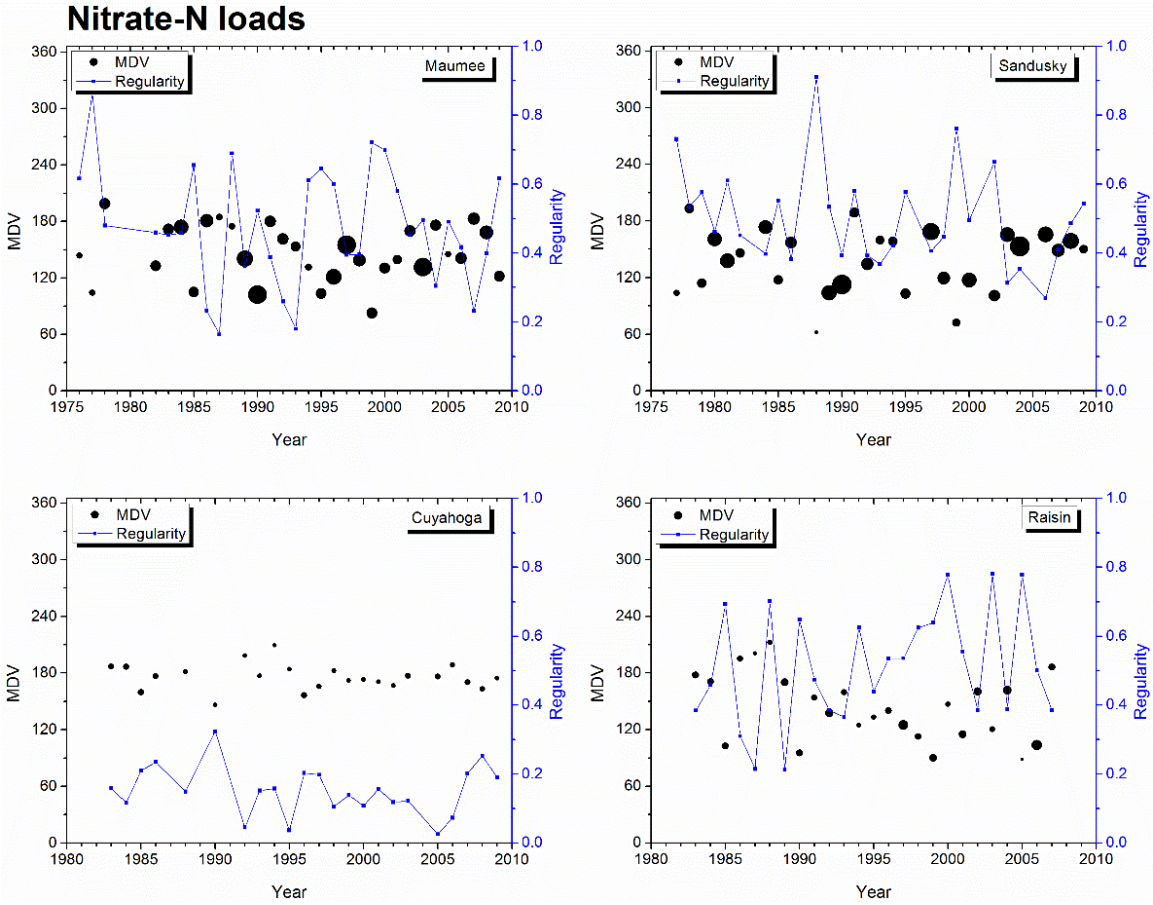

Figure 4.16: Temporal patterns of the mean daily values (MDVs) and their corresponding regularity values for NO_3-N loads for the Maumee, Sandusky, Cuyahoga and Raisin watersheds. The MDVs are represented by the black circular dots and their timing is shown in days after the beginning of the water year. The sizes of the circular dots are proportional to the annual NO_3-N loads per unit area for each water year in the four watersheds over their complete monitoring durations.

The NO_3-N loads per unit area in the Raisin watershed were lower than the other two agricultural watersheds mainly due to lower flow volumes in the watershed attributed to the impoundments. These loads were proportionally higher than the SS and TP loads which are

more likely to be affected by the sedimentation occurring in the impoundment dams. The Cuyahoga watershed saw the least NO_3-N loads per unit area as it had the least area under agriculture and therefore much lesser NO_3-N loads normalized over the complete area of the watershed.

4.4 Summary

This study utilized multiyear daily nutrient (TP and NO_3-N) and sediment (SS) dataset from eight large watersheds lying in the Lake Erie and Ohio River basins to assess temporal patterns in pollutant export from these watersheds. The assessment was done by analyzing the average temporal occurrence and distribution of the top 5 load events for different pollutants and watershed combinations over multiple years of monitoring (8-32 years). Additionally, the patterns in the timing of mean annual precipitation, flow, pollutant concentrations and their respective loads were also examined over the complete duration of monitoring for each watershed. The major conclusions from this research can be summarized as follows:

- There are mechanistic differences in the export of different pollutants, with results indicating that SS and TP pollutographs are closely aligned with the hydrographs. Additionally in the predominantly agricultural tile-drained Midwestern watersheds, typically a lag in NO_3-N pollutographs was seen compared to the hydrographs along with a slower receding curve than SS and TP.
- In the watersheds studied, on average the temporal occurrence of the top 5 NO_3-N load events annually ranged from November to April. For the agricultural watersheds the largest NO_3-N load events typically were even more concentrated temporally, occurring from February to April.
- The temporal patterns in top 5 TP and SS load events annually were very similar to each other, occurring between February and May. These were slightly later

temporally as compared to the top 5 NO_3-N load events and were more distributed on an annual scale with more top load events occurring in the warmer months as compared to NO_3-N.

- There is asynchrony in the largest precipitation and load events in these Midwestern watersheds. Any substantial precipitation event over the winter and early spring months is likely to export large percentages of annual pollutant loads from these watersheds. However, only a very large precipitation event is expected to cause a top 5 pollutant load event annually, over the warmer months with crop growth.
- Pollutant sources along with land-use affect the NO_3-N load event characteristics in these watersheds. An urbanized and point source dominated watershed is likely to have an evenly distributed nitrate loading pattern temporally with lesser significance of the top load events. In comparison an agricultural, tile-drained, non-point source dominated watershed is more likely to have a more concentrated period of nitrate loading on a temporal scale with a few top load events exporting the bulk of annual loads.
- There were no statistically significant trends observed in the timing of the occurrence of the mean annual precipitation, flow, pollutant concentrations and loads in the watersheds studied.
- Flow per unit area in an urbanized watershed was higher than the agricultural watersheds. Also, the regularity of the mean annual flow values for the urbanized watershed were lower indicating a wider annual distribution in flow with less overall fluctuations. Amongst the agricultural watersheds, the lowest flow per unit area was seen in a watershed with numerous impoundment dams which likely impeded the flow increasing the water retention time in the watershed.
- The pollutant concentrations were more evenly distributed throughout the year, but the pollutant loads were more concentrated around certain time periods in a year.

The presence of impoundments potentially aided sedimentation leading to lower SS and TP loads per unit area. Typical loading patterns indicated that higher quantities of loads were exported in relatively wetter years and were more spread out on a temporal scale. Conversely, in the drier years lower annual loads were exported and were concentrated over a small temporal duration.

- The peak nutrient load export and flow in these watersheds was seen in the winter and late spring months. This is temporally separated from the peak algal production and the imminent hypoxic conditions in receiving water bodies, typically seen in the later summer and early fall months. Thereby, any regulatory or management decisions aimed at improving water quality in the downstream water bodies are likely to be more effective by focusing on reducing nutrient load export from Midwestern watersheds over the cooler months.

References

Alexander, R. B., A. H. Elliott, U. Shankar, and G. B. McBride. 2002. "Estimating the Sources and Transport of Nutrients in the Waikato River Basin, New Zealand." *Water Resources Research* 38 (12): 41-423.

Baker, D. B. 1985. "Regional Water Quality Impacts of Intensive Row-Crop Agriculture: A Lake Erie Basin Case Study." *Journal of Soil & Water Conservation* 40 (1): 125-132.

Berens, P. 2009. "CircStat: A MATLAB Toolbox for Circular Statistics." *J Stat Softw* 31 (10): 1-21.

Bosch, N. S. 2008. "The Influence of Impoundments on Riverine Nutrient Transport: An Evaluation using the Soil and Water Assessment Tool." *Journal of Hydrology* 355 (1-4): 131-147.

Bosch, N. S., J. D. Allan, D. M. Dolan, H. Han, and R. P. Richards. 2011. "Application of the Soil and Water Assessment Tool for Six Watersheds of Lake Erie: Model Parameterization and Calibration."*Journal of Great Lakes Research* 37 (2): 263-271.

Cooper, D. M. and C. D. Watts. 2002. "A Comparison of River Load Estimation Techniques: Application to Dissolved Organic Carbon." *Environmetrics* 13 (7): 733-750.

David, M. B., L. E. Gentry, D. A. Kovacic, and K. M. Smith. 1997. "Nitrogen Balance in and Export from an Agricultural Watershed." *Journal of Environmental Quality* 26 (4): 1038-1048.

De Pinto, J. V., T. C. Young, and D. K. Salisbury. 1986. "Impact of Phosphorus Availability on Modelling Phytoplankton Dynamics." *Hydrobiological Bulletin* 20 (1-2): 225-243.

Dixit, A. S., R. I. Hall, P. R. Leavitt, R. Quinlan, and J. P. Smol. 2000. "Effects of Sequential Depositional Basins on Lake Response to Urban and Agricultural Pollution: A Palaeoecological Analysis of the Qu'Appelle Valley, Saskatchewan, Canada." *Freshwater Biology* 43 (3): 319-337.

Gentry, L. E., M. B. David, F. E. Below, T. V. Royer, and G. F. McIsaac. 2009. "Nitrogen Mass Balance of a Tile-Drained Agricultural Watershed in East-Central Illinois." *Journal of Environmental Quality* 38 (5): 1841-1847.

GLWQA.1978.*Great Lakes Water Quality Agreement*. Available at http://www.epa.gov/greatlakes/glwqa/1978/index.html. Last accessed June 6, 2013

Grimvall, A., P. Stålnacke, and A. Tonderski. 2000. "Time Scales of Nutrient Losses from Land to Sea - A European Perspective." *Ecological Engineering* 14 (4): 363-371.

Goolsby, D. A., W. A. Battaglin, B. T. Aulenbach, and R. P. Hooper. 2001. "Nitrogen Input to the Gulf of Mexico." *Journal of Environmental Quality* 30 (2): 329-336.

Hawley, N., T. H. Johengen, Y. R. Rao, S. A. Ruberg, D. Beletsky, S. A. Ludsin, B. J. Eadie, D. J. Schwab, T. E. Croley, and S. B. Brandt. 2006. "Lake Erie Hypoxia Prompts Canada-U.S. Study." *Eos* 87 (32): 313-315.

Heathwaite, A. L., P. J. Johnes, and N. E. Peters. 1996. "Trends in Nutrients." *Hydrological Processes* 10 (2): 263-293.

Kling, G. W., G. W. Kipphut, M. M. Miller, and W. J. O'Brien. 2000. "Integration of Lakes and Streams in a Landscape Perspective: The Importance of Material Processing on Spatial Patterns and Temporal Coherence." *Freshwater Biology* 43 (3): 477-497.

Kyoung, J. L., B. A. Engel, Z. Tang, J. Choi, K. -S Kim, S. Muthukrishnan, and D. Tripathy. 2005. "Automated Web GIS Based Hydrograph Analysis Tool, WHAT." *Journal of the American Water Resources Association* 41 (6): 1407-1416.

Lampman, G. G., N. F. Caraco, and J. J. Cole. 1999. "Spatial and Temporal Patterns of Nutrient Concentration and Export in the Tidal Hudson River." *Estuaries* 22 (2 A): 285-296.

Lewis, J. 1996. "Turbidity-Controlled Suspended Sediment Sampling for Runoff-Event Load Estimation." *Water Resources Research* 32 (7): 2299-2310.

Limburg, K. E., M. A. Moran, and W. H. McDowell. 1986. "The Hudson River Ecosystem." *The Hudson River Ecosystem*.

Markus, M. and M. Demissie. 2006. "Predictability of Annual Sediment Loads Based on Flood Events." *Journal of Hydrologic Engineering* 11 (4): 354-361.

Markus, M., D. J. Wuebbles, X. -Z Liang, K. Hayhoe, and D. A. R. Kristovich. 2012. "Diagnostic Analysis of Future Climate Scenarios Applied to Urban Flooding in the Chicago Metropolitan Area." *Climatic Change* 111 (3): 879-902.

Michalak, A. M., E. J. Anderson, D. Beletsky, S. Boland, N. S. Bosch, T. B. Bridgeman, J. D. Chaffin, et al. 2013. "Record-Setting Algal Bloom in Lake Erie Caused by Agricultural and Meteorological Trends

Consistent with Expected Future Conditions." *Proceedings of the National Academy of Sciences of the United States of America* 110 (16): 6448-6452.

Mourad, D. S. J. and M. van der Perk. 2009. "Spatio-Temporal Patterns of Nutrient Concentrations and Export in a North-Eastern European Lowland Catchment." *Hydrological Processes* 23 (13): 1821-1833.

Preston, S. D., V. J. Bierman Jr, and S. E. Silliman. 1989. "An Evaluation of Methods for the Estimation of Tributary Mass Loads." *Water Resources Research* 25 (6): 1379-1389.

Rabalais, N. N., R. E. Turner, and D. Scavia. 2002. "Beyond Science into Policy: Gulf of Mexico Hypoxia and the Mississippi River." *Bioscience* 52 (2): 129-142.

Randall, G. W. and D. J. Mulla. 2001. "Nitrate Nitrogen in Surface Waters as Influenced by Climatic Conditions and Agricultural Practices." *Journal of Environmental Quality* 30 (2): 337-344.

Raymond, P. A., M. B. David, and J. E. Saiers. 2012. "The Impact of Fertilization and Hydrology on Nitrate Fluxes from Mississippi Watersheds." *Current Opinion in Environmental Sustainability* 4 (2): 212-218.

Richards, R. P. and D. B. Baker. 1993. " Trends in Nutrient and Suspended Sediment Concentrations in Lake Erie Tributaries, 1975-1990." *Journal of Great Lakes Research* 19(2):200-211.

Richards, R. P., D. B. Baker, J. W. Kramer, D. E. Ewing, B. J. Merryfield, and N. L. Miller. 2001. "Storm Discharge, Loads, and Average Concentrations in Northwest Ohio Rivers, 1975-1995." *Journal of the American Water Resources Association* 37 (2): 423-438.

Richards, R. P. and Holloway J. 1987. "Monte Carlo Studies of Sampling Strategies for Estimating Tributary Loads." *Water Resources Research,* 23 (10): 1939-1948.

Robertson, D. M. and E. D. Roerish. 1999. "Influence of Various Water Quality Sampling Strategies on Load Estimates for Small Streams." *Water Resources Research* 35 (12): 3747-3759.

Royer, T. V., M. B. David, and L. E. Gentry. 2006. "Timing of Riverine Export of Nitrate and Phosphorus from Agricultural Watersheds in Illinois: Implications for Reducing Nutrient Loading to the Mississippi River." *Environmental Science and Technology* 40 (13): 4126-4131.

Salles, C., M. G. Tournoud, and Y. Chu. 2007. "Estimating Nutrient and Sediment Flood Loads in a Small Mediterranean River." *Hydrological Processes* 22 (2): 242-253.

Soballe, D. M. and B. L. Kimmel. 1987. "A Large-Scale Comparison of Factors Influencing Phytoplankton Abundance in Rivers, Lakes, and Impoundments." *Ecology* 68 (6): 1943-1954.

Stanley, E. H. and M. W. Doyle. 2002. "A Geomorphic Perspective on Nutrient Retention Following Dam Removal." *Bioscience* 52 (8): 693-701.

Verma, S., A. Bartosova, M. Markus, and R. A. Cooke. 2013. " Annual riverine pollutant load export in Midwestern watersheds: The role of large load events". *Submitted, Journal of Hydrology*

Vörösmarty, C. J., M. Meybeck, B. Fekete, K. Sharma, P. Green, and J. P. M. Syvitski. 2003. "Anthropogenic Sediment Retention: Major Global Impact from Registered River Impoundments." *Global and Planetary Change* 39 (1-2): 169-190.

Zhang Jing, Yan Ju, and Zhang Zai-Feng. 1995. "Nationwide River Chemistry Trends in China: Huanghe and Changjiang." *Ambio* 24 (5): 275-279.

CHAPTER 5

Climate Change Impacts on Flow, Sediment and Nutrient Export in a Great Lakes Watershed Using SWAT

Abstract

Climate change due to elevated global atmospheric carbon dioxide concentrations has the potential to impact the hydrological processes within watersheds in the future. Thereby, it is critical to quantify these impacts for better management of water resources in the coming decades. This research aims at understanding the impacts of projected climate change on the hydrological processes within the Maumee River watershed lying in the Lake Erie basin. The watershed is large (16,395 km^2) and predominantly agricultural (73%) and is the biggest contributor of sediment and nutrient loads to Lake Erie annually. The Soil and Water Assessment Tool (SWAT) was used to evaluate the impacts of projected change in temperature and precipitation for the mid-century (2045-2055) and late-century (2089-2099) time-periods on the flow, sediment and nutrient loading in the watershed. The model was calibrated and validated for a baseline time-period of 1995-2005. Downscaled ensemble projected climate data from three Global Circulation Models (GCMs) namely CGCM3, GFDL-CM2 and HadCM3 for the IPCC A1B scenario was then used to assess future changes in water quantity and quality in the watershed. The results indicated that projected climate change will significantly alter the hydrological processes in the watershed. Compared to the baseline time-period, a 2.9^oC rise in annual average temperature along with a 3.2% fall in annual precipitation in the mid-century time-period is projected to reduce annual flow volumes, and suspended solids (SS), total phosphorus (TP), nitrate (NO_3) loads by 8.5%, 10.4%, 8.5% and 9.9% respectively. Similarly, for the late-century time-period a 4.3^oC rise in annual average temperature along with a 5.6% rise in annual precipitation is projected to increase annual flow volumes, and suspended solids (SS), total phosphorus (TP), nitrate (NO_3) loads by 9.7%, 19.6%, 3.5% and 6.8% respectively. Temporal shifts in climatic conditions were also projected for both the future time-periods with higher temperatures throughout the year along with wetter winters and drier summers. Thus, higher flows, sediment and nutrient loads were projected to occur in the winter and spring months. Implications of these changes would include possible lengthening of crop growing

cycles and the need for increased focus on winter pollutant loadings for TMDL guidelines and overall reduction in annual loadings.

Keywords: Climate change, SWAT, watershed modeling, Lake Erie, sediment loads, nutrient loads

5.1 Introduction

The last century has seen a drastic increase in carbon dioxide and other greenhouse gases emissions (Chaplot, 2007; IPCC, 2012). This increase has been primarily attributed to anthropogenic sources (Wu et al., 2012) and has been quicker over the past few decades (Raupach et al., 2007). Numerous studies have estimated the magnitude and direction of such global mean changes along with studying their impacts on global carbon and water balances (Trenberth, 1999, Trenberth et al., 2007, Meehl et al., 2007, Kundzewicz, 2008, Schuur et al., 2008, Mu et al., 2011). Higher carbon dioxide concentrations in the earth's atmosphere enhance the green-house effect and directly affect the global temperatures and consequently precipitation patterns. There is scientific consensus on the changes in global mean carbon dioxide concentration, temperature, and precipitation happening over the last several decades (Fontaine, 2001). Such global climate change along with increases in carbon dioxide concentrations is already having discernible effects on various environmental systems, including effects on the hydrological cycle at both the global and regional scales (Ficklin et al., 2009). Generally accepted impacts of climate change on hydrological cycle include changes projected in the intensity, frequency, duration, spatial extent, and timing of extreme weather and climate events (IPCC, 2012). Such changes are likely to cause rise of sea level, glacial melting, and variations in precipitation amounts, intensity and distribution along with an increase in the frequency of extreme events such as floods and droughts (IPCC, Dibike and Coulibaly, 2007, Milly et al., 2008, Praskievicz and Chang, 2009).

These changes are projected to further increase in this century, with the magnitude of the changes varying based on several emission scenarios along with land and ocean climatic

feedbacks (Chaplot, 2007; IPCC, 2012). Subsequently, the hydrological cycle is expected to be further impacted with changes occurring in various watershed scale processes such as evapotranspiration, runoff, streamflow, water yields, soil moisture, soil erosion and nutrient losses. Labat et al. (2004), using historical climate data demonstrated that a 1 ^{o}C rise in global temperatures increased the mean global runoff by 4%, attributed to increased oceanic evaporation. The changes in precipitation patterns coupled with increase in potential evapotranspiration might lead to significant changes in river runoff (Kundzewicz et al., 2007). Bronstert et al. (2002) explained the potential increase in surface runoff mainly through infiltration excess processes attributed to increased intensity of precipitation coupled with soil surface crusting. Arnell (2003) showed the effects of climate change on evapotranspiration rates, soil moisture and altered flow regimes in rivers in Britain. Park et al. (2011) simulated future changes in evapotranspiration, groundwater recharge and streamflow based on climate change and land use change both separately and simultaneously for a large forested watershed in South Korea. Bouraoui et al. (2002) demonstrated how climate change modifies the transformation and transport characteristic of nutrients from a watershed in northern England. Changes in precipitation patterns are also expected to directly affect the soil erosive processes from watersheds as simulated by Pruski and Nearing (2002) who indicated that a 1% rise in precipitation amounts and intensity will increase soil erosion by about 1.7% at multiple locations in contiguous US. Overall, changes in runoff, flow regimes, sediment and nutrient export from watersheds attributed to climate change, mainly precipitation variations, would irreversibly affect soil resources and cause both off and on-site effects such as floods, water pollution, reservoir damage, fertility losses and soil erosion (Chaplot 2007). All these studies have described the sensitivity of watershed scale processes to the changes in atmospheric carbon dioxide concentrations, increasing temperature and precipitation. Implications of such changes for water resources, water quality and quantity, agriculture and social issues have thereby been generally identified (Fontaine et al., 2001). However, uniformly accepted conclusions are still

unavailable and less understood along with a lack of quantitative results on the effects of climate change especially at the regional scales.

Anticipating changes in the hydrologic cycle and thereby water resources has generally been done by using physically-based hydrologic models coupled with climate scenarios which are based on General Circulation Models (GCMs). The hydrological models provide a basis to evaluate the relationships between climate parameters, anthropogenic activities along with water resources and predict runoff volumes, water yields, evapotranspiration rates and sediment and nutrient losses. These models are based on equations governing the conservation of mass, momentum and energy. As the parameters of these models have physical meanings, they can use commonly measured hydro-climatic parameters such as precipitation and temperature along with physical characteristics of the watershed such as land-use, soil types, elevation and slope as model inputs to simulate various hydrological processes at varied spatial and temporal scales. In principle, once calibrated, these models can be applied outside the range of conditions used for calibration to understand the sensitivity of the watershed processes to examine the climate change effects. It is imperative to understand that these sensitivity assessments provide invaluable insights into the direction of possible changes in the hydrological systems due to climate change but do not necessarily give projections of the future changes (Arnell and Liv, 2001; Ficklin et al., 2009).

The objective of this study was to assess the overall impact of climate change on the hydrology of a large agricultural watershed in the Lake Erie basin. The physically based, watershed scale hydrologic and water quality model, Soil and Water Assessment Tool (SWAT) (Arnold et al., 1998) was calibrated and validated for flow, sediment and nutrient yields for the duration of 1995-2005. Further, ensemble climate data from three GCMs for mid-century (2045-2055) and late-century (2089-2099) scenarios, downscaled to the watershed level was used as model inputs to analyze future changes in flow, sediment and nutrient yields. The

changes in hydrology based on the future scenarios were compared to the ten year baseline results with the present-day climate. The climate (temperature and precipitation) projections for the future scenarios used in this study were based on the A1B emission scenario, which represents a rapid economic growth and balanced reliance on different sources of energy (IPCC, 2012).

5.2 Methods

5.2.1 Watershed description

With the total basin area of 21,538 km², Maumee is one of the largest Great Lakes basins. The River basin extends from 40° 23' to 42° 5' N Latitude, and between 83° 20' to 85° 15' W Longitude and covers a large part of northwest Ohio along with small portions of the states of Indiana and Michigan (Figure 5.1). Although the river drains out to Lake Erie near the city of Toledo, this study focuses on the river basin draining up to USGS gaging station at Waterville, Ohio (Station #04193500) with a total drainage area of 16,395 km². Meteorological data from the watershed indicate that the mean annual precipitation for the Maumee River watershed ranges from 840 to 940 mm. Similarly, the mean monthly temperature in the watershed ranges from -3.6°C (in December) to 23.1°C (in July). The elevation in the watershed varies from 150 to 470 m from mean sea level. Figure 5.1 also shows the river network in the Maumee River basin.

In Maumee River basin, agricultural area is the major land use which covers about 73% (cropland- 71% and pastureland- 2%) of the watershed area. Other dominant land uses in the basin are developed (urban and built up) and forested land which represent about 10 and 8% of the watershed respectively (NRCS, 2005). A majority of the soils in the basin are formed from the weathering of glacial till. Most of the soils in the basin are poorly drained, rich in organic matter and have high clay content. So, subsurface drains and surface ditches are common in the basin as they drain over 90% of agricultural area (NRCS, 2005). The Maumee River is not only

the largest tributary but also the largest contributor of nutrients and suspended sediments loading to Lake Erie (Myers et al., 2000; Richards et al., 2002). According to the 1997 National Resource Inventory data, the rate of soil erosion in the basin was estimated to be 4,958,700 tons/year (NRCS, 2005).

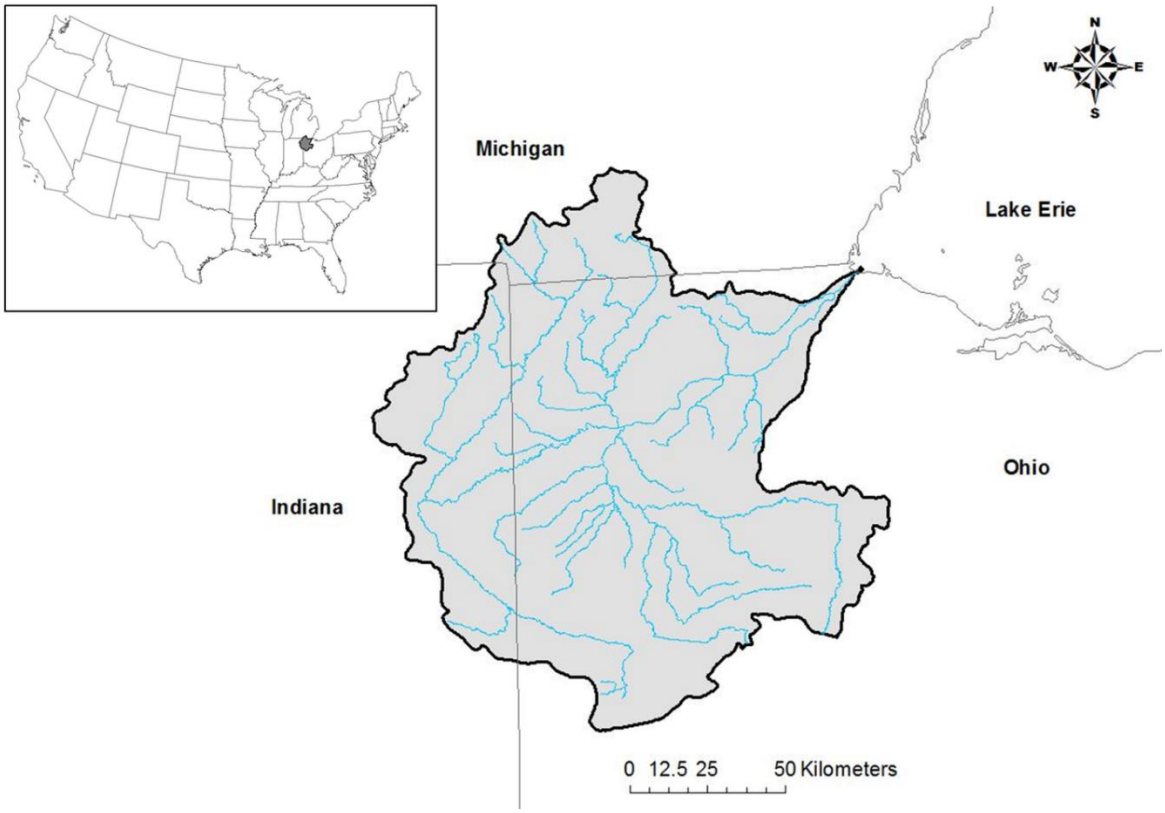

Figure 5.1: The Maumee River watershed along with the stream network, draining into western Lake Erie

5.2.2 Model setup and description

SWAT

The Soil and Water Assessment Tool (SWAT) is a semi-distributed, physically based model which can simulate hydrological processes within a watershed and predict changes in flow and pollutant loadings based on landuse change, nutrient application patterns and various management conditions in the watershed (Bosch et al., 2011, Zahabiyoun et al., 2013) . It is

continuous-time, watershed-scale model which performs simulations on a daily scale (Gassman et al., 2007). SWAT is an interactively coupled climate-landuse model which is primarily used for agricultural non-point pollution modeling (Neitsch et al., 2000). As it is physically based, modeling the crop growth and nutrient cycles and their impacts on water resources, it can be used to test the impacts of climate change on these processes (Chaplot, 2007). As model inputs SWAT relies on spatially distributed data from the watersheds including topography, soils, landuse-landcover, land management and weather (Douglas-Mankin et al., 2010). SWAT is organized by a spatial hierarchy with the watershed being divided into sub-watersheds and sub-watersheds further into smaller units called as Hydrological Response Units (HRUs) (Figure 5.2). HRUs are basic spatial units in SWAT having unique and uniform landcover, soil type and slope. SWAT models all hydrological processes at the individual HRU scale and then compiles the results for sub-watersheds and then watersheds by a weighted average based on area.

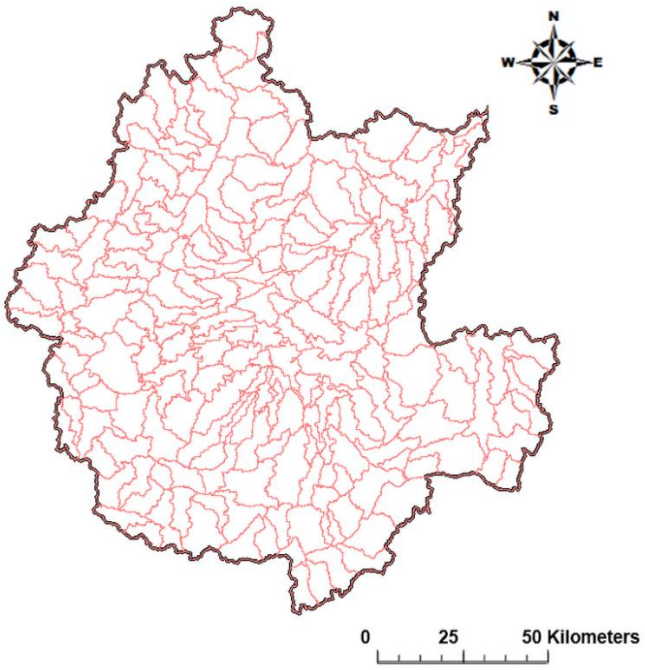

Figure 5.2: The Hydrologic Response Units (HRUs) created by SWAT for the Maumee River watershed

All the hydrological and pollutant transport processes in SWAT are modeled in two divisions, namely the land phase covering the movement of water and pollutants into the main channel and the routing phase dealing with the transport of water and pollutants to the watershed outlet (Neitsch et al., 2005). The SWAT model has been continually developed and improved over the past 20 years and has been extensively applied across the globe to various different watersheds encompassing a wide gamut of land usage, climate, locations and sizes. It's main strengths lie it's capabilities to model watersheds without monitoring data, being computationally efficient, ability to quantify impacts of change in input data on water quality and to perform long-term simulations (Neitsch et al., 2005).

SWAT inputs

In this study, ArcSWAT (version 2.1.5), a Geographic Information System (GIS) interface created for SWAT model, was used to develop the model inputs for the Maumee River basin. Elevation information for the basin was obtained from United States Geological Survey (USGS) National Elevation Dataset. The Digital Elevation Model (DEM) with 30 x 30 m grid resolution was used in this study (Figure 5.3). The river network generated by SWAT was verified using the stream channel network obtained from USGS National Hydrography Dataset (NHD) with 1:100,000-scale. A 30 x 30 m grid cell resolution landcover dataset was obtained from the USGS 2001 National Land Cover Dataset (Figure 5.3). Information on soil types was obtained from the NRCS (Natural Resource Conservation Service) State Soil Geographic Database which had 90× 90 m grid cell resolution. Weather data (daily precipitation, minimum and maximum temperatures) were obtained from the National Oceanic and Atmospheric Administration (NOAA) National Climatic Data Center. Precipitation data from 27 rain gaging stations and temperature data from 21 weather stations were included in this study.

The data on impoundment characteristics were obtained from the USGS National Hydrography Dataset and Allan and Hinz (2004). Land management practices data were

obtained from the USDA National Agricultural Statistics Service (NASS), various local experts, and Ruddy et al. (2006). The point source discharge data was obtained from the EPA Permit Compliance System (PCS) database. Similarly, more complete point source data (average daily water flow, total suspended solids, organic phosphorus, organic nitrogen, nitrate, ammonia, nitrite, mineral phosphorus, chemical/biological oxygen demand, and dissolved oxygen) were also obtained from the local sources, when available. For wetlands, surface area and volume measurement data for typical and flood stage conditions were also collected. Atmospheric nitrogen deposition data was obtained from the National Atmospheric Deposition Program (NADP) dataset.

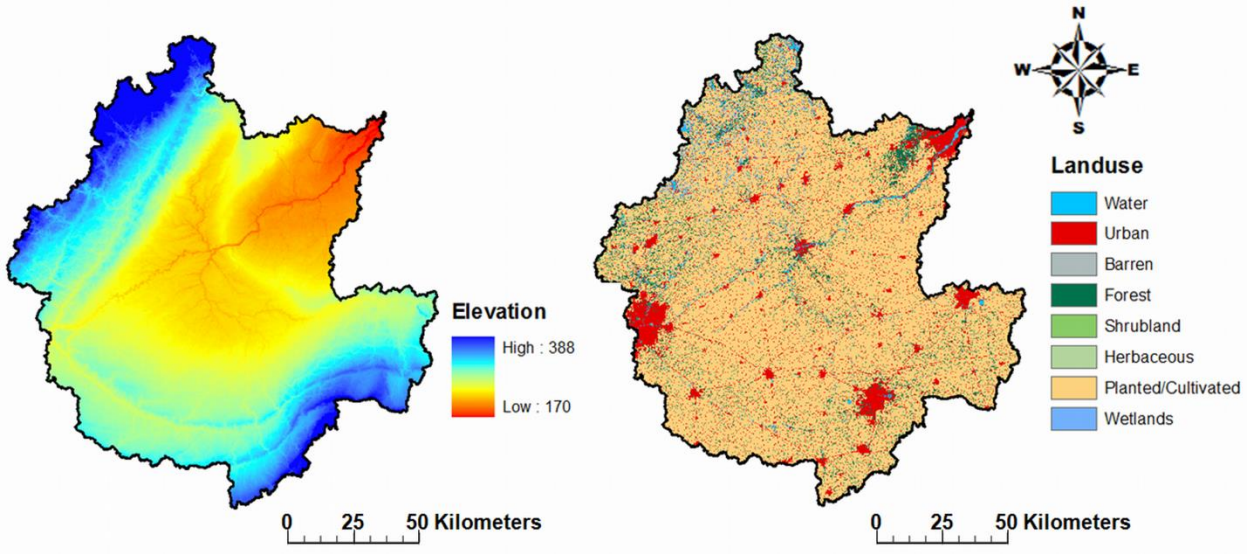

Figure 5.3: The 30x30 m grid digital elevation (DEM) and landuse-landcover layers for the Maumee River watershed used as model inputs in SWAT

Future climate data

For evaluation of the impact of climate change on water quantity and quality, future climate (monthly precipitation and temperature) data were obtained from Bias Corrected and Downscaled WCRP CMIP3 Climate Projections archive (available at: http://gdo-dcp.ucllnl.org/downscaled_cmip3_projections/) for the duration of 2045-2055 and 2089-2099 (Meehl et al., 2007). The archive provides bias corrected and spatially downscaled to 1/8×1/8

degree (12×12 km) resolution precipitation and temperature data from multiple general circulation models (GCMs) output for different IPCC scenarios (Maurer, 2007). Future projected precipitation and temperature data from CGCM3 from Environment Canada, GFDL-CM2 from Geophysical Fluid Dynamics Laboratory of the National Oceanic and Atmospheric Administration (NOAA) in the U.S., and HadCM3 (Hadley Centre Coupled Model, version 3) from the Hadley Centre in the United Kingdom were obtained. In this study, IPCC A1B scenario, which assumes a future world of low population growth but very rapid economic growth and rapid introduction of new and more efficient technology, was used (Parry et al., 2007).

Weather and seasonal forecasts show improved reliability and consistency, when the outputs from multiple models are combined (Knutti et al., 2010). Hence, the averages of three GCM projections were used (ensemble) to drive the SWAT model in this study, rather than using the outputs from a single GCM. The regional climate impact assessments require high-resolution projections (Hayhoe, 2010) and as the GCM projections are on a monthly scale, they need to be downscaled to a daily scale to be used as SWAT model inputs. A relatively simple and popular technique named as "delta" or "change factors" was used in this study to downscale the low-resolution future monthly projections to high-resolution daily projections (Zahabiyoun et al., 2013). In this technique, the future ensemble monthly temperature and precipitation projections (2045-2055, 2089-2099) are compared to the observed baseline values (1995-2005). Further, to calculate the change factors, the "difference" and "proportion" for temperature and precipitation projections respectively were computed for each month (Eq. (5.1) and Eq. (5.2)).

$$\Delta T_m = \left(\bar{T}_{ensemble,fut,m} - \bar{T}_{baseline,obs,m}\right) \tag{5.1}$$

$$\Delta P_m = \left(\frac{\bar{P}_{ensemble,fut,m}}{\bar{P}_{baseline,obs,m}}\right) \tag{5.2}$$

where, ΔT_m and ΔP_m are change factors for temperature and precipitation respectively, m is the month of the year ($1 \leq m \leq 12$). $\bar{T}_{ensemble,fut,m}$ and $\bar{P}_{ensemble,fut,m}$ are future ensemble average monthly temperatures and future ensemble average total monthly precipitations from the three GCM projections respectively. Similarly, $\bar{T}_{baseline,obs,m}$ and $\bar{P}_{baseline,obs,m}$ are average monthly temperatures and average total monthly precipitations from the observed baseline data (1995-2005).

The calculated monthly change factors for both temperature and precipitation were then used to generate high-resolution projection data to be used as SWAT model inputs. Based on the change factors downscaling technique, the future daily time series of climate data was generated as follows:

$$T_{fut,d,m} = \left(T_{obs,d,m} + \Delta T_m\right) \tag{5.3}$$

$$P_{fut,d,m} = \left(P_{obs,d,m} * \Delta P_m\right) \tag{5.4}$$

where, d is the day of the month ($1 \leq d \leq 31$), m is the month of the year ($1 \leq m \leq 12$) and $T_{obs,d,m}$ and $P_{obs,d,m}$ are daily observed temperature and precipitation for the baseline time periods. $T_{fut,d,m}$ and $P_{fut,d,m}$ are daily projected temperature and precipitation for the future time periods calculated after incorporating the change factors to the observed daily data.

5.2.3 Model calibration and confirmation

The model calibration process for monthly flow, suspended soil, nitrate and total phosphorus load is discussed in this section. This study makes use of a calibrated SWAT model for the Maumee River basin reported in an earlier study by Bosch et al. (2011). Hydrological (stream discharge) calibration is a critical step for subsequent water quality (sediment and nutrients) calibration for a watershed-scale water quality model like SWAT. The SWAT model

was calibrated and validated for daily stream discharge measured at the USGS gage station (04193500) on the Maumee River at Waterville, OH for 1995–2005. In order to reduce the impact of initial model parameter values on model output, the first 3 years (1995–1997) data were used for model warm-up and the model output for these three years was not used in calibration process. The observed data for next 4 years (1998–2001) were used for calibration and the remaining 4 years (2002–2005) of observed data for model validation (Bosch et al., 2011).

Various watershed characteristics like Manning's roughness coefficient, potential evapotranspiration, channel erosion, and baseflow parameters were changed from default values to better represent characteristics of the watershed. Table 5.1 shows the various ranges and values of the SWAT parameters used in this study. In order to reflect the slightly less obstructed flow path in this agricultural watershed, Manning's n was set to 0.026. The Hargreaves method was selected for potential evapotranspiration estimation. The Baseflow Filter Program was used to estimate the baseflow alpha factor using 1995-2005 daily flow data (Arnold et al., 1995). Following the approach outlined by Green et al. (2006), tile drainage was implemented in the watershed. Tile drainage was assumed to be present in agricultural lands with poorly drained soils (hydrologic soil group of types C and D). The depth to subsurface drain parameter was set to 1,000 mm, time to drain soil to field capacity parameter was set to 24 hours, and the drain tile lag time parameter was set to 96 hours. Similarly, the depth to impermeable layer parameter was set to 2,500 mm for all agricultural HRUs with poorly drained soils (Bosch et al., 2011). (Please refer to Bosch et al. (2011) for more details on stream discharge calibration and validation process).

Impoundments located on stream channels, including natural lakes and artificial reservoirs, were included in the SWAT model. Impoundments with surface areas greater than 50 ha were incorporated into SWAT as reservoirs, and impoundments of 10 - 50 ha were incorporated as

ponds. Parameter values for surface area and volume under average conditions for each pond and reservoir were entered based on collected data. Water quality parameters to depict N and P settling in impoundments were adjusted on the basis of a study of 27 Midwestern reservoirs (Walker and Kuhner, 1978) that reported median settling rates of 4.7 m/y for N and 14.0 m/y for P.

In SWAT, terrestrial soil denitrification depends on nitrate content of the soil layer, the rate coefficient, soil temperature, soil moisture conditions, organic carbon content, and threshold moisture content. The value of denitrification threshold water content was set to 1.0 to allow denitrification when soils were saturated with water. Similarly, the denitrification exponential rate coefficient was set to 0.15 to better approximate expected denitrification rates according to previous measurements in the literature (Groffman et al., 1992; Hofstra and Bouwman, 2005).

Table 5.1: SWAT model calibration parameters

Parameter	Range (min - max)	Value
Alpha_Bf	0.01-0.3	0.2543
Canmx	0.01-10	5.7317
Ch_K2	0.01-150	0.4174
Ch_N2	0.01-0.1	0.0571
Cn2	-0.5	-6.3791
Epco	0.01-1%	0.6381
Esco	0.01-1	1.0000
Gwqmn	0.01-500	447.58
Revapmin	0.01-500	388.62
Sol_Awc	-0.5	4.9695
Sol_Z	-0.5	-10.903
Surlag	24-Jan	2.8723
Timp	0.01-1	0.0611

The goodness of fit between observed and simulated water quantity and quality parameters were assessed using two popular statistical parameters: coefficient of determination (R^2) and Nash-Sutcliffe efficiency (NSE) coefficient (Nash and Sutcliffe, 1970).

5.3 Results and Discussions

5.3.1 Baseline Climate

The total monthly precipitation observed in the Maumee River watershed over the period 1995-2005 was calculated using daily precipitation records from 27 weather stations lying within and around the watershed boundary. The daily records from all the 27 stations were averaged based on the Thiessen polygon method and average areal precipitation estimates were calculated for the whole watershed. These daily Thiessen weighted values were then summed to compute the monthly totals. The month of May received the maximum precipitation over the 11 year period, averaging about 119mm. The summer months (May-Aug) received the maximum precipitation within a year accounting for almost 44% of total annual precipitation on average. The total annual precipitation varied from 804mm (1999) in the driest year to 1109mm (2003) in the wettest year with the standard deviation being 95mm. On the monthly scale, the maximum precipitation total was observed in July, 2003 at 190mm with the minimum total observed in February, 2004 at 12mm.

Similar to the total monthly precipitation calculations, average monthly temperatures were calculated for the Maumee River watershed. Daily average temperature was calculated for the whole watershed based on the Thiessen polygon method using records from 21 stations lying within and around the watershed boundary. Subsequently, average monthly values were then obtained from the daily records. On average, the results indicated that July was the warmest month with an average temperature of about 23 ^{o}C, and January was the coldest month with an average temperature of -4^{o}C. On an annual scale the coldest year from the period 1995-2005 was 1996 with an average annual temperature being about 9 ^{o}C, and the warmest year was 2001 with an average annual temperature being about 11 ^{o}C. On the monthly scale, the hottest month with an average temperature of 25 ^{o}C was July, 1999 and the coldest month was December, 2000

with an average temperature of about -8 ^{o}C. The highest and lowest maximum average temperatures were typically observed in July at about 29 ^{o}C and January at 0 ^{o}C respectively. Similarly, the highest and lowest minimum average temperatures were also observed in July and January at 17 ^{o}C and -8 ^{o}C respectively.

5.3.2 Climate Projections

Modeled monthly precipitation totals and average monthly temperature data for a mid-century period from 2045-2055 and a late-century period from 2089-2099 from three GCMs namely, CGCM3, GFDL-CM2 and HadCM3 was downloaded for the Maumee River watershed. For these three GCM outputs, IPCC A1B scenario was selected and the ensemble data were compared to the data observed in the Maumee River watershed for the 11 year baseline period from 1995-2005. Table 5.2 summarizes the correction factors obtained for both total monthly precipitation and average monthly temperature for the mid-century and late-century scenarios.

For average monthly precipitation the ensemble model predictions indicated that summer and early fall precipitation (May-Oct) is projected to decrease for the mid-century period. The maximum decrease of about 27% is expected in the months of May and June. Conversely, the average monthly precipitation is expected to increase over the rest of the year for the mid-century period with a maximum increase of 36% expected in November. The results also indicated a large increase in average monthly precipitation of about 30% is also expected for the month of March. On an annual scale the total precipitation is expected to decline from 939mm to 909mm in the baseline and mid-century periods respectively.

For the late century period, a similar temporal pattern in the change of average monthly precipitation was seen, with decreasing precipitation during May-October and increasing precipitation during the rest of the year. However, the largest decreases in average monthly precipitation totals are projected to shift on a temporal scale to the months of July (21%) and

August (23%). The largest increase is projected to occur in March at about 58% compared to the baseline period. Overall, the annual precipitation is projected to increase from 939mm in the baseline period to 991mm in the late-century period.

Table 5.2: The monthly average precipitation totals and average temperatures (Thiessen weighted) for the Maumee River watershed for the baseline period (1995-2005), mid-century period (2045-2055) and late-century period (2089-2099). The baseline period values were computed using observed data, while the future period ensemble values were derived from three GCMs. The correction factors for precipitation totals (P_{Pred}/P_{Obs}) and average temperatures ($T_{Pred}-T_{Obs}$) are also shown for both the future periods.

Precipitation totals (mm)		Jan	Feb	Mar	Apr	May	Jun	Jul	Aug	Sep	Oct	Nov	Dec
Observations	1995-2005	64.72	50.64	56.60	84.99	118.46	99.84	101.74	92.74	80.66	64.36	65.74	58.52
Ensemble Predictions	2045-2055	69.36	57.04	73.51	102.93	86.06	72.84	78.79	76.37	69.97	58.70	89.26	74.57
	2089-2099	74.61	61.69	89.53	106.93	107.56	84.16	80.38	71.42	70.00	80.52	89.29	75.71
Change Factors ($P_{\_}/P_{\_}$)	2045-2055	1.07	1.13	1.30	1.21	0.73	0.73	0.77	0.82	0.87	0.91	1.36	1.27
	2089-2099	1.15	1.22	1.58	1.26	0.91	0.84	0.79	0.77	0.87	1.25	1.36	1.29

Average Temperature (C)		Jan	Feb	Mar	Apr	May	Jun	Jul	Aug	Sep	Oct	Nov	Dec
Observations	1995-2005	-4.00	-1.21	2.82	9.55	15.24	20.94	22.79	21.92	18.07	11.50	4.95	-1.64
Ensemble Predictions	2045-2055	-1.38	0.52	5.75	11.72	17.99	23.41	26.61	26.14	21.56	14.35	6.73	1.83
	2089-2099	0.21	2.29	7.12	13.78	19.26	24.92	27.89	27.68	22.92	16.18	7.58	2.74
Change Factors ($T_{\_}-T_{\_}$)	2045-2055	2.61	1.73	2.92	2.17	2.75	2.47	3.82	4.21	3.49	2.84	1.79	3.47
	2089-2099	4.21	3.50	4.30	4.23	4.02	3.97	5.10	5.75	4.85	4.67	2.63	4.38

The ensemble GCM projections for average monthly temperatures along with their respective correction factors are also summarized in Table 5.2. All the GCMs projected a warmer climate with average monthly temperatures rising in all months for the mid-century and late-century periods. On a monthly scale, compared to the baseline period the maximum rise was projected in August at 4.2°C and 5.8 °C for the mid-century and late-century periods respectively. The minimum rise was projected in February at 1.8 °C and November at 2.6 °C for

the mid-century and late-century periods respectively. Overall, the average annual temperature is projected to increase by 2.9 ^{o}C and 4.3 ^{o}C during the mid-century and late-century periods respectively as compared to the baseline period.

5.3.3 Flow (Stream discharge)

The SWAT model predicted the flow well in the Maumee River watershed for the baseline period. The modeled results from SWAT were compared to the daily flow observed at the USGS gaging station at the outlet of the Maumee River watershed located at Waterville, OH. The first three years (1995-1997) out of the eleven years in the baseline period were used as model warm-up to minimize the impact of initial parameter values on the output. The next four years (1998-2001) were considered as the calibration years while the remaining years from the baseline period (2002-2005) were used for validation purposes. Coefficient of determination (R^2) and NSE values for average monthly flow simulations over calibration and validation periods are shown in Table 5.3. Figure 5.4 shows the average monthly flows observed at the Maumee River watershed plotted against the SWAT simulated values. These statistic values for flow can be categorized as "very good" based on the classification developed by Moriasi et al. (2007).

Interestingly, both the Coefficient of determination (R^2) and NSE statistic values were higher for the validation period than the calibration period. Figure 5.5, shows the comparison of the daily flow observed at the USGS gage at the outlet of the watershed and the daily flow simulated using the SWAT model. Although SWAT under-predicted the peak flows on a daily scale , overall the model successfully simulated the flow conditions in the watershed as visually and statistically indicated by Figures 5.4, 5.5 and Table 5.3 respectively. High goodness of fit statistics for monthly SWAT predictions indicated that the model successfully simulated the physical flow generating processes in the watershed and would be reliable for future climate simulations. Additionally, this was vital as flow calibration is a critical step for water quality predictions (Bosch et al., 2011).

Table 5.3: Calibration and Validation results for monthly flow, suspended solids loads, total phosphorus loads and nitrate-N loads for the Maumee River watershed. Coefficient of determination (R^2) and Nash-Sutcliffe efficiency (NSE) goodness of fit measures are used to compare the observed results to the SWAT modeled results.

	Observed mean	Simulated Mean	R^2	NSE
Calibration				
Flow (m^3/s)	150.61	170.49	0.93	0.91
Suspended Solids loads (Mg)	67395.60	71984.25	0.75	0.72
Total Phosphorus loads (Mg)	150.71	148.92	0.70	0.70
Nitrate-N loads (Mg)	2447.81	2732.55	0.74	0.70
Validation				
Flow (m^3/s)	174.25	184.97	0.96	0.95
Suspended Solids loads (Mg)	64275.58	67973.11	0.90	0.89
Total Phosphorus loads (Mg)	152.84	125.80	0.81	0.77
Nitrate-N loads (Mg)	2519.02	2666.10	0.72	0.69

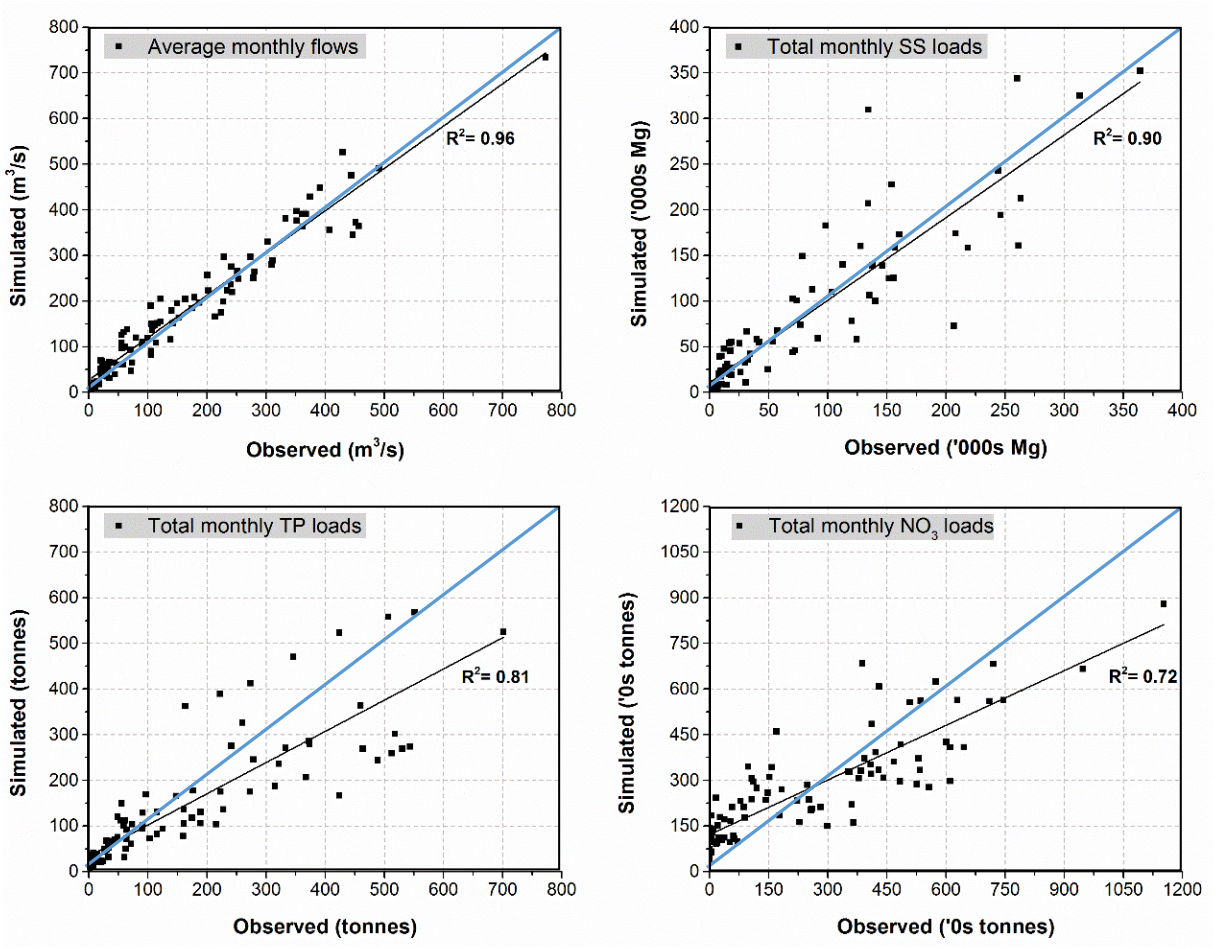

Figure 5.4: Observed monthly averages for the Maumee River watershed compared to the SWAT simulated monthly averages for flow, SS, TP and NO3 loads

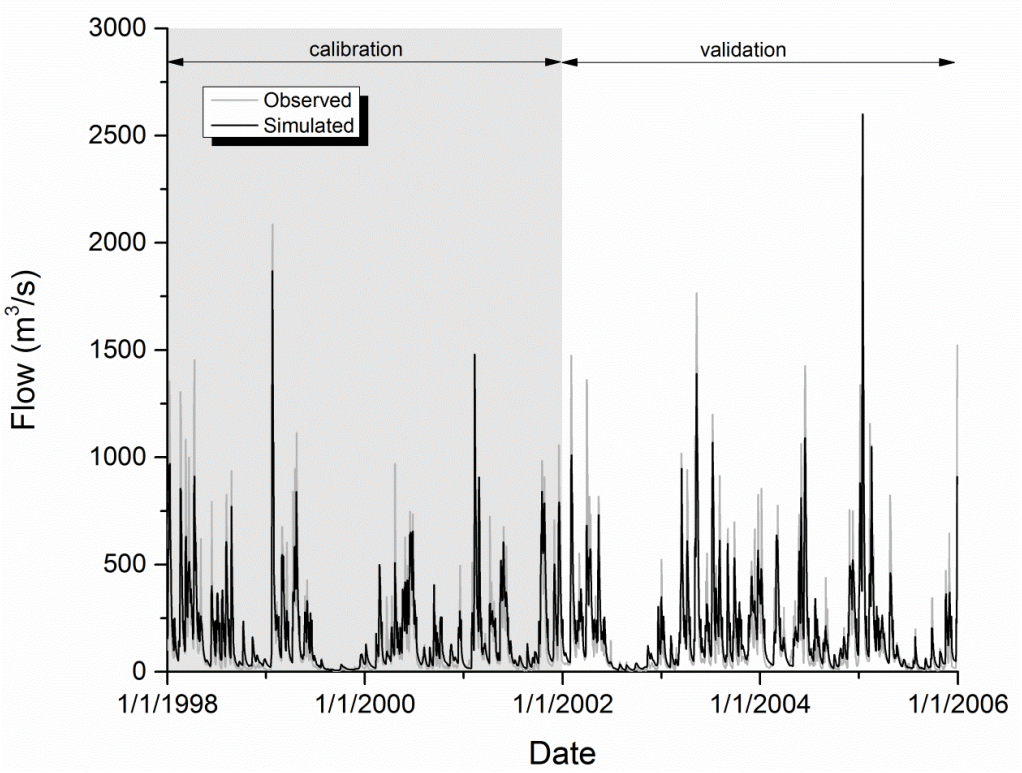

Figure 5.5: Observed daily flow data for the Maumee River watershed (USGS Station #04193500) compared to the daily flow simulations using SWAT for the calibration (1998-2001) and validation time periods (2002-2005).

Changes in average monthly flows attributed to climate change (temperature and precipitation changes) in the mid-century and late-century periods as compared to the baseline period for the Maumee River watershed are presented in the Figure 5.6. The average annual flow over the mid-century and late-century periods is projected to be about 162m^3/s and 195m^3/s respectively. As flow is largely dependent on precipitation, the temporal change in flow patterns for future periods was similar to that of precipitation changes. The summer flows are projected to decline in the Maumee River watershed while the winter flows are expected to rise. As precipitation was projected to decline for the mid-century period on an annual scale when compared to the baseline period, flows were also projected to decrease. Similarly, precipitation was projected to increase in the late-century period as compared to the baseline period and thereby the flows were also projected to increase. However, these changes were not uniform as flow generation from precipitation is a fairly complex process with other variables involved. A

3.2% decrease in annual precipitation accompanied with a 2.9°C rise in average temperatures over the mid-century period decreased the average flow by 8.5%. Similarly, for the late-century period a 5.6% increase in annual precipitation coupled with a 4.3°C rise in average temperatures led to a 9.7% increase in average flow compared to the baseline period. On a temporal scale, the warmer months (May-Sep) saw a decline of 52% and 36% in average flows for mid-century and late-century periods compared to the baseline period respectively. The cooler months (Oct-Apr) saw an increase of 15% and 35% in average flows for mid-century and late-century periods compared to the baseline period respectively. On a monthly scale, the largest decrease in average flows were projected to occur in July (64%) and August (60%) for the mid-century and late-century periods compared to the baseline period respectively. The largest increase was projected in December at 43% and 57% for mid-century and late-century periods compared to the baseline period respectively.

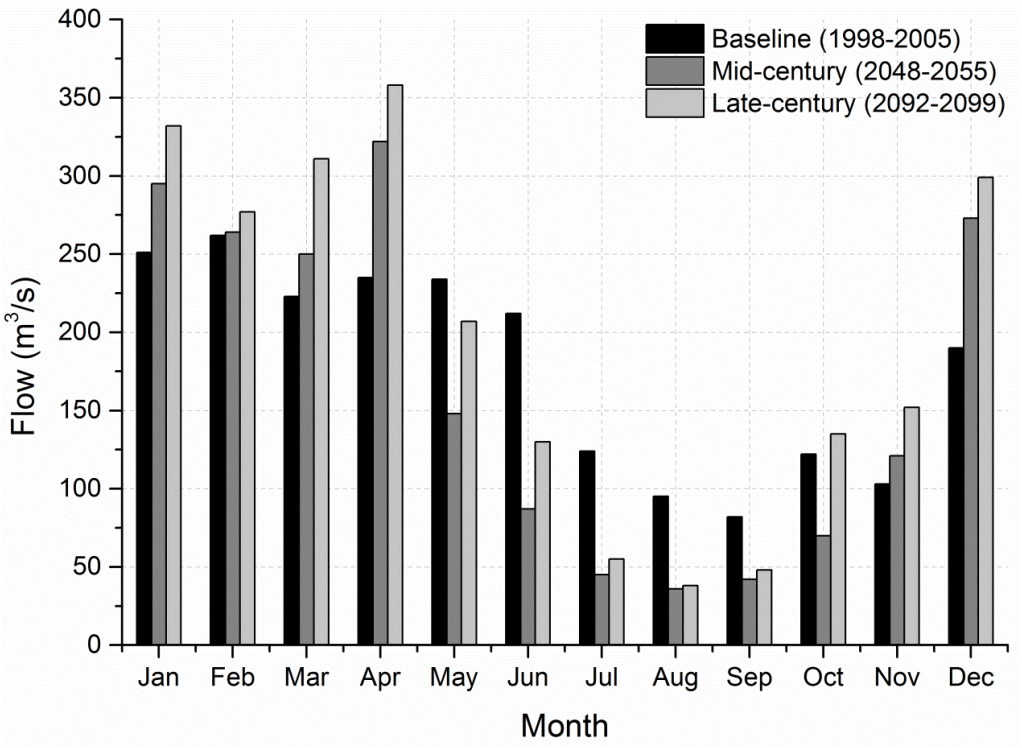

Figure 5.6: Average monthly flow for the mid-century and late-century time periods compared to the reference baseline time period in response to projected changes in temperature and precipitation based on ensemble GCM outputs.

5.3.4 Sediment

Table 5.3 and Figure 5.4 show the monthly observed and predicted sediment loads in the Maumee River watershed for the calibration and validation periods. The monthly sediment loads were calculated based on daily load predictions from SWAT and were compared to the observed loads at the outlet based on extensive sampling data collected by the WQL. Surprisingly, the validation period results were more accurate than the calibration period results indicated by higher goodness of fit values (R^2 and NSE). Figure 5.7 shows the sediment load predictions from SWAT on a daily scale along with the observed loads. It's fairly evident that SWAT under-predicted the peaks when compared to the daily load peaks. This under-prediction can possibly be attributed to the uncertainty in soil erosion and sediment yield methods used in SWAT which are based on MUSLE. MUSLE was originally developed to estimate event-based soil erosion from agricultural fields and small watersheds. Similar under-prediction of sediment loads by SWAT has also been described in few other studies such as Benaman et al. (2005), Maski et al. (2008) and Phomcha et al. (2011). During the baseline period, some of the highest daily flows at the outlet of the Maumee River watershed were observed in January, 2005. There was 3-week period with high flows and no sampling data in the WQL records during this month. Thereby the monthly loads for this month were based on relatively low-flow data and were probably over-predicted as indicated by the very high load peaks in Figure 5.7.

Projected monthly changes in sediment loads in the mid-century and late-century periods and their comparison to the baseline period loads is presented in the Figure 5.8. The sediment loads generally followed the same patterns as precipitation and flow changes. However, there was relatively negligible change projected for sediment loads in January and sediment loads decreased in February even though there was an increase in projected flow for the mid-century period. A similar trend was also seen in projected sediment loads in February for the late-century periods. On a monthly scale, the sediment loads varied between 18% (82% decrease) to

190% (90% increase) and 16% to 238% of the corresponding monthly baseline loads for the mid-century and late-century periods respectively. Similar to flows, typically the sediment loads increased in the cooler months (except February) and decreased in the warmer months for both the future periods. The largest decreases in monthly sediment loads were projected in July-August at about 82% and 81% for the mid-century and late-century periods respectively.

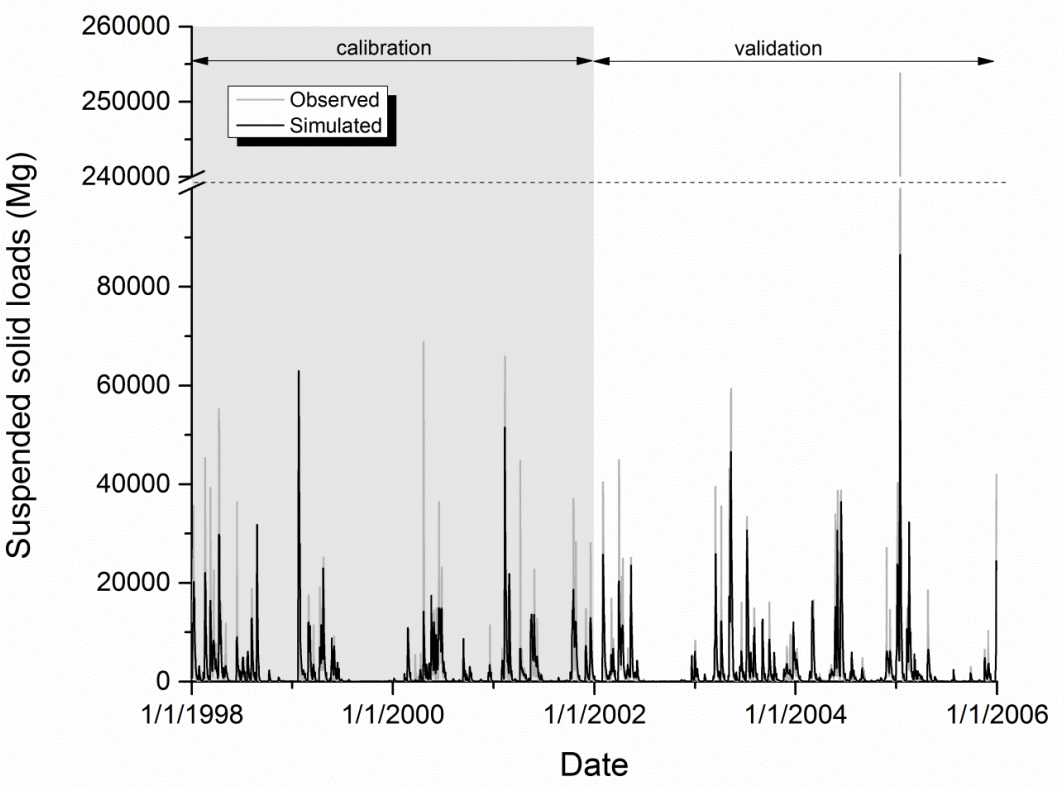

Figure 5.7: Observed daily suspended solid loads for the Maumee River watershed compared to the daily suspended solid loads simulated using SWAT for the calibration (1998-2001) and validation time periods (2002-2005).

The largest increases were projected in November-December and March-April averaging about 69% and 115% for the mid-century and late-century periods respectively. Overall on average on an annual scale, an 8.5% decline in average flow is projected to cause a 10.4% decline in sediment loads for the mid-century period. Similarly, a 9.7% increase in average flow is projected to cause a 19.6% rise in sediment loads over the late-century period.

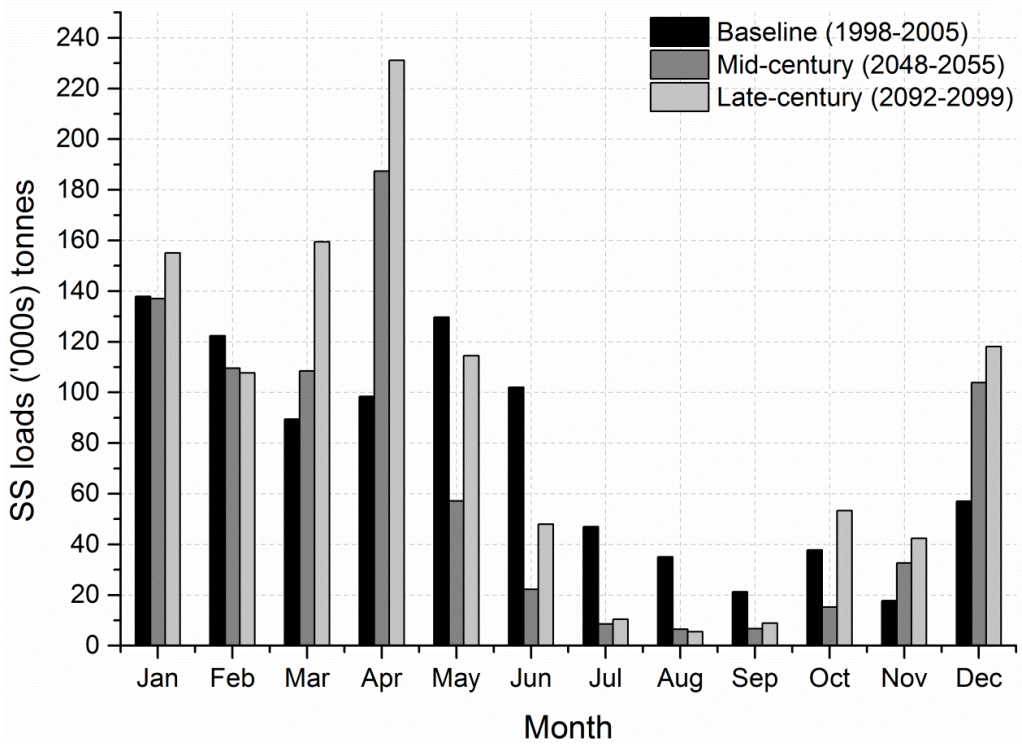

Figure 5.8: Average monthly suspended solid (SS) loads for the mid-century and late-century time periods compared to the reference baseline time period in response to projected changes in temperature and precipitation based on ensemble GCM outputs.

5.3.5 Total Phosphorus

Trends in total phosphorus (TP) loads for the future scenarios were very similar to sediment loads. The TP loads typically followed changes in flow and precipitation patterns. Table 5.3 and Figure 5.4 show the average monthly TP load comparison using the daily data collected at the watershed outlet and daily data simulated using SWAT for the calibration and validation periods in the baseline scenario. The goodness of fit statistics were higher for the validation period as compared to the calibration period and overall the SWAT model predictions for TP loads were slightly worse than sediment predictions. Despite the marginally inferior performance, the goodness of fit statistics were generally classified as “good” for calibration and “very good” for the validation periods indicating acceptable predictions for TP loads using SWAT for the Maumee River watershed. Figure 5.9 shows the daily TP loads observed at the Maumee River

watershed outlet compared to the simulated daily TP loads using SWAT for the baseline period. Similar to sediment, SWAT under-predicted the peak loads for TP loads as well.

Figure 5.10 shows the variations in monthly TP loads as compared to the baseline loads in response to the future changes projected in temperature and precipitation. The monthly loads are expected to vary between 37% to 165% and 38% to 199% of the baseline monthly TP loads for the mid-century and late-century periods respectively. The largest increases in monthly TP loads were projected in November, December and April averaging 63% and 78% for mid-century and late-century periods respectively. The largest decreases were projected to occur in summer months, with a higher decline in the mid-century period at 62% and a lesser decline of 51% in the late-century period. Similar to sediment, the average TP loads in February showed a decline even though there was an increase projected in average flows. Overall, on average on an annual

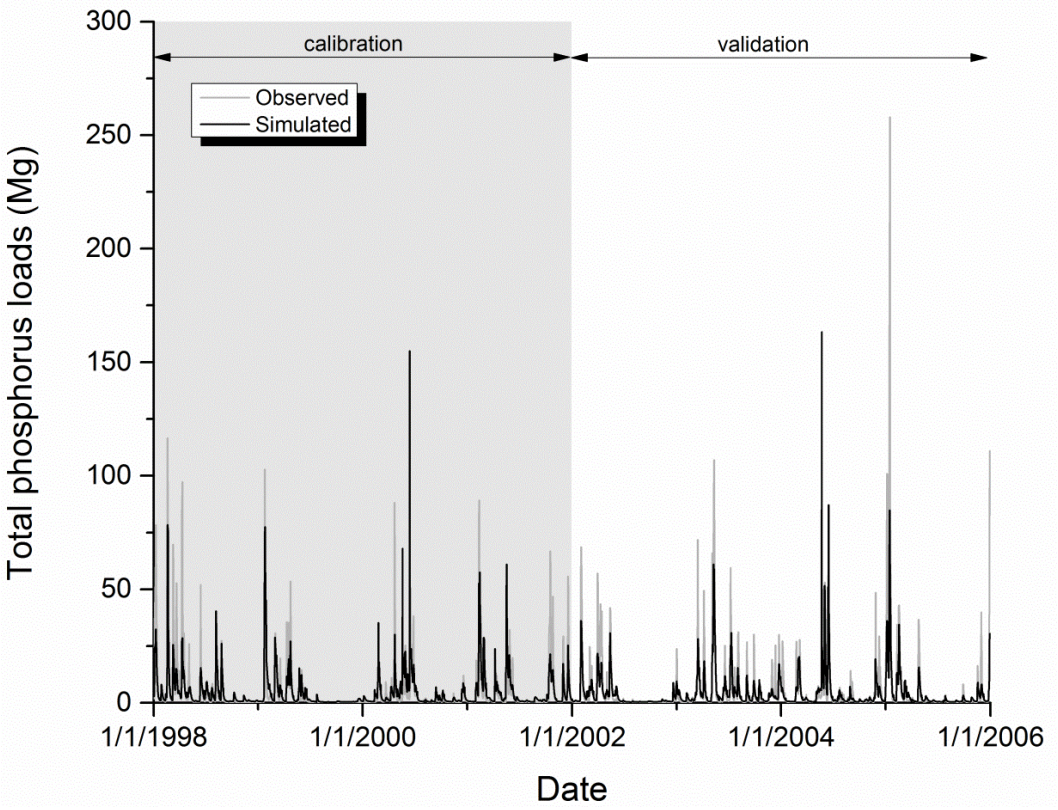

Figure 5.9: Observed daily total phosphorus loads for the Maumee River watershed compared to the daily total phosphorus loads simulated using SWAT for the calibration (1998-2001) and validation time periods (2002-2005).

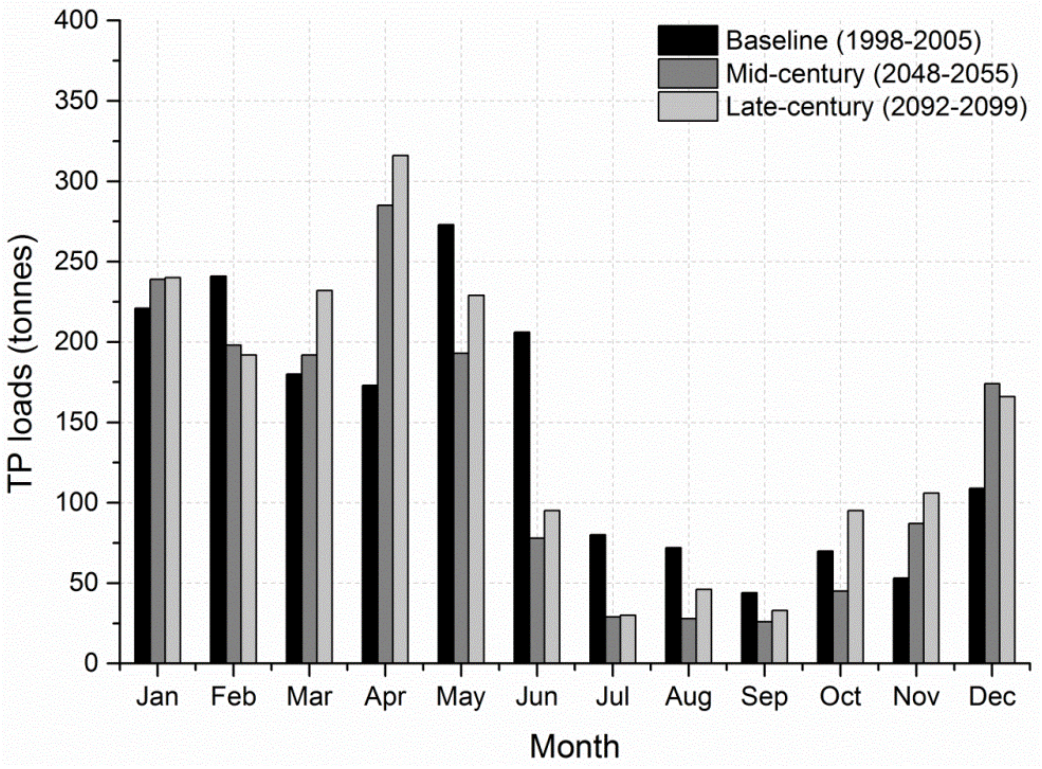

Figure 5.10: Average monthly total phosphorus (TP) loads for the mid-century and late-century time periods compared to the reference baseline time period in response to projected changes in temperature and precipitation based on ensemble GCM outputs.

scale, an 8.5% decline in average flow is projected to cause an 8.5% decline in total phosphorus loads for the mid-century period. Similarly, a 9.7% increase in average flow is projected to cause a mere 3.5% rise in total phosphorus loads over the late-century period.

5.3.6 Nitrate

Table 5.3 and Figure 5.4 show the average monthly nitrate-N loads observed at the mouth of the Maumee River watershed and the comparison to the nitrate-N loads predicted using the SWAT model for both the calibration and validation time periods. Coefficient of determination (R^2) and Nash-Sutcliff efficiency measures were higher for the calibration period being 0.74 and 0.70 respectively, than for the validation period which were 0.72 and 0.69 respectively. Figure 5.11 shows the daily nitrate-N loads for the both the calibration and validation periods using

observed data at the watershed outlet and simulated data from SWAT. Similar to other pollutants such as SS and TP, SWAT under-predicted the nitrate-N load peaks.

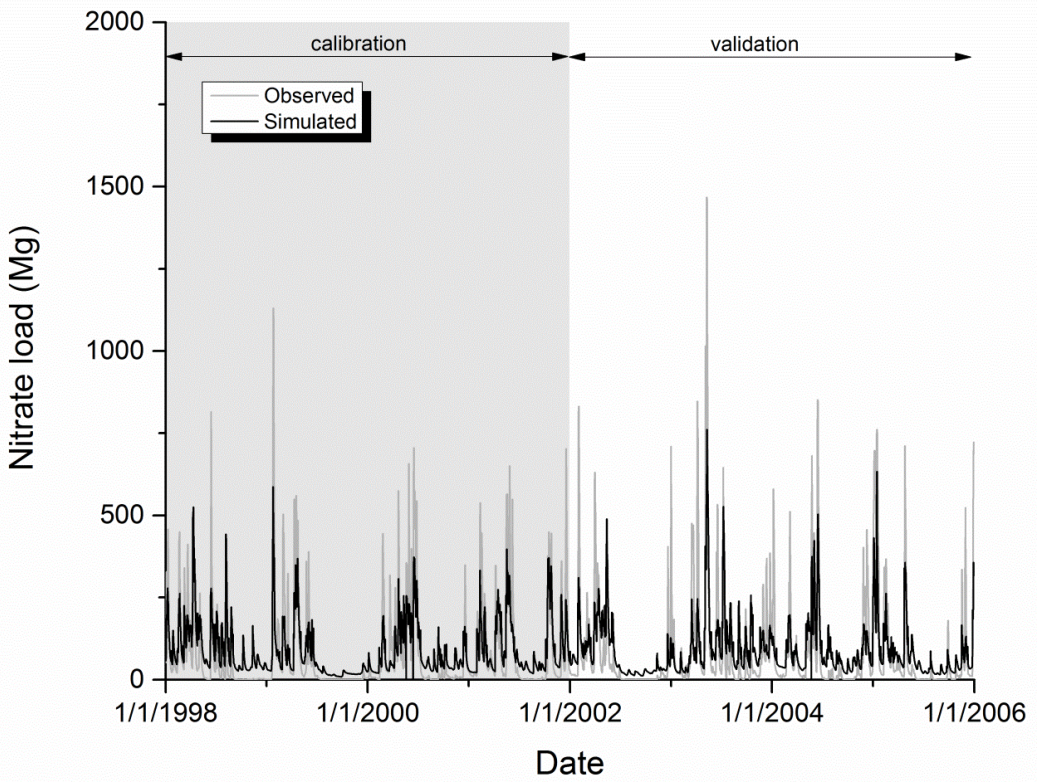

Figure 5.11: Observed daily nitrate-N loads for the Maumee River watershed compared to the daily nitrate-N loads simulated using SWAT for the calibration (1998-2001) and validation time periods (2002-2005).

Figure 5.12 shows the projected variations in average monthly nitrate-N loads for the mid-century and late-century time periods compared to the baseline time period. These changes are in response to projected climate change based on ensemble GCM predictions. The results indicate that the changes in monthly nitrate-N load patterns is going to be very similar to that of changes in average monthly flows. As the flows are expected to rise over winter and spring months, the nitrate-N loads are also expected to increase over these periods for the future time periods.

A decline in nitrate-N loads is projected in the summer months compared to the baseline period for both the future time periods, with it being higher for the mid-century period. October

is the first month after summer which is expected to see higher nitrate-N loads in the late-century period as compared to the baseline period. The relatively warmer months from May to October are projected to see an average decline of 43% in total nitrate-N loads for the mid-century period. Similarly for the late-century time period, the months from May to September

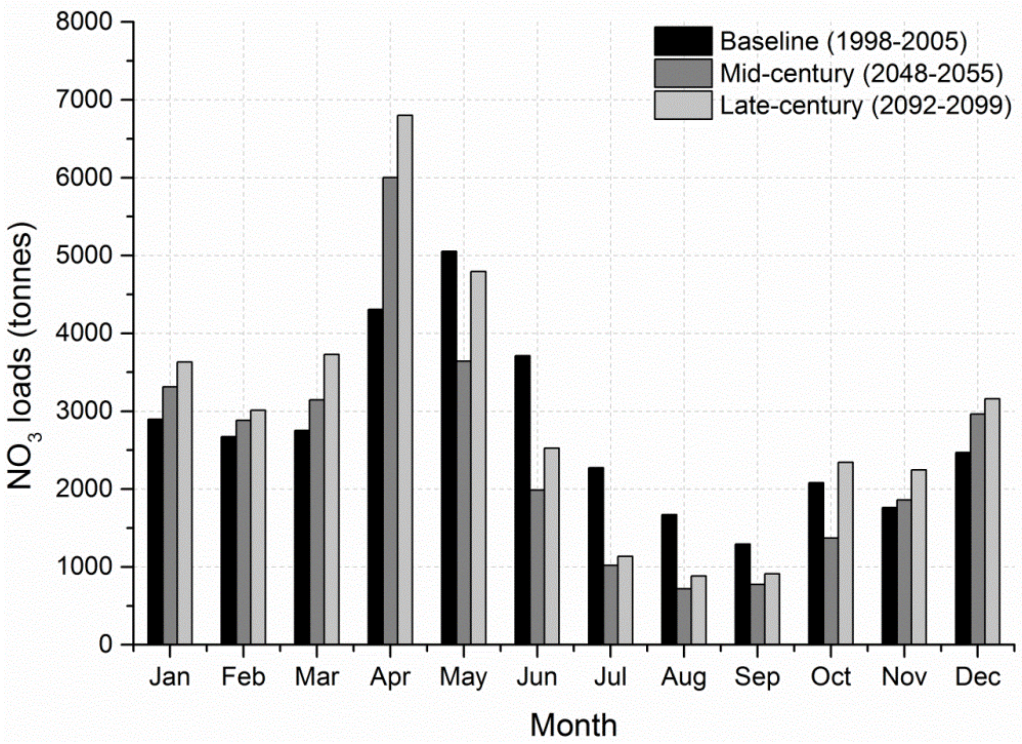

Figure 5.12: Average monthly nitrate-N (TP) loads for the mid-century and late-century time periods compared to the reference baseline time period in response to projected changes in temperature and precipitation based on ensemble GCM outputs.

are expected to see an average decline of 33% in total nitrate-N loads as compared to the baseline time period. The rest of the year i.e. the relatively cooler months are expected to see a rise of 17% and 28% in average monthly nitrate-N loads for the mid-century and late-century time periods respectively. On an individual month level, the maximum rise in nitrate-N loads is projected to occur in April averaging about 39% and 58% more than the baseline time period for the mid and late-century periods respectively. The maximum fall in average monthly nitrate-N loads is expected to occur over July-August averaging 56% and 49% less than the baseline loads for the mid and late-century periods respectively. Overall, for the mid-century time period the

average annual nitrate-N loads declined by 9.9% while they increased by 6.8% for the late-century time period as compared to the baseline time period.

5.4 Implications

The SWAT model was used to quantify the changes in hydrology of the Maumee River watershed in response to the projected climate change in the mid and late century time periods. The implications of these results are vital as they help assess the impacts of impending climate-hydrology changes on agriculture, natural ecosystems and water supply in the Maumee River watershed.

The ensemble GCM predictions indicated that monthly average temperatures are expected to rise throughout the year for the both the mid and late century time periods. This is imperative to the change in crop growth patterns in the future. As described by Ficklin et al. (2009), each crop has its own minimum, optimum and maximum temperature ranges for growth. Higher temperatures during the earlier part of the year coupled with longer optimum temperature periods would potentially shift the crop growing cycle and increase the length of the growing season. Consequently, if the crop growing cycle sees a large enough temporal shift, a two crop annual cycle maybe implemented by farmers instead of the one crop cycle practiced currently.

The future precipitation patterns indicate that summer precipitation totals would decline in the mid-century time period, reducing the overall flow volumes in the Maumee River watershed. This pattern is expected to change in the late-century period when the summer precipitation would rise compared to the mid-century period but would still be lesser than the baseline time period. This decline in summer precipitation along with an increase in crop growth which is also validated by a marginal rise in ET would lead to lesser runoff over the summer months. Thereby, this decline in runoff would affect the water quantity in the Maumee River and can have potentially negative implications on water supply systems and other urban systems which rely

on the Maumee River for their water needs. Additionally, during the latter part of the summer towards the end of the crop cycle, lesser water availability may cause potential droughts leading to crop damage. Conversely, for both the future time periods the winter precipitation and thereby the flow is expected to rise compared to the baseline time period. The projected increase in precipitation over winter months would lead to a high soil moisture conditions and the resulting excess runoff may potentially cause flooding in the watershed.

One direct consequence of modeled increase in winter flows from the Maumee River watershed would be increased sediment and agricultural pollutant transport into Lake Erie. This increased leaching and erosion would potentially affect the natural ecosystem in the lake and probably further worsen the problem of hypoxia. As reported by Royer et al. (2006), majority of agricultural nutrient losses from Midwestern watersheds takes place in winter months which coincides with the non-growing season in the area. Increased flows during this period would possibly further intensify the problem of nutrient leaching from the Maumee River watershed. Moreover, as suggested by Royer et al. (2006) it would become even more critical to focus the TMDL guidelines on periods with higher flows to achieve goals aimed at reducing nutrient and sediment losses from agricultural watersheds.

5.5 Summary

This study demonstrated the impacts of potential climate change on the hydrology of the large and predominantly agricultural Maumee River watershed lying in the Lake Erie basin. The SWAT model was used to simulate the hydrological processes in the watershed for the mid-century (2045-2055) and late-century (2089-2099) time-periods using projected ensemble climate data from three GCMs for the IPCC A1B scenario. The results indicated that the hydrology in the Maumee River watershed is sensitive to climatic variations that are projected to occur in the future. Compared to the baseline period (1995-2005) an increase of 2.9^{o}C in average annual temperatures coupled with a 3.2% decrease in annual precipitation reduced the flow in

the watershed by 8.5% for the mid-century time period. This decrease in annual flow also reduced annual SS, TP and Nitrate-N loads by 10.4%, 8.5% and 9.9% respectively. A 4.3^{o}C rise in annual temperatures along with a 5.6% increase in annual precipitation for the late-century period increased the annual flow in the watershed by 9.7%. This increase in annual flow was accompanied by a 19.6%, 3.5% and 6.8% increase in annual SS, TP and Nitrate-N loads respectively. Apart from the annual variations, the hydrological processes were sensitive to climate change on monthly scales as well. The summer precipitation declined for both the future time periods with a greater decline in the mid-century period, while the winter precipitation rose in both periods. Rising temperatures in general may shift the crop growth cycle on a temporal scale in the watershed and redistribute the water yields leading to a rise in winter months. Consequently, the flow patterns changed on a temporal scale with higher flows simulated for winter and spring months while lower flows simulated for the summer months. As a result, the sediment and nutrient loads also generally saw increases in winter and spring months with a few exceptions.

This study also reflects on the challenges associated with evaluating impacts of climate change on hydrological processes. There are uncertainties related to the future climate projections as there exists a wide degree of variation in projections from different GCM models. Downscaling projected data to a higher-resolution for modeling requirements also adds to a certain degree of uncertainty to the assessment. Additionally, modeling of hydrological processes also has uncertainties of its own such as under-prediction of daily pollutant peaks by SWAT in this study which adds some skepticism over the reliability of future projections.

Overall, the results indicated that modeled changes in the hydrology of the Maumee River watershed over the mid and late-century time periods may have implications associated with water quality and water quantity. The results are not intended to represent actual conditions that will occur in the watershed, but elucidate the general direction and magnitude of changes

that might occur in the hydrology of the watershed. Such projected hydrological changes and potential implications will help water resource managers in the area to make more informed decisions pertaining to water management, agriculture and also take necessary precautions to mitigate the negative impacts associated with excessive nutrient losses, erosion, floods and droughts.

References

Allan, J.D., and L. Hinz .2004. “An assessment of flows for rivers of the great lakes basin”. *Project Report, Great Lakes Protection Fund, Ann Arbor, MI.*

Arnell, N. W. 2003. "Relative Effects of Multi-Decadal Climatic Variability and Changes in the Mean and Variability of Climate due to Global Warming: Future Streamflows in Britain." *Journal of Hydrology* 270 (3-4): 195-213.

Arnell, N.W., and C. Liv. 2001. “Hydrology and water resources. In: McCarthy, J.J., Canziani, O.F., Leary, N.A., Dokken, D.J., White, K.S. (Eds.), Climate Change 2001: Impacts. Adaptation and Vulnerability.” *Cambridge University Press, Cambridge, UK*: 191–233.

Arnold J.G., and P.M. Allen. 1999. “Automated methods for estimating baseflow and ground water recharge from streamflow records.” *J Amer Water Resour Assoc* : 35:411-24.

Arnold, J. G., R. Srinivasan, R. S. Muttiah, and J. R. Williams. 1998. "Large Area Hydrologic Modeling and Assessment Part I: Model Development." *Journal of the American Water Resources Association* 34 (1): 73-89.

Benaman, J., C. A. Shoemaker, and D. A. Haith. 2005. "Calibration and Validation of Soil and Water Assessment Tool on an Agricultural Watershed in Upstate New York." *Journal of Hydrologic Engineering* 10 (5): 363-374.

Bouraoui, F., L. Galbiati, and G. Bidoglio. 2002. "Climate Change Impacts on Nutrient Loads in the Yorkshire Ouse Catchment (UK)." *Hydrology and Earth System Sciences* 6 (2): 197-209.

Bronstert, A., D. Niehoff, and G. Brger. 2002. "Effects of Climate and Land-use Change on Storm Runoff Generation: Present Knowledge and Modelling Capabilities." *Hydrological Processes* 16 (2): 509-529.

Chaplot, V. 2007. "Water and Soil Resources Response to Rising Levels of Atmospheric CO2 Concentration and to Changes in Precipitation and Air Temperature." *Journal of Hydrology* 337 (1-2): 159-171.

Dibike, Y. B. and P. Coulibaly. 2007. "Validation of Hydrological Models for Climate Scenario Simulation: The Case of Saguenay Watershed in Quebec." *Hydrological Processes* 21 (23): 3123-3135.

Douglas-Mankin, K.R., R. Srinivasan, and J.G. Arnold. 2010. “Soil and Water Assessment Tool (SWAT) model: Current developments and applications.” *Transactions of the ASABE,* 53(5), 1423–1431.

Ficklin, D. L., Y. Luo, E. Luedeling, and M. Zhang. 2009. "Climate Change Sensitivity Assessment of a Highly Agricultural Watershed using SWAT." *Journal of Hydrology* 374 (1-2): 16-29.

Fontaine, T. A., J. F. Klassen, T. S. Cruickshank, and R. H. Hotchkiss. 2001. "Hydrological Response to Climate Change in the Black Hills of South Dakota, USA." *Hydrological Sciences Journal* 46 (1): 27-40.

Gassman, P. W., M. R. Reyes, C. H. Green, and J. G. Arnold. 2007. "The Soil and Water Assessment Tool: Historical Development, Applications, and Future Research Directions." *Transactions of the ASABE* 50 (4): 1211-1250.

Green, C. H., M. D. Tomer, M. Di Luzio, and J. G. Arnold. 2006. "Hydrologic Evaluation of the Soil and Water Assessment Tool for a Large Tile-Drained Watershed in Iowa." *Transactions of the ASABE* 49 (2): 413-422.

Groffman, P. M., J. M. Tiedje, D. L. Mokma, and S. Simkins. 1992. "Regional Scale Analysis of Denitrification in North Temperate Forest Soils." *Landscape Ecology* 7 (1): 45-53.

Hayhoe, K. A. 2010. “A standardized framework for evaluating the skill of regional climate downscaled techniques.” *Dissertation. University of Illinois, Urbana-Champaign, Illinois, USA*

Hofstra, N. and A. F. Bouwman. 2005. "Denitrification in Agricultural Soils: Summarizing Published Data and Estimating Global Annual Rates." *Nutrient Cycling in Agroecosystems* 72 (3): 267-278.

Labat, D., Y. Goddéris, J. L. Probst, and J. L. Guyot. 2004. "Evidence for Global Runoff Increase Related to Climate Warming." *Advances in Water Resources* 27 (6): 631-642.

Knutti, R., R. Furrer, C. Tebaldi, J. Cermak, and G.A. Meehl. 2010. “Challenges in combining projections from multiple climate models.” *American Meteorological Society* 23(10), 2739–2758.

Kundzewicz, Z.W., L.J. Mata, N.W. Arnell, P. Döll, P. Kabat, B.Jiménez, K.A. Miller, T. Oki, Z. Sen, and I.A.Shiklomanov.2007. “Freshwater resources and their management. Climate Change 2007: Impacts, Adaptation and Vulnerability. Contribution of Working Group II to the Fourth Assessment Report of the Intergovernmental Panel on Climate Change”. Editors: Parry, M.L., Canziani, O.F., Palutikof, J.P., van der Linden P.J., Hanson, C.E. *Cambridge University Press, Cambridge, UK,* 173–210.

Maski, D., K. R. Mankin, K. A. Janssen, P. Tuppad, and G. M. Pierzynski. 2008. "Modeling Runoff and Sediment Yields from Combined in-Field Crop Practices using the Soil and Water Assessment Tool." *Journal of Soil and Water Conservation* 63 (4): 193-203.

Meehl, G.A., T.F. Stocker, W.D. Collins, P. Friedlingstein, A.T.Gaye, J.M. Gregory, A. Kitoh, R. Knutti, J.M. Murphy, A.Noda, S.C.B. Raper, I.G. Watterson, A.J. Weaver, and Z.-C. Zhao. 2007. "Global climate projections. In Climate Change 2007: The Physical Science Basis. Contribution of Working Group I to the Fourth Assessment Report of the Intergovernmental Panel on Climate Change". Solomon, S., Qin, D., Manning, M., Chen, Z., Marquis, M., Averyt, K.B., Tignor, M., Miller, H.L., Cambridge University Press, Cambridge, United Kingdom and New York, NY, USA.

Milly, P. C. D., K. A. Dunne, and A. V. Vecchia. 2005. "Global Pattern of Trends in Streamflow and Water Availability in a Changing Climate." *Nature* 438 (7066): 347-350.

Moriasi, D. N., J. G. Arnold, M. W. Van Liew, R. L. Bingner, R. D. Harmel, and T. L. Veith. 2007. "Model Evaluation Guidelines for Systematic Quantification of Accuracy in Watershed Simulations." *Transactions of the ASABE* 50 (3): 885-900.

Mu, Q., M. Zhao, and S. W. Running. 2011. "Evolution of Hydrological and Carbon Cycles under a Changing Climate. Part III: Global Change Impacts on Landscape Scale Evapotranspiration." *Hydrological Processes* 25 (26): 4093-4102.

Myers, D.N., K.D. Metzker, and S. Davis. 2000. "Status and trends in suspended-sediment discharges, soil erosion, and conservation tillage in the Maumee River Basin—Ohio, Michigan, and Indiana". *Water Resources Investigations Report: 2000-4091. USGS Information Service, Denver, CO.*

Neitsch, S. L., J. G. Arnold, J. R. Kiniry, J. R. Williams, and K. W. King. 2002. "Soil and Water Assessment Tool Theoretical Documentation Version 2000." *Soil and Water Assessment Tool Theoretical Documentation, Version 2000.*

NRCS. 2005. "Western Lake Erie basin water resources protection plan: Ohio, Indiana and Michigan. Natural Resources Conservation Service". Retrieved October 8, 2012 from ftp://ftp-fc.sc.egov.usda.gov/OH/pub/Programs/Lake_Erie/erie_basin_plan.pdf.

Park, J. -Y, M. -J Park, M. -J H. -K Joh, H. -J Shin, H. -J Kwon, R. Srinivasan, and S. -J Kim. 2011. "Assessment of MIROC3.2 Hires Climate and Clue-s Land use Change Impacts on Watershed Hydrology using Swat." *Transactions of the ASABE* 54 (5): 1713-1724.

Parry, M.L., O.F. Canziani, J.P. Palutikof, P.J. van der Linden, and C.E. Hanson. 2007. “Climate change 2007: Impacts, adaptation and vulnerability. Contribution of Working Group II to the Fourth Assessment Report of the Intergovernmental Panel on Climate Change.” *Cambridge University Press, Cambridge.*

Phomcha, P., P. Wirojanagud, T. Vangpaisal, and T. Thaveevouthti. 2011. "Predicting Sediment Discharge in an Agricultural Watershed: A Case Study of the Lam Sonthi Watershed, Thailand." *ScienceAsia* 37 (1): 43-50.

Praskievicz, S. and H. Chang. 2009. "A Review of Hydrological Modelling of Basin-Scale Climate Change and Urban Development Impacts." *Progress in Physical Geography* 33 (5): 650-671.

Pruski, F. F. and M. A. Nearing. 2002. "Runoff and Soil-Loss Responses to Changes in Precipitation: A Computer Simulation Study." *Journal of Soil and Water Conservation* 57 (1): 7-16.

Raupach, M. R., G. Marland, P. Ciais, C. Le Quéré, J. G. Canadell, G. Klepper, and C. B. Field. 2007. "Global and Regional Drivers of Accelerating CO2 Emissions." *Proceedings of the National Academy of Sciences of the United States of America* 104 (24): 10288-10293.

Richards, R. P., D. B. Baker, and D. J. Eckert. 2002. "Trends in Agriculture in the LEASEQ Watersheds, 1975-1995." *Journal of Environmental Quality* 31 (1): 17-24.

Royer, T. V., M. B. David, and L. E. Gentry. 2006. "Timing of Riverine Export of Nitrate and Phosphorus from Agricultural Watersheds in Illinois: Implications for Reducing Nutrient Loading to the Mississippi River." *Environmental Science and Technology* 40 (13): 4126-4131.

Ruddy, B.C., D.L. Lorenz, and D.K. Mueller. 2006. “County-level estimates of nutrient inputs to the land surface of the conterminous United States, 1982–2001”. *National Water Quality Assessment Program, U.S. Geological Survey.*

Schuur, E. A. G., J. Bockheim, J. G. Canadell, E. Euskirchen, C. B. Field, S. V. Goryachkin, S. Hagemann, et al. 2008. "Vulnerability of Permafrost Carbon to Climate Change: Implications for the Global Carbon Cycle." *Bioscience* 58 (8): 701-714.

Trenberth, K. E. 1999. "Conceptual Framework for Changes of Extremes of the Hydrological Cycle with Climate Change." *Climatic Change* 42 (1): 327-339.

Trenberth, K. E., L. Smith, T. Qian, A. Dai, and J. Fasullo. 2007. "Estimates of the Global Water Budget and its Annual Cycle using Observational and Model Data." *Journal of Hydrometeorology* 8 (4): 758-769.

Walker W.W., and J.Kuhner. 1978. “An empiracal analysis of factors controlling eutrophication in midwestern impoundments.” *In: International Symposium on the Environmental Effects of Hydraulic Engineering Works, University of Tennessee, Knoxville, TN*.

Wu, Y., S. Liu, and O. I. Abdul-Aziz. 2012. "Hydrological Effects of the Increased CO 2 and Climate Change in the Upper Mississippi River Basin using a Modified SWAT." *Climatic Change* 110 (3-4): 977-1003.

Zahabiyoun, B., M. R. Goodarzi, A. R. M. Bavani, and H. M. Azamathulla. 2013. "Assessment of Climate Change Impact on the Gharesou River Basin using SWAT Hydrological Model." *Clean - Soil, Air, Water*.

CHAPTER 6

Data Mining Techniques for Nutrient Load Estimation in the Lake Erie Basin, Ohio

Abstract

Hydrologic monitoring studies have increased significantly over the past few years leading to generation of extensive time-series datasets. A lot of these studies currently focus on monitoring nutrient loads in agricultural, forested and urban streams around the world. Majority of existing modeling techniques used in these studies are not very accurate and also need large amounts of observational flow and concentration data to predict similar quantities of missing concentration data. This study focuses on using data mining techniques which have not been traditionally utilized for load estimation in hydrology, to predict missing nutrient concentrations and their corresponding loads. Data mining techniques as Nearest-Neighbor methods and Decision Trees were used to predict missing nutrient concentrations for two extensively monitored watersheds in the Lake Erie basin, Ohio. Results using these data mining techniques were then compared to the remaining time-series and indicators such as Root Mean Square Error (RMSE) were used to evaluate their performance.

Keywords: Data mining, nearest-neighbor, decision trees, nitrate concentrations, Lake Erie

6.1 Introduction

Intensification of agriculture over the past few decades has led to an increase in nutrient application rates around the world. Consequently nutrient delivery rates to receiving water bodies have increased and have long been identified as major causes of eutrophication in these water bodies (Turner and Rabalais, 1994). Hypoxic conditions attributed to nutrient enrichment have been observed in the Great Lakes since the 1960-70s (Boyce et al., 1987). Lake Erie has been particularly affected by these hypoxic conditions. With successful implementation of various nutrient abatement programs in 1970s in the Great Lakes basin, a marked reduction in

eutrophication was observed in Lake Erie albeit only from point sources. Non-point sources still contributed to nutrient delivery into the lake (Richards, 1985).

From a water resources management and planning perspective and to better understand nutrient dynamics, it is essential to continuously monitor streams draining into these Great Lakes. It is crucial to identify the quantities and timing of movement of nitrogen and other nutrients from agricultural landscapes into receiving streams. Additionally, a comprehensive monitoring plan is needed to gauge impacts of various environmental pressures and responses to management practices.

Long-term range (time-series) streamflow and nutrient concentration measurements are critical to calculate annual or seasonal nutrient loads being delivered into the receiving water bodies (Guo et al., 2002). Rating curve techniques make measuring daily streamflow relatively inexpensive and easy. On the other hand, measuring daily nutrient concentrations across stream cross-sections involve significant time and financial investments. Thereby, most of the hydrological monitoring programs measure streamflow daily and nutrient concentrations at a regular sampling interval (1-week, 4-week etc.). This is further supported by some storm sampling to better quantify nutrient movement during high-flow periods. Further, the missing values in the nutrient concentration time-series are then traditionally estimated using regression and ratio estimators. The accuracy of these estimators is dependent on large amounts of observed streamflow and concentration data. There are also issues of bias arising from transformations between log and linear spaces.

This research focuses on investigating the potential of data mining techniques such as nearest-neighbor methods and decision trees as an alternate way to estimate missing nutrient concentrations in a sparse time-series using continuous streamflow and some concentration observations. Although , there have been a few studies which have used data mining techniques such as neural networks (Yu et al., 2004; Antcil et al., 2009) to estimate missing concentrations

but hardly any which have evaluated the potential and limitations of other techniques such as nearest-neighbors and decision trees for concentration estimation. These techniques were applied to datasets from two watersheds namely, the Maumee and Cuyahoga draining into Lake Erie. Long term time-series datasets of streamflow and nitrate-N were used in the study.

6.2 Material and Methods

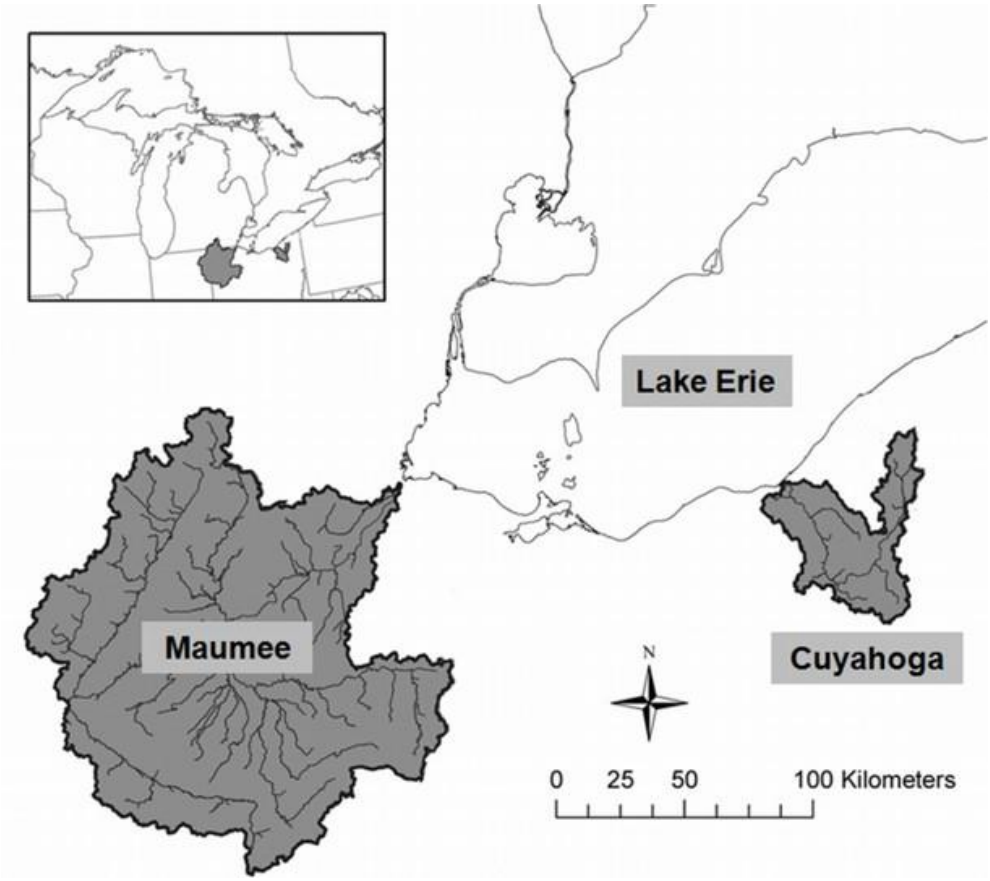

Figure 6.1: Maumee and Cuyahoga watersheds in the Lake Erie basin

6.2.1 Site Descriptions

The Maumee and Cuyahoga watersheds drain into the western and central basins of Lake Erie from Ohio (Figure 6.1). The Maumee watershed has a drainage area of 17,030 square kilometers and the Cuyahoga watershed has an area of about 2100 square kilometers. The

Maumee watershed is predominantly agricultural with about an 80% land-use being agricultural. The Cuyahoga watershed is significantly urbanized with about a 50% of its land-use being urban. Average annual precipitation is slightly higher for the Cuyahoga watershed due to more pronounced lake effects (Bosch et al., 2011).

6.2.2 Datasets

This paper utilized the long term time-series streamflow and nutrient concentration datasets collected by the National Center for Water Quality Research (NCWQR), Heidelberg University, Ohio. These datasets extended for 32 years and 28 years for the Maumee and Cuyahoga watersheds respectively. The datasets consisted of daily streamflow and nitrate-N (NO23) measurements at a gaging station on the downstream end of the watersheds. These daily measurements were also supplemented by more frequent sampling (up to 3 samples a day) during storms (high flow periods).

6.2.3 Data Mining Techniques

The software package Weka (Hall et al., 2009), was used to implement two data mining methods for prediction of missing nitrate-N concentrations in a multiyear time-series.

Instance based classifier (IBk)

IBk is an instance based classifier which is based on the k-nearest-neighbor algorithm. k is the number of nearest neighbors in the training dataset used to define the class of the test instance. This algorithm is a simple machine learning technique which locally assigns a class to the test instance based on a majority vote of its neighbors in the training dataset, with the instance being assigned a class which is most common amongst it k nearest-neighbors. A case with k=1, simply assigns the same class to the test instance as its nearest neighbor's class from the training dataset.

Reduced Error Pruning Tree (REPTree)

REPTree is an algorithm which works on the basic principle of divide and conquer to produce decision trees. Nodes in the decision tree represent points where particular attributes are tested by comparison with a constant value. Further division leads to leaf nodes and they represent the same classification for all the test instances that reach the leaf node. In case of numeric test attributes the nodes create a two way split with values greater or less than a constant. It is an algorithm optimized for speed and it sorts numeric attribute values only once saving considerable time as compared to other decision tree methods.

6.3 Results and Discussion

The IBk classifier was used to predict missing nitrate-N concentrations for the Cuyahoga watershed dataset while the REPTree classifier was used to predict missing nitrate-N concentrations for the Maumee watershed dataset. For both classifiers two techniques namely, cross validation and percentage split were used to evaluate the performance of the classifiers. Nitrate-N was the prediction class using daily measured streamflow, month and a certain number of observed nitrate-N concentrations to train the dataset. Month of measured streamflow was used as a training attribute to account for the seasonality in the nitrate-N concentrations as observed in the watersheds.

In case of cross validation, the complete dataset is divided into a certain number of equal sets (folds). Each fold is then used as a testing dataset while all the remaining folds used as training datasets for the classifiers. This process is repeated till all the folds have been used as a testing dataset at least once. This technique ensures that all instances are tested by the classifier. The percentage split technique is a simple method in which the complete dataset is split into training and testing portions. For example, a percentage split of 66% would entail that 66% of instances in the complete dataset are used to train the classifier while the remaining are used to

test the accuracy of the classifier. The test instances were randomly selected from the complete dataset.

Table 6.1: Performance evaluation of the IBk classifier for Cuyahoga watershed dataset to predict Nitrate-N concentrations using cross validation for training and testing datasets

Metric	Cross Validation			
Folds	10	5	5	5
K-Nearest Neighbors	1	1	2	4
Correlation coefficient	0.86	0.86	0.89	0.90
Mean absolute error	0.41	0.41	0.37	0.35
Root mean squared error	0.63	0.63	0.56	0.52
Relative absolute error (%)	42.36	42.68	38.27	36.59
Root relative squared error (%)	53.61	53.62	47.05	44.25
Total Number of Instances	12103	12103	12103	12103

Performance evaluation of the IBk classifier using cross validation predicted missing nitrate-N concentrations from the Cuyahoga watershed fairly accurately. For 1 nearest-neighbor (k=1), the IBk classifier predicted missing values with a correlation coefficient of 0.86 for both 5 and 10 folds. For a 5 fold cross validation, correlation coefficient increased on increasing the nearest-neighbors to 0.89 and 0.90 for k=2 and k=4 respectively. The Root Mean Square Error (RMSE) was also low ranging from 0.52 to 0.63 for different scenarios (Table 6.1). Figure 6.2 shows the scatter plot between the predicted and observed nitrate-N concentrations for different nearest neighbors for a 5 fold cross validation. The IBk classifier also performed well using the percentage split technique. For a training percentage split of 66% and k=1, the classifier gave a correlation coefficient of 0.85. On decreasing the training dataset percentage to 20% and 10% the correlation coefficient of the predicted and observed nitrate-N concentrations fell marginally to 0.83 and 0.80 respectively. Further, for a training percentage split of 10% the correlation coefficients of the predictions did not change much on increasing the nearest neighbors to 2 and 4. The RMSE varied from 0.64 to 0.74 for different scenarios (Table 6.2). Figure 6.3 shows the

scatter plot between the predicted and observed nitrate-N concentrations for different sizes of the training datasets (percentage split) using the IBk classifier.

Table 6.2: Performance evaluation of the IBk Lazy classifier for Cuyahoga watershed dataset to predict Nitrate-N concentrations using percentage split for training and testing datasets

Metric	Percentage Split				
Training Split (%)	66	20	10	10	10
K-Nearest Neighbors	1	1	1	2	4
Correlation coefficient	0.85	0.83	0.80	0.81	0.80
Mean absolute error	0.41	0.46	0.52	0.50	0.51
Root mean squared error	0.64	0.68	0.74	0.70	0.71
Relative absolute error (%)	42.92	48.22	54.32	51.96	53.73
Root relative squared error (%)	54.47	57.26	62.35	58.95	59.72
Total Number of Instances	4115	9683	10893	10893	10893

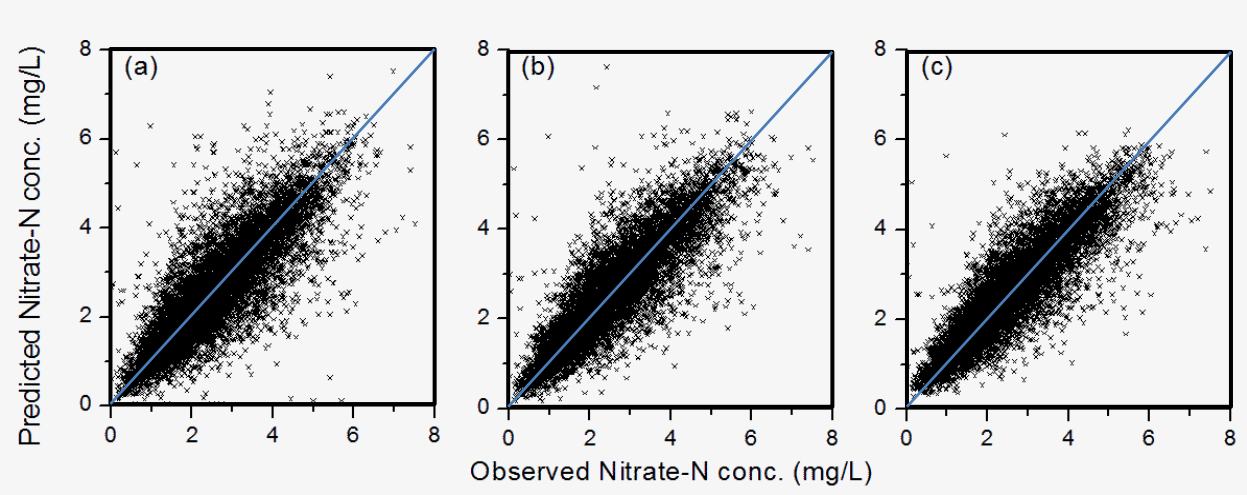

Figure 6.2: Predicted nitrate-N concentrations by the IBk classifier for Cuyahoga watershed using a 5 fold cross validation: (a) k (nearest neighbors) =1 (b) k=2 (c) k=4.

The REPTree classifier was used to predict missing nitrate-N concentrations for the Maumee watershed dataset. Using the cross validation technique the REPTree classifier performed very well giving high correlation coefficients of 0.93 and 0.92 for 10 and 5 folds respectively. The

RMSE was also low at 1.20 and 1.28 for 10 and 5 folds respectively (Table 6.3). The REPTree classifier also perfomed well using the percentage split technique. For a training percentage split of 66% the classifier gave a high correlation coefficient of 0.91 with a low RMSE of 1.35. The correlation coefficient of the predicted and observed nitrate-N concentrations fell to 0.80 and 0.71 on decreasing the training dataset percentage to 20% and 10% respectively. Consequently, the RMSE also increased to 1.94 and 2.29 for a training dataset percentage to 20% and 10% respectively (Table 6.4).

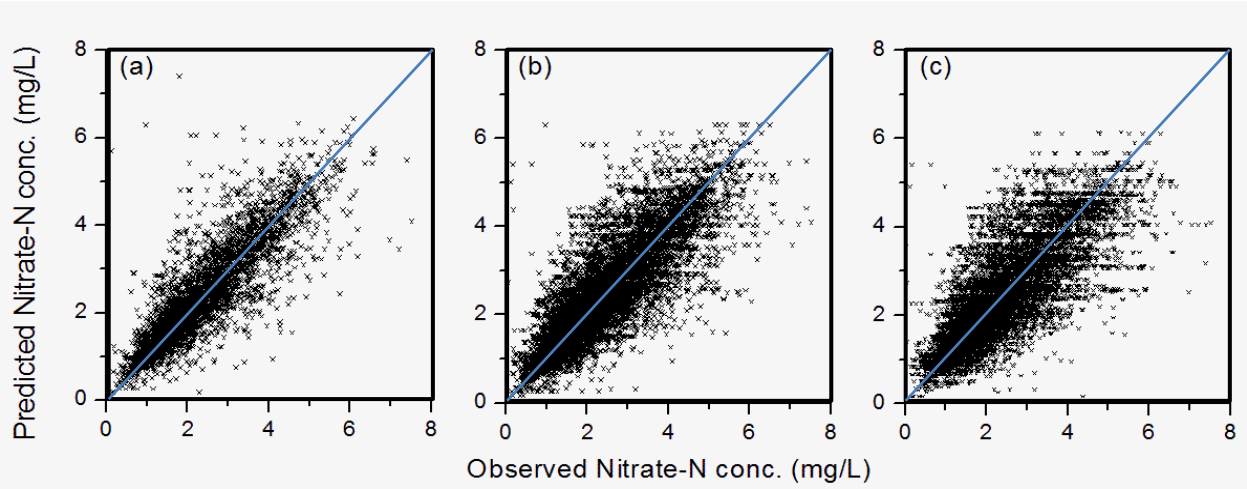

Figure 6.3: Predicted nitrate-N concentrations by the IBk classifier for Cuyahoga watershed using percentage split with a training percentage of: (a) 66 (b) 20 (c) 10

Table 6.3: Performance evaluation of the REPTree classifier for Maumee watershed dataset to predict Nitrate-N concentrations using cross validation for training and testing datasets

Metric	Cross Validation	
Folds	10	5
Correlation coefficient	0.93	0.92
Mean absolute error	0.70	0.76
Root mean squared error	1.20	1.28
Relative absolute error (%)	27.19	29.33
Root relative squared error (%)	37.28	39.73
Total Number of Instances	14555	14555

Table 6.4: Performance evaluation of the REPTree classifier for Maumee watershed dataset to predict Nitrate-N concentrations using percentage split for training and testing datasets

Metric	Percentage Split		
Training Split (%)	66	20	10
Correlation coefficient	0.91	0.80	0.71
Mean absolute error	0.81	1.32	1.62
Root mean squared error	1.35	1.94	2.29
Relative absolute error (%)	31.24	51.30	62.64
Root relative squared error (%)	41.50	60.53	71.25
Total Number of Instances	4949	11644	13099

The REPTree classifier being a decision tree data mining technique gives the same classification or prediction to all instances beyond a certain leaf node in the decision tree. This might lead to same predictions for a certain range of observed instances based on the decision tree created. If the training dataset is small, the ranges of instances having similar predictions might be large. This is fairly evident from Figure 6.4(b) and 6.4(c) where horizontal bands of predicted nitrate-N concentrations can be observed for a large range of observed instances.

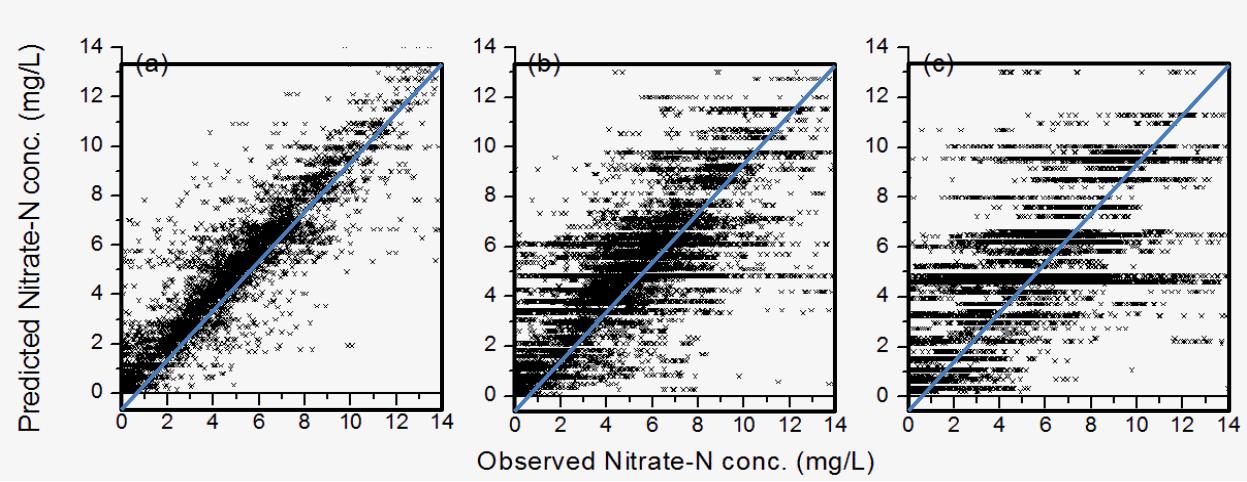

Figure 6.4: Predicted nitrate-N concentrations by the REPTree classifier for Maumee watershed using percentag split with a training percentage of: (a) 66 (b) 20 (c) 10

6.4 Conclusions

This study evaluated the performance of nearest-neighbor (IBk) and decision tree (REPTree) data mining methods to predict missing nitrate-N concentrations from long multi-year time-series from two watersheds in the Lake Erie basin. Two different evaluation techniques, cross validation and percentage split were used for both the data mining methods to create the training and testing datasets. Both data mining techniques were successful in predicting nitrate-N concentrations with high correlation coefficients ranging from 0.80 to 0.90 and 0.71 to 0.93 for the IBk and REPTree methods respectively. These data mining techniques present a host of advantages over the traditional statistical and physical models used in hydrology to predict missing nutrient concentrations. Firstly, these techniques are not constrained by assumptions in data such as linearity and homoscedasticity. Secondly, they aren't constrained by number of parameters used. Thirdly, they eliminate any possible transformation biases arising from converting datasets from log to linear spaces and vice-versa as in case of a few statistical methods. Lastly, these techniques can be implemented fairly quickly using very basic computational power. As both these data mining methods utilized streamflow, month of sampling and some concentration samples to predict the missing concentrations, they can be applied to watersheds with limited concentration data.

The results using these data mining methods are expected to vary with different constituents, watersheds and hydro-climatic zones. Future studies should be directed to evaluate the performance of these data mining methods on a large variety of watersheds from different hydro-climatic zones. Also, studies should quantify the outcome of data availability on the performance of these methods.

References

Turner, R. E., and N. N. Rabalais, Coastal eutrophication near the Mississippi River delta, Nature, (1994)368 (6472): pp 619–621.

Boyce, F.M., Charlton, M.N., Rathke, D., Mortimer and C.H., Bennett, J., Lake Erie research: Recent results, remaining gaps, J. Great Lakes Res. 13, (1987), pp 826–840.

Richards, R.P., Esimating the extent of reduction needed to statistically demonstrate reduced non-point phosphorus loading to Lake Erie, J. Great Lakes Res. 11, (1985), pp 110–116.

Guo, Y., Markus, M., and Demissie, M, Uncertainty of nitrate-N load computations for agricultural watersheds. Water Resources Research, (2002), 38(10), pp 31–312.

Yu, C., Northcott, W. J., and McIsaac, G. F. Development of AN artificial neural network for hydrologic and water quality modeling of agricultural watersheds, Transactions of the ASAE, 47(1), (2004), pp 285–290.

Anctil, F., Filion, M., and Tournebize, J, A neural network experiment on the simulation of daily nitrate-nitrogen and suspended sediment fluxes from a small agricultural catchment, Ecological Modeling, (2009), 220(6), pp 879–887.

Bosch NS, Allan JD, Dolan DM, Han H, Richards RP, Application of the soil and water assessment tool for six watersheds of Lake Erie: Model parameterization and calibration, J Great Lakes Res. (2011), 37(2), pp 263-71.

Hall M., Frank E., Holmes G., Pfahringer B., Reutemann P., Witten I.H., The WEKA Data Mining Software: An Update, SIGKDD Explorations, Volume 11, (2009), Issue 1.

CHAPTER 7

A sensitivity analysis of annual nitrate loads and the corresponding trends in the Lower Illinois River [2]

Abstract

Riverine nutrient concentrations and loads in the Midwestern United States have been identified as a major source of nutrients for the Mississippi River, causing hypoxia in the Gulf of Mexico. The Illinois River is one of the major contributors of nutrients to the Mississippi River, draining more than 40 percent of Illinois and parts of Indiana and Wisconsin. The main goals of this study were to calculate annual average nitrate concentration and annual total loads in the Lower Illinois River and its tributaries for 1975–2010, and to determine how the selection of different approaches affects the calculated trends. The Illinois Environmental Protection Agency (IEPA) has been collecting surface water quality data in Illinois since the early 1970s. This study used nitrite-N+nitrate-N (NO_2+NO_3) samples provided by IEPA and collected from the Illinois River at Havana and Valley City, Sangamon River at Oakford, and La Moine River at Ripley for the period 1975–2010. Discharge data concurrent with routine water quality samples were applied to a suite of approaches to estimate daily concentration and load for the period of analysis, including the seven-parameter regression equation along with several modeling residual adjustment techniques and the Weighted Regression on Time, Discharge, and Season (WRTDS) method. The calculated annual mean concentration and annual total loads for NO_2+NO_3 for the period of record were discussed in relation to different approaches.

Keywords: Illinois River, load estimation, trends, nitrate, regression, residual adjustment

7.1 Introduction

Nutrient loads in the Mississippi River have been a major focus of various studies (Aulenbach et al., 2007; Sprague et al., 2011) due to their significant contribution to hypoxia in

[2] Markus et al., 2013, *Journal of Hydrologic Engineering.* With permission from ASCE. This material may be downloaded for personal use only. Any other use requires prior permission of the American Society of Civil Engineers.

the Gulf of Mexico (EPA Science Advisory Board, 2008; WSTB, 2009). The Illinois River drains predominantly agricultural areas which often provide high loads of nutrients to the Mississippi River. Accurate calculations of seasonal, annual, and long-term nutrient loads passing a given monitoring station are critical in designing appropriate remediation management strategies. Determining nutrient loads typically combines frequently (daily) monitored discharge data and relatively less frequently (monthly or quarterly) monitored nutrient concentration data. As a result, the determination of nutrient loads is an estimation problem subjected to many potential sources of uncertainty, including data and modeling errors. A wide variety of load estimation modeling approaches have been developed and used to estimate loads of various water quality constituents (e.g., Verhoff et al., 1980; Dolan et al., 1981; Ferguson, 1987; Cohn et al., 1989, 1992; Walker, 1996; Guo et al., 2002; Crowder et al., 2007). These different approaches generally could be divided into averaging, ratio, and regression estimators (Preston et al., 1989; Cohn, 1995; Guo et al., 2002). More recently, the residual adjustment techniques such as the composite method (Aulenbach and Hooper, 2006) have been introduced to utilize the autocorrelation in concentration residuals. Similar to the composite method, Verma et al. (2012) proposed triangular and rectangular shape functions to account for residuals in the vicinity of observed concentrations, using proportional and residual adjustment methods. To remove the effects of random variations of streamflow on estimated concentrations and flux, Hirsch et al. (2010) suggested a new approach, weighted regression on time, discharge, and season (WRTDS). This method was applied to study trends in nutrient concentration and flux in the Mississippi River and its tributaries, including the Illinois River for 1980 to 2008 (Sprague et al., 2011).

This study uses the above estimation methods to calculate continuous daily nitrite-nitrogen + nitrate-nitrogen (NO_2+NO_3) concentration and load data in the Lower Illinois watershed. For brevity, in this study the term "nitrate" is used to denote the sum NO_2+NO_3. This research evaluates the selected estimators in estimating the annual nitrate loads, but does not attempt to

synthesize the sources of nitrate variability in this watershed such as denitrification and effects of floodplains and wetlands (e.g., Panno et al., 2008). Specifically, the main goals of this study were (1) to calculate annual average nitrate concentration and annual total loads in the Lower Illinois River and its tributaries for 1975–2010 using several approaches; and (2) to determine how different approaches affect calculated loads and concentrations and their trends. These approaches included the regression estimator (Cohn et al., 1992), coupled with several residual adjustment methods (Aulenbach and Hooper, 2006; and Verma et al., 2012) and the Weighted Regression on Time, Discharge, and Season (WRTDS) method (Hirsch et al., 2010).

7.2 Methodology

The rating curve estimator, based on the seven-parameter linear regression model, was developed specifically for nutrient concentration estimation by Cohn et al. (1992). This regression model was tested by Robertson and Roerish (1999) for small streams in Wisconsin and by Short (1999) for the estimation of nutrient loads from Illinois watersheds. Similar approaches also were presented in load calculations for the Upper Sangamon River in Illinois (Guo et al., 2002) and in the Gulf of Mexico hypoxia assessment (Aulenbach et al., 2007).

The seven-parameter log linear model relies on the correlation between discharge and load, and requires the estimation of the following parameters: a constant, a quadratic fit to the logarithm of discharge, a quadratic fit to time, and a sinusoidal function to remove the effects of annual seasonality (Cohn et al., 1992).

Two general approaches were compared in this study to examine trends in annual nitrate loads and concentrations (Figure 7.1). The first approach includes the rating curve estimator (Cohn, 1995), coupled with several residual adjustment techniques (Aulenbach and Hooper, 2006, and Verma et al., 2012). The second approach was based on the WRTDS (Hirsch et al., 2010). In the subsequent sections, these approaches are described in more detail.

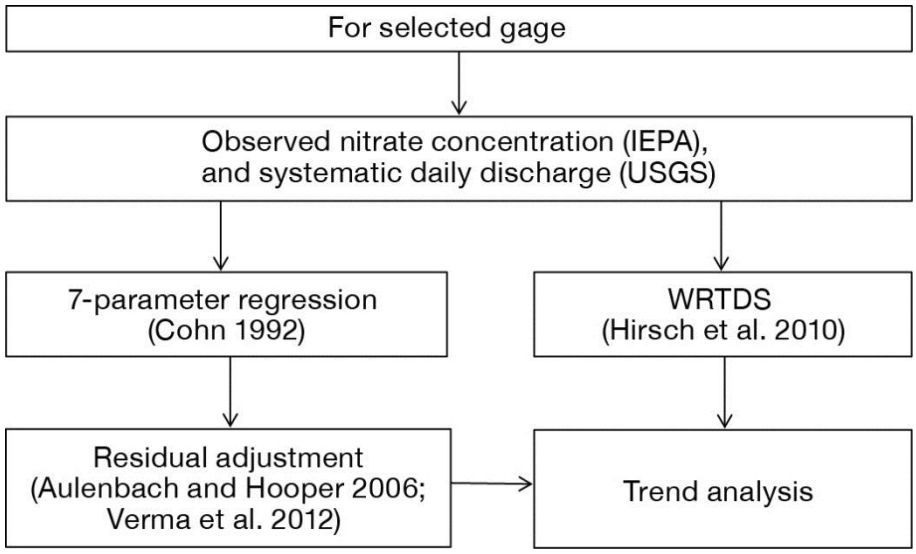

Figure 7.1: Schematic of the methods used in the study

7.2.1 Regression Estimator

The estimator developed by Cohn et al. (1992) is a multiple non-linear regression model which develops and utilizes a relationship between a sparsely collected dependent variable (i.e., concentration) and continuous independent variables such as flow rate and time of year. To achieve a better linear relationship between the dependent and independent variables and to reduce the influence of extreme flows on load calculations, logarithmic transformations are used in the model as follows:

$$\ln(C) = \beta_0 + \beta_1 \ln\left(\frac{Q}{Q'}\right) + \beta_1 \left[\ln\left(\frac{Q}{Q'}\right)\right]^2 + \beta_3 (T - T') + \beta_4 (T - T')^2 + \beta_5 \sin(2\pi T) + \beta_5 \cos(2\pi T) + \varepsilon \quad (7.1)$$

Where ln ( ) denotes natural logarithmic function, C and Q denote the nitrate concentration and flow rate, T denotes time measured in years, ε denotes the errors, which are assumed to be normally distributed with a mean of 0 and a variance of σ_ε^2, β_0, β_1….β_6 denote the various regression parameters estimated from the available dataset, and Q' and T' denote centering variables used in the model. Concentrations from sampled days, along with the corresponding mean daily flow rate and Julian days are used to compute the seven parameters. The model is

then used to estimate log-concentrations and ultimately concentrations on un-sampled days. The complete concentration dataset is then used to obtain load estimates for the monitoring period. Details of this model can be found in Cohn et al. (1992). For shorter time periods, the seven-parameter Eq. (7.1) can be simplified by removing the terms corresponding to β_3 and β_4.

The concentration residual time series term (ε in Eq.7.1) was found to have a significant serial correlation (autocorrelation). For example, for a monthly sampling frequency at a 41-ha experimental basin in Georgia, Aulenbach et al. (2007) found an autocorrelation of 0.20. At two watersheds in central Illinois ranging in size between 3,161 km^2 and 3,424 km^2, Verma et al. (2012) calculated autocorrelation values between 0.25 and 0.30 for a four-week sampling interval. By capturing residual autocorrelation, it is possible to improve load estimates or maintain the same accuracy of load estimates using fewer observations than the traditional methods. The methods capturing the residual autocorrelation are described below, followed by the description of WRTDS and trend tests used in this study.

7.2.2 Composite Method

Aulenbach and Hooper (2006) proposed an alternative approach to estimating constituent loads called the composite method. They used an extensive dataset collected at the outlet of the Panola Mountain Research Watershed (PMRW) near Atlanta, Georgia, USA, to illustrate this method, which combines the strengths of regression and period-weighted approaches. Residual concentrations are computed for all sampled days by subtracting concentrations estimated using the regression model from the corresponding measured values, and a piecewise continuous linear function of the residual concentrations over time is developed. The residual concentration from this composite function is then subtracted from the regression concentrations on unsampled days. Aulenbach and Hooper (2006) demonstrated that the composite method improved load estimation accuracies over short time intervals and allowed for better trend analysis of load estimates. The composite method was based on the principle of autocorrelation

amongst the residual concentrations, and it used a piecewise linear interpolation to distribute residuals in between sampled concentrations. This concept is an advanced form of curve fitting, which has created a new class of error-correction techniques for load estimation models. Based on this concept, by optimizing the distributions used to assign residuals in between sampled concentrations, potentially more accurate new error correction techniques may be developed.

7.2.3 Residual Adjustment

Similar to the composite method, in the study of Verma et al. (2012), the temporal correlation in modeling errors (residuals) were taken into consideration by assigning errors on unsampled days, based on known errors on proximate sampled days. Residual concentrations were calculated on sampled days by finding the difference in regression-model-predicted concentration and observed concentrations. The mid-points of the time interval between all the pairs of consecutive sampled days were then determined. These midpoints were then set as vertices in the estimation of the residuals on adjacent unsampled days. In this study, instead of using stepwise linear interpolation, as in the composite method, rectangular- and triangular-shaped distributions were used to assign errors in the vicinity of a known error (Figure 7.2). For the rectangular distribution, the residual at an unsampled day was assigned the value of the residual on the closest sampled day. For the triangular distribution, the magnitude of the residuals were assumed to be maximum on the sampled days and vary linearly to zero at mid-points of the time-intervals between consecutive sample days.

In addition, Verma et al. (2012) used another set of correction techniques based on proportional concentrations rather than residual concentrations. A proportional concentration is defined as the ratio between the observed/measured concentration and the model estimated concentration on a sampled day. Once the set of proportional concentrations was obtained for all sample observations, the rectangular and triangular distributions again were used to assign concentrations in the vicinity of known proportional concentrations.

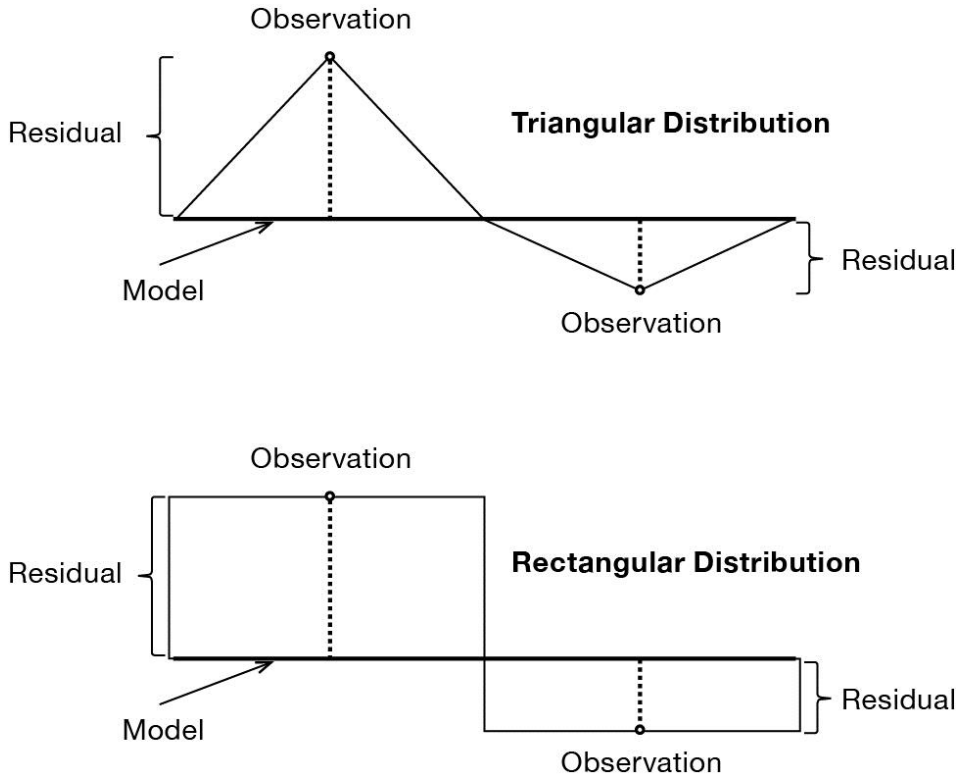

Figure 7.2: Triangular and rectangular distributions adopted from Verma et al. (2012)

7.2.4 Weighted Regressions on Time, Discharge, and Season

The WRTDS method suggested by Hirsch et al. (2010) used the following equation to calculate daily concentration:

$$\ln(C) = \beta_0 + \beta_1 t + \beta_2 \ln(Q) + \beta_3 \sin(2\pi T) + \beta_4 \cos(2\pi T) + \varepsilon \quad (7.2)$$

In Eq. 7.2, ln is natural log, c is concentration, β_i are fitted coefficients, Q is daily mean streamflow, t is decimal time, and ε is the unexplained variation. In the WRTDS method a unique set of coefficients is estimated for every combination of Q and t in the period of record. For every combination of Q and t, the coefficients in Eq. 7.2 are estimated using weighted regression. The weights on each observation in the calibration dataset are based on the distance in time, streamflow, and season between the observation and (Q,t). To remove the effect of random streamflow variations on the annual flux computed by WRTDS, a flow-normalization

(FN) method is suggested (Hirsch et al. 2010). The FN estimates of concentration are computed for a given date using weighted regressions to estimate concentration on that date with the streamflow value set to each one of the historical streamflow values for that day. The FN concentration on that date is then calculated as the mean of the estimated concentration values from each of those weighted regressions.

7.2.5 Kendall's Tau Trend Test

Statistical tests for trends were required to provide an objective way for detecting significant linear trends in the calculated annual average concentrations, total loads, and average discharges. Although there is uncertainty based on selection of trend tests (Keefer et al., 2010), in this study, for consistency, we used the Kendall's Tau test (Kendall, 1955; Helsel and Hirsch, 1995). For each trend test, one has to select a level of confidence with which the null hypothesis (no-trend) will be rejected. In water resources literature, most authors use the confidence level of 95% (Neumann et al., 2003), but others use 90% (Walker, 2003). In this study, however, we used 80-, 90-, 95-, and 99-percent confidence levels to evaluate the degree of change for different datasets.

7.2.6 Şen Trend Test

In a recent paper, Şen (2012) offers a new technique for trend analysis, justified by a set of restrictive assumptions such as independent structure of the time series, normality of the distribution and length of data, characteristics for commonly used trend identification techniques. This new technique for trend detection is based on sub-section time series plots derived from a given time series on a Cartesian coordinate system. In such a plot trend free time series, sub-sections appear along the 45° straight-line. Increasing (decreasing) trends occupy the upper (lower) triangular areas of the square area defined by the variation domain of the variable concerned. More details on the technique and applications are given in Şen (2012).

7.2.7 Watershed Description and Data Sources

The Illinois River drains over 74,000 km^2 primarily in Illinois, but the watershed includes portions of Indiana, Wisconsin, and Michigan. The Illinois River contains numerous backwater lakes, wetlands, and floodplain forest, and the river valley provides significant habitat for fisheries, waterfowl, and other birds and animals, making it an important ecological resource. Land use is predominantly agriculture, but the watershed also receives discharges and runoff from the Chicago metropolitan as well as other urban areas along its length. The river has been further altered by navigation dams, diversion of water from Lake Michigan, along with sedimentation and chemical runoff from agricultural activities. The study area is located in the Lower Illinois River basin (Figure 7.3), which stretches from the Fox River to the Illinois River's confluence at the Mississippi River (Terrio, 2006).

Nitrate data from four water quality monitoring stations operated by the Illinois EPA as part of their statewide ambient network, three of which are collocated with USGS gages, were selected for this project (Wallin and Schafer, 1979; IEPA, 2007). The stations include two on the Illinois River, located at Havana (upstream) and Valley City (downstream), along with a station on the Sangamon River at Oakford and one on the La Moine River at Ripley (Table 7.1 and Figure 7.3). The Sangamon River is the largest tributary to the Illinois River and comprises 19% of the total drainage area at Valley City. Pre-1999 nitrate data were available from Legacy STORET (USEPA, 2011) while newer data are housed in multiple internal IEPA databases. Sample size ranged from 261 from the Sangamon River at Oakford to 407 on the La Moine River at Ripley. Although each station is part of an ambient network routinely sampled over its history on 4- to 6-week intervals, data from other IEPA monitoring projects were included in the analysis when available. The date range for this analysis, 1975 to 2010, was selected to take advantage of the longest timeline available for nitrate data, with the exemption of the Havana gage, for which the monitoring period of record was 1978-2007.

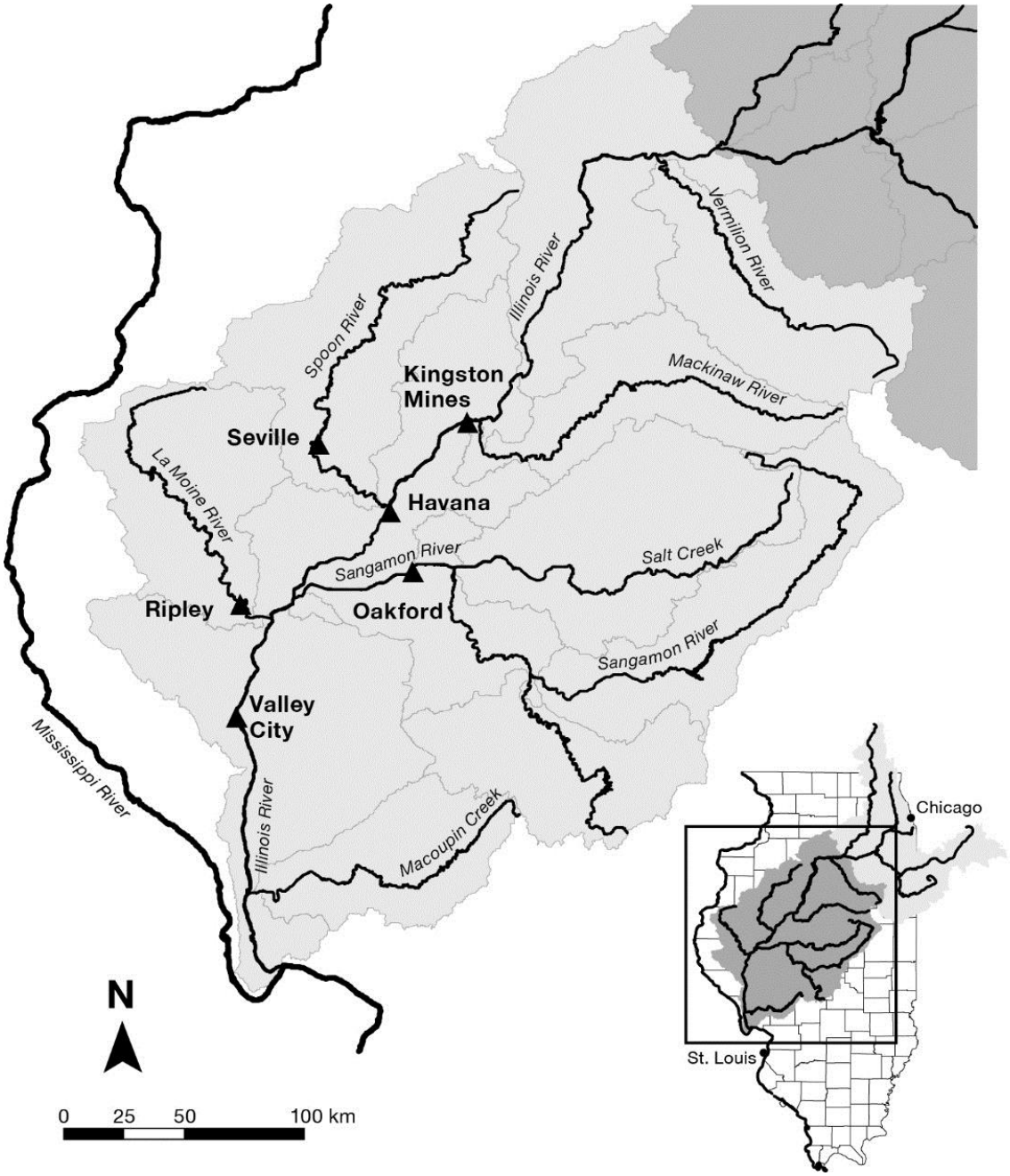

Figure 7.3: Map of the main channel and tributaries in the Lower Illinois River basin

Flow data were compiled from the USGS (http://waterdata.usgs.gov/nwis/). Daily flow data were available from USGS gages at Valley City, Oakford, and Ripley. Daily flow data for the Havana water quality site were determined from a study by Lian et al. (2010), which simulated flows for the entire Illinois River using the Hydrologic Simulation Program-FORTRAN (HSPF). Plots of nitrate concentration, sample date flow data, and linear regressions are shown in Figure

7.4 for the two Illinois River sites and Figure 7.5 for the two tributaries of the Lower Illinois River.

Table 7.1: Streamgages for nitrate concentration and discharge used in this study (1975-2010) * Calculated based on hydrologic modeling (Lian et al. 2010) for 1978-2007

USGS station no.	EPA station no.	Streamgage	Drainage Area (km^2)	Number of samples	Mean discharge (m^3/s)	Mean conc. (mg/L)
05570500	D-31	Illinois River at Havana*	46,845	269	568.3	4.16
05586100	D-32	Illinois River at Valley City	68,465	344	707.3	3.99
05583000	E-25	Sangamon River at Oakford	13,038	261	132.2	4.52
05585000	DG-01	La Moine River at Ripley	3,310	407	30.3	2.93

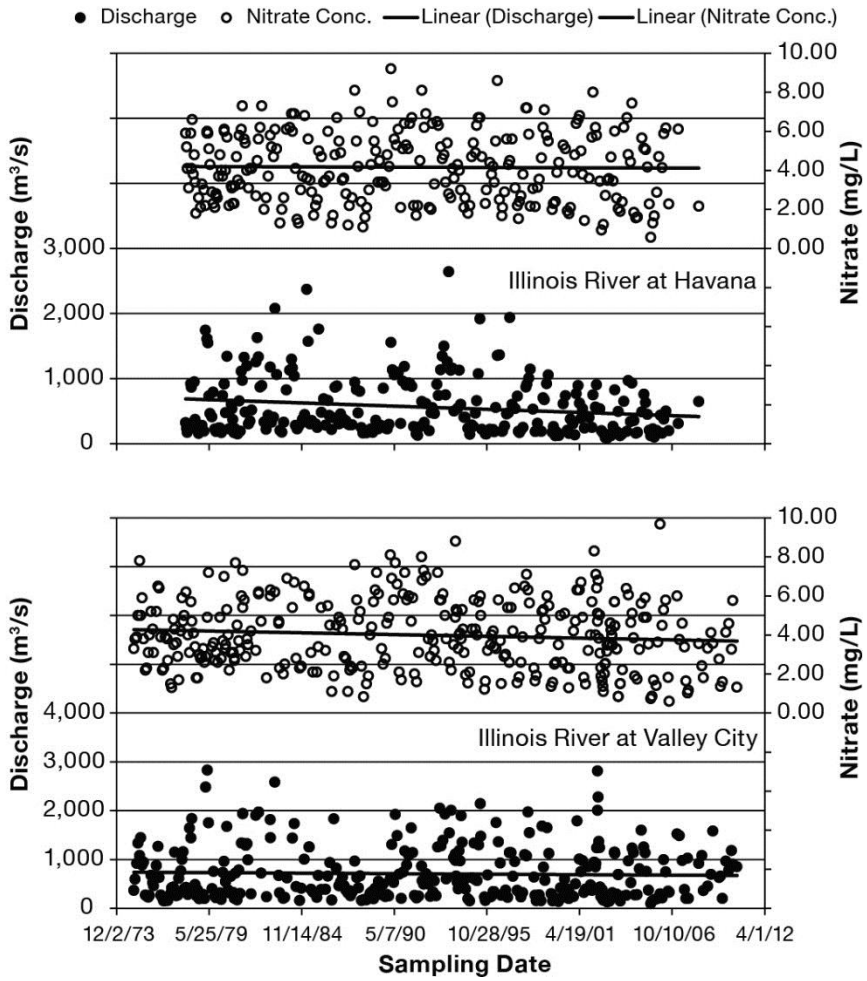

Figure 7.4: Discharge and concentration samples collected at Havana and Valley City on the Illinois River

It is generally thought that flow data concurrent with long-term datasets of water quality samples should provide a good estimate of long-term flow statistics. However, the results show that this notion doesn't always hold true. While there is a substantial decreasing trend in discharge values for days when water quality samples were collected at Havana (Figure 7.4), there is an increase in average annual discharges, calculated based on daily values at this site (Figure 7.6) and the nearest upstream and downstream gages, Kingston Mines and Valley City, respectively. This indicates that trends calculated on the samples alone could result in false determinations even with a long and rich dataset. As such, extending (interpolating) the data beyond the actual observed samples using estimation techniques is beneficial to study trends in nitrate concentrations and loads.

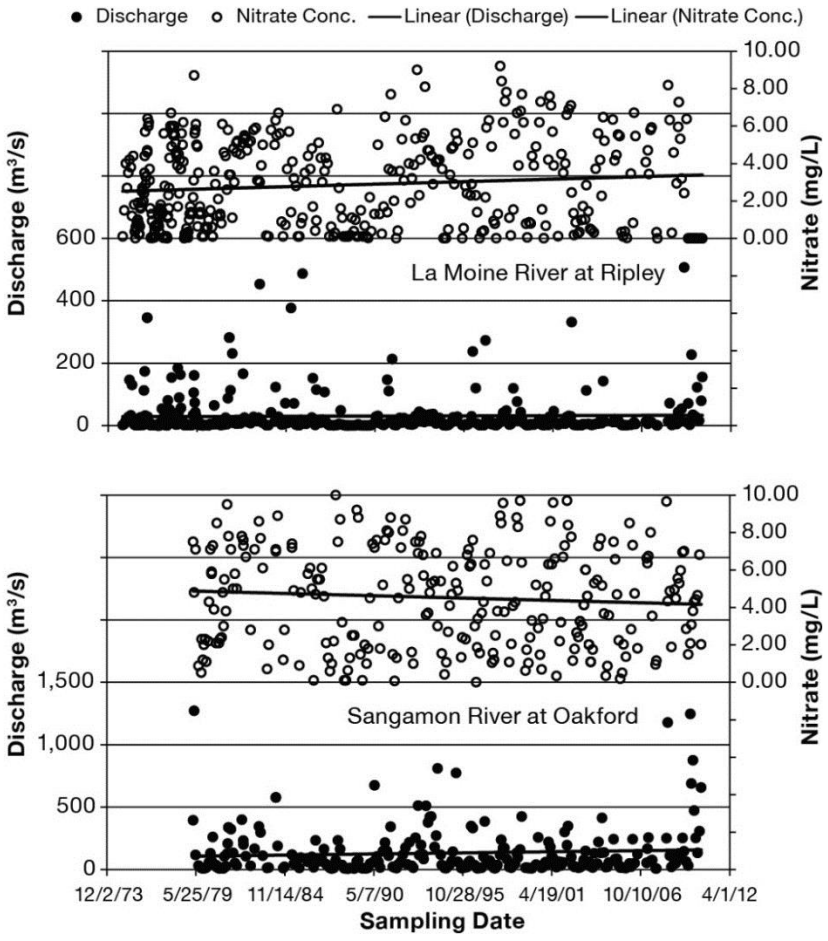

Figure 7.5: Discharge and concentration samples collected at the Lower Illinois River tributaries: Ripley on the La Moine River and Oakford on the Sangamon River

For the Illinois River at Valley City (Figure 7.4) and the two tributaries (Figure 7.5), however, trends in discharge calculated based on samples did not appear to be different from the trends based on the complete daily datasets. Regardless, to provide an objective and consistent analysis, we applied the above described regression-based tools to all four gages in the study. Also, as there was significant variability in flows, it was of our particular interest to test the changes in all four gages using the tool which removes the effects of flow variability (WRTDS).

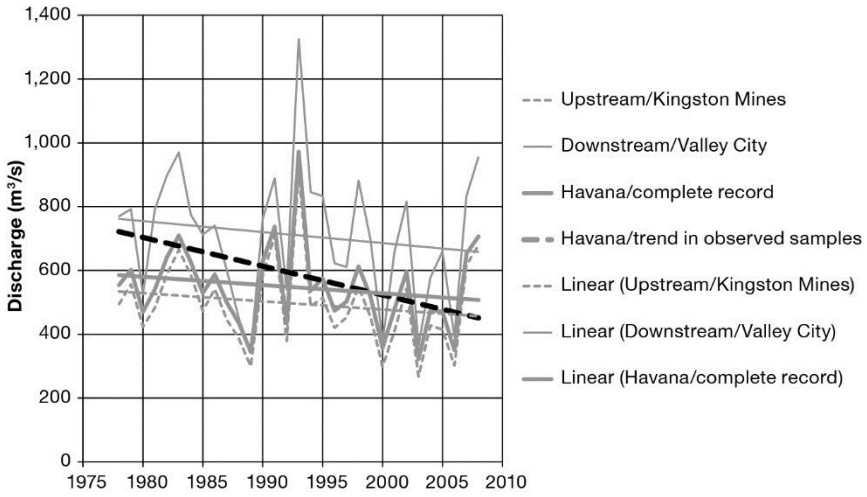

Figure 7.6: Difference in trends based on random observed samples and complete daily records at Havana. The nearest upstream (Kingston Mines) and downstream (Valley City) gages are shown for reference.

7.3 Results

7.3.1 Nitrate Concentration and Loads

The 7-parameter regression method (Cohn et al., 1992), one of the most frequently used models in research and applications (Short, 1999; Turner et al., 2006; Schilling and Spooner, 2006; Aulenbach et al., 2007; Hirsch et al., 2010), was used as a baseline method to calculate annual concentrations and loads. Then we used several residual adjustment methods in conjunction with the 7-parameter method to assess their performance and relative differences.

Figure 7.7 shows the baseline method and the following residual adjustment functions, rectangular residual adjustment (RRA), rectangular proportional adjustment (RPA), triangular residual adjustment (TRA), and triangular proportional adjustment (TPA) from Verma et al. (2012) and the composite method (Aulenbach and Hooper, 2006) at the upstream Havana and downstream Valley City stations on the Illinois River. The figure shows significant differences in annual nitrate concentration between the baseline method and the residual adjustment methods.

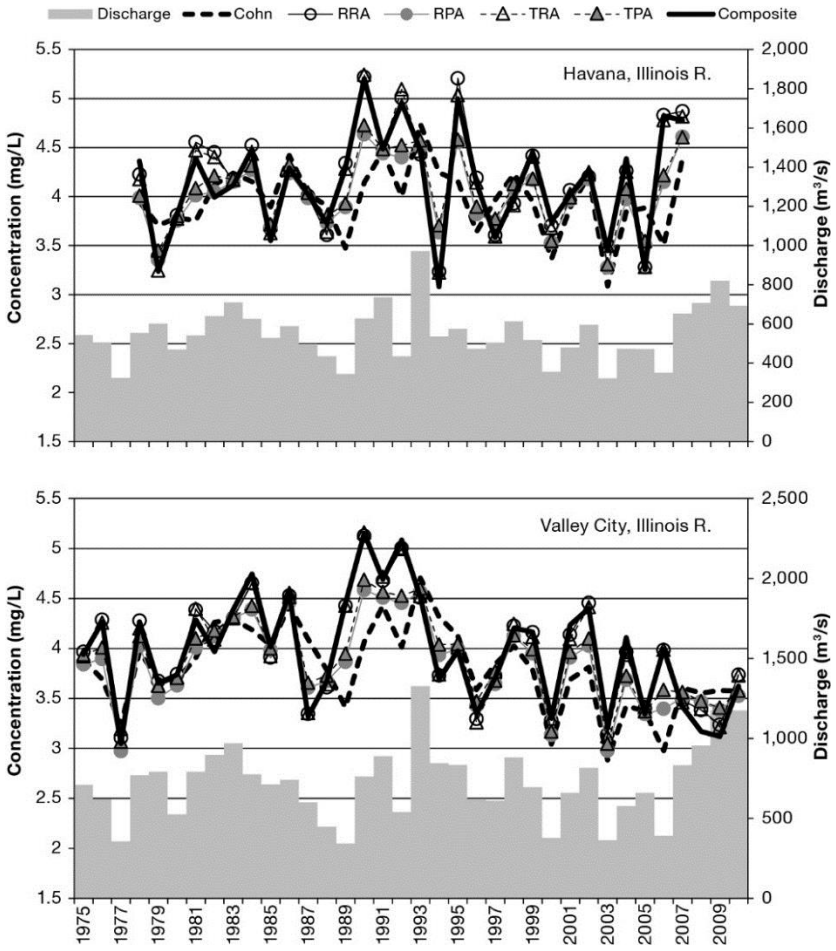

Figure 7.7: Annual average discharge bar-graph and annual average nitrate concentration based on the regression approach (Cohn 1992), various residual adjustment functions, RRA, RPA, TRA, TPA from Verma et al. (2012), and the composite method (Aulenbach and Hooper, 2006)

The baseline method produced approximately 4% lower concentrations and 20% smaller year-to-year variability than all other methods averaged. Among the residual adjustment

methods were two distinct groups of similar results. TPA and RPA produced very similar concentrations forming one group. The three remaining residual adjustment methods, RRA, TRA, and the composite method, also produced similar nitrate concentrations, forming another group.

Next, two approaches representing each group, RPA and the composite method, were selected based on their superior performance in past research (Verma et al., 2012; Aulenbach et al., 2007). Figure 7.8 shows these two approaches, along with the WRTDS method with and without flow normalization. The flow-dependent (not flow-normalized) WRTDS method was denoted as WRTDS, and the flow-normalized WRTDS as FN. While the annual average concentrations at Havana (Figure 7.8, top chart) appear to be relatively constant, the Figure 7.8 bottom chart (Valley City) shows a generally increasing trend in the first half of the record and then a generally decreasing trend in the second half based on RPA, composite, and WRTDS. The FN method shows a relatively constant concentration in the first half of the record and a decrease in the second part. The flow normalized method indicates that the overall reduction in annual nitrate concentration ranges from approximately 4.2 mg/L to about 3.2 mg/L – a 24% reduction. While Sprague et al. (2011) show a relatively constant annual flow-normalized nitrate concentration time-series with minor fluctuations, these results show a significant decrease in the past several years. Although some of these differences might be a result of using different data, different periods of record in the computations, and different parameterization of the WRTDS in the two studies, it appears that the primary reason for these differences is the fact that the WRTDS estimates are “less reliable at the beginning and at the end of the records” (Sprague et al., 2011). This high sensitivity of the WRTDS method to the addition of the high-flow years at the end of the record is reflected in the FN method. The last 2, 3, and 4 years (2009-2010, 2008-2010, and 2007-2010) have the highest 2-year, 3-year, and 4-year flow average on the record, respectively. It is commonly accepted that the concentrations and consequently loads tend to be higher after dry years and lower after wet years (Lucey and

Goolsby, 1993; McIsaac and Libra, 2003). The decreasing FN concentration in the last approximately 8 years at Valley City could be a result of the method sensitivity to a sequence of wet years at the end of the record, and not necessarily an indication of achieving nitrate reduction goals.

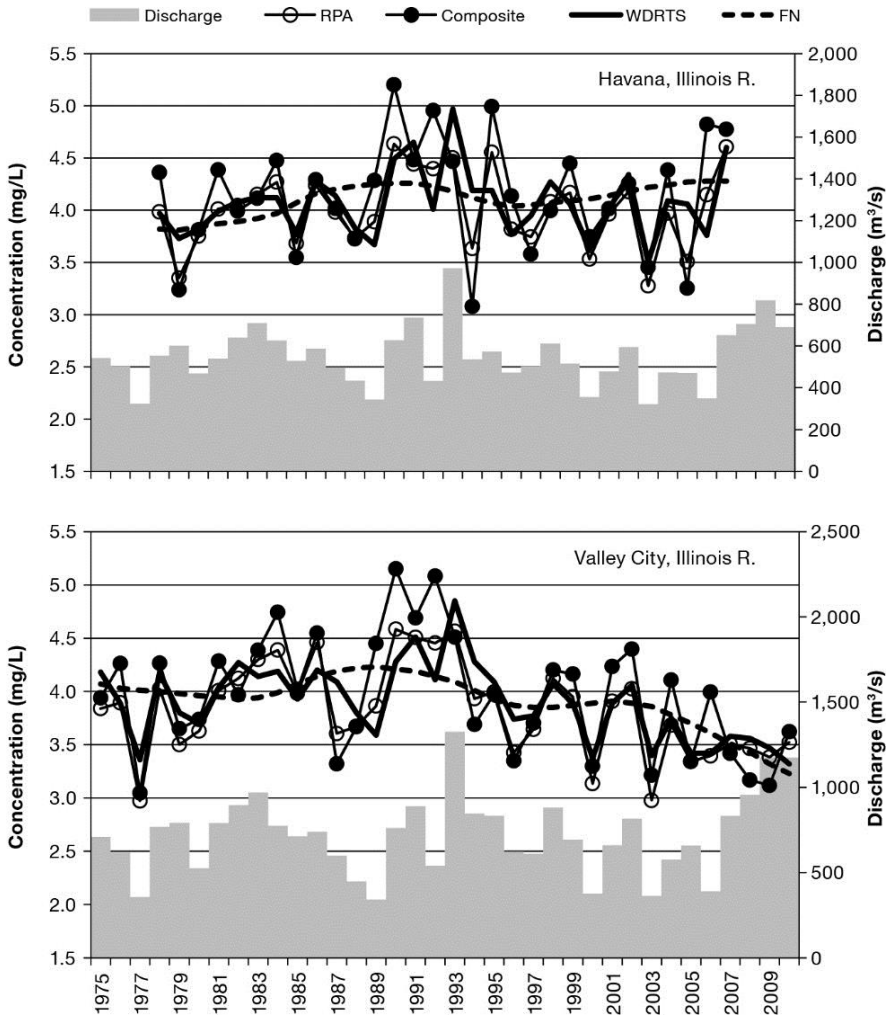

Figure 7.8: Annual average discharge and annual average nitrate concentration based on the rectangular-proportional adjustment RPA (Verma et al. 2012) composite method (Aulenbach and Hooper 2006), flow-dependent WRTDS ("WRTDS"), and flow-normalized WDRTS ("FN")

This sensitivity appears to have an effect on the past approximately 8 years, possibly suggesting that the effects of the end years depend on the characteristics and length of the sequence of years at the end of the record. A long sequence of non-typical conditions (such as the highest 4-year flow average) at the end of the record may result in a longer effect of the

ending years conditions, and conversely, the effect of a more typical ending flow conditions may not propagate back for more than one or two years (similar to Sprague et al., 2011). For trend evaluation, adding several years past 2010 will be of a great importance.

Additionally, the period of nitrate monitoring at Havana (1978-2007) did not match the monitoring periods of other stations in this study (1975-2010). This record, unlike the record at Valley City, ends with a sequence of low and high-flow years, which possibly explains the relatively constant concentration in the past several years (Figures 7.8-7.9, top charts).

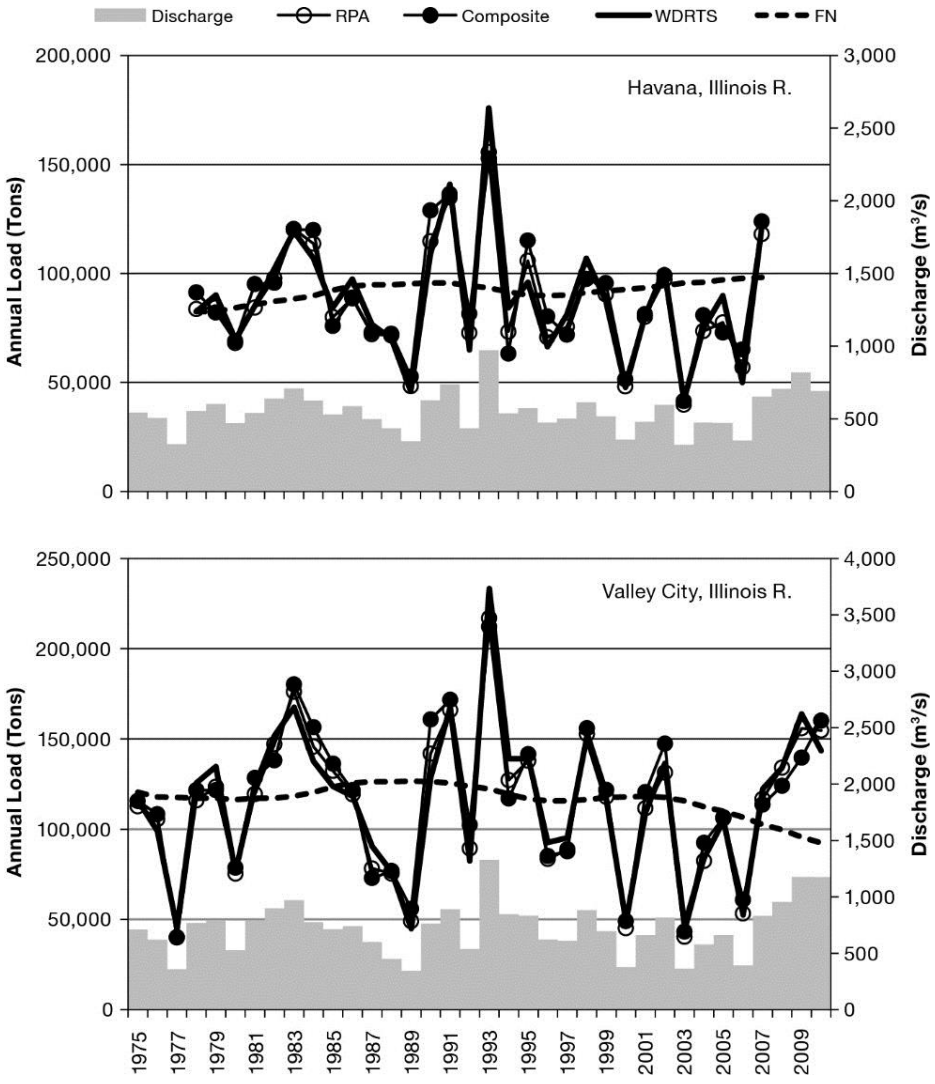

Figure 7.9: Annual average discharge and annual average nitrate loads based on the rectangular-proportional adjustment (Verma et al. 2012) composite method (Aulenbach and Hooper 2006), flow-dependent WDRTS (Hirsch et al. 2010), and flow-normalized WDRTS ("FN")

The corresponding annual average nitrate loads in the Illinois River at Havana and Valley City (Figure 7.9) show a large year-to-year variability as a result of the variability in river discharge. While the differences between RPA, composite, and WDRTS appear insignificant for long-term trend studies, the flow-normalized loads are notably different and appear reasonably consistent with the flow-normalized concentrations for the same locations.

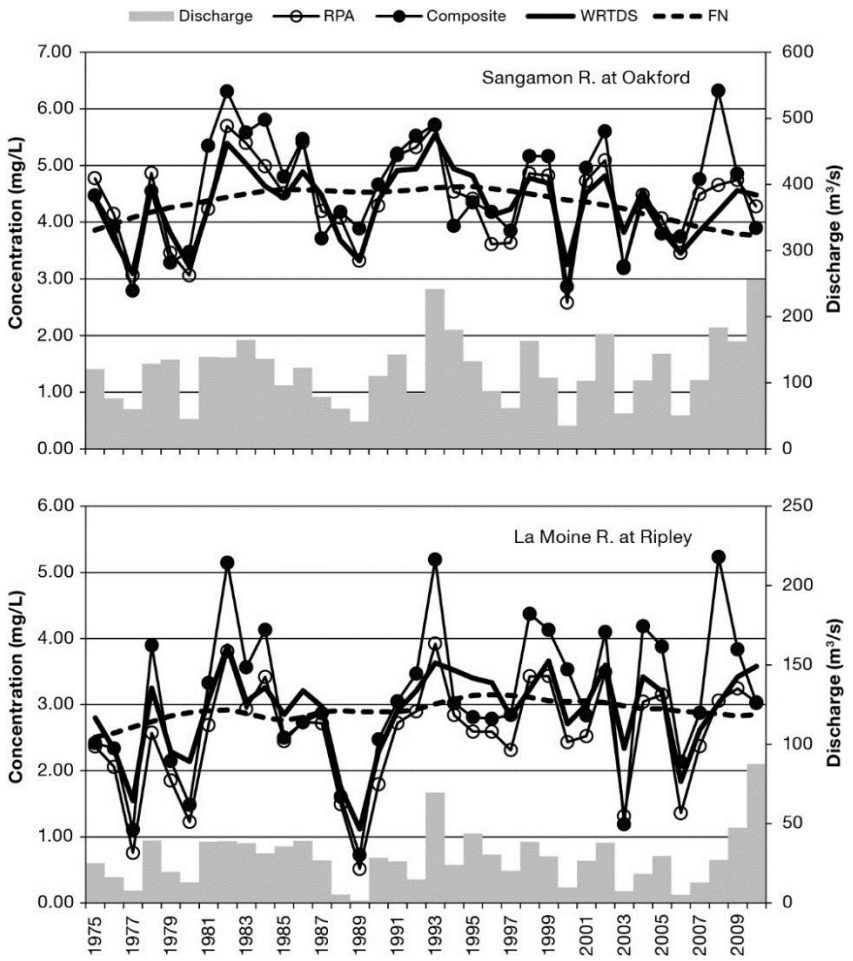

Figure 7.10: Annual average discharge and annual average nitrate concentration based on the rectangular-proportional adjustment (Verma et al. 2012) composite method (Aulenbach and Hooper 2006), flow-dependent WRTDS (Hirsch et al. 2010), and flow-normalized WRTDS ("FN") at the tributaries of the Lower Illinois River

At Havana, the curve showing flow-normalized annual loads exhibits a minor increase, while at the downstream end at Valley City the FN curve shows a significant decrease in the last approximately 8 years of the record, which is consistent with the FN curve for concentration. As

discussed above, because of the sensitivity of the results to the sequence of wet years at the end of record, these results need to be interpreted with caution.

Similar analysis was carried out for the two major tributaries of the Illinois River in this segment, the Sangamon River at Oakford, accounting for 60.3 percent of the drainage area between Havana and Valley City, and the La Moine River accounting for 15.3 percent. Annual average nitrate concentration (Figure 7.10) and annual total nitrate loads (Figure 7.11) show a decrease in nitrate concentration and loads at Oakford on the Sangamon River, and a minor increase at Ripley on the La Moine River.

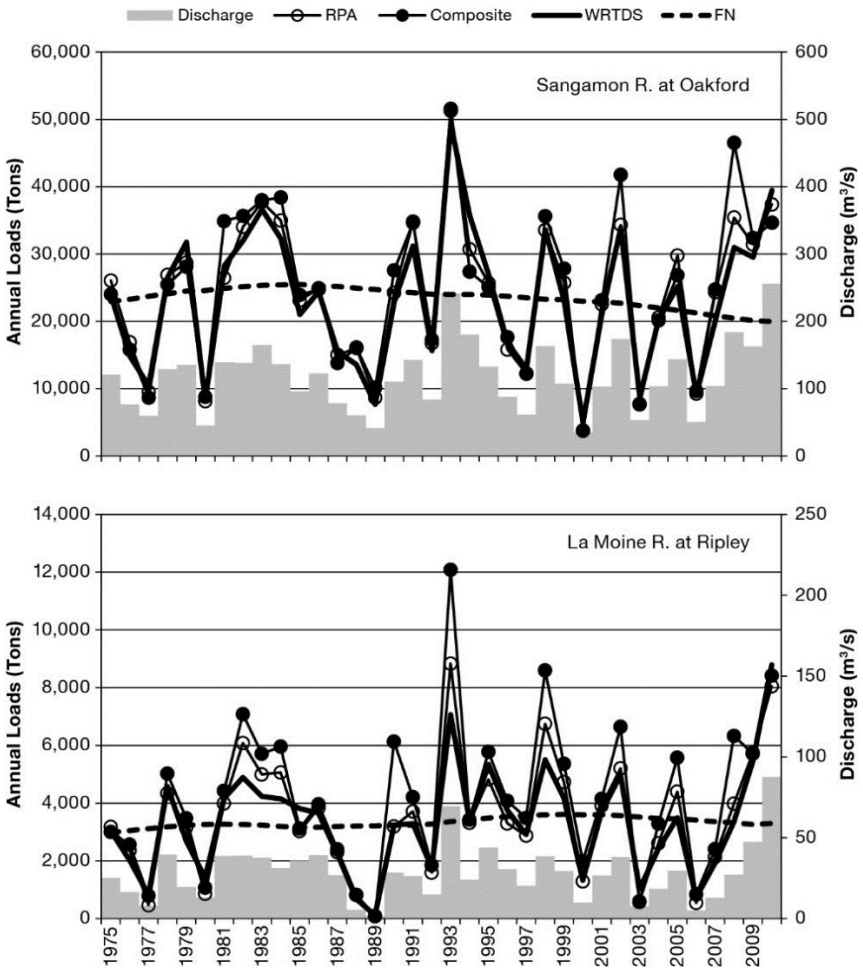

Figure 7.11: Annual average discharge and annual nitrate loads based on the rectangular-proportional adjustment (Verma et al. 2012) composite method (Aulenbach and Hooper 2006), flow-dependent WRTDS (Hirsch et al. 2010), and flow-normalized WRTDS ("FN") at the tributaries of the Lower Illinois River

The annual flow pattern at the Sangamon River is similar to the flow pattern at Valley City on the Illinois River, and the decrease in annual concentrations at the Sangamon River can similarly be attributed to the high-flow years at the end of the record. The concentration and loads at the La Moine River did not show significant changes, possibly due to the differences in flows in the past 4 years. In this watershed, the ending 4 years cover a full range of flow conditions, ranging from a dry year (2007), to the highest year on the record (2010).

7.3.2 Trend Tests

The Kendall's Tau trend test was applied to test the degree of change for different datasets, for 80%, 90%, 95%, and 99% levels of confidence. No trend was detected for concentration, except at Valley City for some of the methods. Table 7.2 shows the results of the Kendall Tau trend method used to determine trends in annual average nitrate concentrations at Valley City. Most of the methods resulted in trends with the levels of confidence under 95%, except TPA (95%) and WRTDS (99%). Similarly, the Kendall Tau trend test was applied to test trends in annual flows and loads, but none of these trends were significant for any of the specified levels of confidence at any site. The absence of trends in flows and loads could partly be explained by the large variability in annual discharge and load data and smaller variability in concentration data.

Table 7.2: Kendall's Tau test with various levels of significance to evaluate the degree of change for annual average concentration at Valley City using different methods (1975-2010)

	Decreasing				Increasing			
Method	99	95	90	80	80	90	95	99
Cohn			■	■				
RRA			■	■				
RPA				■				
TRA				■				
TPA		■	■	■				
Composite			■	■				
WRTDS	■	■	■	■				

Figure 7.12 shows the Şen trend test (Şen, 2012) applied to Valley City on the Illinois River. The test splits the data into two equal parts and compares trends for different flow or concentration ranges. In this case the entire dataset is divided into 1975–1992 and 1993–2010, which are referred to as the early and late periods, respectively. The left chart in the figure indicates that daily discharge values under 2000 m3/s have increased from the early to the late period, and that the discharges above 2000 m3/s have decreased. The average increase in discharge is 12.6%, as the majority of highly skewed daily discharge values (96.1%) belong to the range under 2000 m3/s. Similarly, the right chart indicates that the concentration decreased for the entire observed range, in particular for the values above 3.5 mg/L, which resulted in an average decrease of 6.7%.

It should be noted, however, that both Kendall Tau and Şen tests have limitations. The Kendall Tau test is based on the assumption that the trend is linear. This assumption does not seem to be met for all datasets in this study. For example, Figures 7.8 and 7.9, suggest that annual average concentrations at Valley City are best characterized by increases up through the early 1990s and decreases since that time, particularly in the last 10 years. The Şen test divides the entire dataset in two equal parts, making it well suited for data with an abrupt change occurring approximately in the middle of the record. However, the data in this study have more complex patterns. Some of the driest (e.g., 1989) and wettest (e.g., 1993) historical years on the record are a part of this 36-year record. These years could represent statistical outliers, making it more difficult to ascertain if “true” linear or nonlinear trends exist.

In addition, the trends in concentration might have been affected by the periods of record, such as the sequences of wet years, at the end of the monitoring records. While the record at Havana, which did not include the past 3 years (2008-2010), had no trend in concentration, the Valley City gage, which included the last 3 years, showed a decreasing trend in concentration

with various levels of significance. The addition of future monitoring data as they become available will give us more insight in the processes and trends in these streams in the future

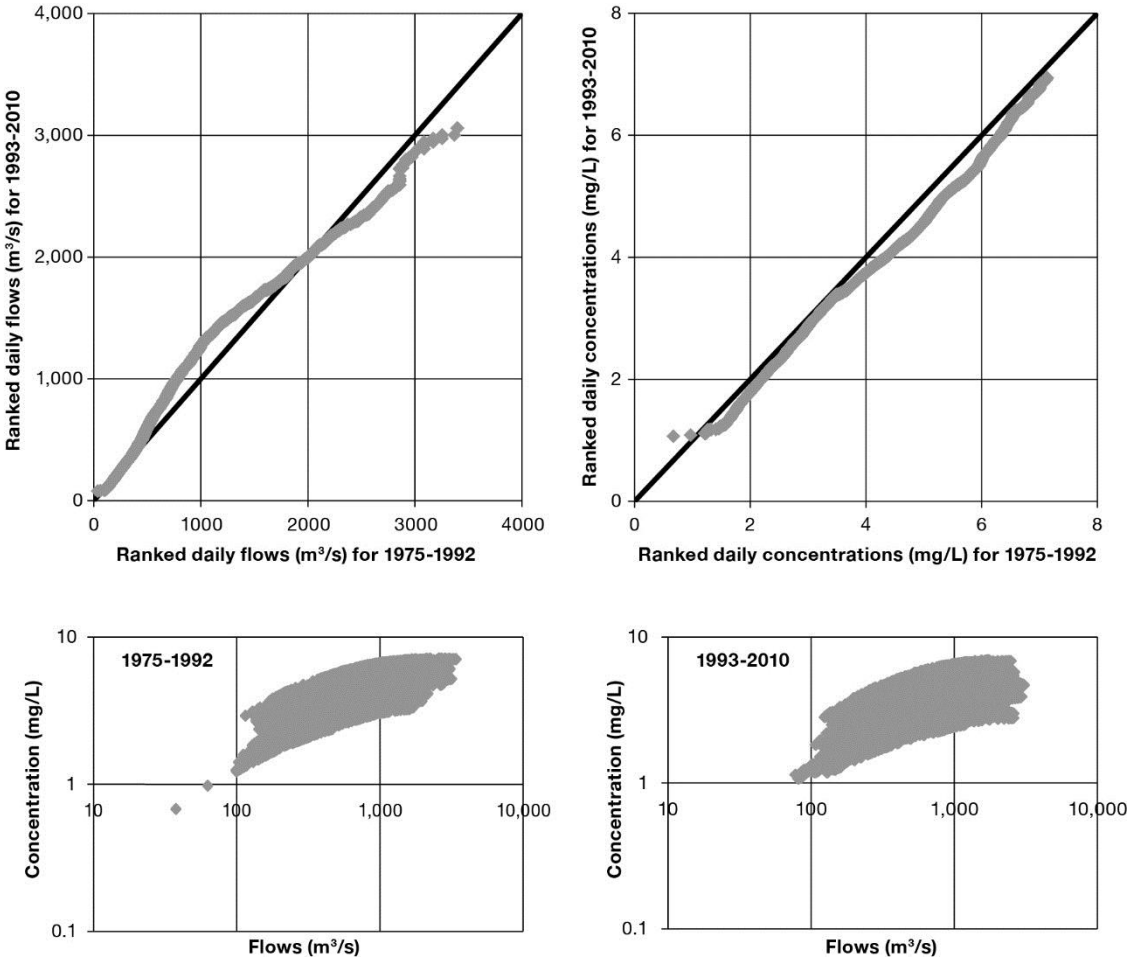

Figure 7.12: Trend tests for daily discharge (top left) and concentration (top right) at Valley City based on the Sen test (Sen 2012) showing an average increase in discharge (12.6%) and decrease in concentration (6.7%). Bottom charts show relationships between flow and concentration for two time periods.

7.4 Conclusions

The goal of the study presented here is twofold. First, we compared several methods for annual load estimation using a 36-year nitrate monitoring dataset observed at the Lower Illinois River basin. Second, using the selected methods we evaluated long-term changes in average annual nitrate concentrations and total annual loads at four stations in the watershed.

This research indicated that trends calculated on the samples alone could result in false determinations even with a long and rich dataset. Thus, extending the data beyond the actual observed samples using estimation techniques can be very beneficial to study long-term trends in nitrate concentrations and loads.

The results of this study also indicated that load estimation methods and trend analyses are highly sensitive to different periods of record. The reliability of annual concentration and loads and their trends based on all methods, particularly the FN method, is affected by the sequence of high-flow years at the end of the record. The presence of low and high outliers and driest and wettest historic years on the record added to the complexity of the analysis. On the other hand, the results were not as sensitive to the method selection. Annual nitrate loads and their trends based on RPA, composite, and WRTDS methods were reasonably similar, particularly for larger watersheds, such as the Illinois River at Valley City.

For these watersheds, the findings of the study highlight the role of data variability and signify the value of each observation year. This underscores the importance of identifying and maintaining sites with long-term nutrient and flow data records for future examination of changes in loads, ultimately affecting hypoxia in the Gulf of Mexico. Further monitoring and refinement of load calculation methods and quantification of their uncertainties are an important part in evaluating progress toward the EPA Science Advisory Boards' (2008) recommended 45% reduction in the loads of nutrients to the Gulf of Mexico.

Acknowledgements

This research was partially supported by the EPA/Illinois Indiana Sea Grant (Grant EPA GL-00E00683-0). In addition, this research was a part of the Illinois River Conservation Reserve Enhancement Program (CREP) funded by the Illinois Department of Natural Resources. Debbie Bruce and Rich Mollahan served as project managers. Dr. Robert Hirsch (USGS) kindly provided us with the WRTDS software and manual. We would like to thank Dr. Greg McIsaac (University of Illinois) for very useful comments and suggestions. The authors also would like to acknowledge the contribution of the Illinois Water Survey staff: Yanqing Lian for providing hydrologic data, Lisa Sheppard for editing, and Sara Olson for preparation of figures.

References

Aulenbach, B. T., Buxton, H. T., Battaglin, W. A., and Coupe, R. H., 2007, "Streamflow and nutrient fluxes of the Mississippi-Atchafalaya River Basin and subbasins for the period of record through 2005." U.S. Geological Survey Open-File Report 2007–1080.

Aulenbach, B. T., Buxton, H. T., Battaglin, W. A., Coupe, R. H., 2007. Streamflow and Nutrient Fluxes of the Mississippi-Atchafalaya River Basin and Subbasins for the Period of Record through 2005: US Geological Survey Open-File, Report 2007–1080.

Aulenbach, B. T., and Hooper, R. P., 2006, "The composite method: An improved method for stream-water solute load estimation." *Hydrological Processes*, 20, 3029–3047.

Cohn, T. A., 1995, "Recent advances in statistical methods for the estimation of sediment and nutrient transport in rivers." *Review of Geophysics*, *Supplement*, 1117–1123.

Cohn, T. A., Caulder, D. L., Gilroy, E. J., Zynjuk, L. D., and Summers, R. M., 1992, "The validity of a simple statistical model for estimating fluvial constituent loads: An empirical study involving nutrient loads entering Chesapeake Bay." *Water Resour. Res.*, 28(9), 2353–2363.

Cohn, T. A., DeLong, L. L., Gilroy, E. J., Hirsch, R. M., and Wells, D. K., 1989, "Estimating constituent loads." *Water Resour. Res.*, 25(5), 937–942.

Crowder, D. W., Demissie, M., and Markus, M., 2007, "The accuracy of sediment loads when log-transformation produces nonlinear sediment load-discharge relationships." *J. of Hydrol.*, 336(3-4), 250–268.

Dolan, D. M., Yui, A. K., and Geist, R. D., 1981, "Evaluation of river load estimation methods for total phosphorus." *Journal of Great Lakes Research*, 7(3), 207–214.

EPA Science Advisory Board, 2008, "Hypoxia in the Northern Gulf of Mexico, An update by the EPA Science Advisory Board." Washington DC, EPA Science Advisory Board, EPA SAB-08-003.

Ferguson, R. I., 1987, "Accuracy and precision of methods for estimating river loads." *Earth Surface Processes and Landforms*, 12(1), 95–104.

Guo, Y., Markus, M., and Demissie, M., 2002, "Uncertainty of nitrate-N load computation for agricultural watersheds." *Water Resources Research,* 38(10), 1185.

Helsel, D. R., and Hirsh, R. M., 1995, "*Statistical methods in water resources*." New York: Elsevier Science Publishing Company, Inc., 529 p.

Hirsch, R. M., Moyer, D. L., and Archfield, S. A., 2010, "Weighted regressions on time, discharge, and season (WRTDS), with an application to Chesapeake Bay river inputs." *J. Am. Water Resour. Assoc.* 46, 857–880.

Illinois Environmental Protection Agency, 2007, Illinois Water Monitoring Strategy 2007-2012. Illinois EPA, Bureau of Water, Springfield, IL. http://www.epa.state.il.us/water/water-quality/index.html

Keefer, L., Bauer, E., and Markus, M., 2010, "*Hydrologic and Nutrient Monitoring of the Lake Decatur Watershed: Final Report 1993–2008, 2010*." ISWS CR 2010-07 Illinois State Water Survey, Champaign, IL.

Kendall, M. G., 1955, "*Rank correlation methods*." New York: Hafner Publishing Co.

Lian, Y., Chan, I.-C., Xie, H., and Demissie, M., 2010, "Improving HSPF modeling accuracy from FTABLES: Case study for the Illinois River basin." *Journal of Hydrologic Engineering*, 15(8), 642–650.

Lucey, K. J., Goolsby, D. A., 1993, Effects of climatic variations over 11 years on nitrate-nitrogen concentrations in the Raccoon River, Iowa, *Journal of Environmental Quality*, 22(1):38–46.

Markus, M., Demissie, M., Short, M., Verma, S., and Cooke, R., 2013, A Sensitivity Analysis of Annual Nitrate Loads and the Corresponding Trends in the Lower Illinois River, *Accepted, Journal of Hydrologic Engineering*

McIsaac, G. F., and Libra, R. D., 2003, Revisiting nitrate concentrations in the Des Moines River 1945 and 1976–2001, *J. Environ. Qual.*, 32:2280–2289.

Neumann, D. W., Rajagopalan, B., and Zagona, E. A., 2003, "Regression model for daily maximum stream temperature." *J. Environ. Engrg*, 129(7), 667–674.

Panno, S. V., Kelly, W. R., Hackley, K. C., Hwang, H. -H., and Martinsek, A. T., 2008, "Sources and fate of nitrate in the Illinois River Basin, Illinois." *Journal of Hydrology*, 359(1-2), 174–188.

Preston, S., Bierman, V. J., and Silliman, S. E., 1989, "An evaluation of methods for the estimation of tributary mass loads." *Water Resour. Res.*, 25(6), 1379–1389.

Robertson, D. M., and Roerish, E. D., 1999, "Influence of various water quality sampling strategies on load estimates for small streams." *Water Resour. Res.*, 35(12), 3747–3759.

Şen, Zekâi, 2012, "An Innovative Trend Analysis Methodology." Journal of Hydrologic Engineering, doi:http://dx.doi.org/10.1061/(ASCE)HE.1943-5584.0000556.

Schilling, K. E., Spooner, J., 2006, Effects of watershed-scale land use change on stream nitrate concentrations, *J. Environ. Qual.*, 35:2132–2145.Short, M. B., 1999, *"Baseline Loadings of Nitrogen, Phosphorus, and Sediments from Illinois Watersheds."* Illinois Environmental Protection Agency, IEPA/BOW/99-020, Springfield, IL.

Sprague, L. A., Hirsch, R. M., and Aulenbach, B. T., 2011, "Nitrate in the Mississippi River and its tributaries, 1980 to 2008: Are we making progress?" *Environmental Science and Technology* 45(17), 7209–7216.

Terrio, P. J., 2006, "*Concentrations, fluxes and yields of nitrogen, phosphorus and suspended sediment in the Illinois River Basin, 1996-2000*." U.S. Geological Survey Scientific Investigations Report 2006-5078.

Turner, R. E.; Rabalais, N. N.; Justic, D., 2006, Predicting summer hypoxia in the northern Gulf of Mexico: Riverine N, P, and Si loading. Mar. *Pollut. Bull.* 52(139–148) USEPA, 2011, http://www.epa.gov/storet/legacy/gateway.htm .

Verhoff, F. H., Yaksich, S. M., and Melfi, D. A., 1980, "River nutrient and chemicaltransport estimation." *Journal of the Environmental Engineering Division*, *ASCE, EE3*, 591–608.

Verma, S., Markus, M., Cooke, R.A., 2012. Development of error correction techniques for nitrate-N load estimation. *J. Hydrol.* 432, 12–25.

Wallin, T. R. and Schaeffer, D. J., 1979, "Illinois redesigns its ambient water quality monitoring network." *Env. Mng*. 3(4), 313–319.

Walker, W. W., 1996, *Simplified procedures for eutrophication assessment and prediction: User manual*, U.S. Army Corps of Engineers, Waterways Experiment Station Instruction Report W-96-2.

Walker, W. W., 2003, "Consideration of variability and uncertainty in phosphorus total maximum daily loads for lakes." *Journal of Water Resources Planning and Management*, 129(4), 337–344.

WSTB (Water Science and Technology Board), 2009, "*Nutrient Control Actions for Improving Water Quality in the Mississippi River Basin and Northern Gulf of Mexico*." National Research Council of the National Academies, National Academies Press, Washington, D.C.

CHAPTER 8

Summary and next steps

The overall goal of this study was to improve the understanding of anthropogenic and natural impacts on various processes of the hydrologic cycle, mainly by predicting and analyzing annual pollutant loads and their corresponding trends from large Midwestern watersheds. To achieve this goal, I first assessed the role of large load events in predicting annual pollutant (sediment and nutrients) loads using regression relationships. Then I identified temporal patterns in pollutant load export from these watersheds for efficient monitoring and resource allocation. I next evaluated the impacts of projected climate change for a mid-century and late-century period on hydrology and water quality in a large agricultural watershed using a physically-based model. Then I explored the applicability of two data mining techniques which have scarcely been used in hydrology to predict missing nutrient concentrations. Finally, I evaluated impacts of available data to predict missing nutrient concentrations, loads and corresponding trends for a large agricultural basin in Midwestern United States by comparing a few traditional, improved and modified statistical approaches. Development, application and evaluation of three different modeling approaches to predict annual pollutant loads and analyzing their corresponding trends in large Midwestern watersheds enabled me to draw these main conclusions:

- Mechanistic differences exist in export of sediment and phosphorus which are mainly exported by surface runoff as compared to nitrates which are primarily exported by subsurface-tile drain systems. Top 5 load events annually carry more than 55% of total pollutant loads and they can be used to predict total annual loads with high accuracies (median errors less than 12.5%) using regression relationships. These prediction accuracies were maximum for sediment and improved on reducing the

spatial extent of watersheds analyzed i.e. lowest prediction errors were seen at individual watershed level. The regression equations are spatially transferable without loss of prediction accuracies for watersheds with similar land-use and in the same geographical region.

- A strong temporal pattern in pollutant export was observed with nitrate export happening primarily in between November and April and sediment and phosphorus export concentrated between February and May, with sediment export being more evenly distributed over the year. No significant statistical trends were observed in the timing of mean daily values of hydrological parameters over long monitoring durations. Pollutant concentrations were considerably more temporally distributed as compared to loads which were concentrated over the high flow periods in late winter and early spring months. The presence of impoundments reduced the overall loads by limiting flow and aiding sedimentation.
- Future climate changes are projected to have an impact on the hydrology of Midwestern watersheds as indicated by simulations using future climate data and a physically-based calibrated SWAT model. In a typical large Midwestern watershed, for the mid-century time period (2045-55) the ensemble GCM projections indicated a rise in average annual temperatures accompanied by a decline in overall annual precipitation amount compared to a baseline time period of 1995-2005. These changes are expected to reduce total flow volumes annually which will also reduce overall pollutant load export from the watershed. For the late-century time period, ensemble GCM projections indicated a further rise in mean average annual temperatures and an increase in annual precipitation. These changes are expected to increase annual flow volumes and total annual pollutant load export. Temporally, for both the future scenarios the temperatures are expected to increase for all months, while the cooler months (winter-spring) are expected to be wetter and see a higher

load export while the warmer months are expected to be drier with a decline in load export. Additionally, due to overall warming, an increase in the length of the crop growing season is expected.

- Two data mining methods including the instance based nearest neighbor IBk classifier and decision tree based REPTree classifier were successful in predicting missing nitrate concentrations with high correlation coefficients ranging from 0.80 to 0.90 and 0.71 to 0.93 respectively for two large watersheds in the Lake Erie basin. The multiyear datasets comprised of daily measured flow, Julian day and nitrate concentrations. Part of the complete dataset was used to calibrate the classifiers using cross validation and a simple percentage split and then flow and Julian day were used to predict concentrations for the remaining data. As expected, prediction errors declined on increasing calibration data used in the percentage split method. Increasing the nearest neighbors used to make predictions offset the impacts of a small calibration percentage for the IBk classifier. Increasing folds beyond 5, did not change the prediction errors significantly for both the data mining methods.
- Average annual pollutant concentrations, loads and their respective trends are sensitive to amounts of data used for calculations. Just depending on sparse low frequency sampling can lead to false trend calculations even for longer datasets. Extending the datasets by predicting missing concentrations is beneficial for long term pollutant load trend analysis. Additionally, statistical approaches such as the seven-parameter regression equation along with several modeling residual adjustment techniques and the Weighted Regression on Time, Discharge, and Season (WRTDS) method gave similar projections indicating low sensitivity to method selection, especially for average annual values for a large watershed.

The work summarized here contributes to the understanding of anthropogenic and natural impacts on water resources by applying and improving different modeling approaches to predict

pollutant loads and trends. At the same time, there are several key areas in which the research could be expanded and improved:

- Apply regression equations to evaluate predictability of annual loads from large load events for watersheds in different landscapes, locations and having different climate patterns.
- Use data mining approaches to quantify the relationship between commonly measured and predicted hydro-climatic parameters such as precipitation intensity, total precipitation, stream flow, temperature, antecedent moisture index, land-use percentages, soil types, point source loads, fertilizer application times etc. and large load events. This approach will potentially aid in identifying watershed specific "triggers" to better predict the criticality of a future high flow event.
- Use more data mining approaches to estimate missing pollutant concentrations and their corresponding loads. Compare these predictions to observed loads and quantify the uncertainties associated.
- Use GCM predictions for different IPCC scenarios and future periods for a wide range of watershed sizes and landuses to estimate the changes in water quantity and quality. Infer changes in overall water balances and their potential impacts on water supply systems and crop growing patterns.
- Evaluate the impacts of projected climate change on performance of sub-surface tile drain systems in Midwestern watersheds
- Evaluate the impacts of potential landuse change and urbanization on hydrology and water quality of Midwestern watersheds
- Do an overall comparative analysis of the three modeling approaches (statistical, physically-based, data mining) for pollutant load estimation for the same dataset to quantify the relative advantages and disadvantages of the three different approaches.